2

AD-A207 215

AFWAL-TR-86-3017
VOLUME II

ADVANCED DURABILITY ANALYSIS
VOLUME II - ANALYTICAL PREDICTIONS, TEST RESULTS AND ANALYTICAL CORRELATIONS

S. D. Manning

General Dynamics Corporation
Fort Worth Division
P.O. Box 748
Fort Worth, Texas 76101

J. N. Yang

United Analysis Incorporated
2100 Robin Way Court
Vienna, Virginia 22180

February 27, 1989

FINAL REPORT OCTOBER 1984 - FEBRUARY 1989

FLIGHT DYNAMICS LABORATORY
AIR FORCE WRIGHT AERONAUTICAL LABORATORIES
AIR FORCE SYSTEMS COMMAND
WRIGHT-PATTERSON AIR FORCE BASE, OH 45433-6553

NOTICE

WHEN GOVERNMENT DRAWINGS, SPECIFICATIONS, OR OTHER DATA ARE USED FOR ANY PURPOSE OTHER THAN IN CONNECTION WITH A DEFINITELY GOVERNMENT-RELATED PROCUREMENT, THE UNITED STATES GOVERNMENT INCURS NO RESPONSIBILITY OR ANY OBLIGATION WHATSOEVER. THE FACT THAT THE GOVERNMENT MAY HAVE FORMULATED OR IN ANY WAY SUPPLIED THE SAID DRAWINGS, SPECIFICATIONS, OR OTHER DATA, IS NOT TO BE REGARDED BY IMPLICATION, OR OTHERWISE IN ANY MANNER CONSTRUED, AS LICENSING THE HOLDER, OR ANY OTHER PERSON OR CORPORATION; OR AS CONVEYING ANY RIGHTS OR PERMISSION TO MANUFACTURE, USE, OR SELL ANY PATENTED INVENTION THAT MAY IN ANY WAY BE RELATED THERETO.

THIS REPORT HAS BEEN REVIEWED BY THE OFFICE OF PUBLIC AFFAIRS (ASD/CPA) AND IS RELEASABLE TO THE NATIONAL TECHNICAL INFORMATION SERVICE (NTIS). AT NTIS, IT WILL BE AVAILABLE TO THE GENERAL PUBLIC, INCLUDING FOREIGN NATIONS.

THIS TECHNICAL REPORT HAS BEEN REVIEWED AND IS APPROVED FOR PUBLICATION.

Howard A. Wood, Jr

FOR MARGERY E. ARTLEY
Project Engineer

James L. Rudd

JAMES L. RUDD, Tech Mgr
Fatigue, Fracture & Reliability Group
Structural Integrity Branch

FOR THE COMMANDER

Tony G. Gerardi

TONY G. GERARDI, Chief
Structural Integrity Branch
Structures Division

IF YOUR ADDRESS HAS CHANGED, IF YOU WISH TO BE REMOVED FROM OUR MAILING LIST, OR IF THE ADDRESSEE IS NO LONGER EMPLOYED BY YOUR ORGANIZATION PLEASE NOTIFY AFWAL/FIBEC, WRIGHT-PATTERSON AFB, OH 45433-6553 TO HELP US MAINTAIN A CURRENT MAILING LIST.

COPIES OF THIS REPORT SHOULD NOT BE RETURNED UNLESS RETURN IS REQUIRED BY SECURITY CONSIDERATIONS, CONTRACTUAL OBLIGATIONS, OR NOTICE ON A SPECIFIC DOCUMENT.

Unclassified

SECURITY CLASSIFICATION OF THIS PAGE

REPORT DOCUMENTATION PAGE

1a. REPORT SECURITY CLASSIFICATION Unclassified	1b. RESTRICTIVE MARKINGS
2a. SECURITY CLASSIFICATION AUTHORITY	3. DISTRIBUTION/AVAILABILITY OF REPORT Approved for public release; distribution unlimited
2b. DECLASSIFICATION/DOWNGRADING SCHEDULE	
4. PERFORMING ORGANIZATION REPORT NUMBER(S)	5. MONITORING ORGANIZATION REPORT NUMBER(S) AFWAL-TR-86-3017, Volume II
6a. NAME OF PERFORMING ORGANIZATION General Dynamics - FWD 6b. OFFICE SYMBOL (If applicable)	7a. NAME OF MONITORING ORGANIZATION Flight Dynamics Lab. (AFWAL/FIBEC) Air Force Wright Aeronautical Laboratories
6c. ADDRESS (City, State and ZIP Code) P.O. Box 748 Fort Worth, Texas 76101	7b. ADDRESS (City, State and ZIP Code) Wright-Patterson AFB OH 45433-6553
8a. NAME OF FUNDING/SPONSORING ORGANIZATION Wright Aeronautical Laboratories 8b. OFFICE SYMBOL (If applicable) FIBEC	9. PROCUREMENT INSTRUMENT IDENTIFICATION NUMBER F33615-84-C-3208
8c. ADDRESS (City, State and ZIP Code)	10. SOURCE OF FUNDING NOS. PROGRAM ELEMENT NO.: 62201F; PROJECT NO.: 2401; TASK NO.: 01; WORK UNIT NO.: 89
11. TITLE (Include Security Classification) Advanced Durability Analysis - Vol. II - Analytical Predictions, Test Results & Analytical Correlations	

12. PERSONAL AUTHOR(S)
S. D. Manning and J. N. Yang

13a. TYPE OF REPORT	13b. TIME COVERED	14. DATE OF REPORT (Yr., Mo., Day)	15. PAGE COUNT
Final	FROM Oct 84 TO Feb 89	89 02 27	287

16. SUPPLEMENTARY NOTATION
The associate investigator for this report was Dr. J. N. Yang of United Analysis, Inc.

17. COSATI CODES FIELD	GROUP	SUB. GR.
0103	1404	1305

18. SUBJECT TERMS (Continue on reverse if necessary and identify by block number)
Durability, fatigue, equivalent initial flaw size (EIFS), initial fatigue quality (IFQ), ~~time to~~ crack initiation (~~TTCI~~), ~~deterministic and~~ stochastic crack growth. (MJM)

19. ABSTRACT (Continue on reverse if necessary and identify by block number)

Advanced durability analysis "design tools" have been developed for metallic aircraft structures. These tools can be used to evaluate durability design requirements for functional impairments due to (1) excessive cracking and (2) fuel leakage/ligament breakage. The methodology accounts for the initial fatigue quality variation of structural details, the crack growth accumulation for a population of structural details under specified design conditions and structural properties. Step-by-step procedures are provided. This volume is limited to the analytical methods, technical aspects, concepts and philosophy for the durability analysis of metallic aircraft structures.

The methodology reflects a probabilistic approach, a fracture mechanics philosophy and both deterministic and stochastic crack growth methods. It can be used to predict the probability of crack exceedance at any service time and/or the cumulative distribution of the time

20. DISTRIBUTION/AVAILABILITY OF ABSTRACT UNCLASSIFIED/UNLIMITED ☒ SAME AS RPT. ☐ DTIC USERS ☐	21. ABSTRACT SECURITY CLASSIFICATION Unclassified
22a. NAME OF RESPONSIBLE INDIVIDUAL Margery E. Artley	22b. TELEPHONE NUMBER (Include Area Code) (513) 255-6104 22c. OFFICE SYMBOL AFWAL/FIBEC

DD FORM 1473, 83 APR EDITION OF 1 JAN 73 IS OBSOLETE.

Unclassified

SECURITY CLASSIFICATION OF THIS PAGE

1

18. (continued) probability of crack exceedance, cumulative distribution of TTCI.

cont'd

~~19. (continued)~~ to reach any crack size. The methodology applies to the small crack size range associated with excessive cracking (e.g., <0.05") and to large through-the-thickness cracks (e.g., 0.5" - 0.75") associated with fuel leakage/ligament breakage.

Keyword

No matter what form, location or combination the as-manufactured flaws may have in fastener holes (e.g., scratches, burrs, microscopic imperfections, etc.) or whatever the source of fatigue cracking may be, a practical method of representing the reality of the as-manufactured condition is needed for durability analysis. This is taken care of by the equivalent initial flaw concept.

Initial fatigue quality of a structural detail (e.g., fastener holes, cutouts, fillets, lugs, etc.) is represented by an equivalent initial flaw size distribution. An equivalent initial flaw (EIFS) is an artificial crack size which results in an actual crack size at an actual point in time when the initial flaw is grown forward. It is determined by back-extrapolating fractographic results. It has the following characteristics: (1) an EIFS is an artificial crack assumed to represent the initial fatigue quality of a structural detail in the as-manufactured condition whatever the source of fatigue cracking may be, (2) it has no direct relationship to actual initial flaws in fastener holes such as scratches, burrs, microdefects, etc., and it cannot be verified by NDI, (3) it has a universal crack shape in which the crack size is measured in the direction of crack propagation, (4) EIFSs are in a fracture mechanics format but they are not subject to such laws and limitations as the "short crack effect," (5) it depends on the fractographic data used, the fractographic crack size range used for the back-extrapolation and the crack growth rate model used, (6) it must be grown forward in a manner consistent with the basis for the EIFS, and (7) EIFSs are not unique - a different set is obtained for each crack growth law used for the back-extrapolation.

Recommendations for durability analysis are as follows: (1) define the equivalent initial flaw size distribution (EIFSD) using fractographic data in the small crack size region (e.g., 0.01"-0.05"), (2) use fractographic data pooling procedure and statistical scaling technique to estimate the EIFSD parameters in a "global sense" for a "single hole population" basis (3) use the deterministic crack growth approach (DCGA) in the small crack size region and (4) use the two-segment deterministic-stochastic crack growth approach (DCGA-SCGA) for applications in the large crack size region (e.g., 0.50"-0.75"); the two-segment deterministic crack growth approach (DCGA-DCGA) is also reasonable but it is slightly less conservative than the DCGA-SCGA.

Procedures have been developed for defining initial fatigue quality. These procedures could be used to standardize the way initial flaw sizes are determined from fractographic data. A better understanding of initial flaw sizes (i.e., what they are and limitations) has been developed. For consistent durability analysis predictions, equivalent initial flaws must be used in the same context for which they were defined. This means that equivalent initial flaws must be grown forward in the same manner the EIFSs were established by back-extrapolating fractographic results.

FOREWORD

This report was prepared by General Dynamics, Fort Worth Division, under the "Advanced Durability Analysis" program (Air Force Contract F33615-84-C-3208) for the Air Force Wright Aeronautical Laboratories (AFWAL/FIBEC). Margery E. Artley was the Air Force Project Engineer; Dr. John W. Lincoln of ASD/ENFS and James L. Rudd of AFWAL/FIBEC were technical advisors. Dr. S. D. Manning of the General Dynamics' Structures Technology Staff was the program manager and co-principal investigator along with Dr. J. N. Yang of United Analysis Incorporated (Vienna, VA).

The advanced durability analysis methodology developed under this program is evaluated in this report (Vol. II). Analytical predictions, test results and analytical correlations are considered. Other volumes for this program are as follows:

- Volume I - Analytical Methods
- Volume III - Fractographic Test Data
- Volume IV - Executive Summary
- Volume V - Durability Analysis Software User's Guide

Table of Contents

Table of Contents (Continued)

Table of Contents (Continued)

Table of Contents (Concluded)

LIST OF FIGURES

List of Figures (Continued)

List of Figures (Continued)

List of Figures (Continued)

List of Figures (Continued)

List of Figures (Continued)

List of Figures (Continued)

List of Figures (Continued)

List of Figures (Continued)

List of Figures (Continued)

List of Figures (Concluded)

LIST OF TABLES

List of Tables (Continued)

List of Tables (Concluded)

SECTION I
INTRODUCTION

The purpose of this Volume is to evaluate the advanced durability analysis methodology documented in Volume I [1] and the test/fractographic results documented in Volume III [2].

SECTION II

EVALUATION OF DURABILITY TEST/FRACTOGRAPHIC RESULTS

2.1 INTRODUCTION

Test and fractographic results acquired under this program (Volume III) [2] are reviewed, evaluated and compared in this section with results from two previous test programs [3, 4]. The overall test program and results are described. Test and fractographic results are evaluated; conclusions and recommendations are presented.

2.2 TEST PROGRAM

A two-phase test program was conducted. Dog-bone specimens were fatigue tested to failure under spectrum loading. Fractographic and strain survey results were acquired. Details of the test program, test and fractographic results are given in Volume III [2].

The Phase I test matrix is described in Table 1 and specimen details are shown in Fig. 1. Data acquired under Phase I was used to (1) evaluate/verify statistical scaling method for multi-hole dog-bone specimens and (2) investigate the initial fatigue quality and crack growth behavior of countersunk fastener holes.

The Phase 2 test matrix is described in Table 2. Specimen details are shown in Figs. 2 and 3. The purpose of these tests was to (1) acquire data for verifying the durability analysis extension for large through-the-thickness cracks associated with fuel leaks and ligament breakage, and (2) conduct a strain survey to verify the present bolt load transfer for a double-reversed dog-bone type specimen.

Table 1. Phase 1 Test Matrix.

SPECIMEN	MATERIAL	TEST SERIES	NO. HOLES PER SPECIMEN	% LOAD TRANSFER	LOAD SPECTRA	MAX. STRESS LEVEL (KSI)	FASTENER I.D.	NO. SPECIMEN
	7475-T7351	I(a)	3	0	F-16 400HR	34	MS90353-08(1/4)	15
		I(b)			B-1 BOMBER	36		16

Note: All tests performed at room temperature in lab air

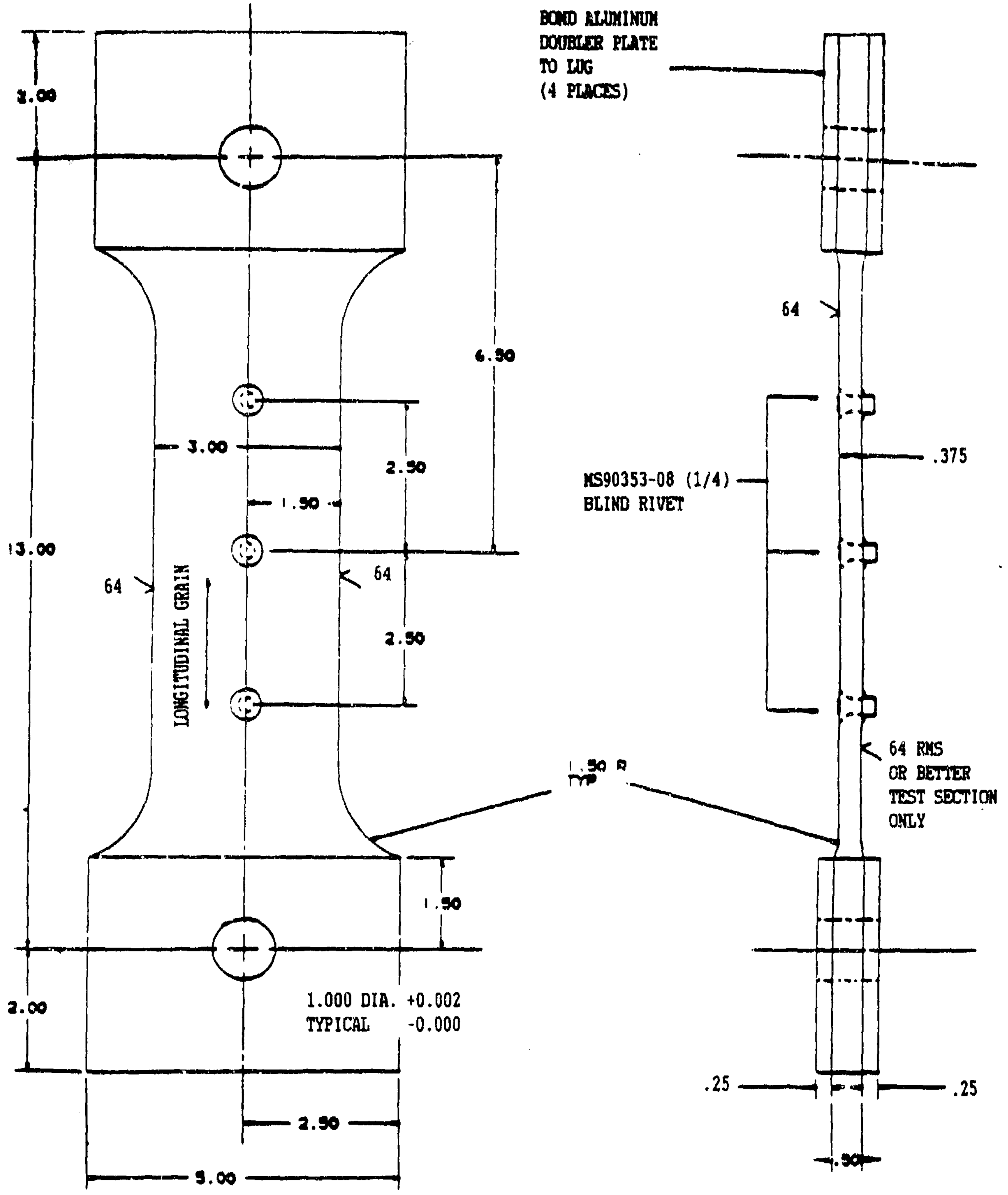

NOTES: 1. MATERIAL: 7475-T7351 Aluminum Plate (1/2" stock)
2. Match drill holes using Modified Winslow Spacematic (no deburring)
3. Drill and install MS90353-08 Rivets per M198
4. All dimensions in inches

Figure 1. **Design Details for WFI Data Set Specimens.**

Table 2. Phase 2 Test Matrix.

Specimen	Material	Test Series	No. Holes per Specimen	Load Transfer	Load Spectra	Max Stress Level (ksi)	Fastener Type	Fastener Dia (in)	Fastener ID	No. Specimens Tested
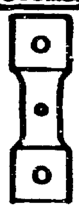 (Fig 2)	7475-T7351 Al	IV(a)	1	0	F-16 400-Hr	34	PH	1/4	NAS6204	9
		IV(b)			B-1 Bomber	34				8
		IV(c)			F-16 C/D	34 / 40.8				5 / 8
		IV(h)			F-16 400-Hr	34	Open Hole (1/4" Dia.)			15
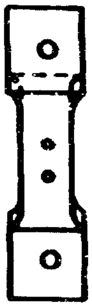 (Fig 3)		IV(d)	4	15%	F-16 400-Hr	34	CSK	1/4	MS90353-08	15
		IV(e)				40.8				
		IV(f)			B-1 Bomber	34				
		IV(g)				40.8				
		IV(i)			Strain Survey	—				1

Note: All tests performed at room temperature in lab air

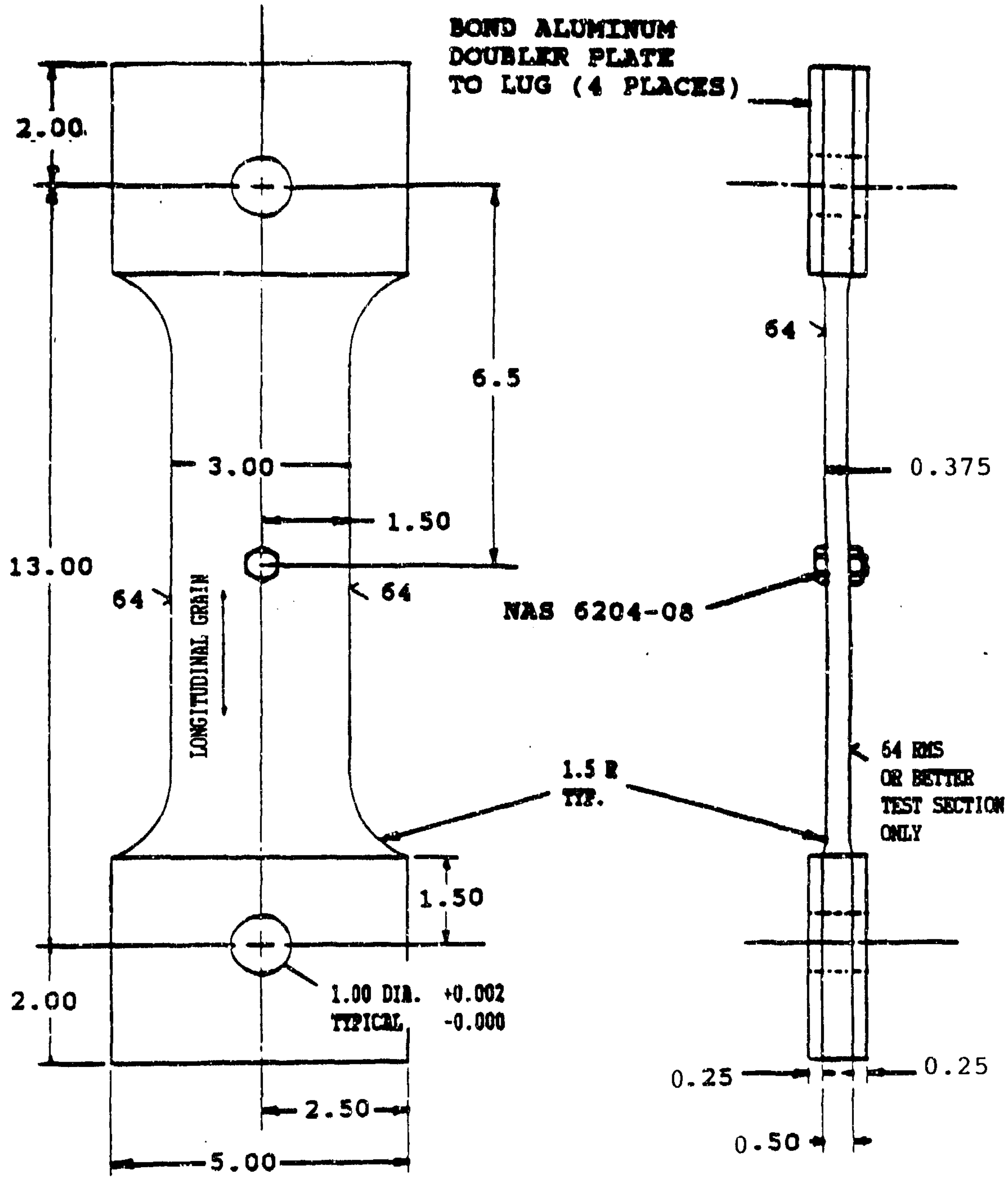

NOTES: 1. MATERIAL: 7475-T7351 Aluminum Plate (1/2" stock)
2. Match drill holes using Modified Winslow Spacematic (no deburring)
3. Drill and install NAS 6204-08 Bolt per M198
4. All dimensions in inches

Figure 2. Dog-Bone Specimen with Single Hole.

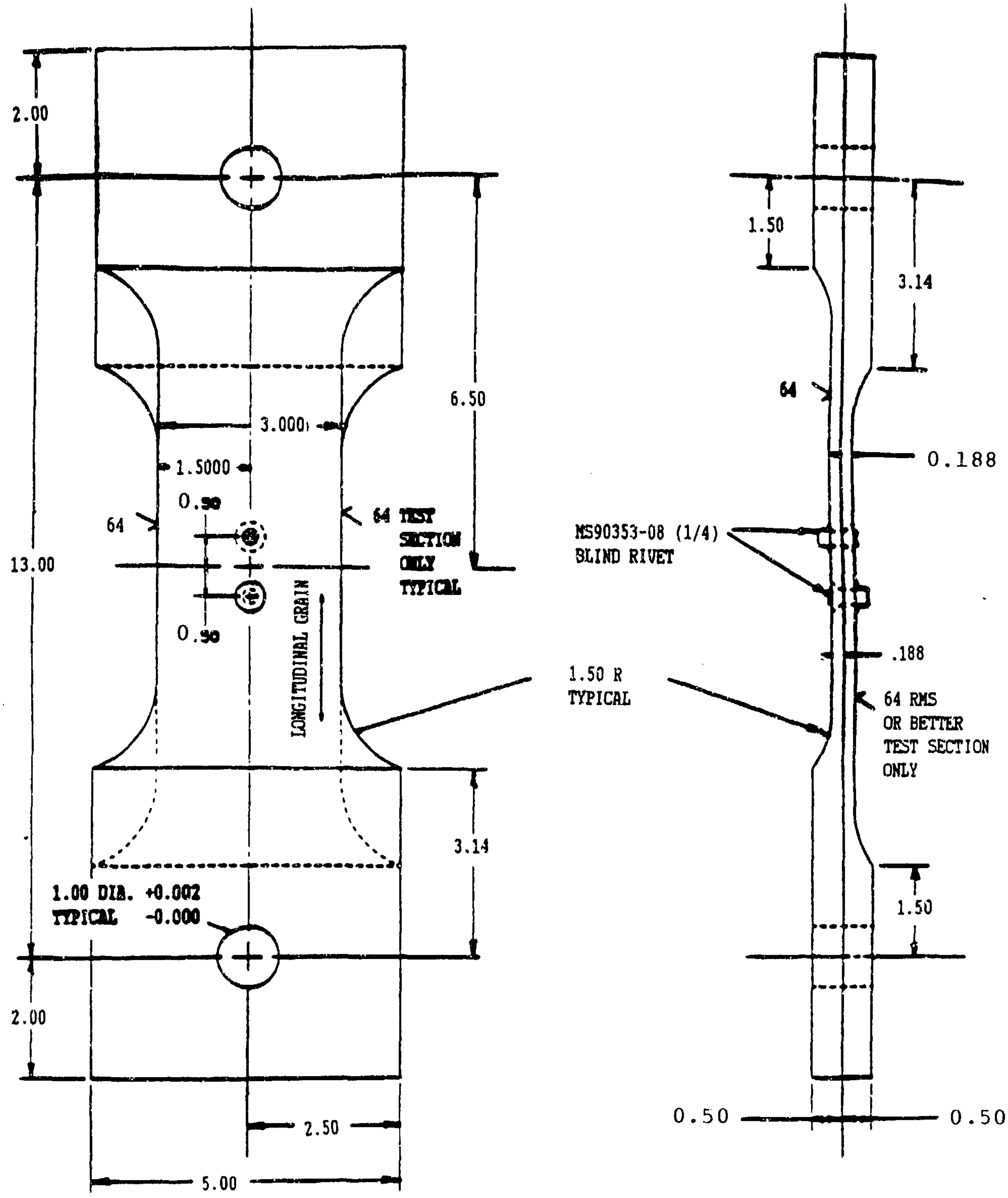

NOTES: 1. MATERIAL: 7475-T7351 Aluminum Plate (1/2" stock)
2. Match drill holes using Modified Winslow Spacematic (no deburring)
3. Drill and install MS90353-08 Rivets per M198
4. All dimensions in inches

Figure 3. **Double-Reversed Dog-Bone Specimen (15% Load Transfer).**

Specimen details are shown in Figs. 4 through 6 for those specimens used in the "Fastener Hole Quality" [2] and "Durability Methods Development" [4] programs. Applicable fractographic results for these specimens are referred to in this Volume (II).

2.3 FRACTOGRAPHIC DATA SCREENING

Fractographic data should be screened before using the data for any durability analysis purpose. Screening is essential to determine the uniformity, quality and behavior of the fractographic data. Software has been developed for surveying and plotting the fractographic data for a given data set. The software is briefly described in Appendix A and details are given in Volume V [5].

A comprehensive fractographic data screening investigation is documented in Appendix B. Each data set from this program was surveyed and the fractographic data (i.e., a(t) versus t) was plotted. Refer to Appendix B for details.

2.4 CRACK INITIATION ORIGINS AND TRENDS

Crack initiation origins and trends were investigated for both straight-bore and countersunk fastener holes. Results from this program were also compared with those from two other programs [3,4].

The following crack initiation origins were observed.

1. Some fatigue cracks originated in the bore of the fastener hole for straight-bore holes. Multiple origins and crack branching in the bore of the hole were observed for both fighter and bomber load spectra and for specimens with or without a fastener in the hole. For example, specimen for

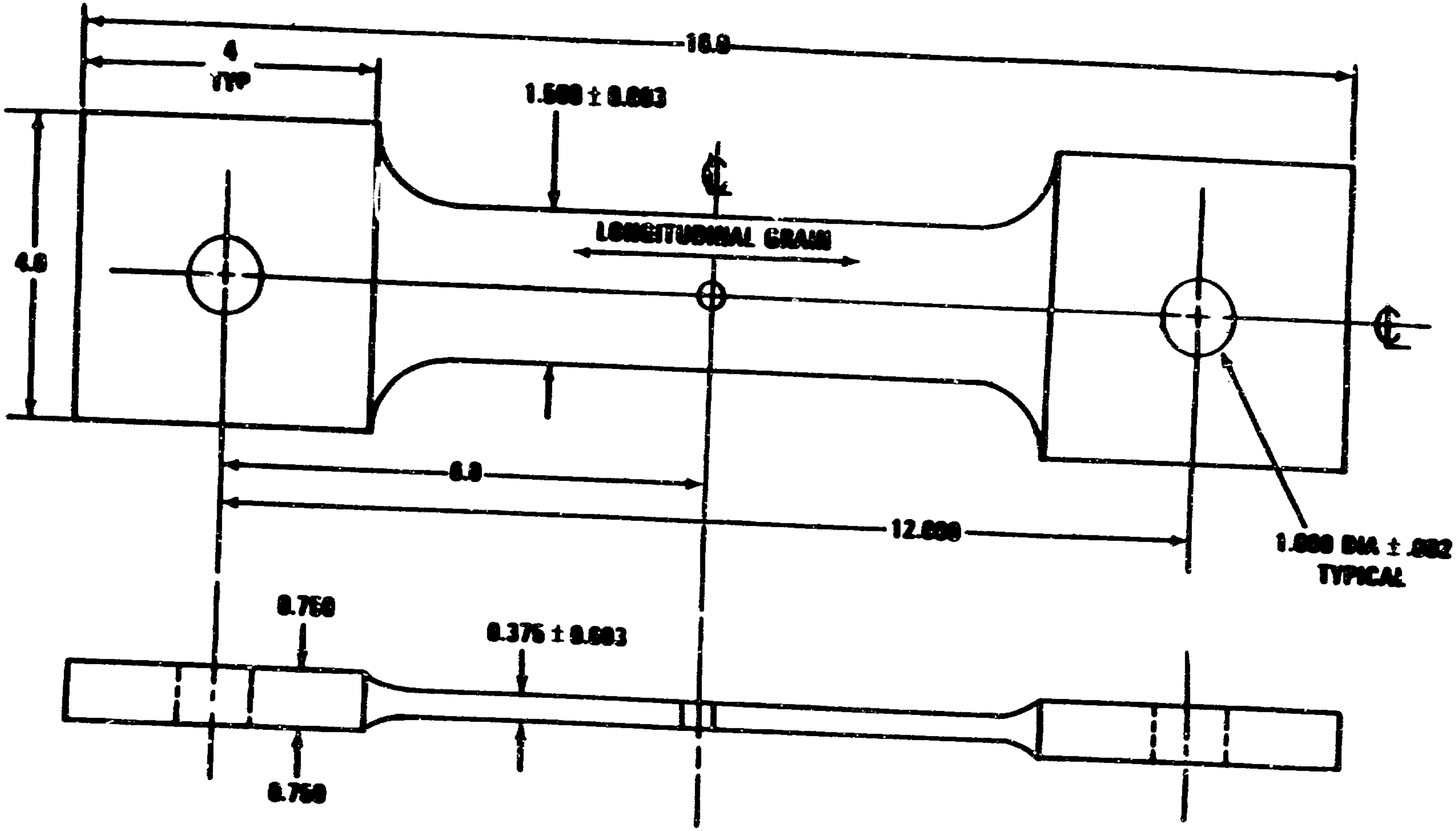

Figure 4. <u>No-Load Transfer Specimen Geometry.</u>

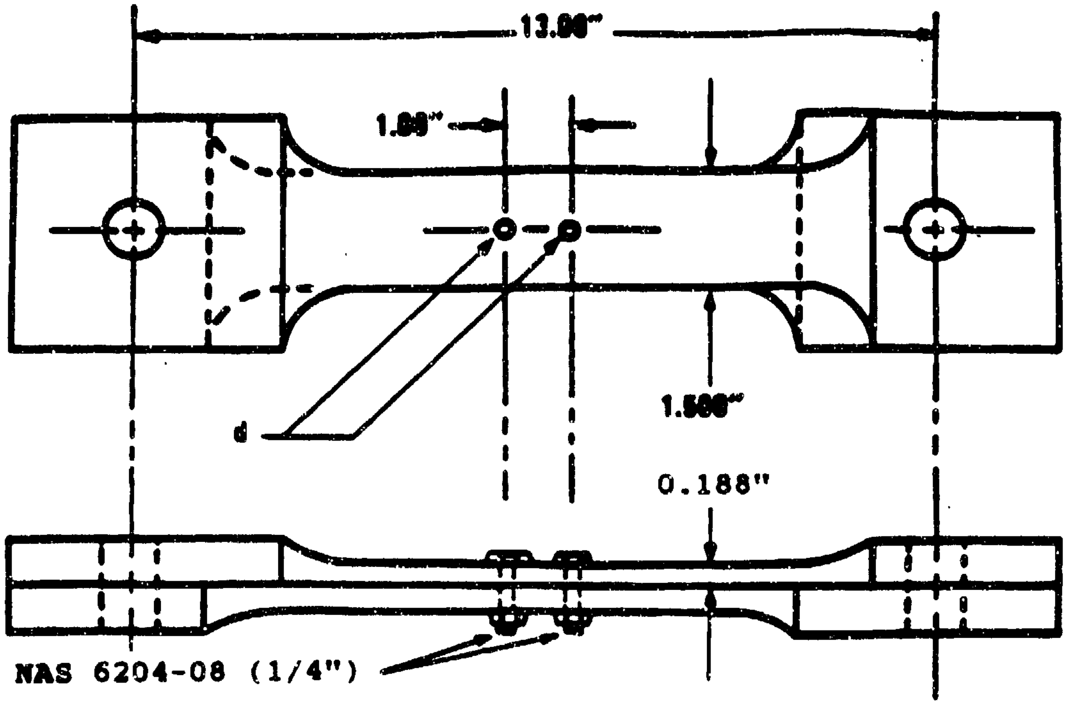

Figure 5. Double-Reversed Dog-Bone Specimen Design with Straight Shank Bolts.

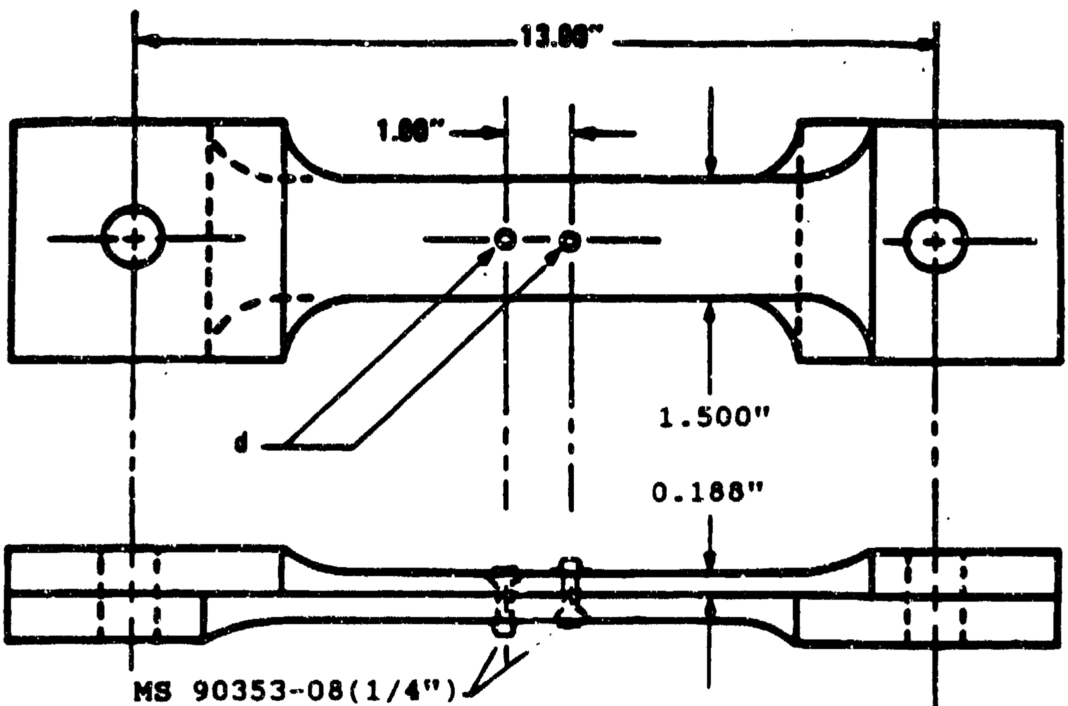

Figure 6. Double-Reversed Dog-Bone Specimen Design with Blind Countersunk Rivets.

the WWPFO data sets contained a single straight-bore hole without a fastener installed. All data sets with a straight-bore fastener hole were a "no load transfer" type (i.e., bolt passive).

2. Most fatigue cracks originated in the bore of the countersunk fastener holes for the WFI and WBI data sets (both "no load transfer" type specimen). A few fatigue cracks also originated on the surface of the countersink.

3. For data sets with countersunk fastener holes with bolt load transfer, most fatigue cracks originated at the corner of the fastener hole at the interface. Some cracks originated on the surface of the countersink. Also, in one or two cases fatigue cracks originated on the faying surface instead of the fastener hole.

The fatigue crack initiation origins and trends observed for this program for both straight bore and countersunk fastener holes are very comparable with those for the "Fastener Hole Quality" program [3] and the prototype "Durability Methods Development" program [4].

2.5 STRAIN SURVEY

A strain survey was performed in Phase 2 on a double reversed dog-bone specimen like the one shown in Fig. 3. The purpose of the strain survey was to estimate the actual amount of bolt load transfer, as a function of the applied load level, for this type of specimen. Details of the strain survey are given in Appendix G.

The double-reversed dog bone specimen shown in Fig. 3 is a "15% bolt load transfer design." If the fasteners perfectly fit the holes, the specimen will theoretically transfer 15% of the applied load to specimen through the bolts. The actual amount of bolt load transfer for this type specimen varies depending on the fastener type and fit.

The percent bolt load transfer is an important consideration for durability analysis for (1) tuning or curve fitting the analytical crack growth program [e.g., 1] to the fractographic data base that is used to define IFQ or the EIFSD parameters and (2) determining the service crack growth master curve (SCGMC) for desired durability analysis conditions.

2.6 FRACTOGRAPHIC DATA APPLICATIONS

The fractographic data acquired under this program are used extensively in this Volume (II) to (1) conduct initial fatigue quality studies for fastener holes, (2) evaluate/verify the statistical scaling method developed in Volume I [1], (3) evaluate the sensitivity of crack growth rate parameters Q and σ_z with respect to the fractographic crack size range used, (4) study mean EIFSs for different data sets, (5) investigate the initial flaw size for different EIFSD functions and crack exceedance probabilities and (6) evaluate/compare time-to-crack initiation (TTCI) and time-to-failure (TTF) statistics and trends for narrow (W = 1.5") and wide (W = 3.0") specimen data sets.

Most of the investigation mentioned above are documented in other sections of this Volume (II), such as Sections III and IV and Appendices B, C and E-J.

TTCIs (mean, high and low extremes) for a_0 = .05" are compared in Tables 3-5 for various data sets. The mean TTCI is denoted by an open or solid circle and the extremes by tic marks. An open circle is used to denote data sets from either the "Fastener Hole Quality" program [3] or the "Durability Methods Development" program [4].

Table 3. Comparison of TTCIs (a_0 = 0.05") for Narrow and Wide Specimen Data Sets (Straight Bore Holes with NAS 6204-08 Bolt).

DATA SET	σ (ksi)	WIDTH (in.)	% LT	TTCI (a_0 = 0.05")
WPF (N=33)	34	1.5	0	
WWPF (N=13)	34	3.0	0	
WWPFO (N=14)	34	3.0	0	(open hole w/o bolt)
WPB (N=32)	34	1.5	0	
WWPB (N=12)	34	3.0	0	

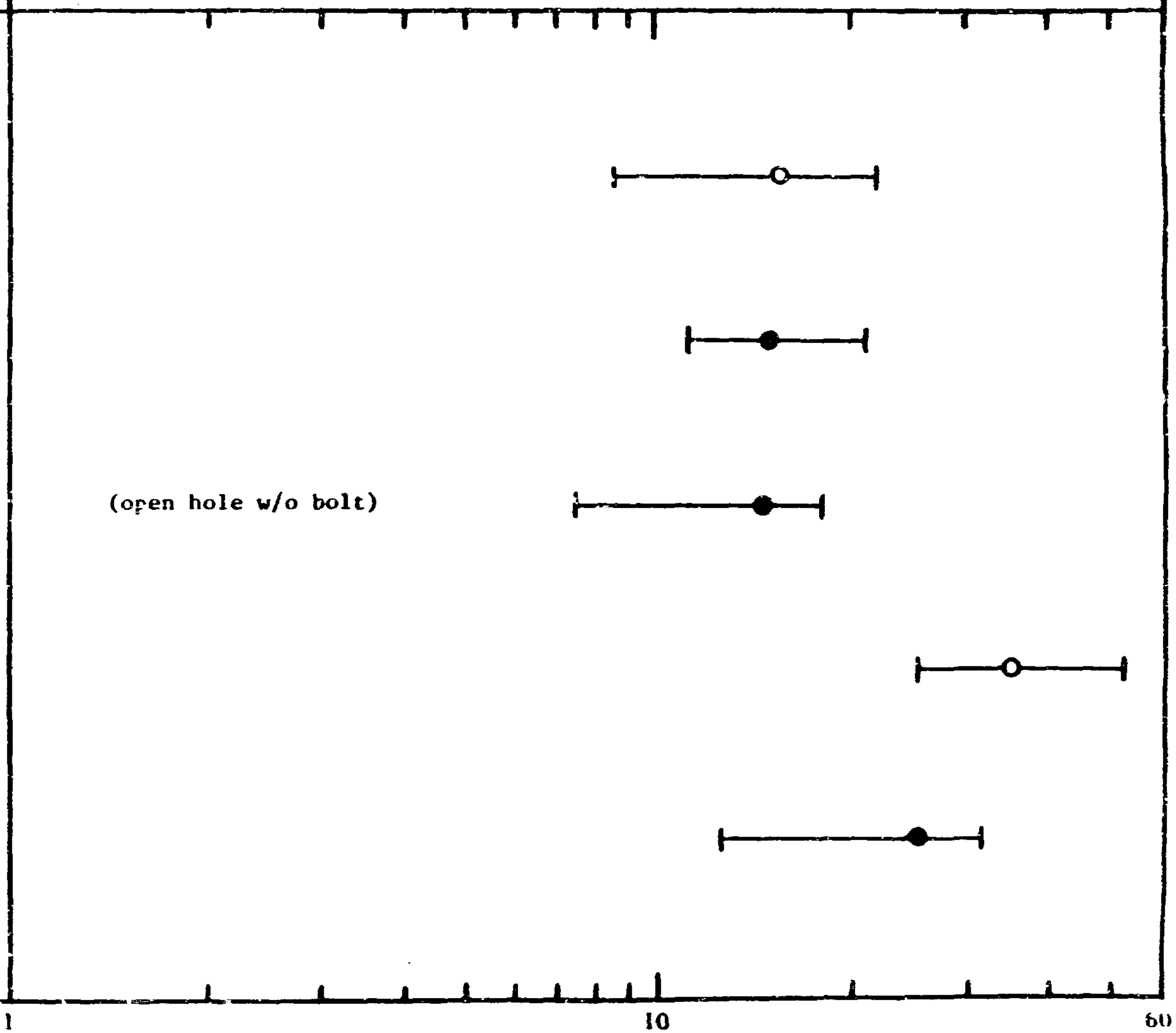

Table 4. Comparison of TTCIs (a_0 = 0.05") for Narrow and Wide Specimen Data Sets (Countersunk Holes with MS 90353-08 Rivets).

DATA SET	σ (ksi)	WIDTH (in.)	% LT
AFXLR4 (N=10)	32	1.5	15
AFXMR4 (N=9)	34	1.5	15
AFXHR4 (N=10)	38	1.5	15
WAFXMR4 (N=14)	34	3.0	15
WAFXHR4 (N=13)	40.8	3.0	15

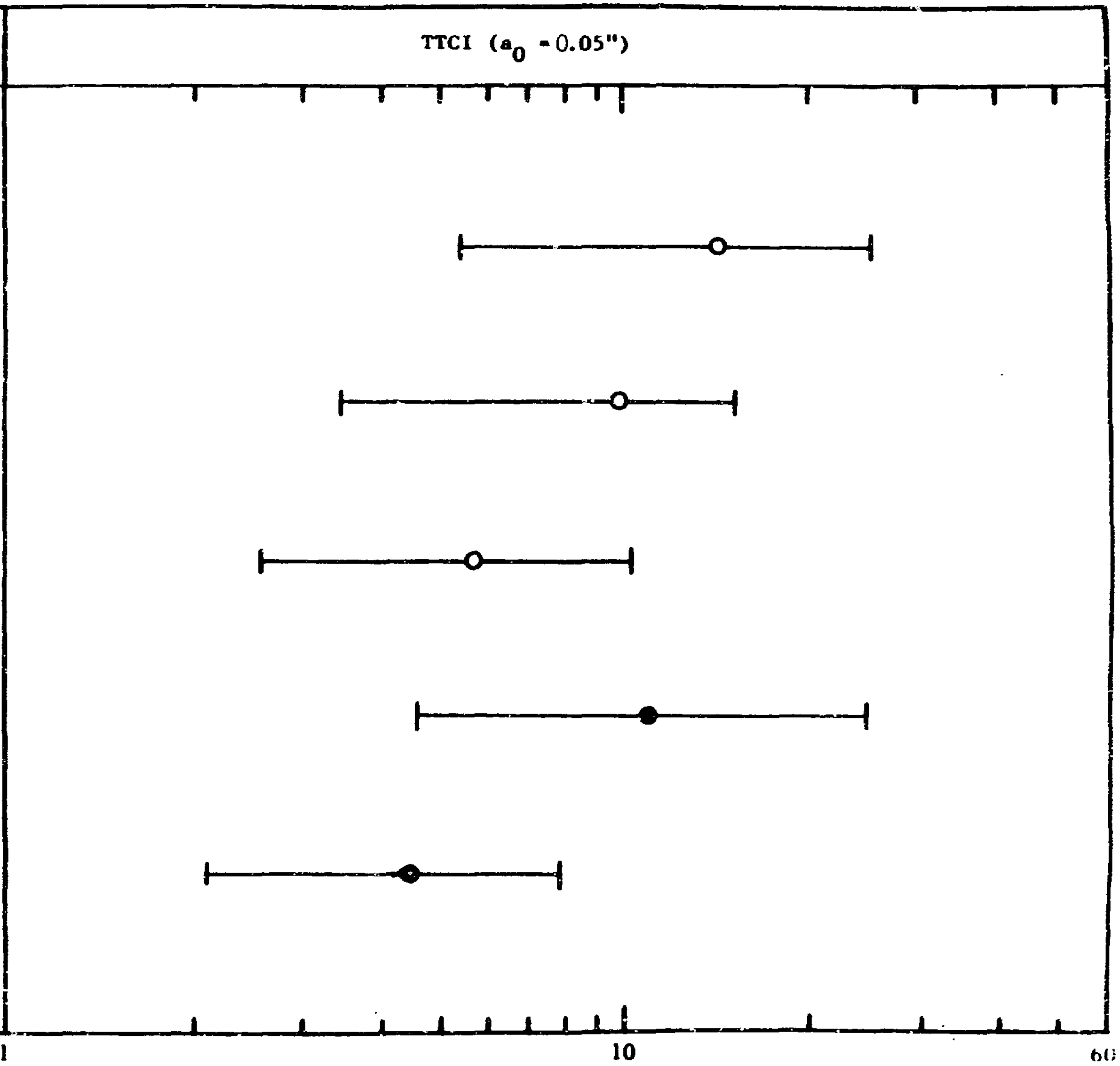

Table 5. Comparison of TTCIs (a_0 = 0.05") for Wide Specimen Data Sets.

DATA SET	σ (ksi)	WIDTH (In.)	% LT
WWPCL (N=4)	34	3.0	0
WWPCH (N=6)	40.8	3.0	0
WFI (N=14)	34	3.0	0
WBI (N=12)	36	3.0	0
WXWPB (N=15)	34	3.0	15
WABXHR4 (N=15)	40.8	3.0	15

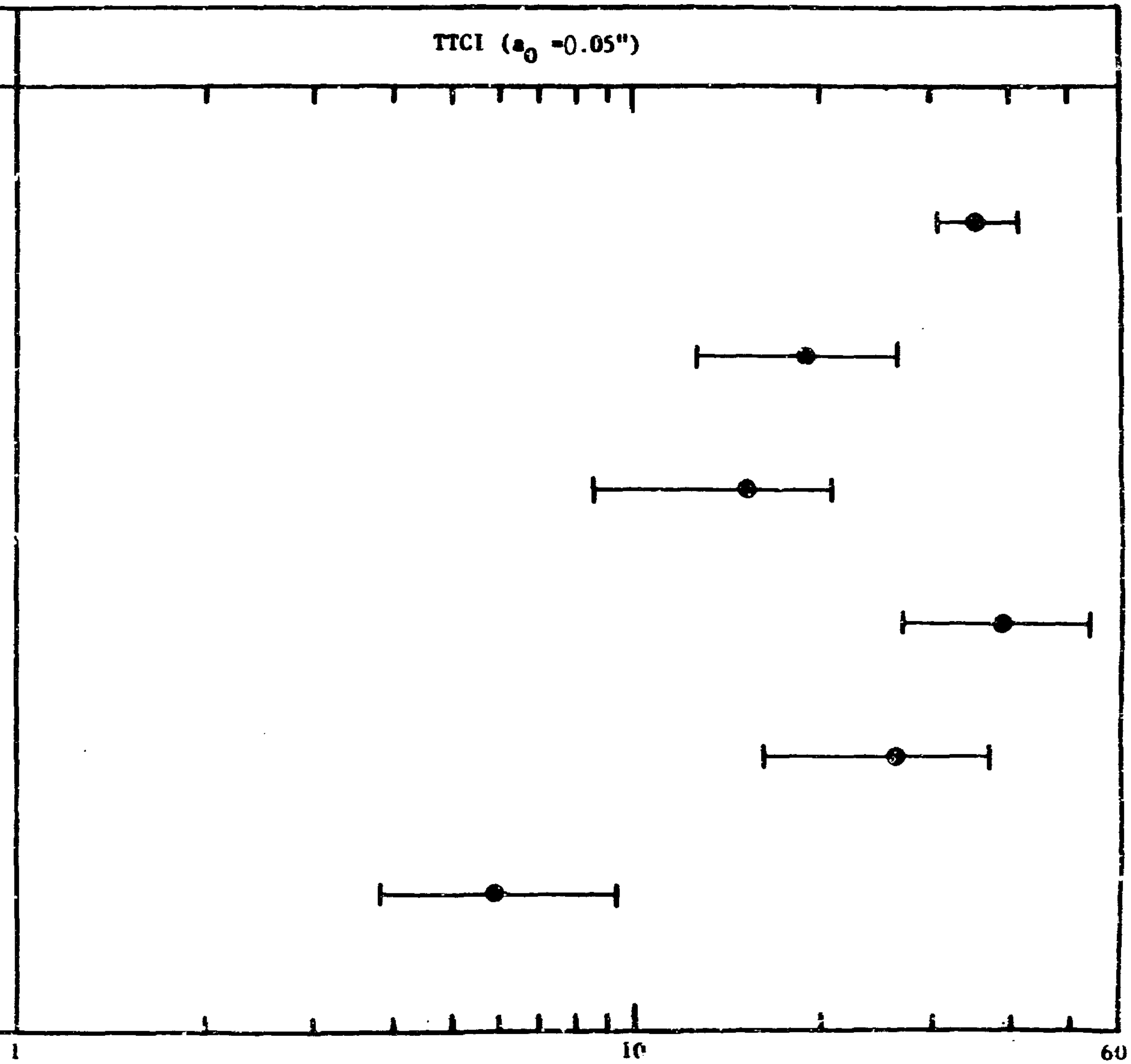

In Table 3, the mean and extreme TTCI values for narrow and wide specimen data sets are compared for the fighter and bomber load spectra. For example, the results for the narrow specimen data set WPF are compared with the wide specimen data sets WWPF and WWPFO. The specimen details for data sets WWPF and WWPFO are identical except no bolt is installed in the fastener hole for the WWPFO data set. In this case the mean and extreme TTCIs for the narrow and wide specimen data sets are the same order of magnitude.

TTCIs for the WPB data set (bomber load spectrum) are compared with those for the WWPB data in Table 3. In this case, the mean and extreme TTCIs, for some reason, do not have the same degree of agreement as those for the fighter data set.

TTCI results for selected countersunk data sets are shown in Table 4. The specimens and test conditions for data sets AFXMR4 and WAFXMR4 are identical except the latter is 3.0" wide and the former is 1.5" wide. In this case, the mean TTCIs and extremes compare reasonably well. This suggests that specimen width doesn't have a significant affect on the TTCIs for a relatively small referenced crack size (i.e., $a_0 = 0.05"$). Since other data sets do not have comparable stress levels, the results cannot be compared directly.

The TTCI mean and extreme values are shown in Table 5 for six other fractographic data sets acquired under this program. Data sets WWPCL and WWPCH reflect straight-bore fastener holes and the other data sets reflect countersunk fastener holes.

2.7 CONCLUSIONS, RECOMMENDATIONS AND GUIDELINES

The following observations, conclusions and recommendations are based on the extensive evaluations and experience with the test and fractographic results of this program and two other programs [3,4].

1. Test specimens for acquiring IFQ data should be fatigue tested to failure. "Mixing and Matching" fractographic results for both failures and runouts (or survivors) may lead to one of the following potential problems. The fractographic data (i.e., a(t) versus t) for each test specimen may not cover the desired AL-AU crack size range. Hence, fractographic results may have to be "extrapolated" to a given crack size and/or service time.

2. Fractographic data should be surveyed and censored before using the data for any durability analysis purpose. Data screening is needed to determine the quality and character of the data and to reject suspicious data. Questionable fractographic data should be censored from the data set.

3. Software is available for an IBM or IBM-compatible PC for plotting fractographic results for any data set [5]. This software is useful for studying the behavior of fractographic data for a selected AL-AU range and for identifying fatigue cracks with abnormal behavior.

4. The fractographic data sparsity problem needs to be investigated further. For example, fractographic data may not be available, for one reason or another, in the desired AL-AU crack size range. There are three possibilities regarding the fractographic data: (1) it covers the selected AL-AU range completely (i.e., $a(t) \leq AL$ and $a(t) > AU$), (2) it has some data in the AL-AU range, and (3) it has no data in the

AL-AU range. If the (a(t), t) fractographic data does not cover the AL-AU range, then data may have to be extrapolated for the durability analysis.

5. When fractographic data is extrapolated, don't extrapolate too far beyond the limits of the actual data. Two problems with extrapolations are (1) extrapolated values may be meaningless if they are far removed from the limits of the actual size, and (2) there's no way to separate the effects of fractographic data extrapolations and interpolations on the overall variability.

6. Considerable scatter was observed for some of the fractographic data sets. The following factors probably contributed to the scatter: (1) inherent variability of material properties, (2) specimen manufacturing variability, (3) testing procedures/environment, and (4) fractographic readers and readings.

7. Considerable care should be used to prepare the test specimens for fractographic evaluation because fracture surfaces can be easily damaged by saw marks when cracks are broken open.

8. The TTCI mean and extremes for the WPF (W = 1.5"), the WWPF (W = 3.0") and the WWPFO (W = 3.0") straight-bore data sets (a_0 = 0.05") were comparable. This was expected for relatively small fatigue cracks in fastener holes.

9. The fractographic data acquired under this program was very useful for evaluating/refining the durability analysis methods described in Volume I [1]. The data was particularly useful for (1) investigating/evaluating the IFQ of fastener holes, (2) evaluating/justifying the statistical scaling method developed, (3) estimating the % bolt load transfer for double-reversed dog-bone specimens, and (4) conducting numer-

ous durability related studies.

10. Only straight shank and countersunk clearance fit fasteners in 7475-T7351 aluminum were investigated under this program. The effect of interference fit fasteners and cold working on the IFQ of fastener holes needs to be investigated. Whatever type fastener is used, however, the same general guidelines presented herein apply.

11. The double-reversed dog-bone type specimens used in this program were "designed" for 15% bolt load transfer. The actual amount of bolt load transfer varied depending upon the fastener type and fit. From the strain survey we determined that the actual amount of % bolt load transfer was approximately 7% for the specimen used at 100% specimen load. Only one reversed dog-bone specimen was used in the strain survey. We would expect the actual amount of the % bolt load transfer to vary for each specimen - depending on the particular fastener type and fit for each specimen. The % bolt load transfer for a given fractographic data set can be estimated in one of the following two ways: (1) strain survey or (2) by tuning or curve fitting the analytical crack growth program to the EIFS master curve.

12. In a few cases fatigue cracks originated on the faying surface instead of the bore of the hole. Two possible reasons for this behavior are (1) surface finish too rough, and (2) mating surface rubbing together at the faying surface.

SECTION III

DEMONSTRATION/EVALUATION OF INITIAL FATIGUE QUALITY

3.1 INTRODUCTION

The purpose of this section is to demonstrate and evaluate the refined methods, described in Volume I [1], for determining the initial fatigue quality of countersunk and straight-bore fastener holes. Initial fatigue quality (IFQ) characterizes the initially manufactured state of a structural detail or details (e.g., fastener holes, lugs, cutouts, fillets, etc.) with respect to initial flaws in a part, component, or airframe prior to service. Actual initial flaws in a fastener hole are typically random scratches, burrs, microscopic imperfections, etc. Initial flaws are represented by the equivalent initial flaw size (EIFS) in this program. An EIFS is an artificial crack size which results in an actual crack size at an actual point in time when the EIFS is grown forward. It is determined by back-extrapolating fractographic results using a suitable empirical crack growth rate model. The IFQ, represented by an equivalent initial flaw size distribution (EIFSD), is the "cornerstone" of the durability analysis method. Once the IFQ has been determined and justified for durability analysis, it can be used to make predictions for the probability of crack exceedance at any service time, τ , and the cumulative distribution of service time to reach any crack size, x_1.

In this section, we will determine the EIFSD parameters for the Weibull compatible distribution for countersunk and straight bore fastener holes (with clearance fit and no cold working) and then justify the resulting EIFSD for durability analysis. For this purpose, we will use available fractographic results for 7475-T7351 aluminum [2-4] and available durability software [5]. This section concerns IFQ and fatigue cracking in the small crack size region (e.g., AL - AU = 0.01" - 0.05"). However, the IFQ results of this section will be used later in Section III to demonstrate and evaluate the durability analysis extension for the large crack size region (e.g., AL - AU = 0.05" - 1").

The general procedure for estimating the EIFSD parameters for the Weibull compatible distribution using fractographic results is presented in Volume I [1]. The procedure, essential equations, and details are summarized in this section. The same approach for determining IFQ applies to both countersunk and straight-bore fastener holes.

3.2 METHOD FOR DETERMINING INITIAL FATIGUE QUALITY

The general procedure for defining IFQ is summarized below and key elements are described in Figs. 7-9.

1. Select a suitable EIFSD function for representing the initial fatigue quality (e.g., Weibull compatible or Lognormal, or lognormal/compatible). The Weibull compatible distribution function proposed by Yang and Manning [6,7] has been found to be reasonable for representing the EIFS cumulative distribution [6-16].

$$F_{a(0)}(x) = \exp\left\{-\left[\frac{\ln(x_u/x)}{\phi}\right]^{\alpha}\right\} \; ; \; 0 \leq x \leq x_u \qquad (1)$$
$$= 1.0 \qquad ; \; x > x_u$$

in which $F_{a(0)}(x) = P[a(0) \leq x]$, $a(0)$ = EIFS = crack size at time $t = 0$, x_u = EIFS upper bound limit, and α and ϕ are empirical parameters.

2. Select fractographic data set(s) to be used to determine the EIFSD. The data sets should be for the same material, same type load spectrum (e.g., fighter, bomber, or trans-

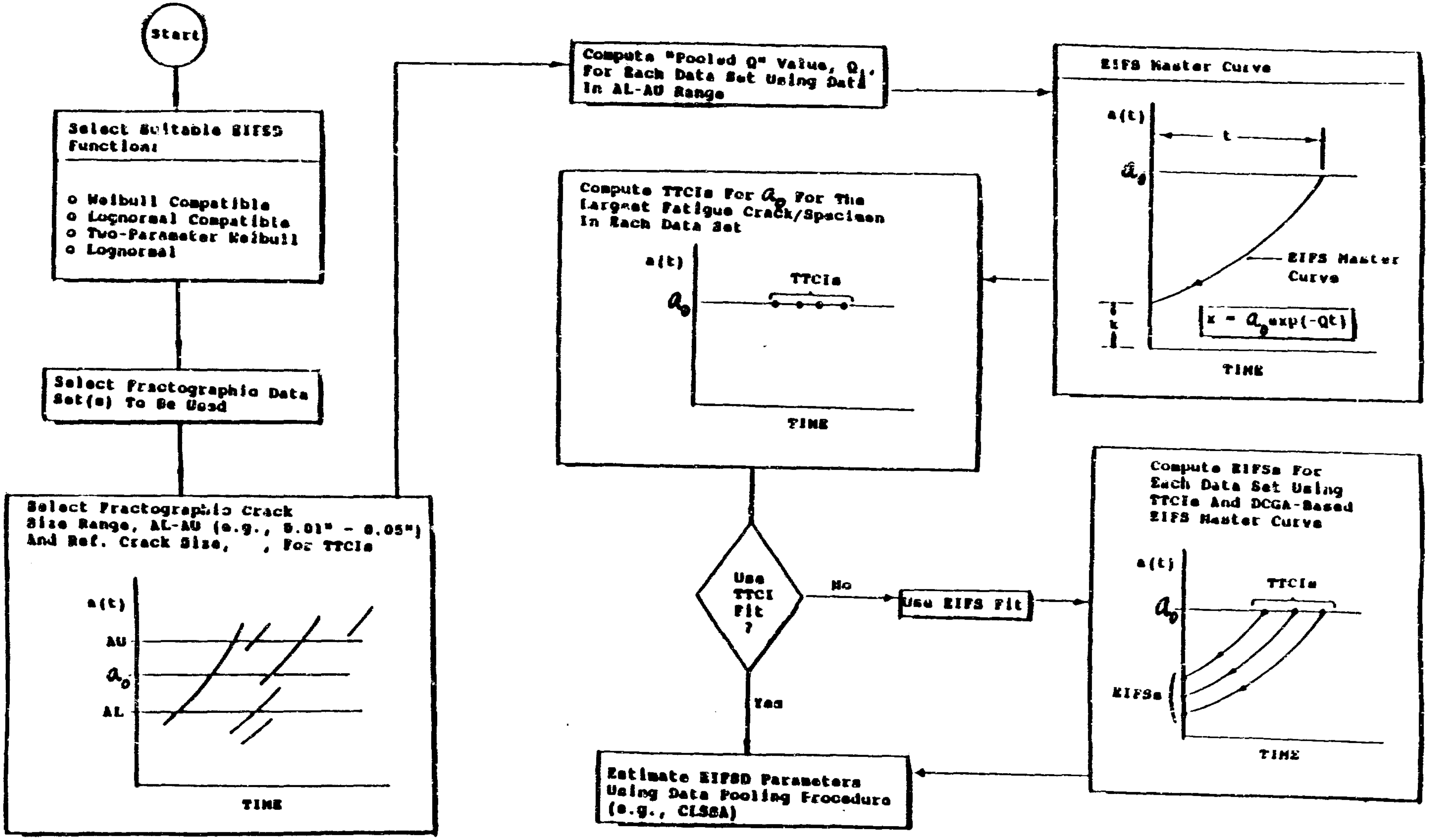

Figure 7. Initial Steps in Procedure Leading to Estimation of EIFSD Parameters.

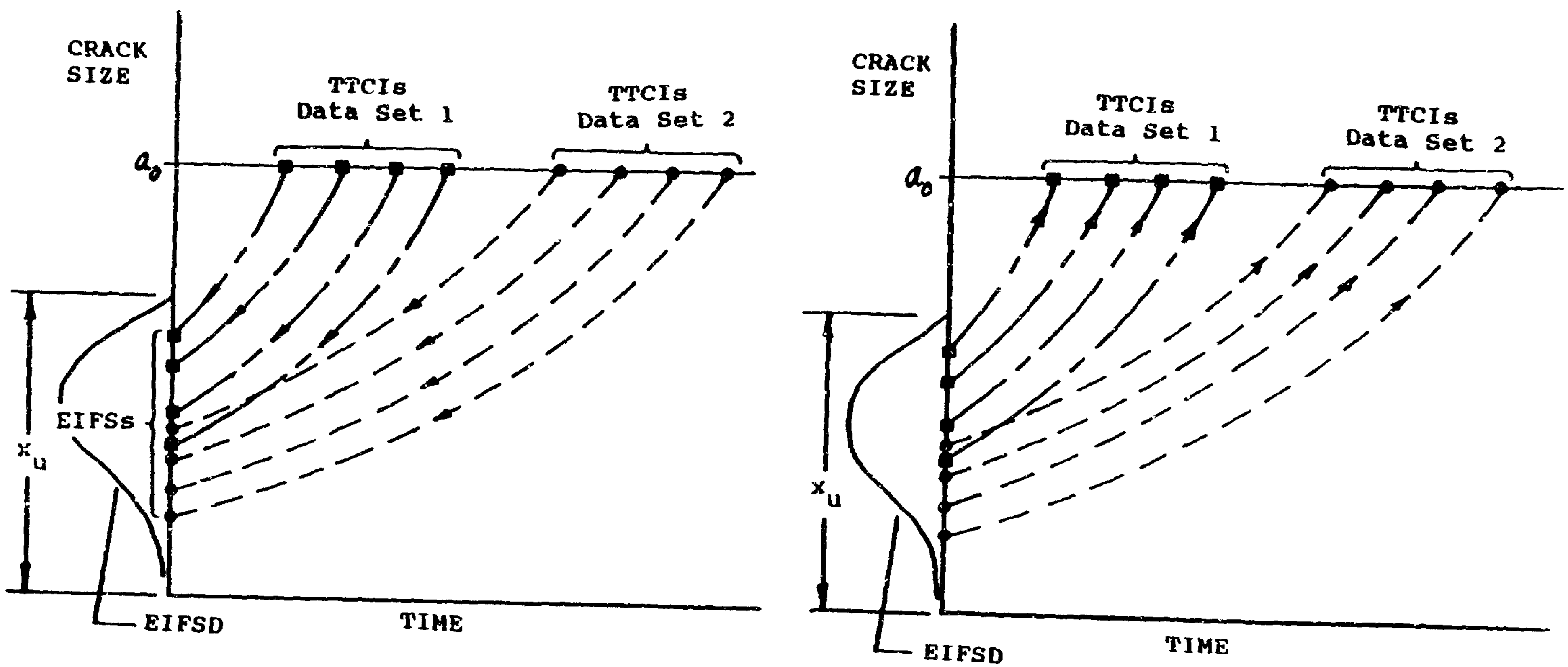

(a) Estimate EIFSD Parameters Using EIFSs

(b) Estimate EIFSD Parameters Using TTCIs

Figure 8. Two Different Philosophies for Estimating EIFSD Parameters Using Fractographic Data Pooling Procedures and DCGA.

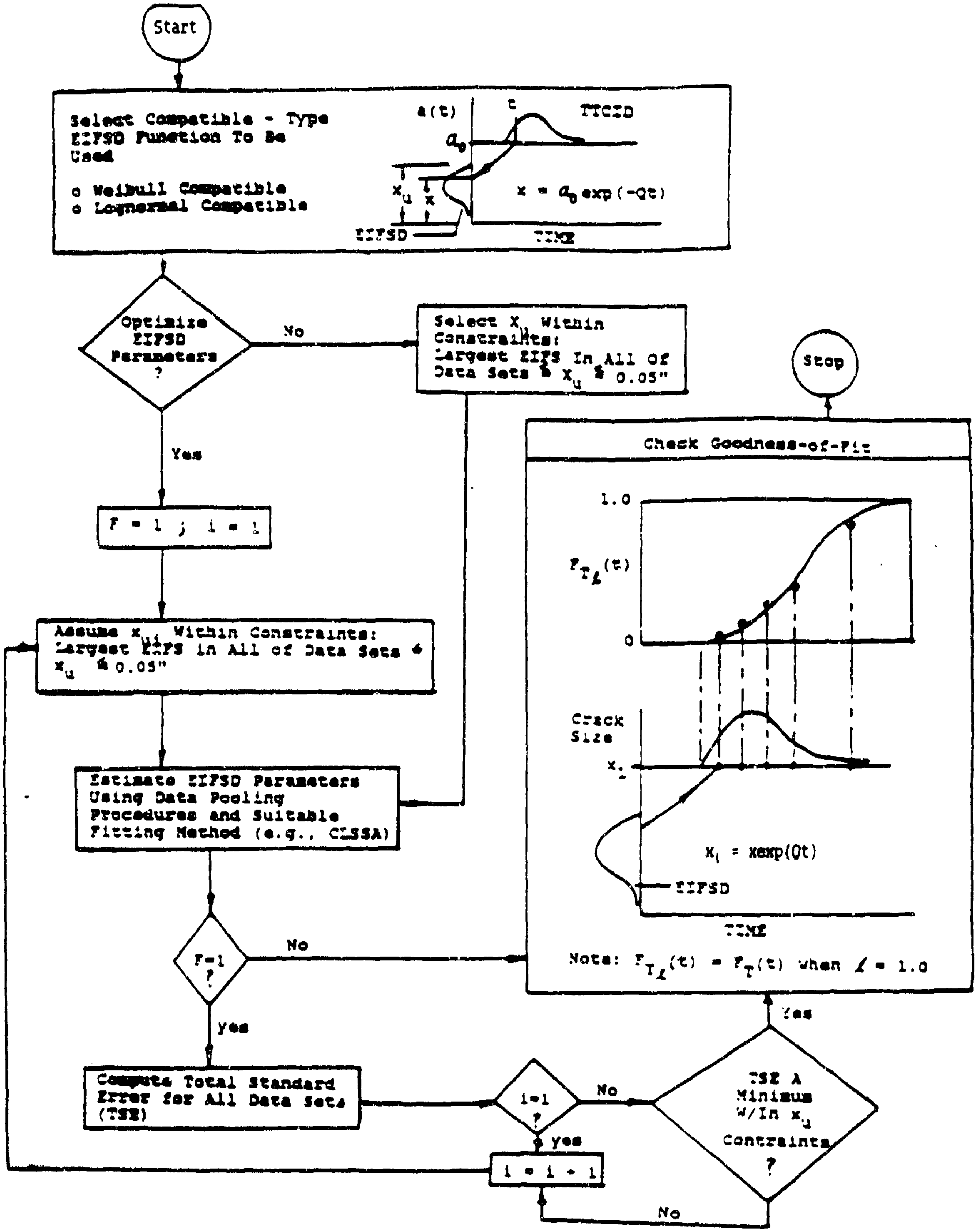

Figure 9. General Procedure for Optimizing EIFSD Parameters and Checking Goodness-of-Fit for Compatible Type EIFSD Function.

port) and type fastener/hole/fit (e.g., straight-bore or countersunk). Screen and censor the data for any unusual abnormalities.

3. Select fractographic crack size range, AL-AU. Fractographic data in this range will be used to determine the crack size-time relationship and deterministic crack growth rate parameters. Also select a reference crack size, a_0, for the TTCIs for each fractographic data set, see Fig. 7. Use the largest fatigue crack per speciman in each data set.

4. Estimate the crack growth rate parameters Q in the model suggested by Yang and Manning for the small crack size region [6,7]

$$da(t)/dt = Qa(t) \tag{2}$$

in which $da(t)/dt$ = crack growth rate, $a(t)$ = crack size at time, t, and Q is an empirical crack growth rate parameter.

This model, Eq. 2, has been found to be very reasonable for durability analysis [8-11,14,16]. Integration of Eq. 2 leads to a relation between a(0) or EIFS and the crack size a(t) at any service time t, i.e.,

$$EIFS = a(0) = a(t)\exp(-Qt) \tag{3}$$

If a_0 is the reference crack size, say 0.03", and T is the time to initiate the crack size a_0, i.e., $a(T) = a_0$, then the deterministic relation between EIFS = a(0) and TTCI = T, is referred to as the "EIFS master curve." Such an EIFS master curve is obtained from Eq. 3 by setting t = T and $a(T) = a_0$, as follows

$$EIFS = a_0\exp(-QT) \tag{4}$$

Hence, for every TTCI = T in a given fractographic data set, there is a corresponding EIFS value and vice versa as shown in Eq. 4 (also, see Volume I [1]).

Q in Eqs. 2-3 is an empirical crack growth rate parameter, which can be used from a particular fractographic data set. This parameter is used to define EIFSs for a given fractographic data set using Eq. 4.

Suppose the ith fractographic data set contains a total of m fatigue cracks, where each fatigue crack is denoted by $j = 1, 2, \ldots, m$. The jth fatigue crack has a total number of N pairs of fractographic data in the AL-AU range, denoted by $[a_j(t_k), t_k]$, i.e., $a_j(t_k)$ = kth crack size for the jth fatigue crack at service time t_k in the AL-AU range, where $k = 1, 2, \ldots, N$.

The crack growth rate parameter for a single fatigue crack, say the jth fatigue crack, denoted by Q_j, is estimated from fractographic data of the jth fatigue crack in the AL-AU range using Eq. 3 and the least squares fit procedure as follows

$$Q_j = \frac{N\sum_{k=1}^{N} X_k Y_k - \sum_{k=1}^{N} X_k \sum_{k=1}^{N} Y_k}{N\sum_{k=1}^{N} X_k^2 - \left(\sum_{k=1}^{N} X_k\right)^2} \tag{5}$$

in which $X_k = t_k$ and $Y_k = \ln a_j(t_k)$.

Q_j given in Eqs. 3-5 is the crack growth rate parameter for the jth crack and it is obtained using the fractographic data of the jth crack. Let Q_i be the crack growth rate parameter for the ith data set consisting of m cracks. Then, Q_i is referr-ed to as the "pooled Q" value for the ith data set. It is obtained using all the fractographic data in the ith data set, i.e., all fractographic data for m cracks in the AL-AU range, and the least squares fit procedure. Q_i or the "pooled Q" value for the ith data set can be obtained as follows

$$Q_i = \exp\left[\frac{1}{m}\sum_{j=1}^{m} \ln Q_j\right] \tag{6}$$

where, Q_j = crack growth rate parameter Q for the jth fatigue crack and m = total number of fatigue cracks in the ith data set (i.e., j = 1, 2, ..., m).

5. Determine TTCI values for each data set(s) for the chosen reference crack size, a_0, by either interpolation or extrapolation of fractographic results. Refer to Fig. 7.

6. Use (i) the data pooling procedure described in Volume I [1], (ii) TTCI results from Step 5, and (iii) the combined least square sums approach (CLSSA), to estimate and optimize the Weibull compatible EIFSD parameters (i.e., α and ϕ for a given x_u) given in Eq. 1. Other EIFSD functions could also be used if appropriate (e.g., lognormal compatible, lognormal, two-parameter Weibull, etc.). The general procedure for optimizing the EIFSD parameters is described in Fig. 9 and Volume I [1].

> NOTE: The EIFSD parameters can be estimated using either a "TTCI fit" or a "EIFS fit." Either fitting method will yield the same EIFSD parameter values. The formulation for the "EIFS fit" is given elsewhere [1,21]. In the durability analysis design handbook [21] the "EIFS fit" is recommended because the EIFS statistics (mean and standard deviation) provide a basis for comparing and cataloging initial fatigue quality results from various sources; whereas, TTCI statistics (mean and standard deviation) do not

provide such a basis. The "TTCI fit" formulation, reflected in the following, is considered herein as a part of the overall evaluation of methods for estimating EIFSD parameter values.

The Weibull compatible EIFSD parameters α and ϕ in Eq. 1 can be determined for a given x_u as follows. Let M = total number of fractographic data sets to be used for estimating the EIFSD parameters. For each fractographic data set there is a corresponding "TTCI" or "EIFS" data set. Therefore, M also applies to either TTCI or EIFS data sets. The ith TTCI data set (i.e., i = 1, 2, ..., M) contains a number of N_i TTCIs based on the largest fatigue crack per specimen, where each TTCI is denoted by j = 1, 2, ..., N_i. Further, let Q_i = pooled crack growth rate parameter for the ith fractographic data set based on Eq. 6 and ℓ_i = scaling factor for the ith fractographic data set.

Then, α and ϕ for a given x_u can be determined as follows:

$$\alpha = \frac{n\Sigma XY - (\Sigma X)(\Sigma Y)}{n\Sigma X^2 - (\Sigma X)^2} \tag{7}$$

$$\phi = \exp\left\{\frac{\alpha n \Sigma X - \Sigma Y}{\alpha n}\right\} \tag{8}$$

The terms in Eqs. 7 and 8 are defined as follows:

$$X_{ij} = \ln\left[\ln(x_u/a_0) + Q_i t_{ij}\right] \tag{9}$$

$$Y_{ij} = \ln\left\{-(1/\ell_i)\ln\left[1 - \frac{j}{(N_i+1)}\right]\right\} \tag{10}$$

$$
\begin{aligned}
\Sigma X &= \sum_{i=1}^{M} \sum_{j=1}^{N_i} X_{ij} \\
\Sigma X^2 &= \sum_{i=1}^{M} \sum_{j=1}^{N_i} X_{ij} \\
\Sigma Y &= \sum_{i=1}^{M} \sum_{j=1}^{N_i} Y_{ij} \\
\Sigma XY &= \sum_{i=1}^{M} \sum_{j=1}^{N_i} X_{ij} Y_{ij} \\
n &= \sum_{i=1}^{M} N_i
\end{aligned}
\tag{11}
$$

All notations in Eqs. 9 - 11 have been previously defined except the following. In Eq. 9, t_{ij} = jth TTCI value for the ith TTCI data set (i.e., j = 1, 2, ..., N_i). In Eq. 10, the TTCIs for the ith data set are ranked in ascending order, i.e., j = 1, 2, ..., N_i. Similar expressions to those in Eqs. 9 and 10 have been developed for an "EIFS fit" [1, 21].

The expression for the total standard error is given in Eq. 12 [1],

$$
TSE = \sqrt{\frac{\sum_{i=1}^{M} \sum_{j=1}^{N_i} \left\{ \frac{j}{(N_i + 1)} - 1 + \exp\left\{ - l_i \left[\frac{\ln(x_u / a_{ij}) + Q_i t_{ij}}{\phi} \right]^{\alpha} \right\} \right\}^2}{\sum_{i=1}^{M} N_i}}
\tag{12}
$$

where all terms have been previously defined in Eqs. 6-11. Equation 12 is used in the optimization of EIFSD parameters.

For a given x_u there is a corresponding α, ϕ and TSE. Within the user's selected limits for minimum and maximum x_u values, the TSE can be minimized with respect to x_u using a trial and error procedure.

7. Verify the goodness-of-fit of the resulting EIFSD us-

ing the fractographic data sets that have been used to estimate the EIFSD parameters. For example, correlate theoretical predictions for (i) the probability of crack exceedance, $p(i, \tau)$, at a given service time, τ, and (ii) the cumulative distribution of service time to reach any crack size x_1, $F_{T(x_1)}(\tau)$ with actual fractographic results for those data sets that have been used to define the IFQ, see Fig. 10. Other fractographic data sets (e.g., for different stress levels, load spectra, % load bolt load transfer, etc.) that have not been used to estimate the EIFSD parameters can also be used to justify the candidate EIFSD for durability analysis.

Software is available for an IBM or IBM-compatible PC for implementing the procedures described above, including a goodness-of-fit plotting capability. The software user's guide is given in Volume V [5].

3.3 DEMONSTRATION FOR DOG-BONE SPECIMENS

The general procedure described in Section 3.2 is used to demonstrate and evaluate the IFQ methods for countersunk and straightbore fastener holes in 7475-T7351 aluminum (clearance-fit fasteners without cold working) in the following.

3.3.1 Countersunk Fastener Hole Specimens

Three fractographic data sets from the "Durability Method Development" program [4] will be used to determine the IFQ of countersunk fastener holes. The three data sets, referred to as "AFXLR4", "AFXMR4", and "AFXHR4", are described in Table 6. Specimen geometry and design details for these data sets are shown in Fig 6. The fractographic results, i.e., a(t) versus t data, for each fatigue crack in each data set were screened for abnormal behavior (see Figs. B.23-B.28). Only one fatigue crack, i.e. crack number 8, was deleted from the AFXLR4 data set, see Fig. 11. Fractographic data screening is an important

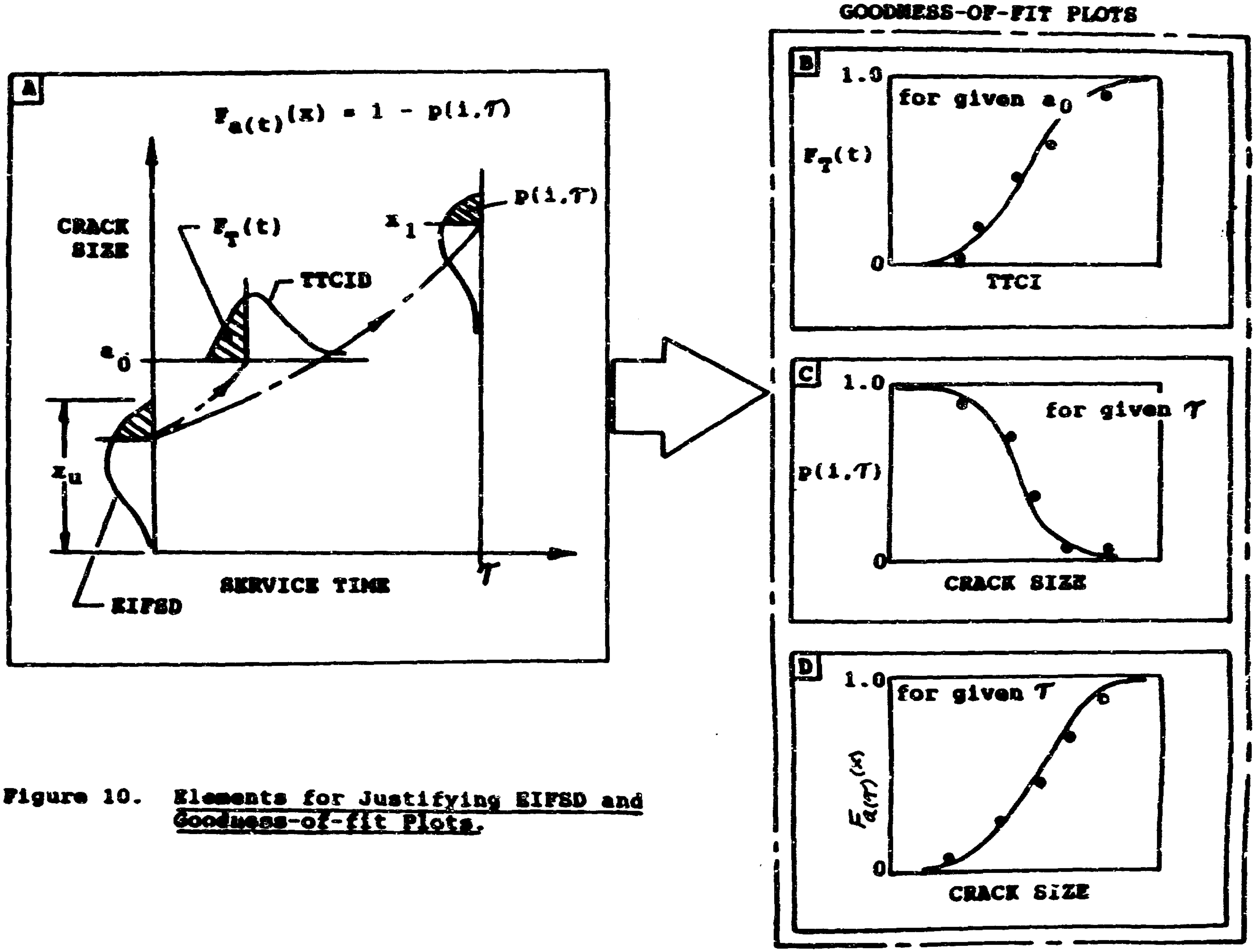

Figure 10. Elements for Justifying EIFSD and Goodness-of-fit Plots.

Table 6. Description of Fractographic Data Sets Used to Determine the IFQ for Countersunk Fastener Holes

Data Set	No. of Specimens Used (4)	(3) KSI	LT %	W (In)	t (In)	Fastener (2)	Load Spectrum	Ref.
AFXLR4	10/11 (5)	32	15	1.5	.1875	MS 90353-08 (1/4D)	F-16 400 Hr	4
AFXMR4	9/9	34	↓	↓	↓	↓	↓	
AFXHR4	10/10	38						

NOTES:
(1) Material: 7475-T7351 Aluminum
(2) Blind pull-through rivet (countersunk head)
(3) Gross section stress
(4) XX/YY = No. of specimens used/total no. of specimen in data set
(5) Deleted crack No. 8 from data set (ref. Fig. 11)

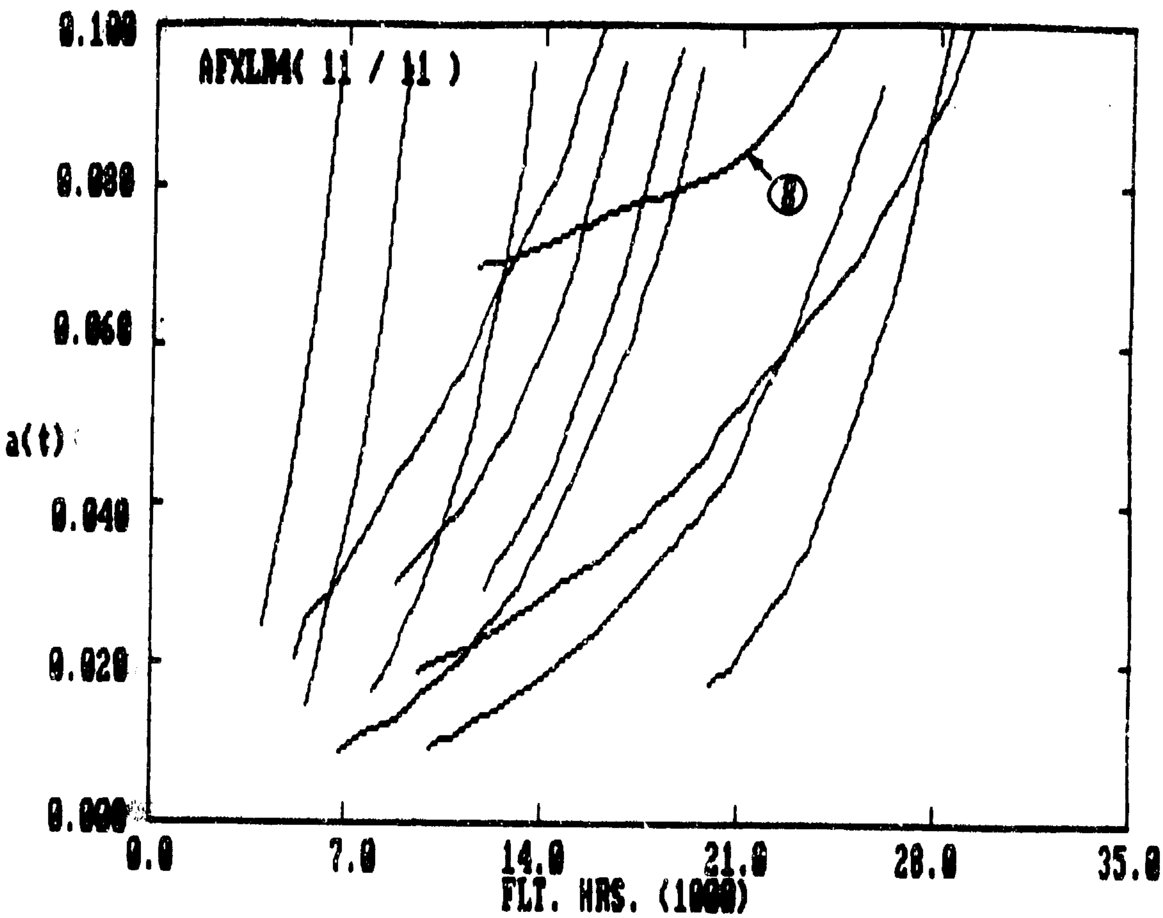

Figure 11. Fractographic Data Survey for AFXLR4 Data Set in the AL-AU = 0-.1" Crack Size Range.

consideration in determining IFQ.

The IFQ or EIFSD will be determined for each of the three data sets shown in Table 6 separately. Then, these three data sets will be pooled together as a "pooled data set" to increase the sample size. The IFQ will be determined for the pooled data set using the data pooling procedures described in Volume I [1]. Elements of this procedure for determining an EIFSD for the pooled data set are conceptually described in Fig. 12. Once the EIFSD has been determined, the candidate EIFSD must be justified for desired durability analysis applications. An EIFSD, based on one or more fractographic data sets, should be justified by showing that the given EIFSD can be grown forward to make reasonable predictions for one or more of the following: (1) cumulative distribution of TTCI, $F_T(t)$, at a given reference crack size x_1, (2) probability of crack exceedance, $p(i,\tau)$, at any given service time, τ, and (3) cumulative distribution of crack size, $F_{a(t)}(x)$, at a given service time, t. Elements for justifying an EIFSD for durability analysis are described in Fig. 10.

The IFQ analysis that follows is divided into three parts: (1) estimate the deterministic crack growth rate parameter, pooled Q (2) estimate the EIFSD parameters (i.e., α and ϕ for given x_u) for the Weibull compatible distribution function, and (3) justify the EIFSD for desired durability analyses. Details are provided in the following subsections.

3.3.1.1 Estimation of Crack Growth Rate Parameters. Pooled Q values for AFXLR4, AFXMR4, and AFXHR4 data sets obtained using Eq. 6, are summarized in Table 7. Q values were determined using the software documented in Volume V [5]. Example problems and computer output for Q are given in Volume V. The Q values shown in Table 7 will be used to estimate the EIFSD parameters.

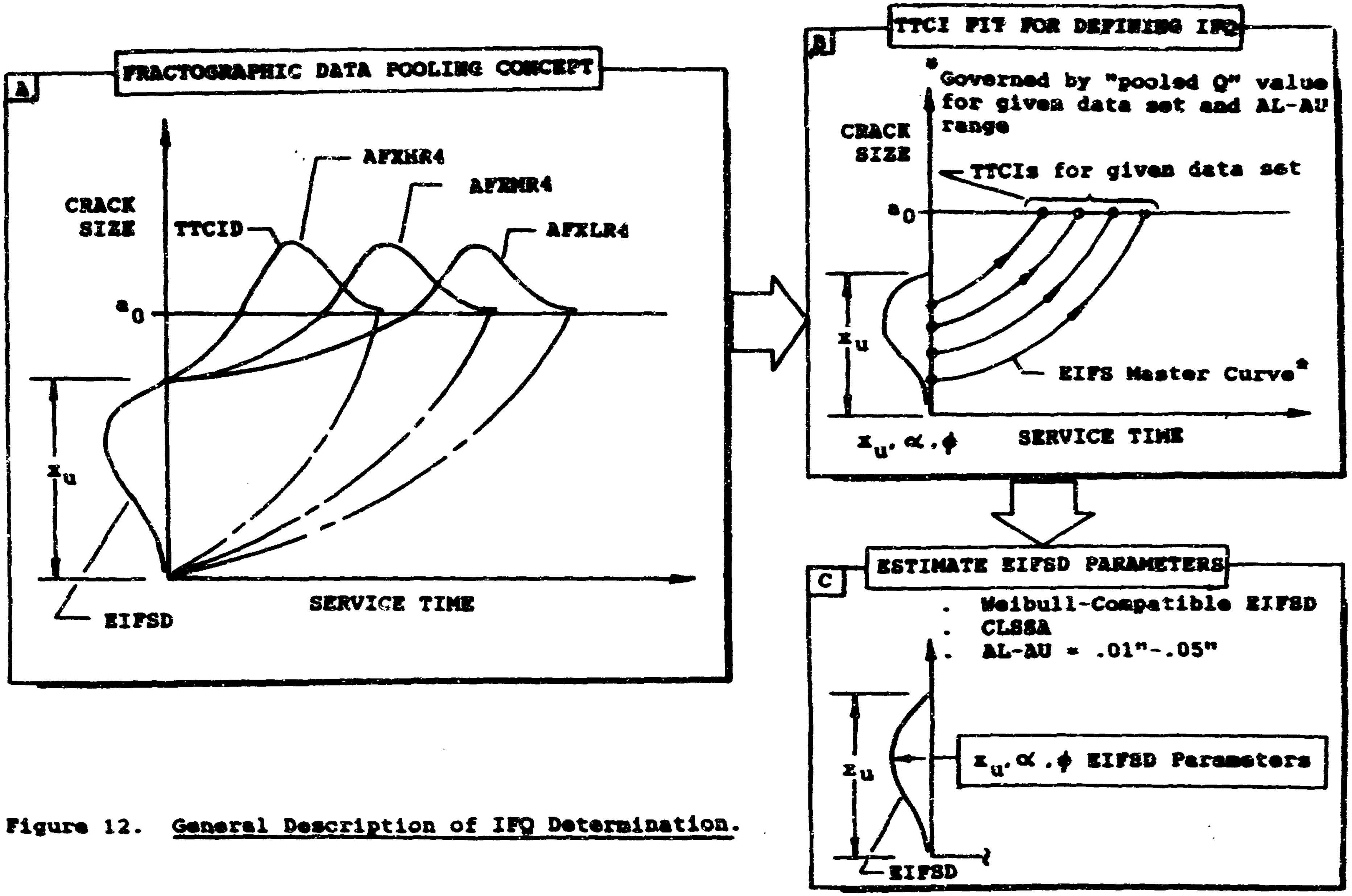

Figure 12. General Description of IFQ Determination.

Table 7. Summary of Pooled Q Values for Double-Reversed Dog-Bone Specimens (15% LT) with Countersunk Fastener Holes.

Data Set	% LT	No. Cracks	(KSI)	W (IN.)	t (IN.)	AL-AU	$Q \times 10^4$ (1/HR)	Load Spectrum
AFXLR4	15	10	32	1.5	.1875	.01"-.05"	2.101	F-16 400 HR
AFXMR4	↓	9	34	↓	↓	↓	2.514	↓
AFXHR4		10	38				6.062	

3.3.1.2 Estimation of EIFSD Parameters. The EIFSD parameters (i.e., α and ϕ) for the Weibull compatible distribution, Eq. 1, for a given x_u will be estimated for individual fractographic data sets and for the pooled data sets. Essential features, conceptually described in Fig. 12, will be briefly discussed.

The cumulative distribution of TTCI, $F_T(\tau)$, can be obtained using the distribution of EIFS given by Eq. 1 and the EIFS master curve relationship given in Eq. 12. The resulting expression, given in Eq. 13, is derived in Volume I [1].

$$F_T(\tau) = 1 - \exp\left\{-\left[\frac{Y(\tau)}{\phi}\right]^{\alpha}\right\}; \; Y(\tau) \geq 0 \tag{13}$$

where

$$Y(\tau) = \ln(x_u/x_1) + Q\tau \; ; \; \tau \geq 0 \tag{14}$$

In Eq. 13, x_u = EIFS upper bound limit, x_1 = a_0 = reference crack size for TTCIs, and τ = TTCIs for given x_1.

It can easily be shown that Eqs. 13 and 14 are simply the three-parameter Weibull distribution as follows:

$$F_T(\tau) = 1 - \exp\left\{-\left[\frac{\tau - \epsilon}{\phi/Q}\right]^{\alpha}\right\} \; ; \; \tau \geq \epsilon \tag{15}$$

$$= 0 \qquad ; \; \tau < \epsilon$$

where

$$x_u = x_1 \exp(-Q\tau) \tag{16}$$

Recall that the Weibull compatible EIFS distribution given by Eq. 1 was derived from Eqs. 15 and 16, where $\phi = Q\beta$ with β being the scale parameter of TTCI.

The EIFSD parameters in Eq. 13 can be estimated for a given x_u value using either the combined least square sums approach (CLSSA), Eqs. 7-11, the method of moments (MM), or the homogeneous EIFS (HEIFS) approach [1]. Detailed procedures and equations are given in Volume I [1], and software for determining α and ϕ is documented in Volume V [5].

A statistical scaling factor ℓ which accounts for the number of fastener holes per specimen, is used to determine the EIFSD parameters. The scaling concept is developed and discussed in Volume I. For example, each specimen in the AFXLR4, AFXMR4, and AFXHR4 data sets contains 4 fastener holes per specimen (i.e., two holes per dog bone and there are two dog bones per specimen). However, fractographic data were acquired for only the largest fatigue crack in any one of 4 holes per specimen. Hence, $\ell = 4$ should be used.

EIFSD parameters for individual data sets and for pooled data sets, based on the CLSSA, are summarized in Table 8 for selected x_u values (i.e., .02", .03" and .05"). These results are based on $\ell = 4$. Similar EIFSD parameter values have been obtained using the method of moments [42]. Mean EIFS values for each of the three data sets are also shown for comparison. The mean EIFS values or each data set should first be compared before all data sets are pooled together to determine the EIFSD parameters for the pooled data sets. Ideally, the mean EIFS values or each data set used in the data pooling procedure should be of he same order of magnitude. Data sets with large differences in mean EIFS values should be carefully scrutinized before such data sets are used to estimate the EIFSD parameters.

3.3.1.3 <u>Goodness-of-Fit Plots</u>. A given EIFSD should be justified by showing that reasonable predictions for $F_T(t)$, $p(i,\tau)$, or $F_{a(t)}(x)$ can be made for (1) those data sets that were used to define the IFQ and/or (2) data sets that were not considered in the EIFSD determination. Basic concepts of such

Table 8. Summary of IFQ Model Parameters for Countersunk Data Sets.

DATA SET	σ (ksi)	NO. OF CRACKS USED	AL - AU	POOLED $Q \times 10^4$ (1/Hr.)	x_u (In.)	α	ϕ	ℓ	MEAN EIFS (In.)	METHOD (5)
AFXLR4 (1)	32	10/11	.01"-.05"	2.101	0.03 0.03 0.05	1.960 2.309 2.450	5.708 5.020 5.918	4	.0042	CLSSA MM CLSSA
AFXMR4 (1)	34	9/9	.01"-.05"	2.514	0.03 0.05	1.960 2.545	4.355 4.646	4	.0062	CLSSA CLSSA
AFXHR4 (1)	38	10/10	.01"-.05"	6.062	0.03 0.05 0.05	1.870 2.240 2.607	6.857 7.108 6.386	4	.0034	CLSSA CLSSA MM
AFXLR4 AFXMR4 (2) AFXHR4	32 34 38	10/11 9/9 10/10	.01"-.05"	2.101 2.514 6.062	0.02 0.03 0.05	1.330 1.716 2.132	6.794 6.308 6.453	4 4 4	.0042 .0062 .0034	CLSSA

Notes: (1) Individual fractographic data set
(2) Pooled fractographic data sets
(3) Scaling factor used to define IFQ
(4) Weibull compatible EIFSD function used
(5) CLSSA = Combined Least Square Sums Approach; MM = Method of Moments; a_{0i}=0.05" (ref. crack size for TTCIs)

justification procedures are shown in Figs. 13 and 14.

Expressions for $p(i,\tau)$ and $F_{a(t)}(x)$ developed in Volume I [1], are given in Eqs. 17 and 18, respectively. The expression for $Y(\tau)$ in Eq. 17 is given in Eq. 14.

$$p(i,\tau) = 1 - exp\left\{-\left[\frac{Y(\tau)}{\phi}\right]^{\alpha}\right\}; \; Y(\tau) \geq 0 \tag{17}$$
$$= 0 \qquad ; \; Y(\tau) \leq 0$$

$$F_{a(t)}(x) = 1 - p(i,\tau) \tag{18}$$

Let $T(x_1)$ be the time to reach any specific crack size x_1 and $F_{T(x_1)}(\tau)$ be the corresponding cumulative distribution, i.e., $F_{T(x_1)}(\tau) = P[T(x_1) \leq \tau]$. The distribution function of $T(x_1)$ is the probability that the crack will reach a crack size x_1 before the service time τ. Such a probability is equal to the probability that the crack size $a(\tau)$ at service time τ will exceed x_1, which is simply tha probability of crack exceedance. Hence,

$$F_{T(x_1)}(\tau) = P[T(x_1) \leq \tau] = P[a(\tau) \geq x_1] = p(i,\tau) \tag{19}$$

Therefore, the cumulative distribution of service time to reach any crack size x_1 is obtained by computing the crack exceedance probability, $p(i,\tau)$, at different values of τ.

Various goodness-of-fit plots for $F_{T(x_1)}(t)$ and $p(i,\tau)$ are shown in Figs. 15-30 for testing different EIFSDs for the AFXLR4, AFXMR4, and AFXHR4 data sets. Plots are presented for each of the three data sets using the EIFSD for a single data set and for pooled data sets. Different goodness-of-fit plots are presented so that comparisons can be made for different sets of EIFSD parameters.

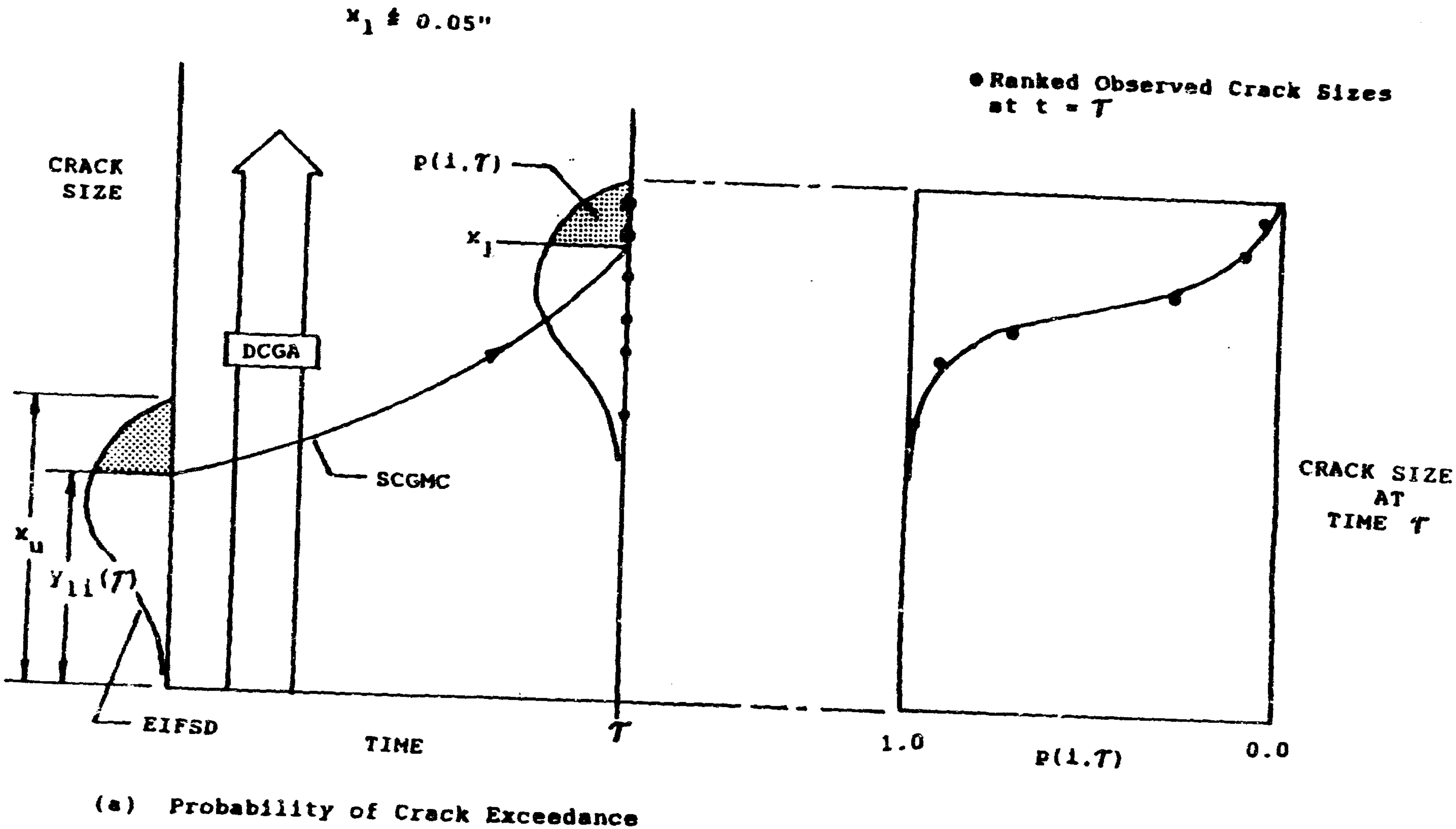

Figure 13. Probability of Crack Exceedance and Goodness-of-Fit for Small Crack Size Range.

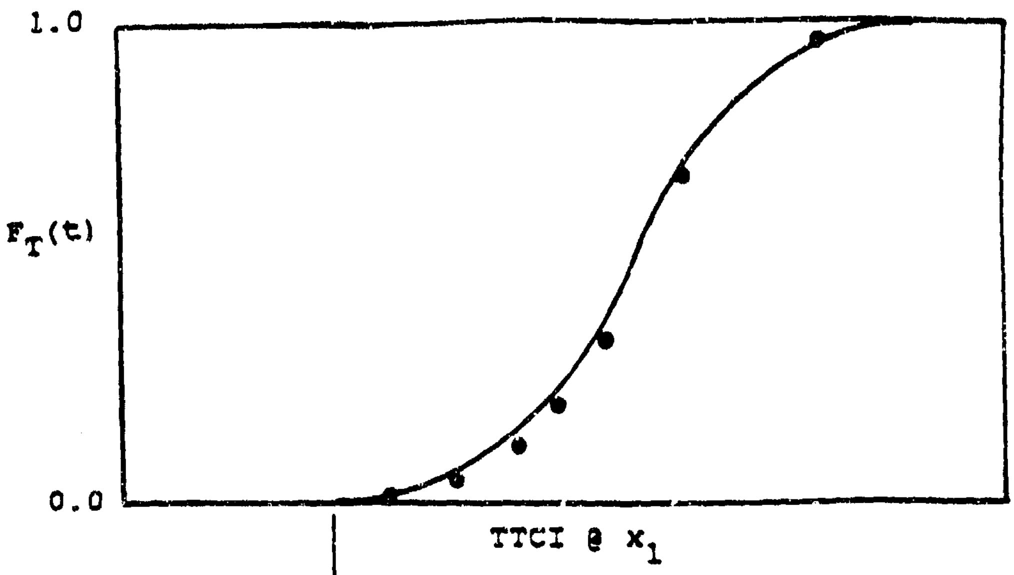

(b) $F_T(t)$ Goodness-of-Fit

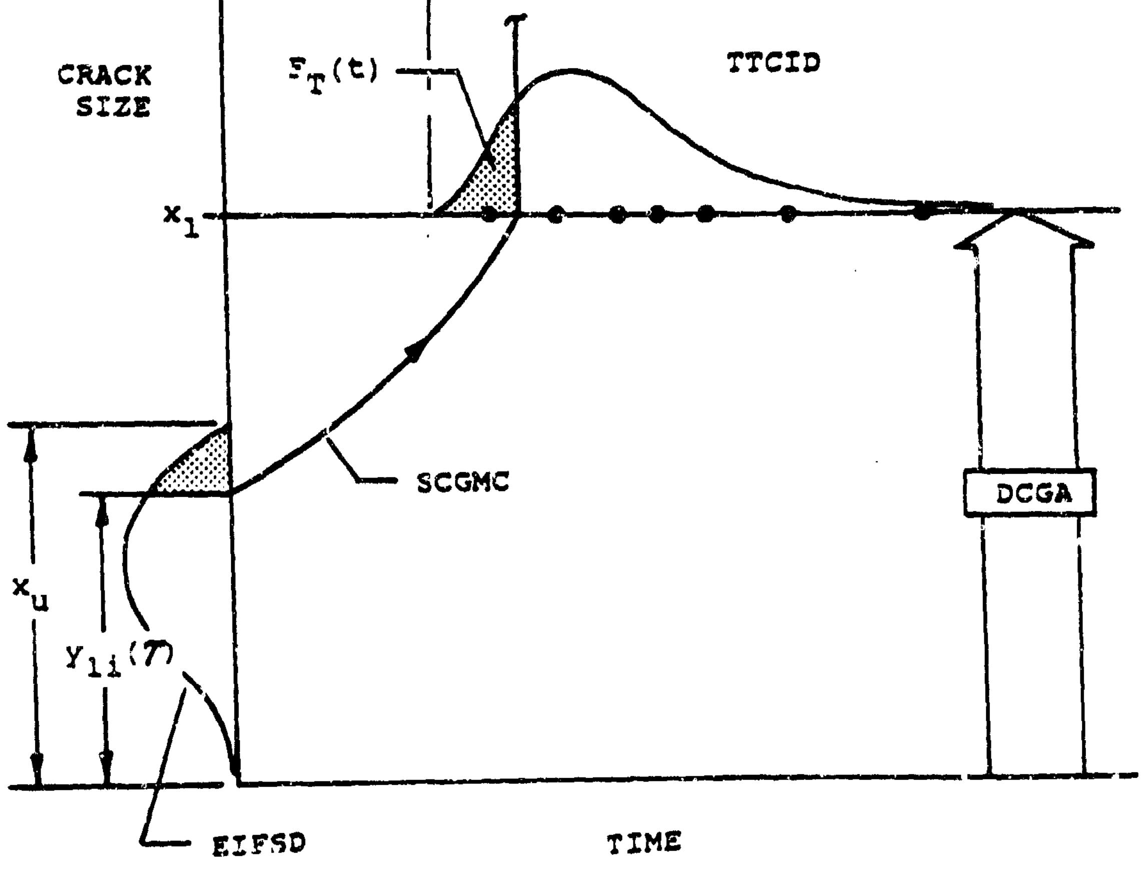

(a) Cumulative Distribution of TTCI

Figure 14. Cumulative Distribution of TTCI and Goodness-of-Fit for Small Crack Size Range.

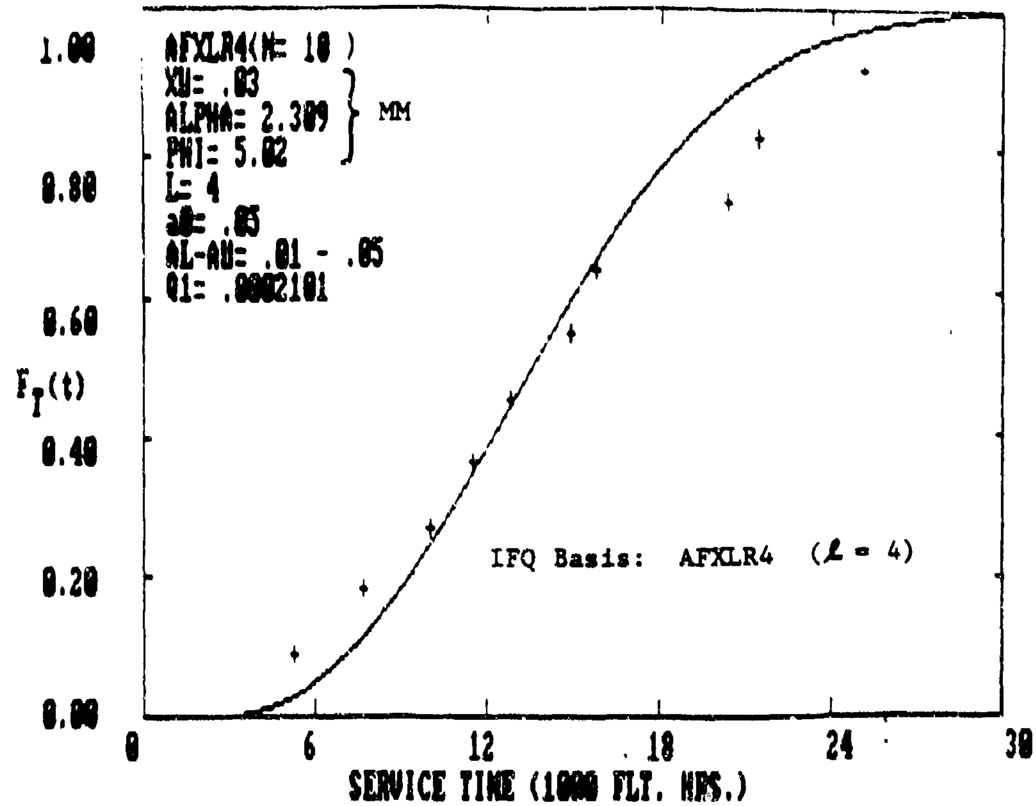

Figure 15. $F_T(t)$ Versus TTCI Plot for AFXLR4 (IFQ Basis: AFXLR4: x_u=.03", α =2.309, ϕ=5.02, ℓ =4, Method of Moments)

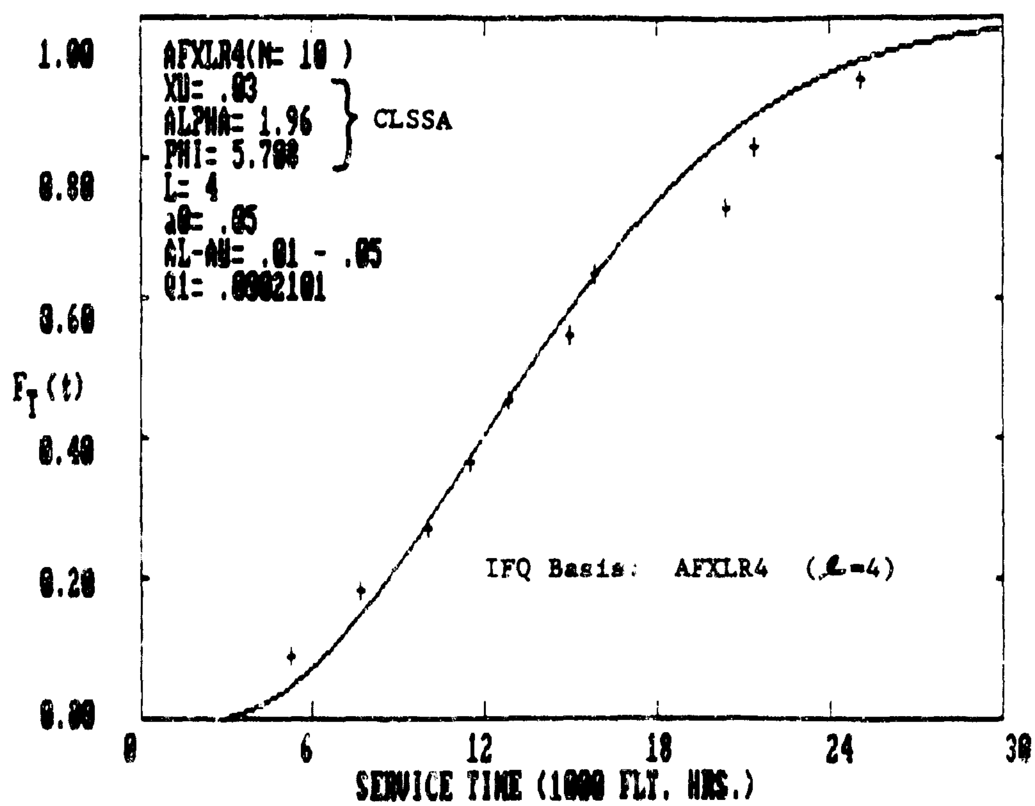

Figure 16. $F_T(t)$ Versus TTCI Plot for AFXLR4 (IFQ Basis: AFXLR4; x_u = .03", α= 1.96, ϕ= 5.708, ℓ =4; CLSSA)

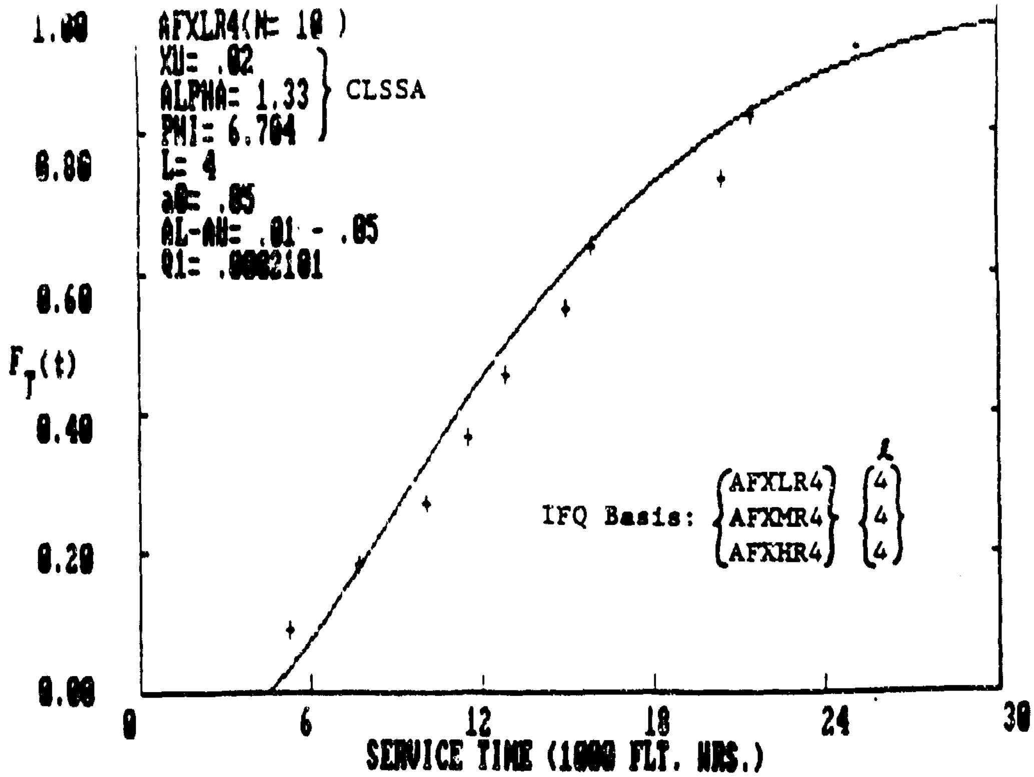

Figure 17. $F_T(t)$ Versus TTCI Plot for AFXLR4 (IFQ Basis: AFXLR4 + AFXMR4 + AFXHR4; x_u =0.02", α= 1.33, ϕ= 6.704, ℓ=4, CLSSA)

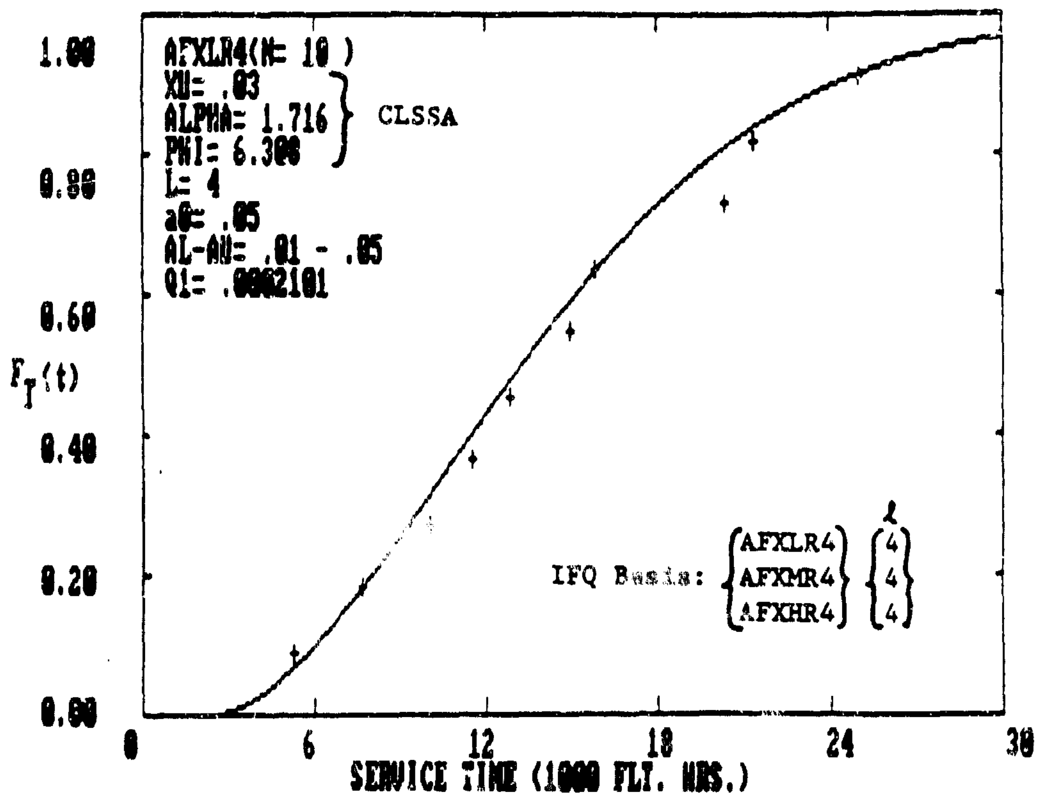

Figure 18. $F_T(t)$ Versus TTCI Plot for AFXLR4 (IFQ Basis: AFXLR4 + AFXMR4 + AFXHR4; x_u =0.03", α= 1.716, ϕ= 6.309, ℓ=4; CLSSA)

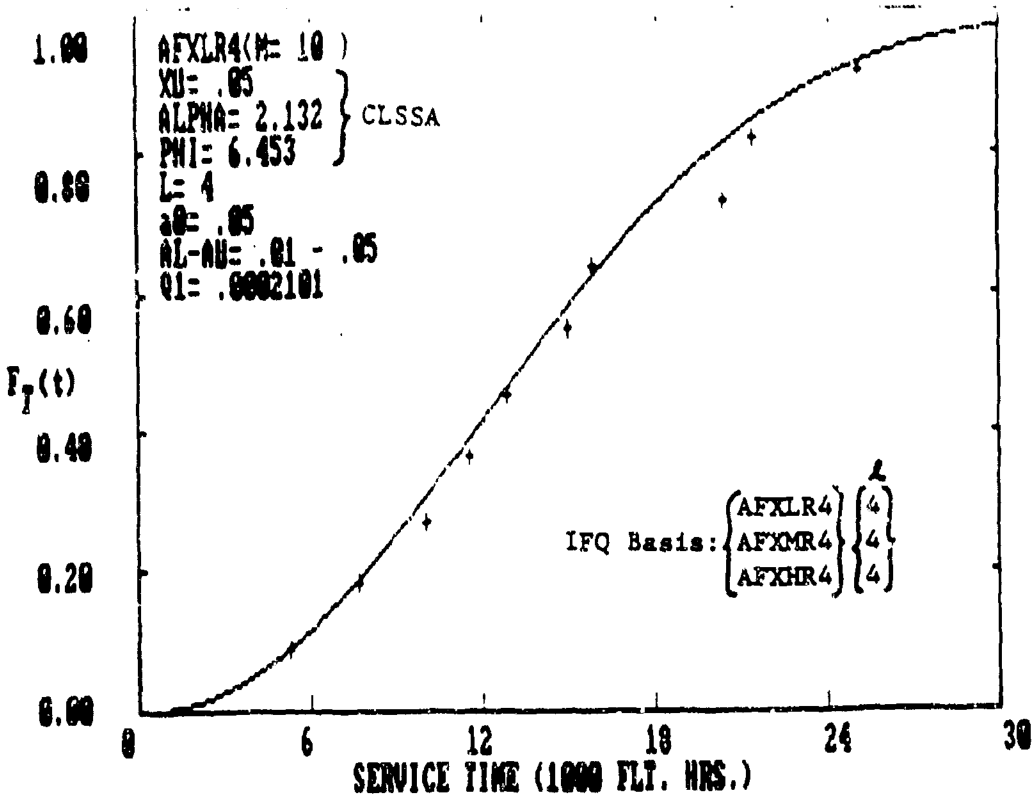

Figure 19. $F_T(t)$ Versus TTCI Plot for AFXLR4 (IFQ Basis: AFXLR4 + AFXMR4 + AFXHR4; x_u = 0.05", α = 2.132, ϕ = 6.453, $\mathcal{L}$ = 4; CLSSA)

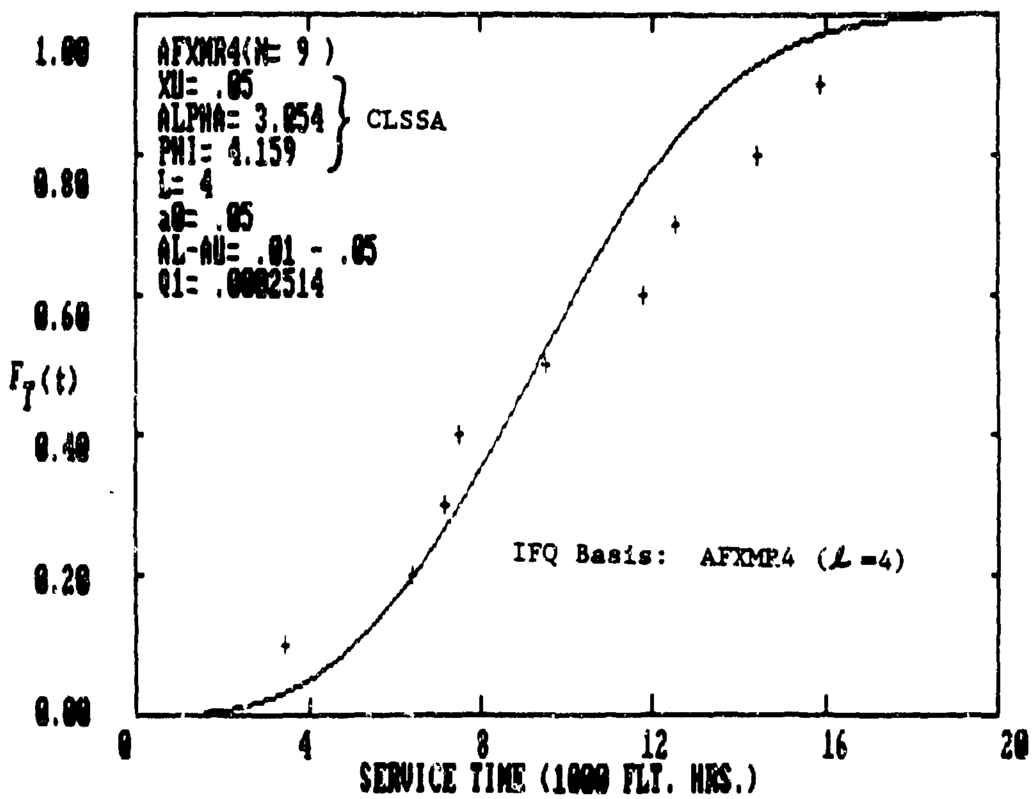

Figure 20. $F_T(t)$ Versus TTCI Plot for AFXMR4 (IFQ Basis: AFXMR4; x_u = 0.05", α = 3.054, ϕ = 4.159, $\mathcal{L}$ = 4; CLSSA)

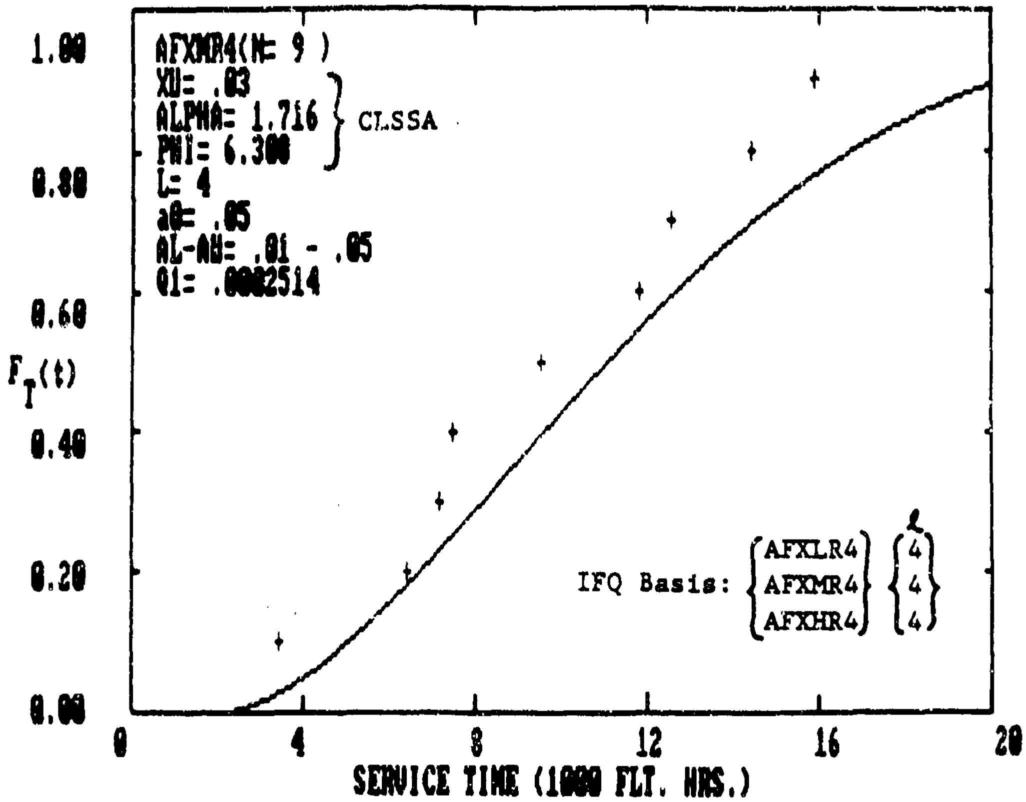

Figure 21. $F_T(t)$ Versus TTCI Plot for AFXMR4 (IFQ Basis: AFXLR4 + AFXMR4 + AFXHR4; x_u =0.03" α = 1.716, ϕ =6.308, ℓ=4; CLSSA)

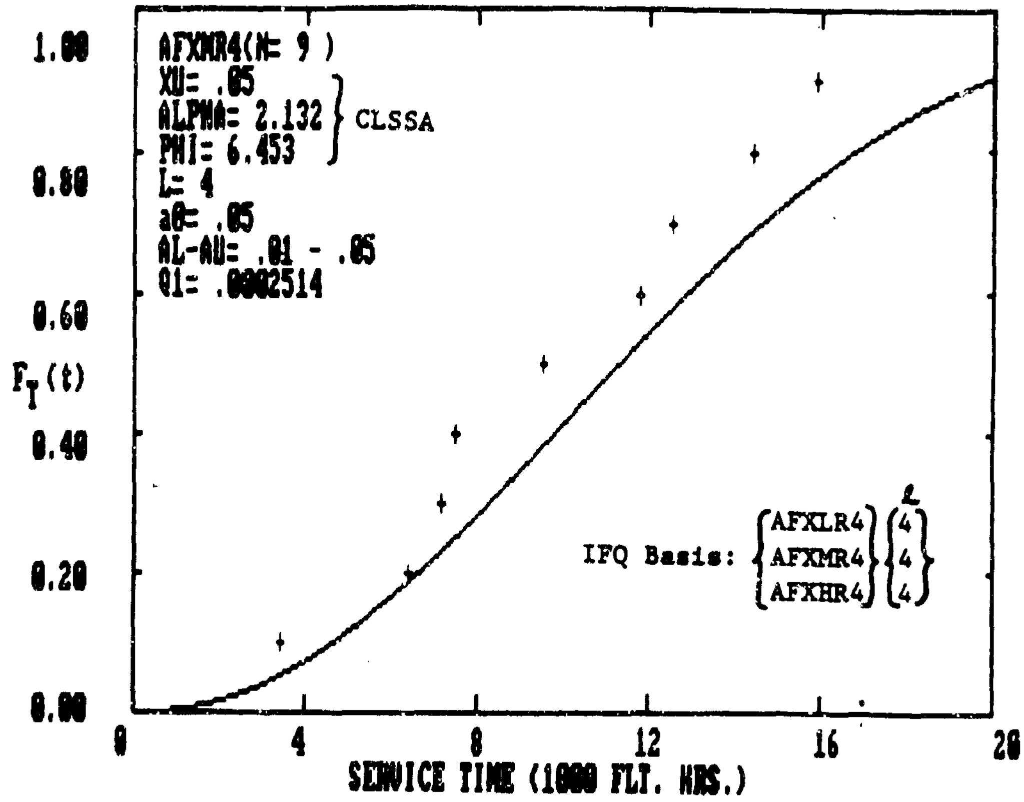

Figure 22. $F_T(t)$ Versus TTCI Plot for AFXMR4 (IFQ Basis: AFXLR4 + AFXMR4 + AFXHR4; x_u =0.05" α = 2.132, ϕ = 6.453, ℓ=4; CLSSA)

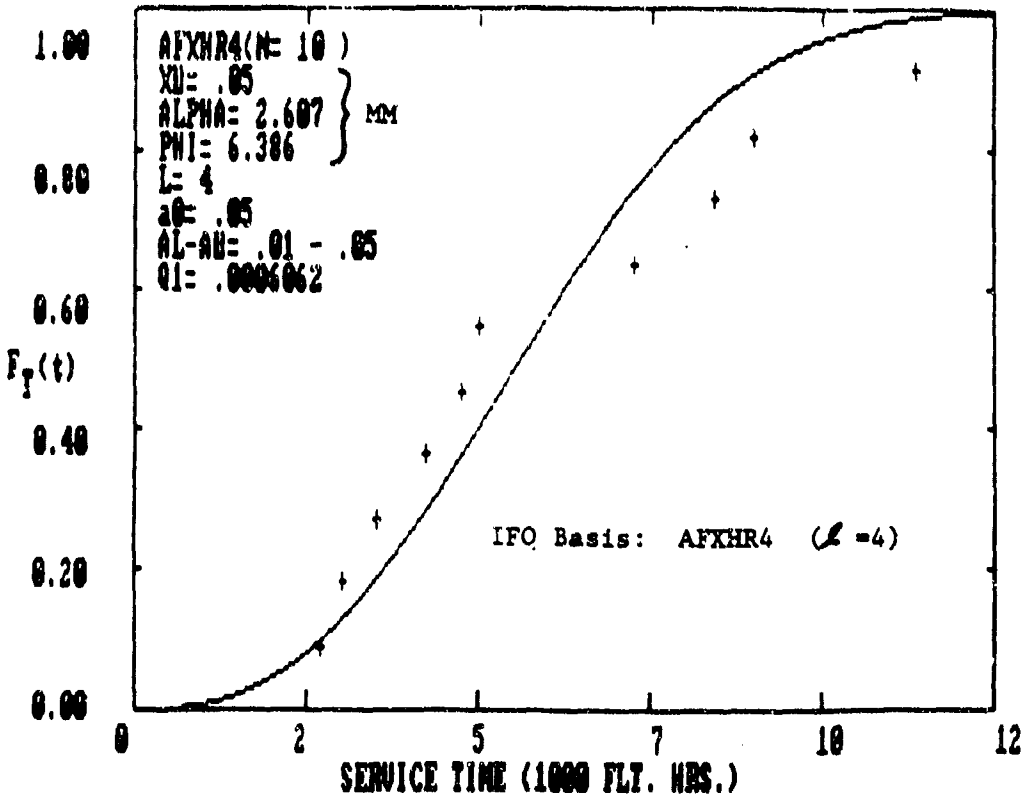

Figure 23. $F_T(t)$ Versus TTCI Plot for AFXHR4 (IFQ Basis: AFXHR4; $x_u = 0.05''$, $\alpha = 2.607$, $\phi = 6.386$, $\ell = 4$; Method of Moments)

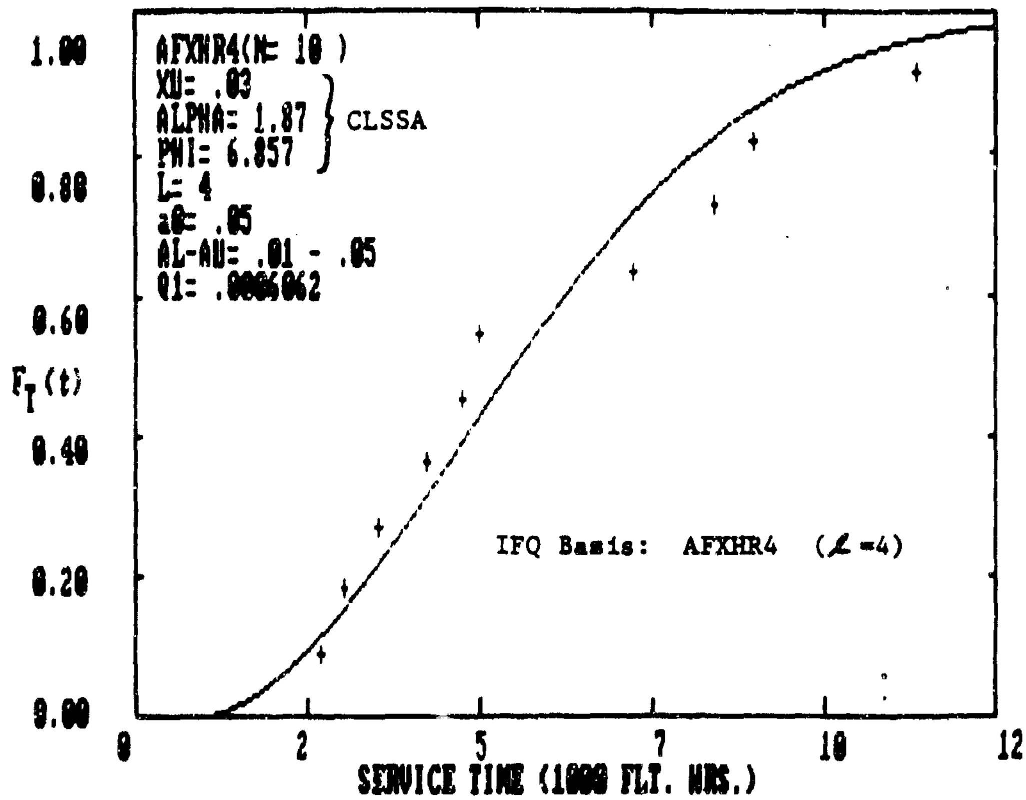

Figure 24. $F_T(t)$ Versus TTCI Plot for AFXHR4 (IFQ Basis: AFXHR4; $x_u = 0.03''$, $\alpha = 1.87$, $\phi = 6.857$, $\ell = 4$; CLSSA)

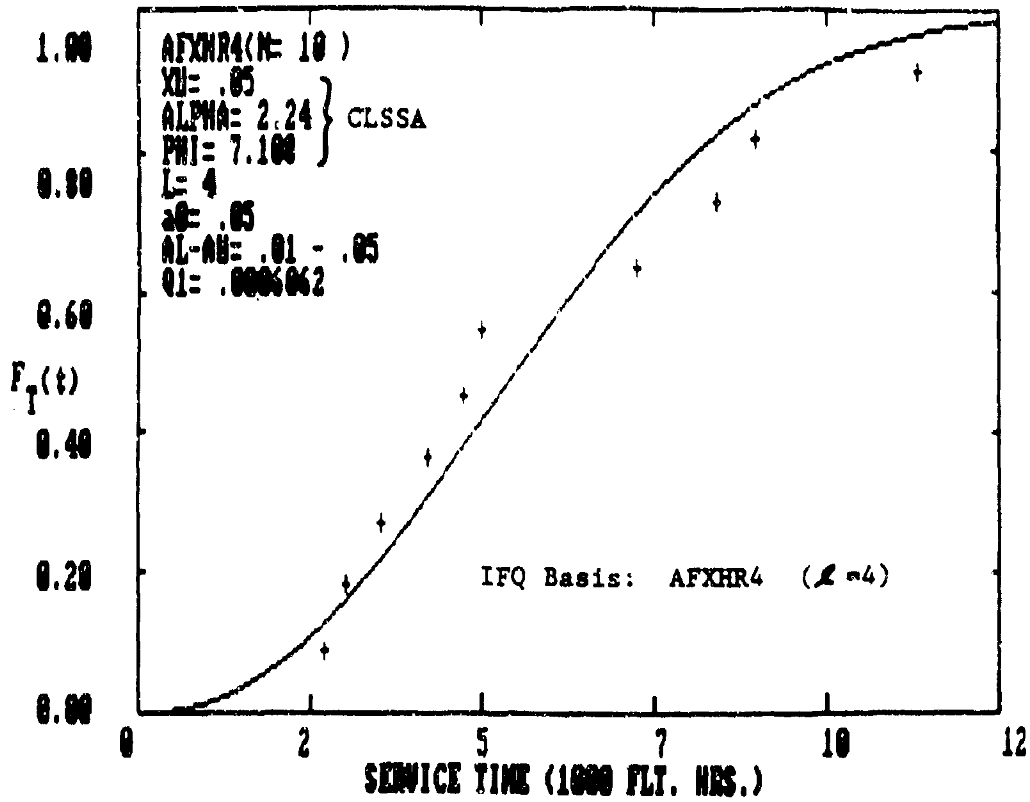

Figure 25. $F_T(t)$ Versus TTCI for AFXHR4 (IFQ Basis: AFXHR4; x_u = 0.05", α = 2.24, ϕ = 7.108, ℓ = 4; CLSSA)

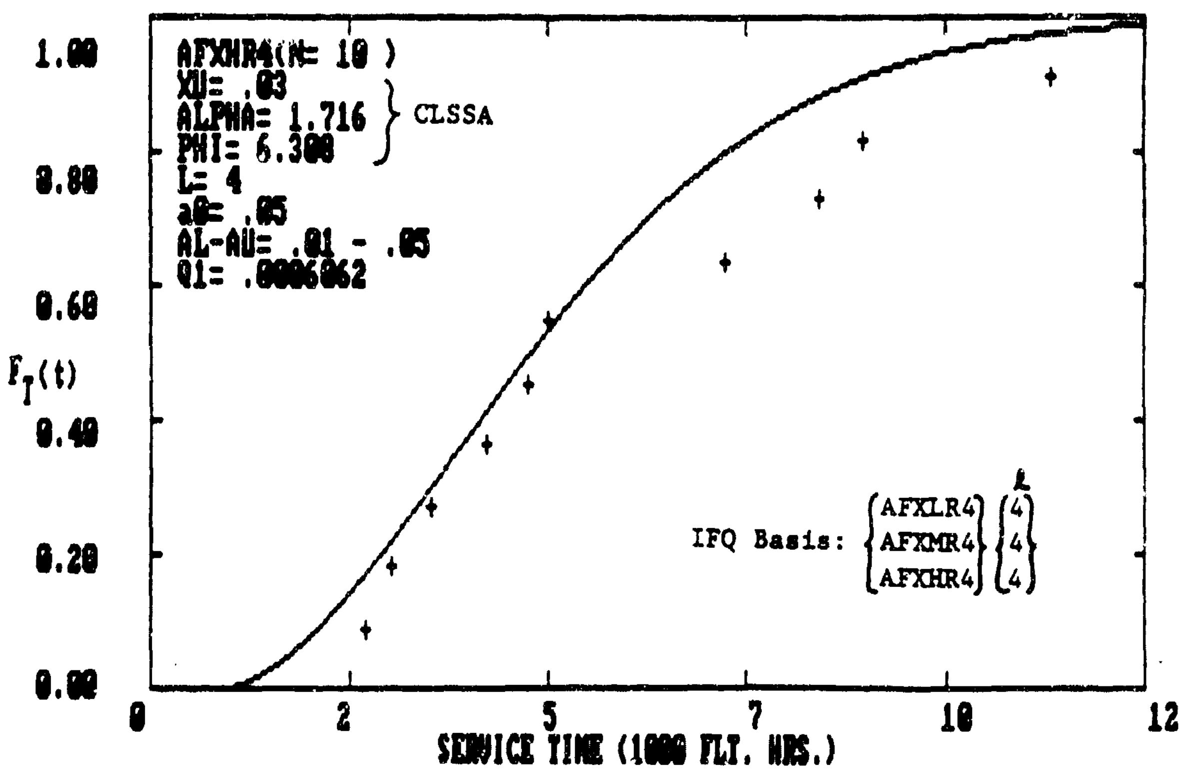

Figure 26. $F_T(t)$ Versus TTCI for AFXHR4 (IFQ Basis: AFXLR4 + AFXMR4 + AFXHR4; x_u =0.03" α = 1.716, ϕ = 6.308, ℓ =4; CLSSA)

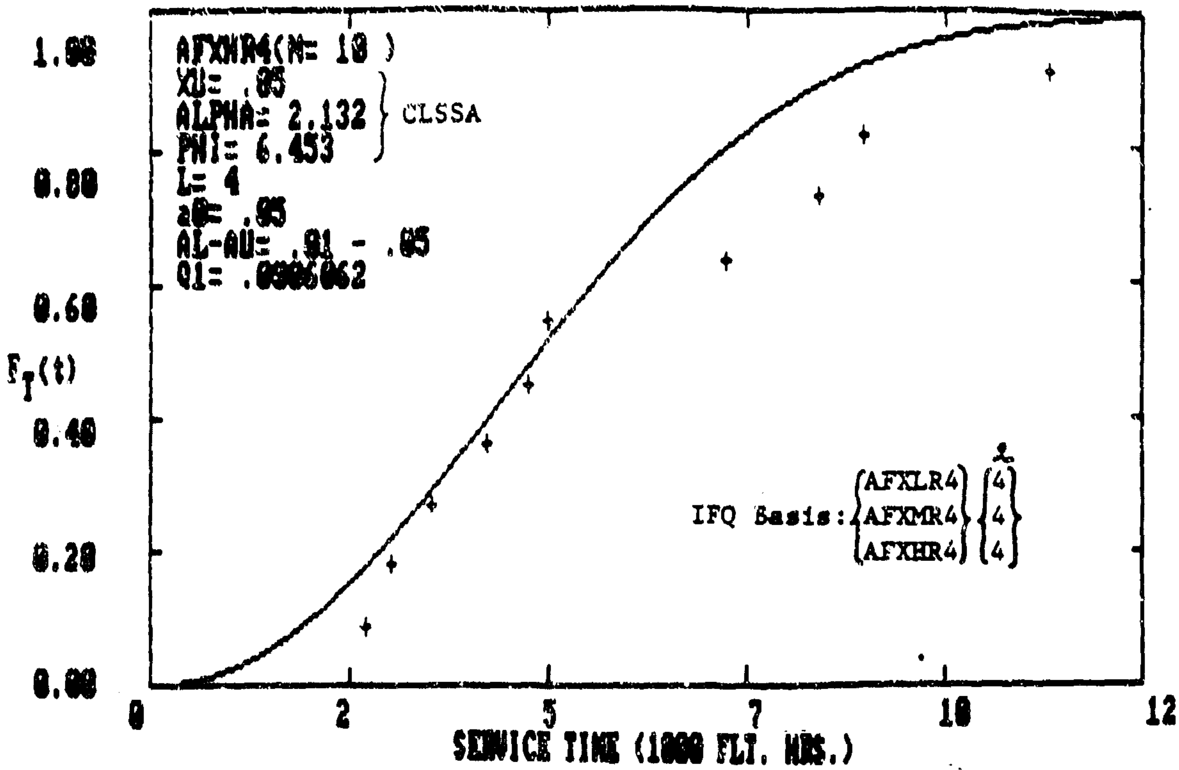

Figure 27. $F_T(t)$ Versus TTCI for AFXHR4 (IFQ Basis: AFXLR4 + AFXMR4 + AFXHR4; $x_u = 0.05"$, $\alpha = 2.132$, $\phi = 6.453$, $\ell = 4$; CLSSA)

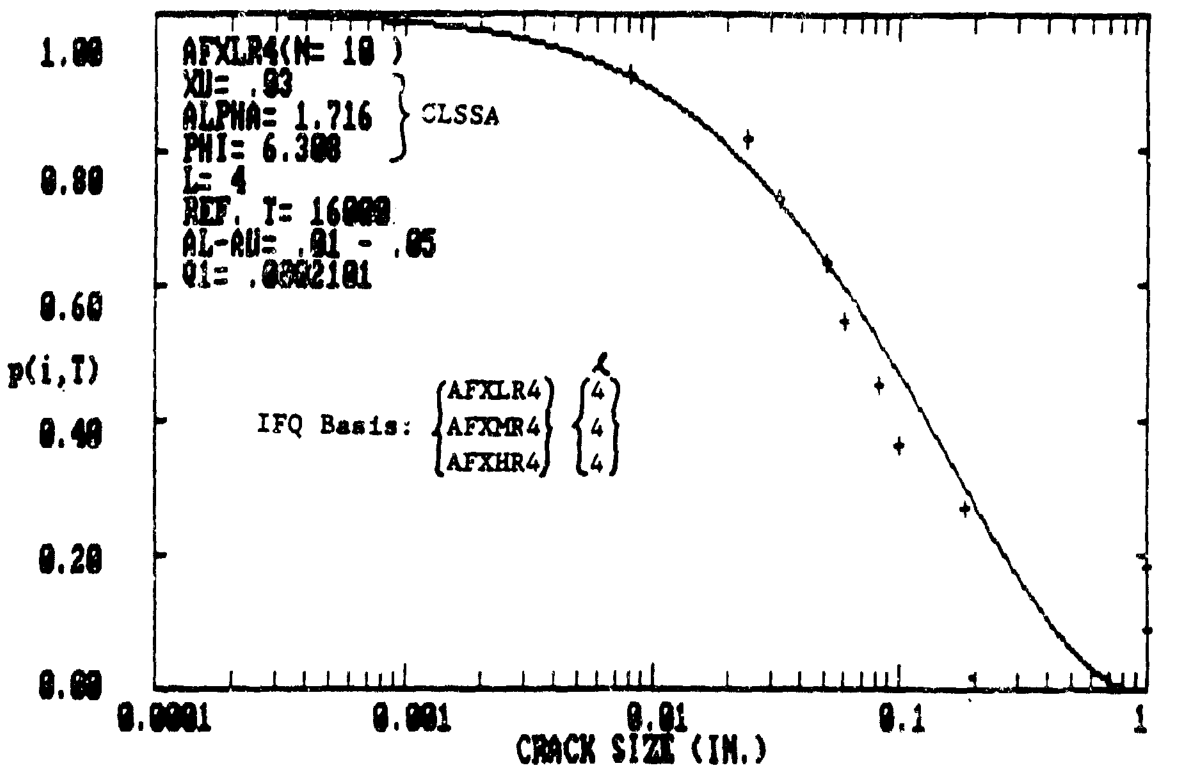

Figure 28. p(i, τ) Versus Crack Size for AFXLR4 (IFQ Basis: AFXLR4 + AFXMR4 + AFXHR4; $x_u = 0.03"$, $\alpha = 1.716$, $\phi = 6.308$, $\ell = 4$; CLSSA)

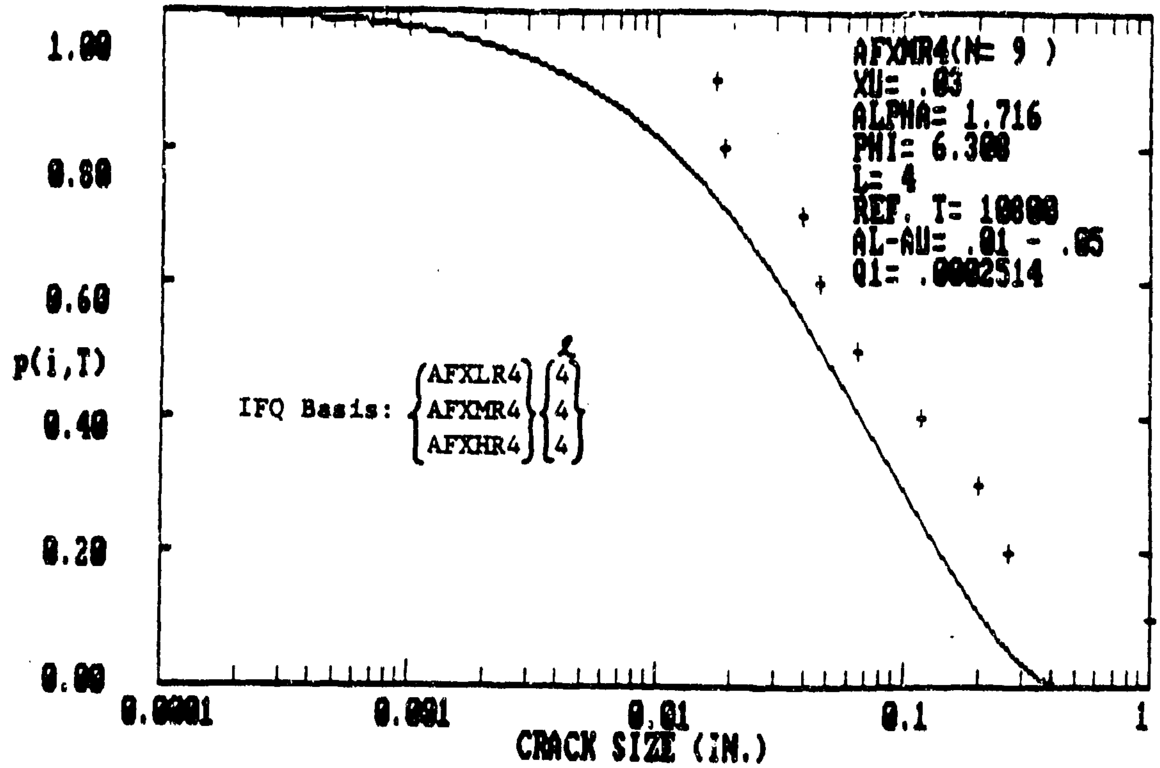

Figure 29. p(i, τ) Versus Crack Size for AFXMR4 (IFQ Basis: AFXLR4 + AFXMR4 + AFXHR4; x_u = 0.03", α = 1.716, ϕ = 6.308, $\mathcal{L}$ = 4; CLSSA)

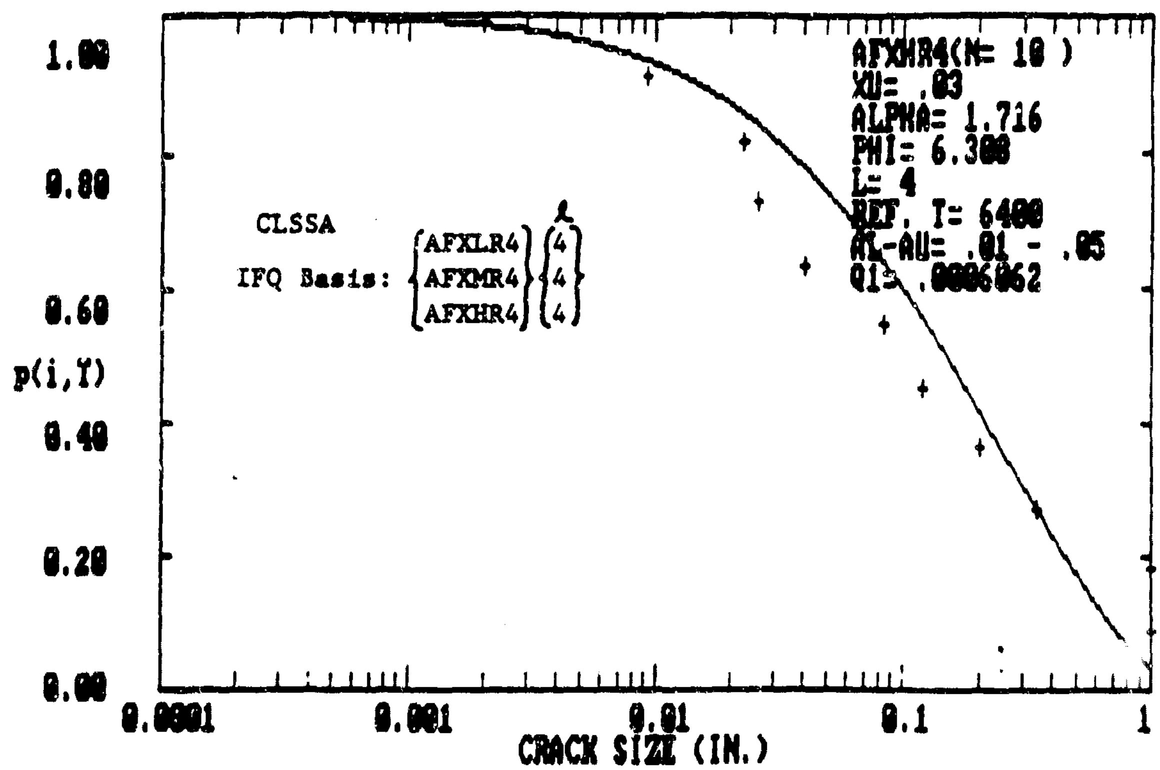

Figure 30. p(i, τ) Versus Crack Size for AFXHR4 (IFQ Basis: AFXLR4 + AFXMR4 + AFXHR4; x_u = 0.03", α = 1.716, ϕ = 6.308, $\mathcal{L}$ = 4; CLSSA)

3.3.1.4 Discussion of Results. The following observations, comments, and conclusions are based on Figs. 15-30.

1. The EIFSD parameters for the Weibull compatible distribution depend on the chosen fractographic crack size range, AL-AU. A fractographic crack size range of AL-AU = 0.01" - 0.05" was used in the demonstration.

2. The EIFS parameters have been estimated using the CLSSA and the method of moments (MM) [1,42]. Goodness-of-fit plots for $F_T(t)$ versus TTCI using the MM and the CLSSA are shown in Figs. 15 and 16, respectively. In general, however, the CLSSA seems to give a better overall fit than the MM. This has been expected because α and ϕ are determined by minimizing the total sum squared error.

3. With the IFQ that is determined from pooled data sets (i.e., AFXLR4 + AFXMR4 + AFXHR4) goodness-of-fit plots for $F_T(t)$ are shown in Figs. 17-19 for the AFXLR4 data set and in Figs. 26 and 27 for the AFXHR4 data set. These plots reflect different x_u values. For all three data sets x_u = 0.03" appears to give the best fit in the lower tail. Plots for x_u = 0.05" also give reasonable fits for the three data sets The theoretical predictions based on x_u = 0.02" do not correlate as well with actual test results as either x_u = 0.03" or 0.05".

4. The crack exceedance probability plots, $p(i, \tau)$, in Figs. 28 - 30 are shown for crack sizes up to 1.0". Theoretical predictions are based on the corresponding EIFS master curve. The crack size range of most interest for justifying the EIFSD is for AL-AU = 0.01" - 0.05".

5. The theoretical predictions for $F_T(t)$ and $p(i, \tau)$ based on the IFQ that is determined from the pooled data sets,

correlate reasonably well with the actual test results for each of the three countersunk fastener hole data sets, separately. We then conclude that the EIFSD parameters x_u = .03", α = 1.716, and ϕ = 6.308 (for the pooled data sets) are reasonable for the durability analysis of countersunk fastener holes in 7475-T7351 aluminum for the situation considered. The EIFSD parameters x_u = .05", α = 2.132, and ϕ = 6.453 are also considered reasonable for durability analysis. A slightly more conservative durability analysis prediction for x_u = 0.05" than for x_u = 0.03" would be expected. The EIFSD parameters x_u = 0.02", α = 1.33, and ϕ = 6.704 are a poor third choice for representing the IFQ.

3.3.2 Straight-Bore Fastener Hole Specimens

Two fractographic data sets from the "Fastener Hole Quality" (FHQ) program [3] will be used to determine the initial fatigue quality (IFQ) of stright-bore fastener holes in 7475-T7351 aluminum. The two data sets, referred to as "WPF" and "XWPF" are described in Table 9. Specimen geometry and design details for WPF and XWPF data sets are shown in Figs. 4 and 5, respectively. The specimens for both data sets have NAS 6204 (1/4" dia) protruding head bolts installed with a clearance fit. No special life enhancement hole processing, such as cold working and interference fit bushings, were reflected in any of the test specimens considered.

The fractographic results (i.e., a(t) versus t data) for the largest fatigue crack per specimen in the bore of the hole of each specimen in each data set were screened for extreme behavior. Screening was conducted using the computer software in Volume V [5]. Fractographic results in AL-AU = 0-.05" are shown in Figs. 31 and 32 for the WPF and XWPF data sets, respectively. Two fatigue cracks were deleted from each of the two data sets as indicated in Figs. 31 and 32.

Table 9. Description of Fractographic Data Sets Used to Determine the IFQ for Straight-Bore Fastener Holes

Data Set (1)	No. of Specimens Used	(4) (KSI)	% KT	W (In.)	Fastener	Load Spectrum	Ref. Fig.
WPF	31/33 (2)	34	0	1.5	NAS6204-8	F-16 400 HR	4
(5)							
XWPF	31/33 (3)	34	15	1.5			5

Notes:

(1) 7475-T7351 Aluminum
(2) Deleted fatigue cracks #2 and 6
(3) Deleted fatigue cracks #11 and 16
(4) Gross section stress for peak spectrum load
(5) Ref. FHQ program [3]

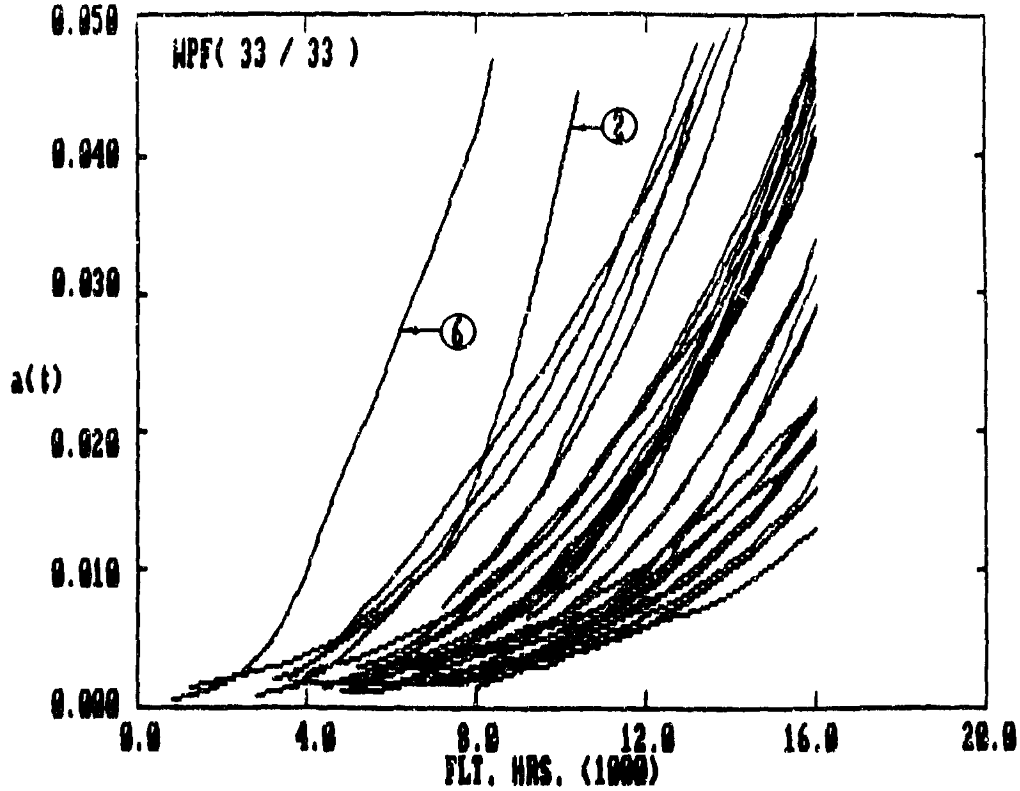

Figure 31. Fractographic Data Survey for WPF Data Set in the AL-AU = 0-.05" Crack Size Range.

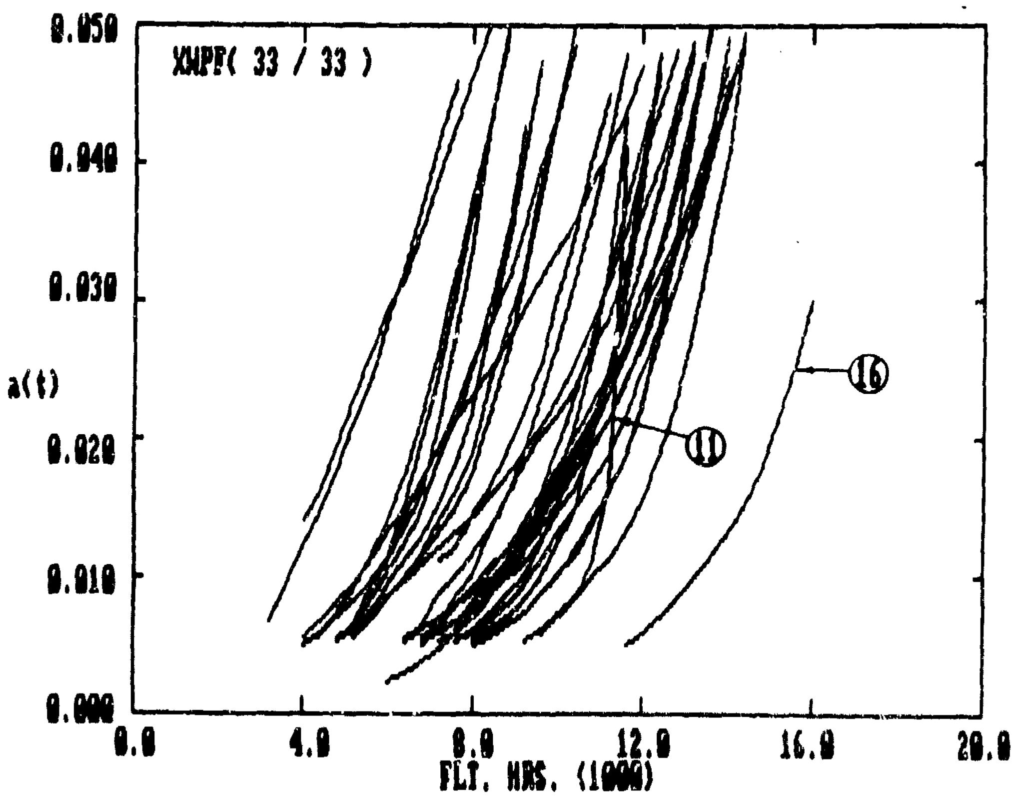

Figure 32. Fractographic Data Survey for XWPF Data Set in the AL-AU = 0-.05" Crack Size Range.

Two criteria were used to censor the fractographic data: (1) eliminate fatigue cracks with abnormally fast crack growth rates (e.g., cracks no. 2 and 6 for the WPF and crack no. 11 for the XWPF data set), and (2) delete cracks with little useful data in the desired AL-AU range, e.g., the crack data is sparse for fatigue crack no. 16 of the XWPF data set and would require extrapolation to $a_0 = 0.05"$. There are no hard and fast rules for fractographic data censoring. However, fractographic data screening is essential when defining the IFQ to assure data consistency and compatibility.

The IFQ analysis procedures described previously for countersunk fastener holes will be repeated herein for straight-bore hole specimens in the following.

3.3.2.1 Estimation of Crack Growth Rate Parameters. The crack growth parameter Q in Eqs. 10 - 12 is determined for the WPF and XWPF data sets using the same procedure described in Section 3.3.1.1 for countersunk fastener holes. Pooled Q values were determined using the applicable fractographic data in the AL-AU range = 0.01"-0.05". Pooled Q values for the WPF and XWPF data sets are shown in Table 10. Similar Q values are also shown in Table 10 for the WWPF, LYWPF and HYWPF data sets. Experimental results for these three data sets will be used later to correlate with theoretical predictions for $p(i,\tau)$ or $F_{T(x_1)}(\tau)$. In this case predictions will be based on an EIFSD determined using two data sets (i.e., WPF and XWPF) and the data pooling procedure described in Volume I [1]. Specimen geometries for the WWPF, LYWPF and HYWPF data sets are also shown in Table 10. Specimen geometrics for the WWPF data set are shown in Fig. 2. Except for specimen width, the specimen for the WWPF data set is identical to that for the WPF data set in the test section. The width of the WPF and WWPF specimens is 1.5" and 3.0", respectively.

Table 10. Summary of Pooled Q Values for Data Sets Used for Straight-Bore Fastener Hole Demonstration

(1) Data Set	Number of Specimens Used	(4) (KSI)	W (In.)	% LT	(5) AL-AU	(6) $Qx10^4$ (1/HR.)	Load Spectrum	Ref. Fig.
WPF	31/33 (2)	34	1.5	0	.01"-.05"	2.329	F-16 400 HR.	4
XWPF	31/33 (3)	34	1.5	15		3.671		5
WWPF	13/13	34	3.0	0		2.742		2
LYWPF	5/6	30.6	1.5	15		2.140		5
HYWPF	8/8	40.6	1.5	15		9.969		5

Notes:
(1) Ref. FHQ program [3]
(2) Deleted fatigue crack #2 and 6
(3) Deleted fatigue crack #11 and 16
(4) Gross section stress for peak spectrum load
(5) Fractographic crack size range used to compute Q
(6) Based on Eq. 3

3.3.2.2 Estimation of EIFSD Parameters. EIFSD parameters are estimated using fractographic results for individual data sets and for pooled data sets. Three different initial fatigue quality (IFQ) cases are considered as shown in Table 11. The IFQ for cases 1 and 2 is based on the fractographic data for individual data sets (i.e., WPF and XWPF). Statistical scaling factors of $\ell = 1$ and 4 were used for the WPF and XWPF data sets, respectively for IFQ case 3. The statistical scaling procedure used is described in Volume I [1].

Specimens for the WPF data set have a single fastener hole (Fig. 4), whereas each specimen for the XWPF data set (Fig. 5) contains two common fastener holes in two dog-bones or a total of four holes per specimen. Fractographic results are available for the largest fatigue crack in each specimen for both data sets.

The EIFSD parameters for the Weibull-compatible distribution function (i.e., α and ϕ), Eq. 1, will be estimated for $x_u = 0.03"$ using the WPF and XWPF data sets described in Table 9. The same procedures, equations, and details used in Section 3.3.1.2 for countersunk fastener holes will be used for the straight-bore fastener hole demonstration.

EIFSD parameters α and ϕ can be estimated for a given x_u using either an "EIFS fit" or a "TTCI fit" and the combined least square sums approach (CLSSA). Details of the estimation procedure are given in Volume I [1]. In this section α and ϕ were estimated for each IFQ case using $x_u = 0.03"$, an "EIFS fit," and the CLSSA. Software for an IBM or IBM-compatible PC, documented in Volume V [5], was used to determine the EIFSD parameters. Results for the three IFQ cases are summarized in Table 11.

Table 11. Summary of EIFSD Parameters for Straight-Bore Fastener Holes Based on Weibull-Compatible Distribution Function

IFQ Basis	No. Spec.	AL-AU (In.)	$Q \times 10^4$ (1/HR)	ℓ	x_u (In.)	α	ϕ	IFQ Case
WPF	31	.01-.05	2.329	1	.03	6.920	3.808	1 (1)
XWPF	31		3.671	4		5.136	5.440	2 (1)
{WPF, XWPF}	{31, 31}		{2.329, 3.671}	{1.0, 4.0}		4.782	4.658	3 (2)

NOTES: (1) Based on individual fractographic data set
(2) Based on pooled fractographic data sets

3.3.2.3 Goodness-of-Fit Plots. A candidate EIFSD can be tested as follows. The EIFSD is grown forward to predict the probability of crack exceedance, $p(i,\tau)$, at any service time and/or the cumulative distribution of service time, $F_T(t)$, at any given crack size. Then, analytical predictions can be plotted and correlated with available fractographic results to determine if reasonable predictions can be obtained with the candidate EIFSD. Such plots are referred to as "goodness-of-fit plots." The three IFQ cases shown in Table 11 are evaluated in the following.

$p(i,\tau)$ predictions, based on IFQ cases 1 and 2 (individual data sets), are correlated with fractographic results as shown in Figs. 33 and 34 for the WPF and XWPF data sets, respectively. Similar plots for $F_T(t)$ are shown in Figs. 35 and 36 for the same data sets.

$p(i,\tau)$ predictions based on IFQ case 3 for pooled data sets (i.e., WPF and XWPF), are correlated with fractographic results in Figs. 37 and 38 for the WPF and XWPF data sets, respectively. Similar plots for $F_T(t)$ are shown in Figs. 39 and 40.

Predictions for $p(i,\tau)$ and/or $F_T(t)$ were also made and correlated with fractographic results for three data sets (i.e., WWPF, LYWPF and HYWPF) not used to estimate the IFQ. Theoretical predictions were based on IFQ case 3. Results for the WWPF data set are shown in Figs. 41 and 42 for $p(i,\tau)$ and $F_T(t)$, respectively. Specimen details for the WWPF data set are shown in Fig. 2. Crack growth parameters for determining $p(i,\tau)$ and $F_T(t)$ and other details are shown in Table 10.

$F_T(t)$ predictions for the LYWPF and HYWPF data sets were also made using IFQ case 3 (Table 11). Specimen details are shown in Fig. 5 and other particulars are shown in Table

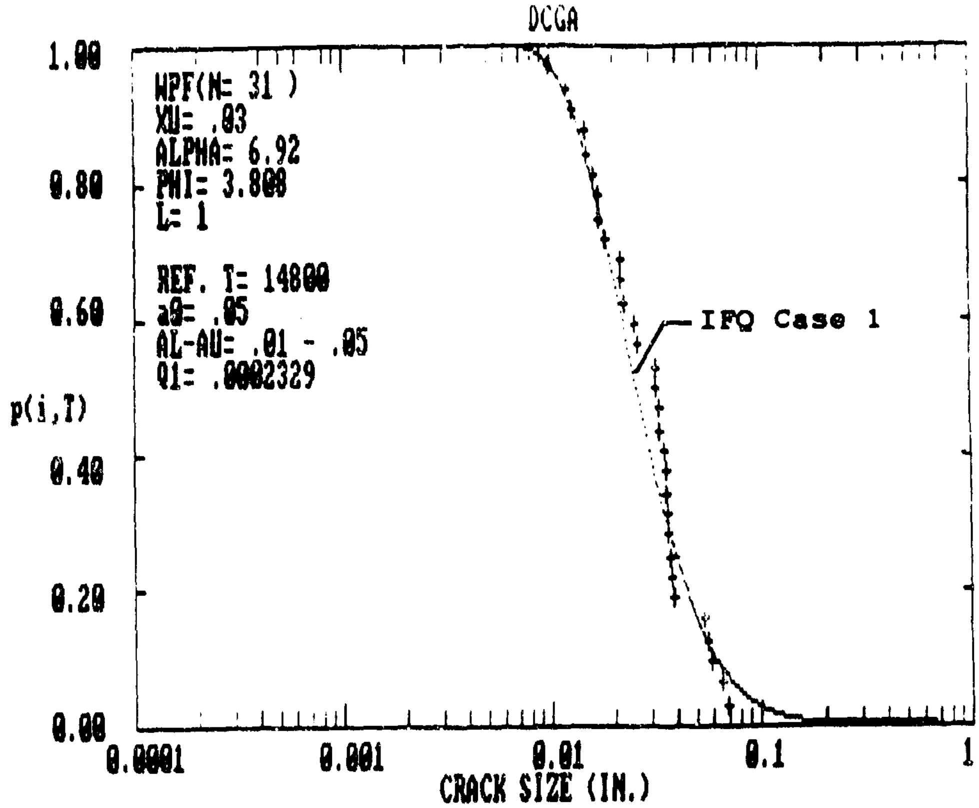

Figure 33. p(i,τ) Versus Crack Size Goodness-of-Fit Plot for WPF Data Set (IFQ Basis: Case 1) at τ = 14800 Flight Hours.

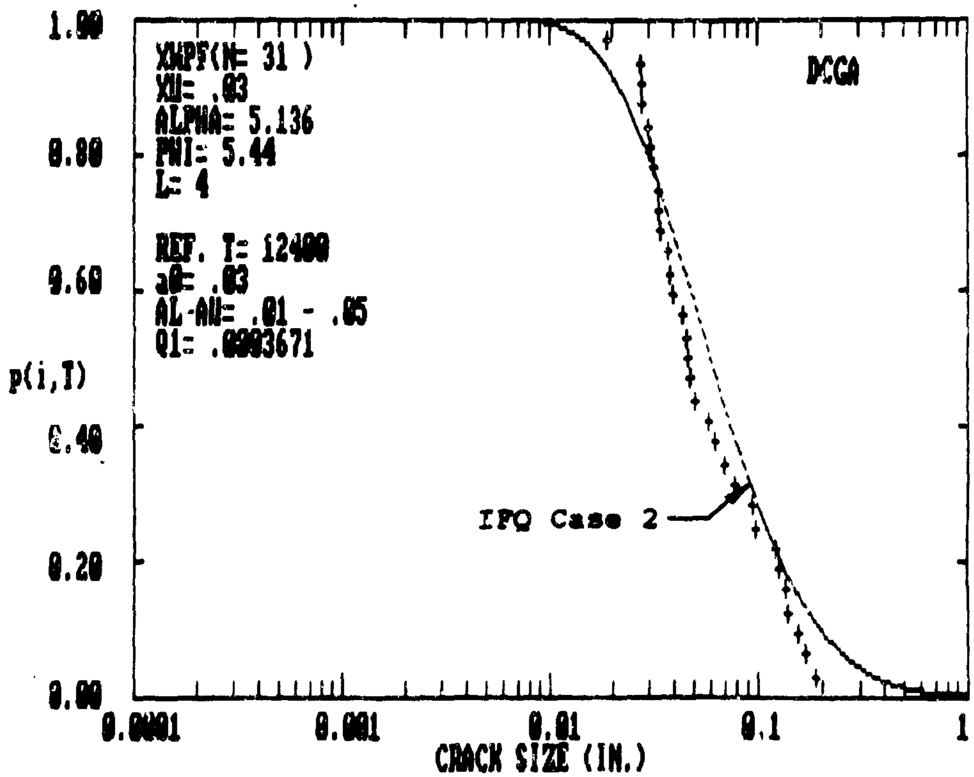

Figure 34. p(i,τ) Versus Crack Size Goodness-of-Fit Plot for XWPF Data Set (IFQ Basis: Case 2) at τ = 12400 Flight Hours.

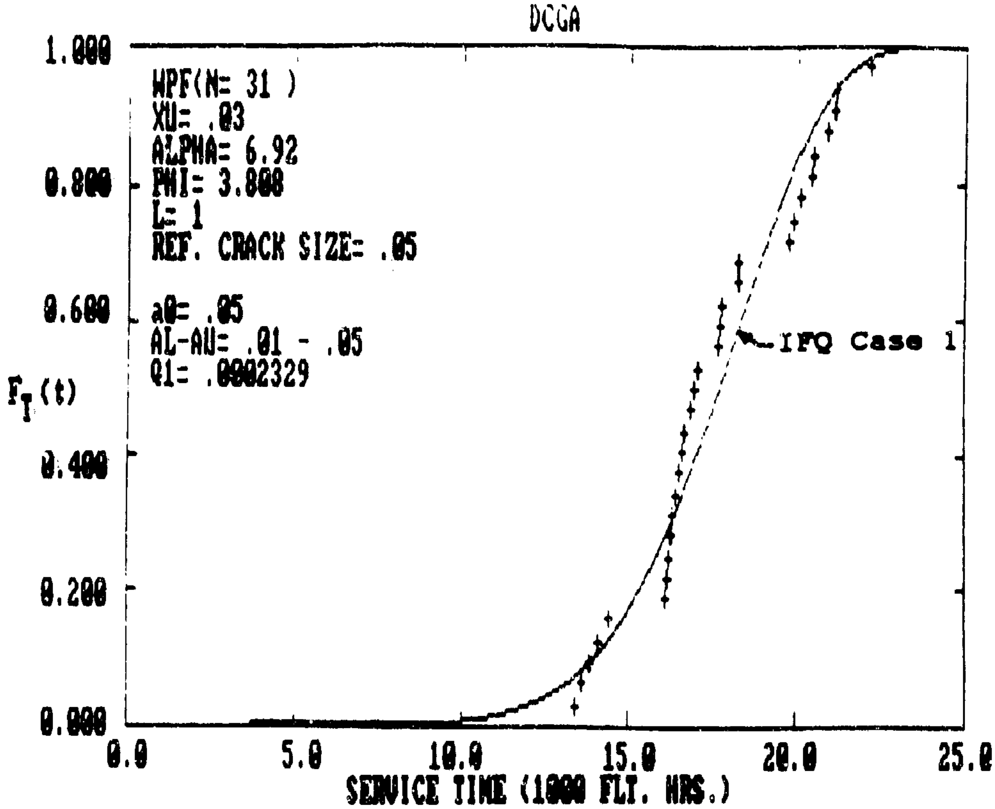

Figure 35. $F_T(t)$ Versus TTCI Goodness-of-Fit Plot for WPF Data Set (IFQ Basis: Case 1) at a_o = .05".

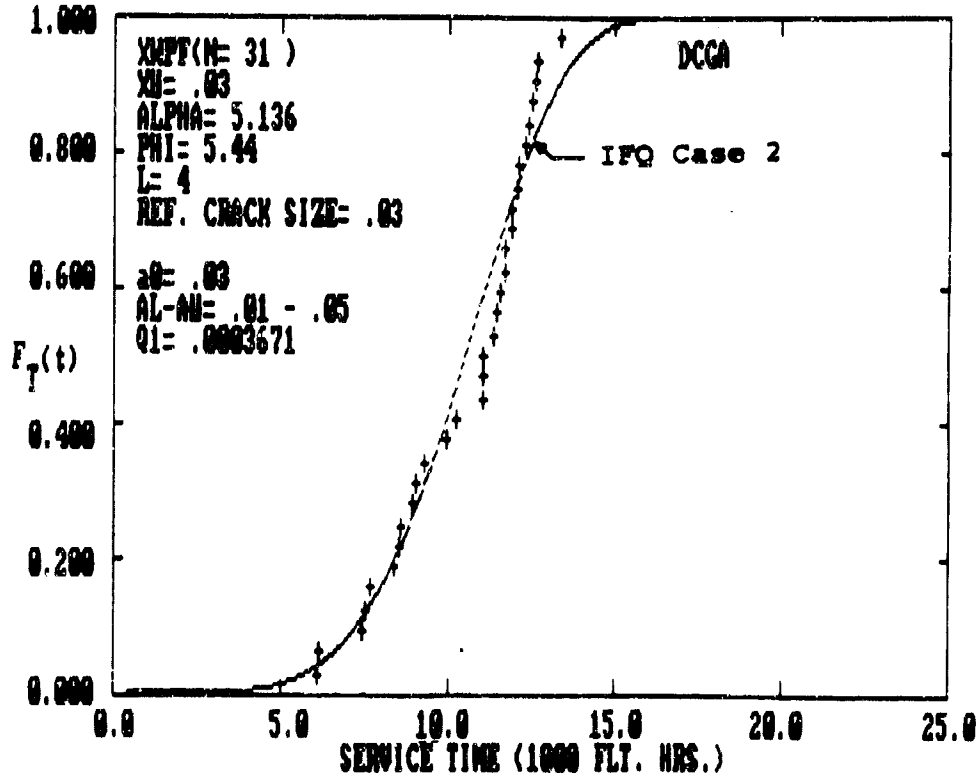

Figure 36. $F_T(t)$ Versus TTCI Goodness-of-Fit Plot for XWPF Data Set (IFQ Basis: Case 2) at a_o = .05".

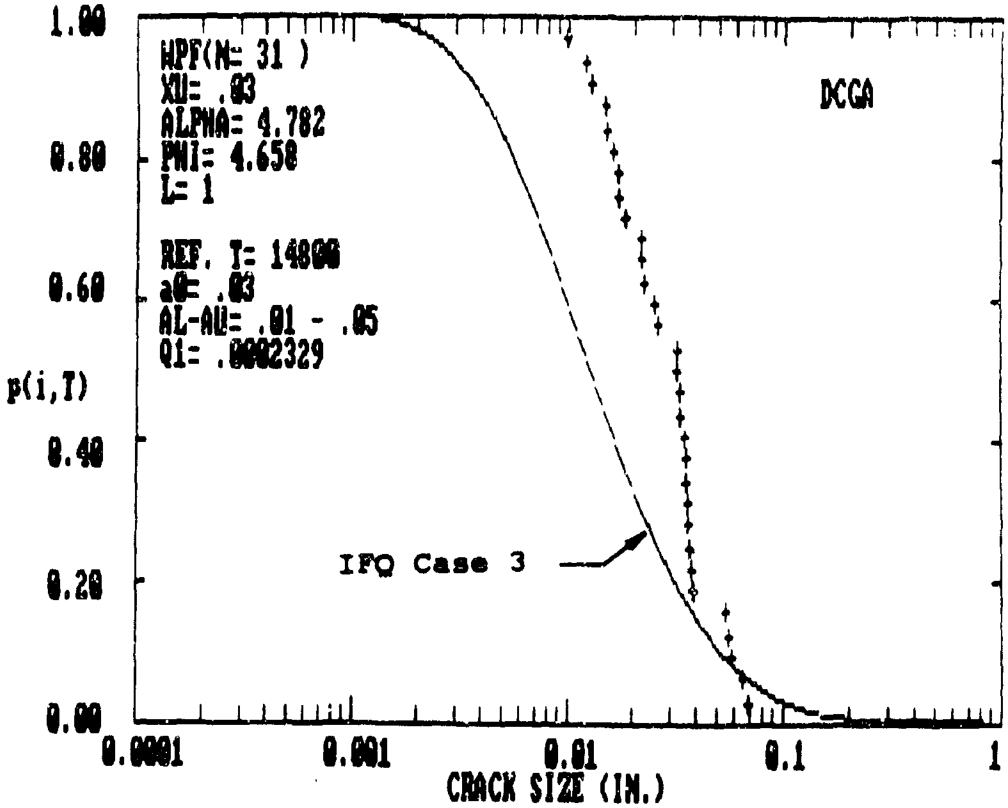

Figure 37. p(i,$\mathcal{T}$) Versus Crack Size Goodness-of-Fit Plot for WPF Data Set (IFQ Basis = WPF+XWPF) at $\mathcal{T}$ = 14800 Flight Hours.

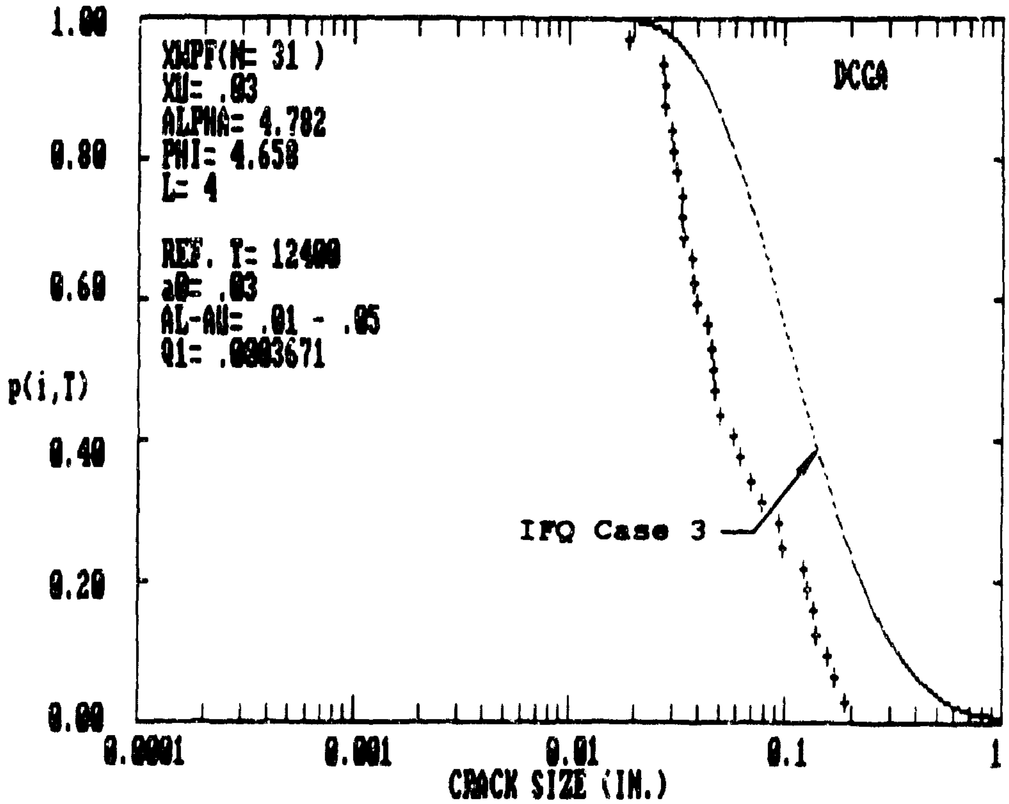

Figure 38. p(i,$\mathcal{T}$) Versus Crack Size Goodness-of-Fit Plot for XWPF Data Set (IFQ Basis = WPF+XWPF) at $\mathcal{T}$ = 12400 Flight Hours.

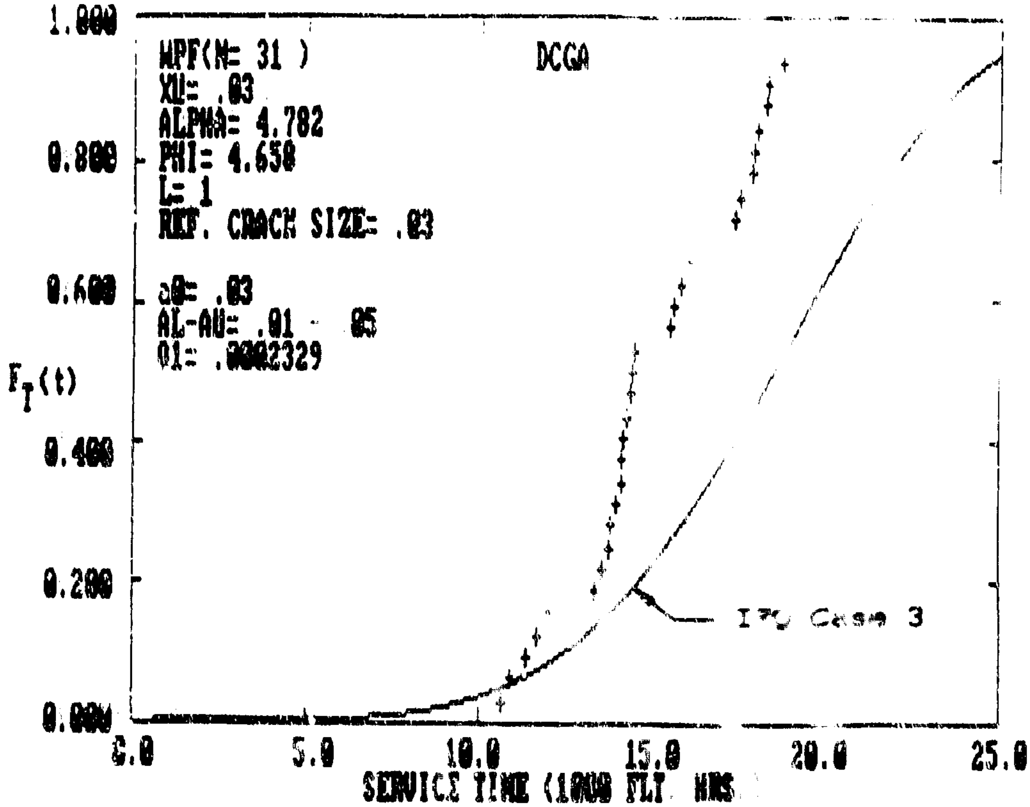

Figure 39. $F_T(t)$ Versus TTCI Goodness-of-Fit Plot for WPF Data Set (IFQ Basis = WPF+XWPF) for a_0 = 0.03".

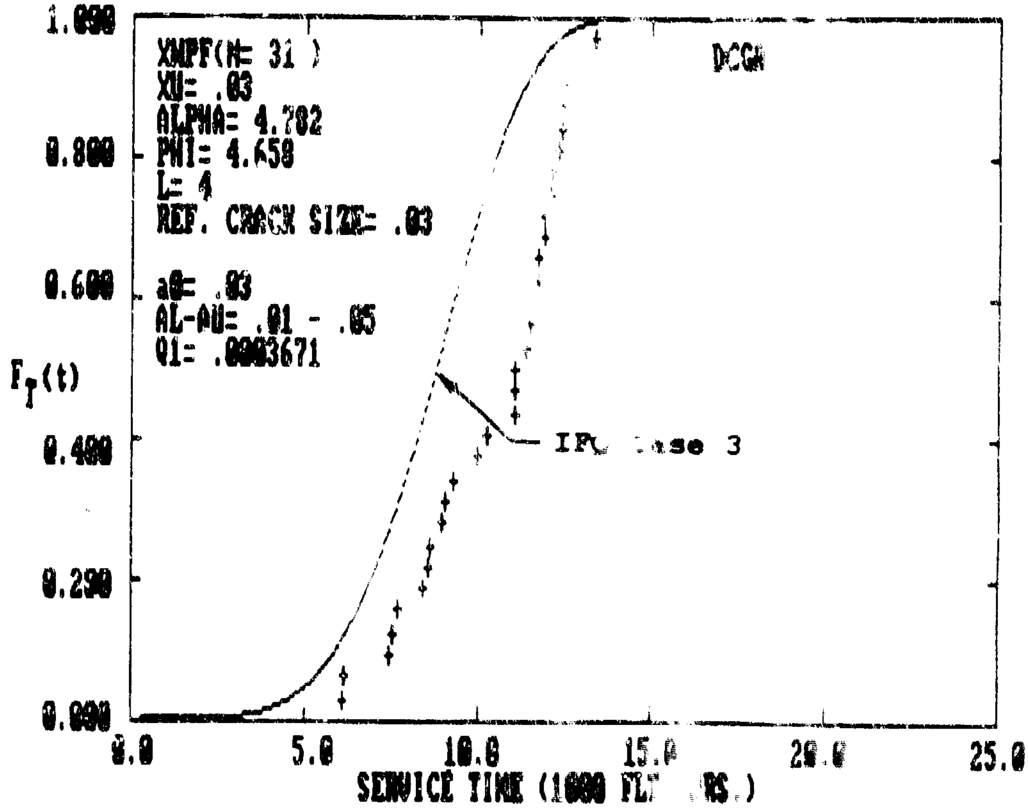

Figure 40. $F_T(t)$ Versus TTCI Goodness-of-Fit Plot for XWPF Data Set (IFQ Basis = WPF+XWPF) for a_0 = 0.03".

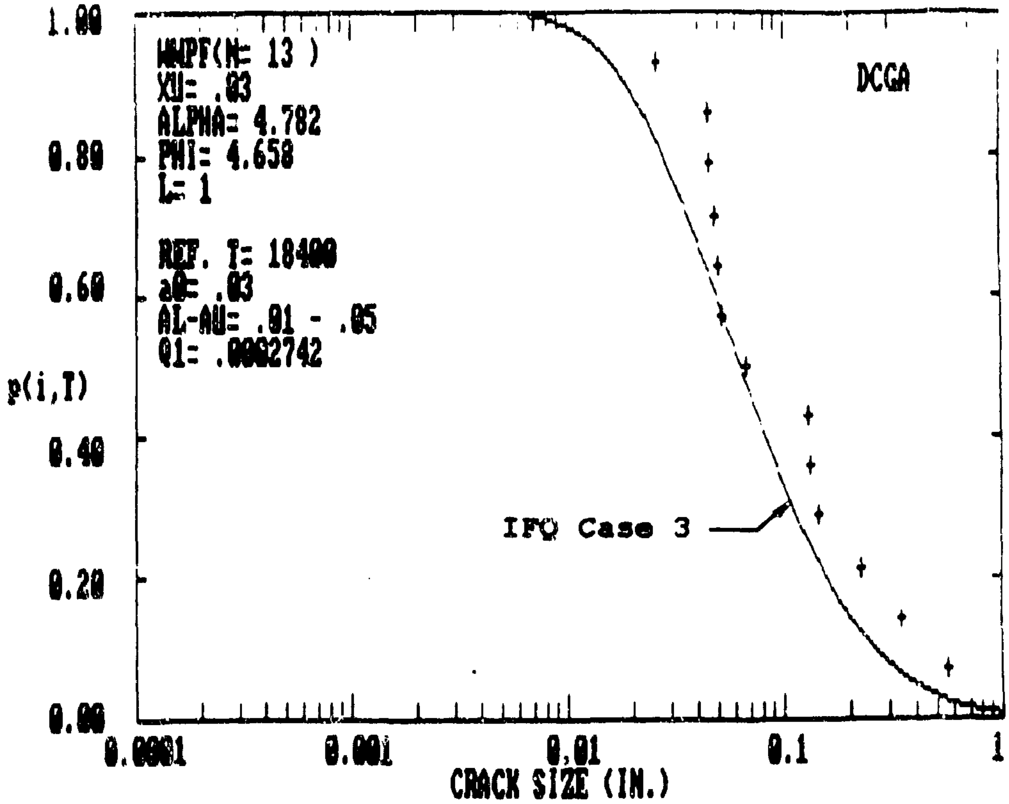

Figure 41. <u>p(i,$\mathcal{T}$) Versus Crack Size Goodness-of-Fit Plot for WWPF Data Set (IFQ Basis = WPF+XWPF) at $\mathcal{T}$ = 18400 Flight Hours.</u>

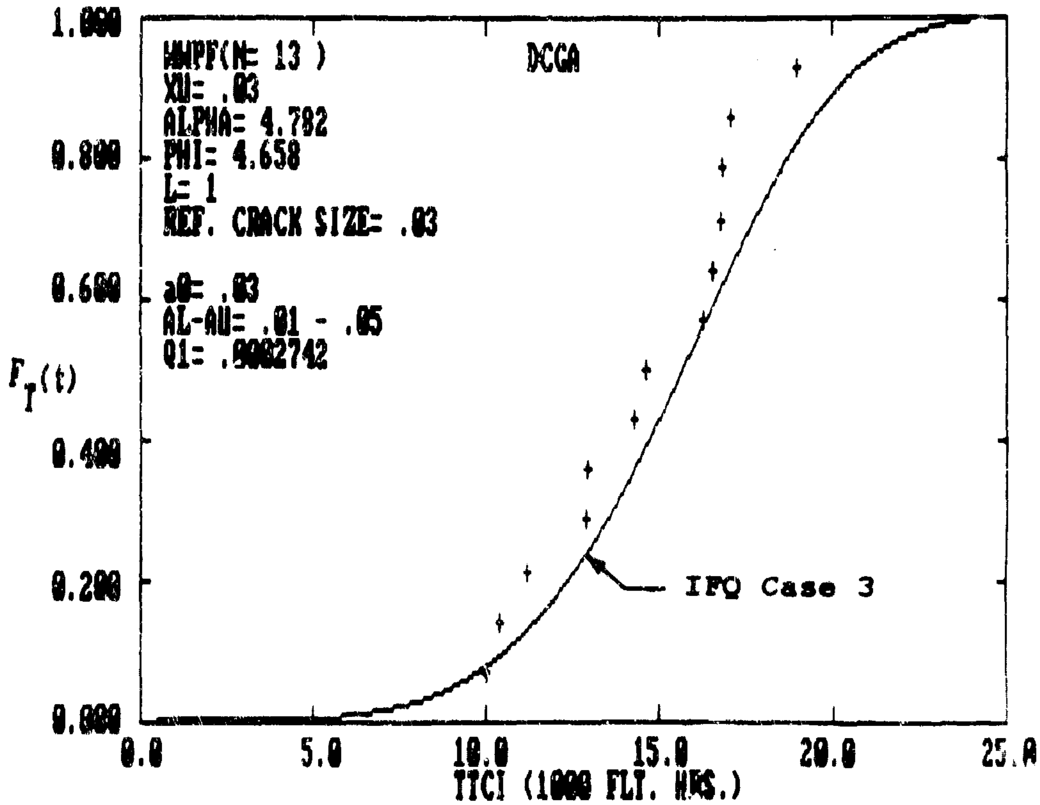

Figure 42. <u>$F_T(t)$ Versus TTCI Goodness-of-Fit Plot for WWPF Data Set (IFQ Basis = WPF+XWPF) for a_o = 0.03".</u>

10. $F_T(t)$ predictions are correlated with actual fractographic results for the LYWPF and HYWPF data sets in Figs. 43 and 44, respectively. Experimental results for all plots shown in Figs. 33-44 are based on the largest fatigue crack per specimen -- irrespective of the number of fastener holes per specimen.

3.3.2.4 Discussion of Results. The following observations, comments and conclusions are based on the demonstration presented herein.

1. $p(i, \mathcal{T})$ and $F_T(t)$ predictions for an individual fractographic data set (i.e., WPF and XWPF) correlated very well with fractographic results when the IFQ was based on the fractographic results of that given data set. For example, see Figs. 33-36.

2. Theoretical predictions for $p(i, \mathcal{T})$ and $F_T(t)$ for the WPF and XWPF data sets, based on IFQ case 3 (see Table 11), did not correlate as well with experimental results as those based on IFQ cases 1 and 2. For example, compare results shown in Figs. 33-40.

3. The WWPF, LYWPF and HYWPF fractographic data sets were not used to define the IFQ for any of the three IFQ cases shown in Table 11. Theoretical predictions for $p(i, \mathcal{T})$ and $F_T(t)$, based on the DCGA, correlated reasonably well with experimental results for the WWPF data set (see Figs. 41 and 42). Poorer correlations were obtained for the LYWPF and HYWPF data sets as shown in Figs. 43 and 44, respectively. Better correlations were obtained for the HYWPF data set than for the LYWPF data set. Theoretical predictions for $F_T(t)$ were more conservative (i.e., shorter service times to reach a specified crack size) than the experimental results for both the LYWPF and HYWPF data sets. It should be noted that the LYWPF and HYWPF data sets had a limited number of useable

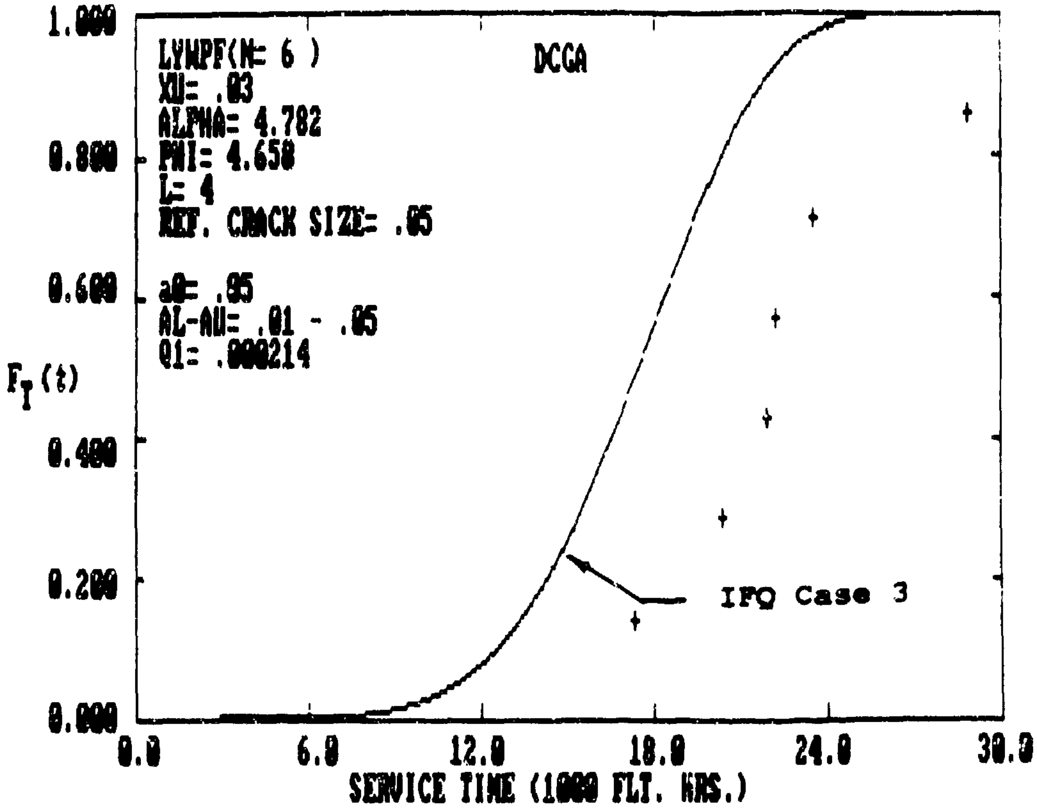

Figure 43. $F_T(t)$ Analytical and Experimental Correlations for LYWPF Data Set.

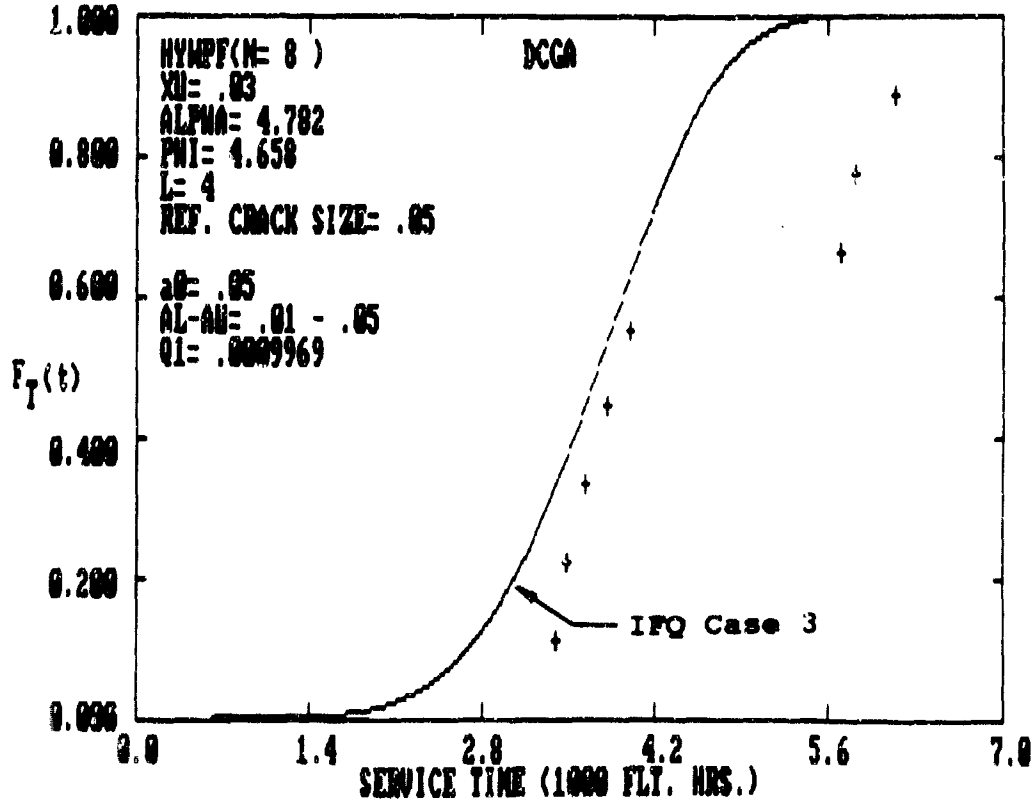

Figure 44. $F_T(t)$ Analytical and Experimental Correlations for HYWPF Data Set

fatigue cracks per data set (e.g., N = 6 for LYWPF and N = 8 for HYWPF).

4. Goodness-of-fit plots for $p(i, \tau)$ and/or $F_T(t)$ are essential to justify an EIFSD and statistical scaling for durability analysis.

5. The following aspects of statistical scaling need to be investigated further: (1) statistical independence of dominant fatigue cracks in fastener holes, (2) effect of variable stress level on scaling, (3) effect of bolt load transfer and variance on scaling, and (4) how to deal with fractographic data sets with significantly different mean EIFS values when estimating the EIFSD parameters using the data pooling procedure.

SECTION IV

DEMONSTRATION/EVALUATION OF DURABILITY ANALYSIS EXTENSION

4.1 INTRODUCTION

The purpose of this section is to demonstrate and evaluate the durability analysis extension for predicting the probability of crack exceedance in the large crack size range that may result in functional impairment such as fuel leaks and ligament breakage. Various theoretical approaches have been proposed for the durability analysis extension in Vol. I[1]. In this section, only the two-segment deterministic-deterministic (DCGA-DCGA) and deterministic-stochastic (DCGA-SCGA) crack growth analysis methodologies will be demonstrated, because these two approaches are the most promising. Other durability extension methodologies will be presented in the Appendix.

The demonstration/evaluation is performed at two levels: (1) coupon specimens, and (2) full-scale aircraft structure. Fractographic results for 1.5" wide double-reversed dog-bone type specimens [4] and the Weibull-compatible EIFSD function, given in Eq.1, are used to define the initial fatigue quality (IFQ) of straight-bore holes and countersunk fastener holes.

Durability analysis predictions will be made for 3" wide double-reversed dog-bone type specimens and for the F-16 lower wing skins. Analytical predictions will be correlated with actual test results for 3" wide test specimens [2] and for the F-16 durability test article [4]. Specifically, straight-bore holes and countersunk fastener holes in 7475-T7351 aluminum will be considered. The durability analysis extension will cover the large crack size regions, involving functional impairment, such as fuel leakage and ligament breakage.

The advanced durability analysis methodology is documented in Volume I [1]. Volume I should be referred to for further details about equations, concepts and methods. Key equations from Volume I, which will be used in the durability analysis, will be presented in the following.

This section includes the demonstration/evaluation of the following three parts: (1) countersunk fastener holes in dog-bone specimen (2) straight bore holes in dog-bone specimen, and (3) F-16 lower wing skins. Details of the investigation are given in the following sections. Results of this investigation are discussed, and observations/conclusions and recommendations are presented.

4.2 EQUATIONS FOR DURABILITY ANALYSIS EXTENSION

Two-segment crack growth approaches for the durability analysis extension are described in Fig. 45. Key equations for the durability analysis extension, derived in Volume I [1], for the two-segment DCGA-DCGA and DCGA/SCGA are presented in the following.

4.2.1 Deterministic-Deterministic Crack Growth Approach (DCGA-DCGA)

In the crack size region smaller than a reference crack size a_0, referred to as the first region, the service crack growth rate model is given by

$$da(t)/dt = Q_1 [a(t)]^{b_1} \; ; \; a(t) \leq a_0 \tag{20}$$

The service crack growth rate model in the crack size region larger than a_c, referred to as the second region, is

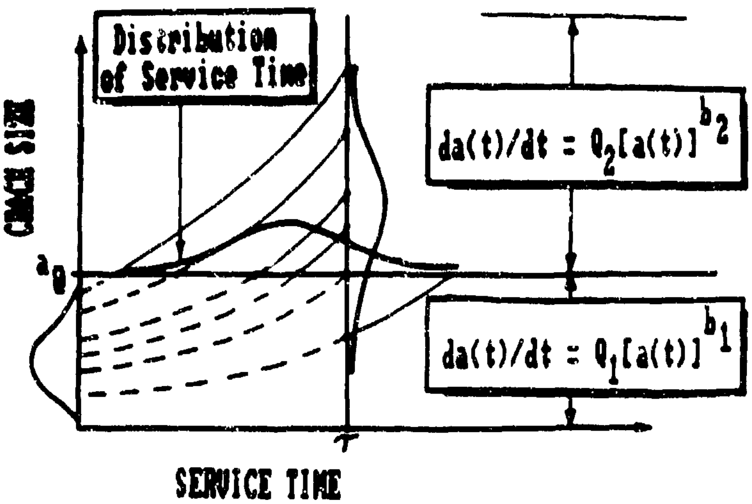

(a) Two-Segment Deterministic Crack Growth Approach (DCGA-DCGA)

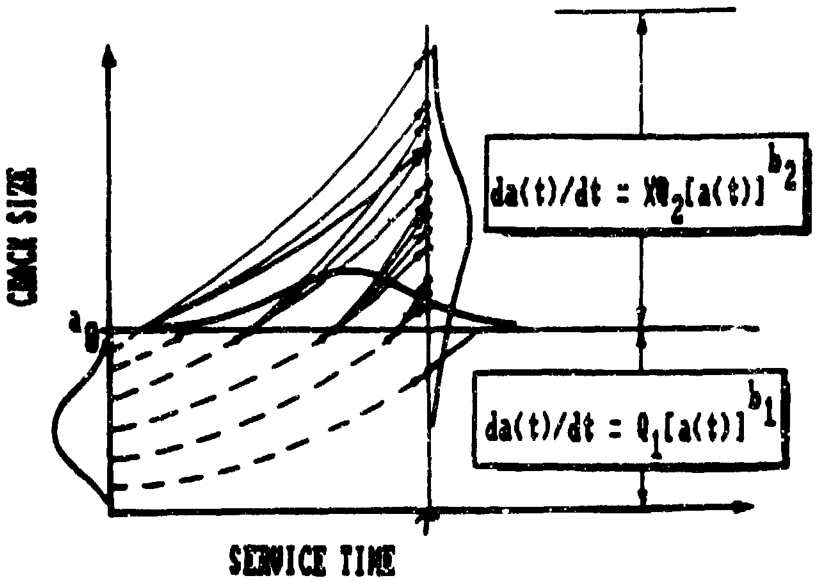

(b) Two-Segment Deterministic-Stochastic Crack Growth Approach (DCGA-SCGA)

Figure 45. Two-Segment Crack Growth Approaches for Durability Analysis Extension.

$$da(t)/dt = Q_2[a(t)]^{b_2}; \quad a(t) \geq a_0 \tag{21}$$

With the EIFSD given in Eq. 1 and the service crack growth rate models given in Eqs. 20 and 21 for $b_1 = b_2 = 1$, the distribution function, $F_{a(\mathcal{T})}(x_1) = P[a(\mathcal{T}) \leq x_1]$, of the crack size, $a(\mathcal{T})$, at any service time $\mathcal{T}$ can be derived as

$$F_{a(\mathcal{T})}(x_1) = F_{a(0)}[y(x_1;\mathcal{T})] \tag{22}$$

in which

$$y(x_1;\mathcal{T}) = x_1 \exp(-Q\mathcal{T}); \quad x_1 \leq a_0 \tag{23}$$

and

$$y(x_1;\mathcal{T}) = \left\{(x_1)^{Q_1/Q_2}\right\} \exp(\Lambda - Q_1\mathcal{T}); \quad x_1 > a_0 \tag{24}$$

where

$$\Lambda = [1 - (Q_1/Q_2)] \ln a_0 \tag{25}$$

The probability of crack exceedance, $p(i, \mathcal{T})$, and the distribution of service time to reach a given crack size x_1, $F_{T(x_1)}(\mathcal{T})$, are derived as follows

$$p(i,\mathcal{T}) = 1 - F_{a(\mathcal{T})}(x_1) = F_{T(x_1)}(\mathcal{T}) \tag{26}$$

in which $F_{a(\tau)}(x_1)$ is given by Eqs. 22 - 25.

In using Eq. 26 for computing either the probability of crack exceedance $p(i,\tau)$ or the distribution of service time to reach any crack size x_1, $F_{T(x_1)}(\tau)$, the following distinction should be made: (1) for the crack exceedance probability $p(i,\tau)$ prediction, τ is a selected fixed service time and x_1 is a variable crack size for crack exceedance, and (2) for $F_{T(x_1)}(\tau)$ prediction, x_1 is a selected fixed crack size and t is a service time variable.

When the predictions are made for the largest crack in specimens with ℓ holes, i.e., the scaling factor is ℓ, the solutions for $p(i,\tau)$ and $F_{T(x_1)}(\tau)$ are given in the following.

$$p(i,\tau) = F_{T(x_1)}(\tau) = 1 - \left\{F_{a(0)}[y(x_1;\tau)]\right\}^{\ell} \tag{27}$$

4.2.2 Equations for the Two-Segment DCGA-SCGA

The service crack growth rate model in the first region is given in Eq. 20 whereas a stochastic crack growth rate model is used in the second region

$$da(t)/dt = X Q_2 [a(t)]^{b_2} \; ; \; a(t) \geq a_0 \tag{28}$$

in which X is a lognormal random variable with a unit median value. Thus, the statistical variability of the crack growth rate in the large crack size region is taken into account by the lognormal random variable X. Equation 28 is referred to as the lognormal random variable model [12-17, 39-40].

The probability density function of the lognormal random variable X with a median 1.0 is given by

$$f_X(u) = \frac{\log e}{\sqrt{2\pi}\, u\, \sigma_z} \exp\left\{-\frac{1}{2}\left[\frac{\log u}{\sigma_z}\right]^2\right\}; \; u \geq 0 \qquad (29)$$

$$= 0 \qquad ; \; u < 0$$

in which σ_z is the standard deviation of the normal random variable Z = log X. Equation 29 is used when σ_z is estimated using the log to base 10 form. If σ_z is based on the natural log form, $f_X(u)$ given in Eq. 30 should be used.

$$f_X(u) = \frac{1}{\sqrt{2\pi}\, u\, \sigma_z} \exp\left\{-\frac{1}{2}\left[\frac{\ln u}{\sigma_z}\right]^2\right\}; \; u \geq 0 \qquad (30)$$

$$= 0 \qquad ; \; u < 0$$

Two different expressions for σ_z, derived in Appendix C of Volume I [1], are given in Eqs. 31 and 32 for the natural log basis.

$$\sigma_z = \sqrt{\frac{1}{N}\sum_{j=1}^{m}\sum_{k=1}^{N_j}\left[\ln\left(da(t)/dt\right)_{jk} - \ln Q - \ln a_j(t_k)\right]^2} \qquad (31)$$

$$\sigma_z = \sqrt{\frac{1}{m}\sum_{j=1}^{m}\left[\ln(Q_j/Q)\right]^2} \qquad (32)$$

In Eqs. 31 and 32, m = the total number of fatigue cracks in the fractographic data set, N_j = number of da(t)/dts for a(t)s in the second region for the jth fatigue crack, $N = \sum_{j=1}^{m} N_j$ = total number of [da(t)/dt, a(t)] pairs in the second region $(da(t)/dt)_{jk}$ = the kth crack growth rate value for the jth fatigue crack , $a_j(t_k)$ = crack size for the jth fatigue crack , $a_j(t_k)$ = crack size for the jth fatigue crack at the kth service time t_k (i.e., k = 1, 2, ..., N_j), Q_j = crack growth rate parameter for the jth fatigue crack defined by Eq. 5 and Q = "pooled Q" value for the fractographic data set defined by Eq. 6 in which $Q = Q_i$.

The distribution function, $F_{a(\tau)}(x_1) = P[a(\tau) \leq x_1]$, of the crack size, $a(\tau)$, at any service time τ can be derived from the distribution functions of a(0) and X given by Eqs. 1 and 29, respectively, through the transformation of Eqs. 20 and 28. The result for $b_1 = b_2 = 1$ is given as follows

(i) for $x_1 \leq a_0$

$$F_{a(\tau)}(x_1) = F_{a(0)}[y(x_1;\tau)] \tag{33}$$

in which $F_{a(0)}(y)$ is given by Eq. 1 and

$$y(x_1;\tau) = x_1 \exp(-Q_1 \tau) \tag{34}$$

(ii) for $x_1 > a_0$

$$F_{a(\tau)}(x_1) = \int_0^{\infty} F_{a(0)}[G(x_1;\tau \mid X = u)] f_X(u) du \tag{35}$$

in which $f_X(u)$ is given in Eq. 30 or 31 and

$$G(x_1;\tau \mid X = u) = a_0 \exp(-Q_1 \tau)(x_1/a_0)^{\gamma/u} \tag{36}$$

$$\gamma = Q_1/Q_2 \tag{37}$$

The probability of crack exceedence at a particular service time, $p(i,\tau)$, and the distribution function of service time to reach a given crack size x_1, $F_{T(x_1)}(\tau)$, are obtained from the distribution of $a(\tau)$ derived above

$$p(i,\tau) = F_{T(x_1)}(\tau) = 1 - F_{a(\tau)}(x_1) \qquad (38)$$

For the prediction of largest cracks in specimens with a scaling factor of ℓ, Eq. 27 should be used.

4.2.3 Extent of Damage Statistics

The extent of damage in an aircraft structure can be quantitatively defined in terms of the number of structural details expected to exceed any given crack size x_1 at a given service time τ. The mean and upper/lower bound limits for the "extent of damage" can be estimated using the Binomial distribution [1,9-11,21,23,41]. From a functional impairment standpoint, the extent of damage can be interpreted as the average number of locations where the accumulated crack size exceeds limiting crack sizes for functional impairment. For example, a through-the-thickness crack in a fuel tank may cause fuel leakage and the dimension between adjacent structural details may be considered as a crack size limit for ligament breakage.

The number of details in the ith stress region with a crack size greater than x_1 at the service time τ, is a statistical variable, the mean value $N(i,\tau)$, and the standard deviation, $\sigma_N(i,\tau)$, are determined using the Binomial distribution:

$$\bar{N}(i,\tau) = N_i\, p(i,\tau) \qquad (39)$$

$$\sigma_N(i,\tau) = \left\{N_i\, p(i,\tau)[1 - p(i,\tau)]\right\}^{1/2} \qquad (40)$$

in which N_i denotes the total number of details in the ith stress region. The average number of details with a crack size exceeding x_1 at the service time τ for m stress regions, $L(\tau)$, and the standard deviation, $\sigma_L(\tau)$, can be computed using Eqs. 41 and 42, respectively.

$$\bar{L}(\tau) = \sum_{i=1}^{m} \bar{N}(i,\tau) \tag{41}$$

$$\sigma_L(\tau) = \left[\sum_{i=1}^{m} \sigma_N^2(i,\tau)\right]^{1/2} \tag{42}$$

Equations 41 and 42 can be used to quantify the extent of damage for a single detail, a group of details, a part, a component, or an airframe. $\bar{L}(\tau)$ approximately corresponds to a 50% probability. Upper and lower bound limits for the "extent of damage" can be estimated using the Binomial distribution, e.g., $\bar{L}(\tau) \pm z\sigma_L(\tau)$, with z being the number of standard deviations, from the mean, $\bar{L}(\tau)$. Equations 39 - 42 are valid when the crack growth accumulation for each detail is statistically independent [6,9,23].

4.3 DEMONSTRATION FOR DOUBLE REVERSED DOG-BONE SPECIMENS

4.3.1 Countersunk Fastener Hole Specimens

The initial fatigue quality of countersunk fastener holes will be determined using the narrow specimen (Fig. 6) test results, i.e., AFXLR4, AFXMR4 and AFXHR4 data sets. Then, the durability analysis prediction will be made for the test results of wide specimen (Fig. 3), i.e., WAFXMR4 and WAFXHR4 data sets where large fatigue cracks exist. Correlations between the theoretical predictions and test results will be made to demonstrate the validity of the durability analysis methodology. The procedures are given as follows:

The WAFXMR4 and WAFXHR4 data sets are described in Table 12. Specimen design details are shown in Fig. 3. Specimen design details for the WAFXMR4 and WAFXHR4 data sets are the same as those for the AFXLR4, AFXMR4 and AFXHR4 data sets except the specimen width. For the latter three data sets the specimen width is 1.5" and for the former two data sets it is 3.00".

Table 12 Summary of Q and σ_z for WAFXMR4 and WAFXHR4 Data Sets

DATA SET (1)	% LT	NO. CRACKS	MAX. STRESS (ksi)	WIDTH (In.)	CRACK SIZE RANGE $a_0 - AU'$	Q x10^4 (1/Hr.)	σ_z (2)
WAFXMR4	15	14	34	3.00	.05"-.5"	2.906	.449
WAFXHR4	15	13	40.8	3.00	.05"-.5"	3.854	.322

Notes: (1) Ref. Fig. 3 for specimen design details (7475-T7351 aluminum)
(2) Ref. Eq. 32 (Natural log basis)

1. Use the EIFSD parameters obtained from the pooled data set (i.e., AFXLR4, AFXMR4 and AFXHR4) in Section 3.3.1 to define the IFQ of countersunk fastener holes in 7475-T7351 aluminum for x_u = 0.03". These parameter values are x_u = 0.03", α = 1.716 and ϕ = 6.308 (see Table 13).

2. Determine the crack growth rate parameter Q_1 for WAFXMR4 and WAFXHR4 data sets in the small crack size region, (i.e., AL-AU = 0.01" - 0.05"), using the pooled Q values from AFXMR4 and AFXHR4 data sets, respectively. Determine the crack growth rate parameter Q_2 and the corresponding variability σ_z for WAFXMR4 and WAFXHR4 data sets in the large crack size region (i.e., a_0 - AU' = 0.05"-.5") using the fractographic results for WAFXMR4 and WAFXHR4 data sets, respectively.

3. Predict the crack exceedance probability $p(i,\tau)$ in the large crack size region and the distribution of service time $F_{T(x_1)}(\tau)$ to reach any specified large crack size x_1. The two-segment DCGA-DCGA and DCGA-SCGA approaches will be used.

4. Correlate analytical predictions with the actual test results for two wide specimen data sets; i.e., WAFXMR4 and WAFXHR4. The investigation plan is described in Fig. 46.

WAFXMR4 and WAFXHR4 data sets were tested using the F-16 400 hour spectrum with a maximum peak gross stress of 34 ksi and 40.8 ksi, respectively. Theoretically, there is no significant difference in the peak stress at the edge of the fastener hole for narrow (W = 1.5") or wide (W = 3.0") specimen subjected to the same gross section stress. The narrow specimen has a slightly larger net section stress than the wide specimen. However, the narrow specimen has a smaller stress concentration factor than the wide specimen. These compensating factors are the reason the maximum peak stress

Table 13. Summary of IFQ Parameters for Pooled Countersunk Data Sets.

DATA SET	NO. CRACKS	MAX. STRESS (ksi)	ℓ	AL-AU	$Q \times 10^4$ (1/HR.)	x (IN.)	α	ϕ	MEAN EIFS $\times 10^4$
AFXLR4	10	32	4	.01"-.05"	2.101	.02	1.330	6.704	42.40"
AFXMR4	9	34	4		2.514	.03	1.716	6.308	62.43"
AFXHR4	10	38	4		6.062	.05	2.132	6.453	34.29"

Notes: 1. CLSSA used
2. Used data pooling procedure

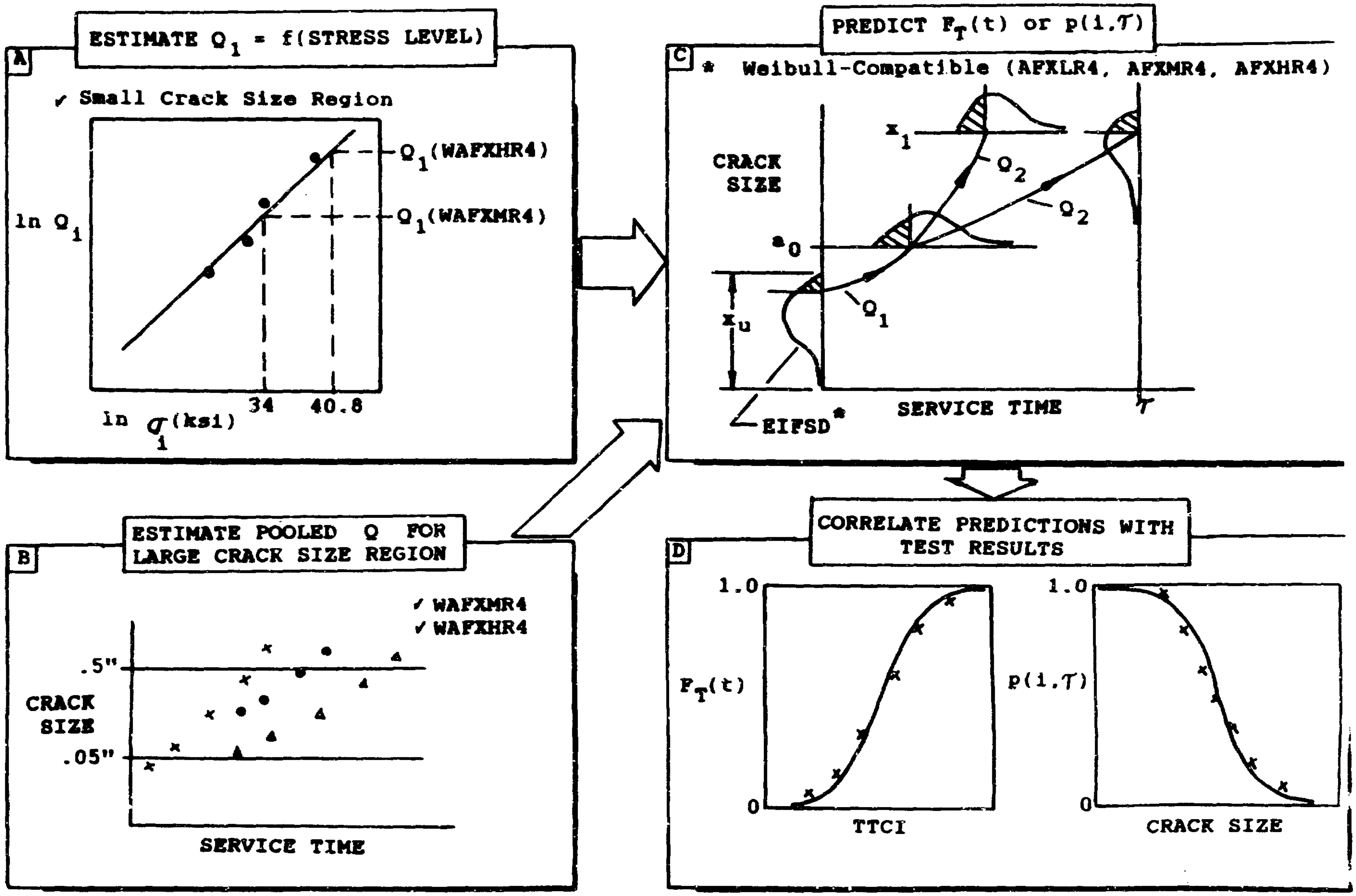

Figure 46. General Approach Used to Demonstrate the Two-Segment DCGA for WAFXMR4 and WAFXHR4 Data Sets.

at the edge of the fastener hole is virtually the same for both narrow and wide specimens subjected to the same gross section stress.

4.3.1.1 <u>Estimation of Service Crack Growth Parameters</u>. The crack growth behavior in the small and large crack size region must be characterized to implement the two-segment DCGA-DCGA and DCGA-SCGA. In the following demonstrations, AL-AU = 0.01" - 0.05" is chosen for the small crack size region whereas a_0-AU′ = 0.05" - 0.5" is chosen for the large crack size region.

In reality, however, crack growth rate data are usually not available for service conditions in which the crack exceedance probability should be predicted. For instance, crack growth rate data in various stress regions of the F-16 lower wing skins are not available. Hence, crack growth parameters Q_1 and Q_2 should be estimated using either an analytical crack growth program [e.g., 18,19] or suitable fractographic results [e.g., 2-4] if available. In any case, Q_1 should be compatible with the basis in which the EIFS master curve(s) is established for defining the EIFSD parameters. This aspect is discussed in Volume I [1].

EIFSD parameters for countersunk fastener holes were defined in Section 4.2.3 using three narrow width (w = 1.5") specimen data sets (i.e., AFXLR4, AFXMR4, AFXHR4). Pooled Q values for these three data sets are shown in Table 13.

The crack growth rate parameters Q_1 and Q_2 vary with respect to service loading conditions. However, when all service loading conditions are identical, such as loading spectra, percentage of load transfer, type of fastener holes, etc., except the maximum gross section stress level σ, a very reasonable model relating the crack growth rate parameter Q and the maximum gross section stress has been proposed by

Yang and Manning as follows [6,8,20].

$$Q = C\sigma^{V} \tag{43}$$

in which C and V are empirical parameters.

Thus, if fractographic data sets are available under several different gross stress levels, σ, the empirical parameters C and V can be determined from Eq. 43 using the least square fit procedure. Then, an alternate approach to determine the crack growth rate parameters Q_1 and Q_2 is to use Eq. 43. For demonstrative purpose, since applicable fractographic results in the small crack size region are available for AFXLR4, AFXMR4 and AFXHR4 narrow specimen data sets, Eq. 43 will be used to determine the crack growth rate parameters Q_1 for WAFXMR4 and WAFXHR4 data sets as well as various stress regions in the lower wing skin of F-16 aircraft.

In the small crack size region of AL-AU = 0.01" - 0.05", Q values versus gross stresses for the AFXLR4, AFXMR4 and AFXHR4 data sets shown in Table 13 are plotted in Fig. 47 as solid circles. Using the model of Eq. 43 and a least-squares-fit procedure, a straight line is obtained in Fig. 47; with C = 4.829×10^{-4} and V = 6.38. With the values of C and V given above as well as the gross stresses for WAFXMR4 and WAFXHR4 data set, Q_1 values for these two data sets are computed from Eq. 43 as 2.851×10^{-4} per hour and 9.126×10^{-4} per hour, respectively.

Fractographic results available in the large crack size range, i.e., a_0 - AU$'$ = 0.05" - 0.5", for AFXLR4, AFXMR4 and AFXHR4 data sets are not sufficient to determine the respective pooled Q_2 values, because the specimens for these data sets are only 1.5" wide. As a result, the crack growth rate parameters Q_2 and the corresponding variabilities σ_z in segment 2, i.e., a_0 - AU$'$ = 0.05" - 0.5", for WAFXMR4 and WAFXHR4

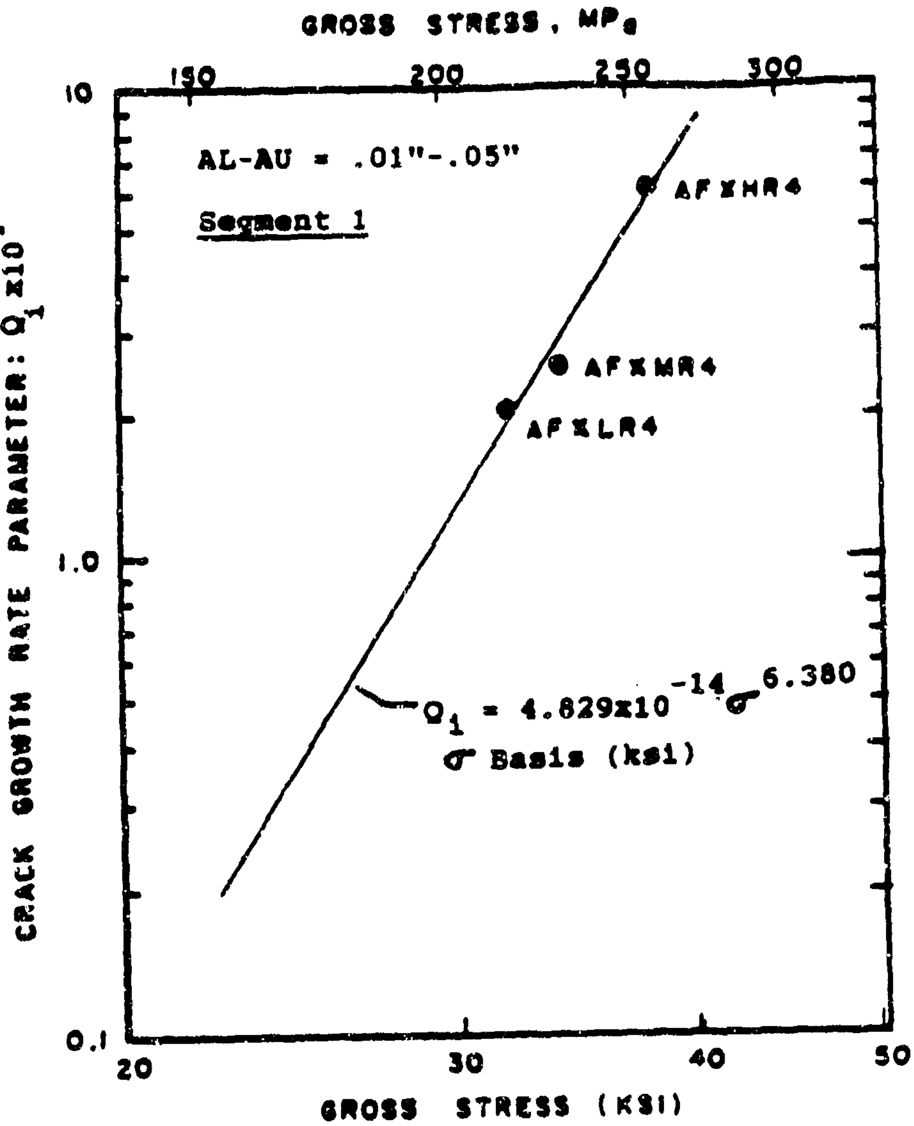

Figure 47. Crack Growth Parameter Q Versus Gross Stress for Narrow Specimen Data Sets (AFXLR4, AFXMR4, AFXHR4).

were determined using the fractographic results of these two data sets. Q_2 and σ_z values for WAFXMR4 and WAFXHR4 are summarized in Table 12 in which the value of Q_2 is denoted as Q.

4.3.1.2 <u>Theoretical/Experimental Correlations</u>. Theoretical predictions for the probability of crack exceedance $p(i,\tau)$, and the cumulative distribution of service time to reach any crack size x_1, $F_{T(x_1)}(t)$, for the WAFXMR4 and WAFXHR4 data sets have been computed using the DCGA-DCGA and the DCGA-SCGA. All results are based on the following EIFSD parameters for the Weibull compatible distribution function: $x_u = 0.03"$, $\alpha = 1.716$, $\phi = 6.308$ (see Table 13).

The following results are presented for the DCGA-DCGA: (1) Probability of crack exceedance plots at $\tau = 11608$ and 7000 flight hours are shown in Figs. 48 and 49, respectively for the WAFXMR4 and WAFXHR4 data sets. (2) The cumulative distributions of service time to reach a crack size $x_1 = 0.73"$ and 0.59" are shown in Figs. 50 and 51, respectively for WAFXMR4 and WAFXHR4. In these figures, the theoretical predictions are shown by the solid curves; whereas, experimental results are displayed by solid circles.

Using the DCGA-SCGA, theoretical/experimental correlation plots corresponding to Figs. 48-51 are presented in Figs. 52 - 55.

4.3.1.3 <u>Discussion of Results.</u> The following observations are made based on the results presented in Figs. 48-55:

1. The DCGA-DCGA predictions correlated reasonably well with the experimental results for the WAFXMR4 and the WAFXHR4 data sets in the central portion of the population. However, the correlation was poor at the tail portion of the distribution (see Figs. 48 - 51).

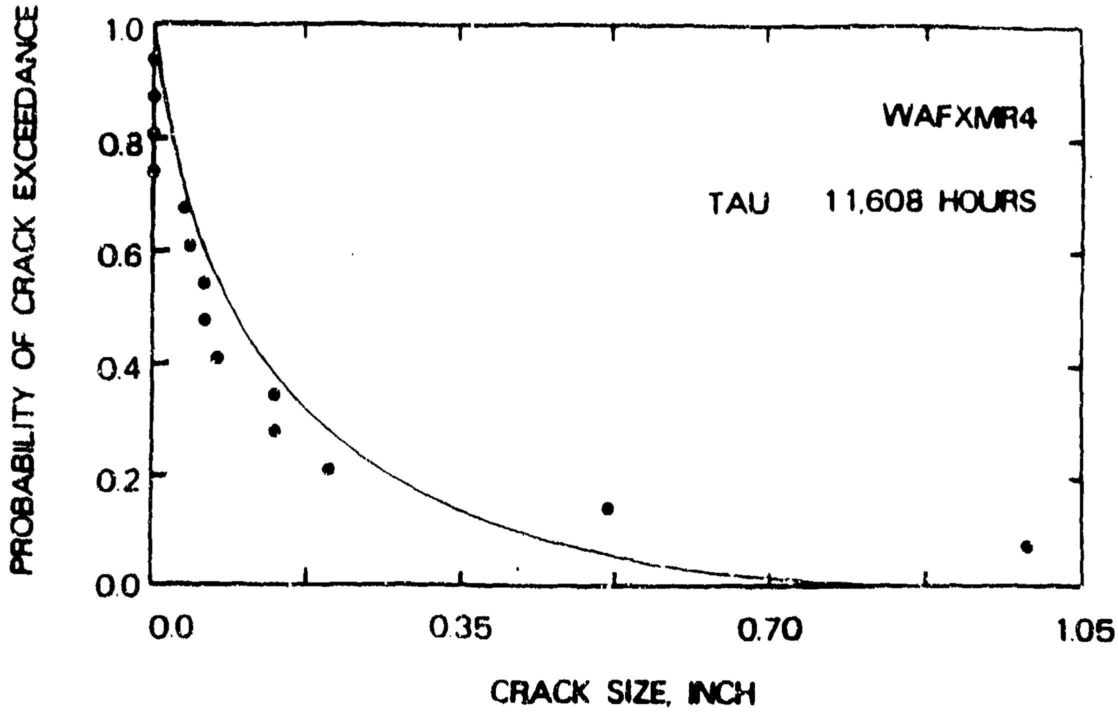

Figure 48. Correlations Between Theoretical Predictions and Experimental Results (WAFXMR4 Data Set) for Crack Exceedance Probability $p(i,\tau)$ at τ = 11608 Flight Hours Based on DCGA-DCGA.

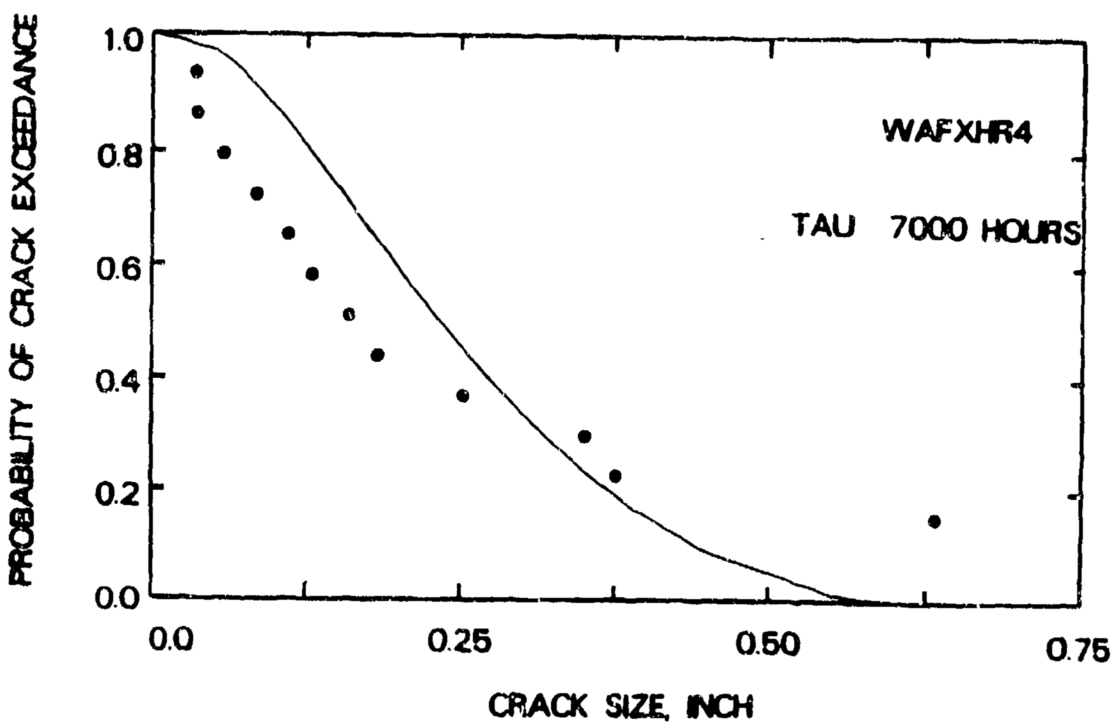

Figure 49. Correlations Between Theoretical Predictions and Experimental Results (WAFXHR4 Data Set) for Crack Exceedance Probability $p(i,\tau)$ at τ = 7000 Flight Hours Based on DCGA-DCGA.

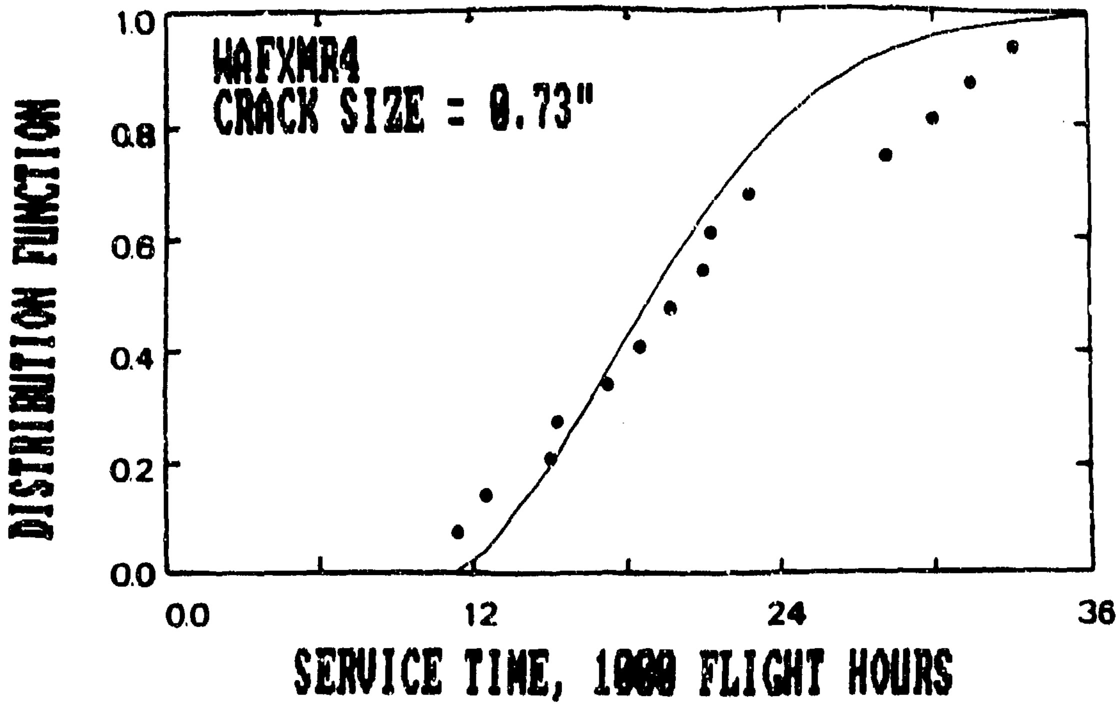

Figure 50. Correlations Between Theoretical Predictions and Experimental Results (WAFXMR4 Data Set) for Cumulative Distribution of Service Time to Reach Crack Size x_1 = .73" Based on DCGA-DCGA.

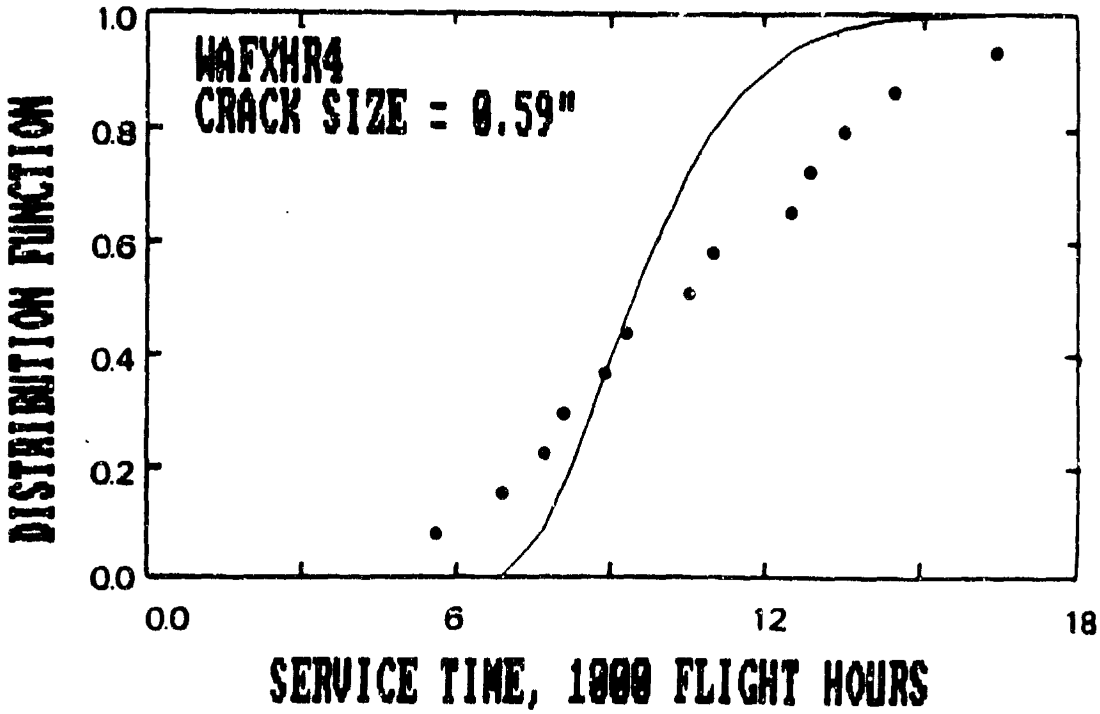

Figure 51. Correlations Between Theoretical Predictions and Experimental Results (WAFXHR4 Data Set) for Cumulative Distribution of Service Time to Reach Crack Size x_1 = .59" Based on DCGA-DCGA.

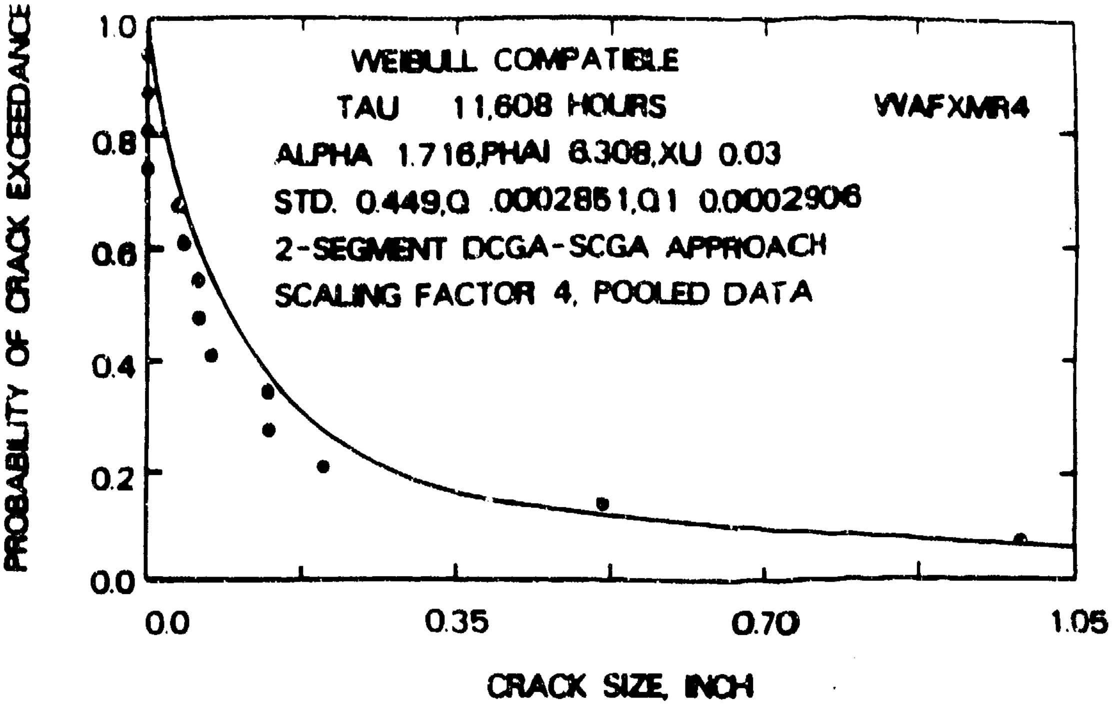

Figure 52. Correlations Between Theoretical Predictions and Experimental Results (WAFXMR4 Data Set) for Crack Exceedance Probability p(i, τ) at τ = 11608 Flight Hours Based on DCGA-SCGA.

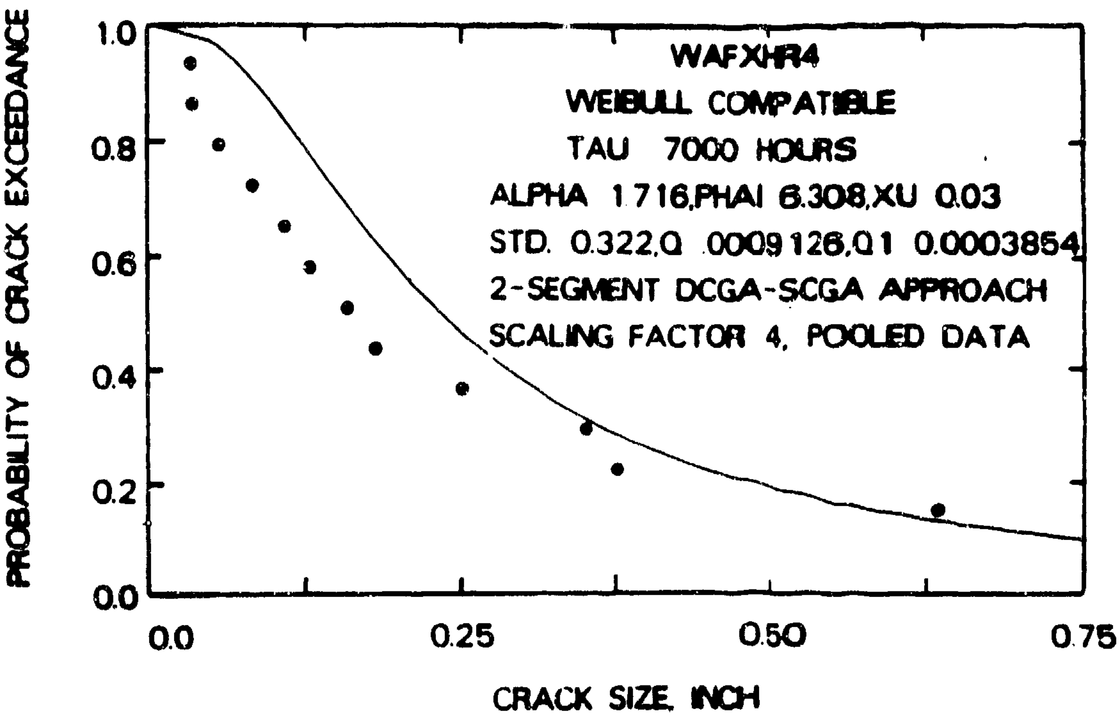

Figure 53. Correlations Between Theoretical Predictions and Experimental Results (WAFXHR4 Data Set) for Crack Exceedance Probability p(i, τ) at τ = 7000 Flight Hours Based on DCGA-SCGA.

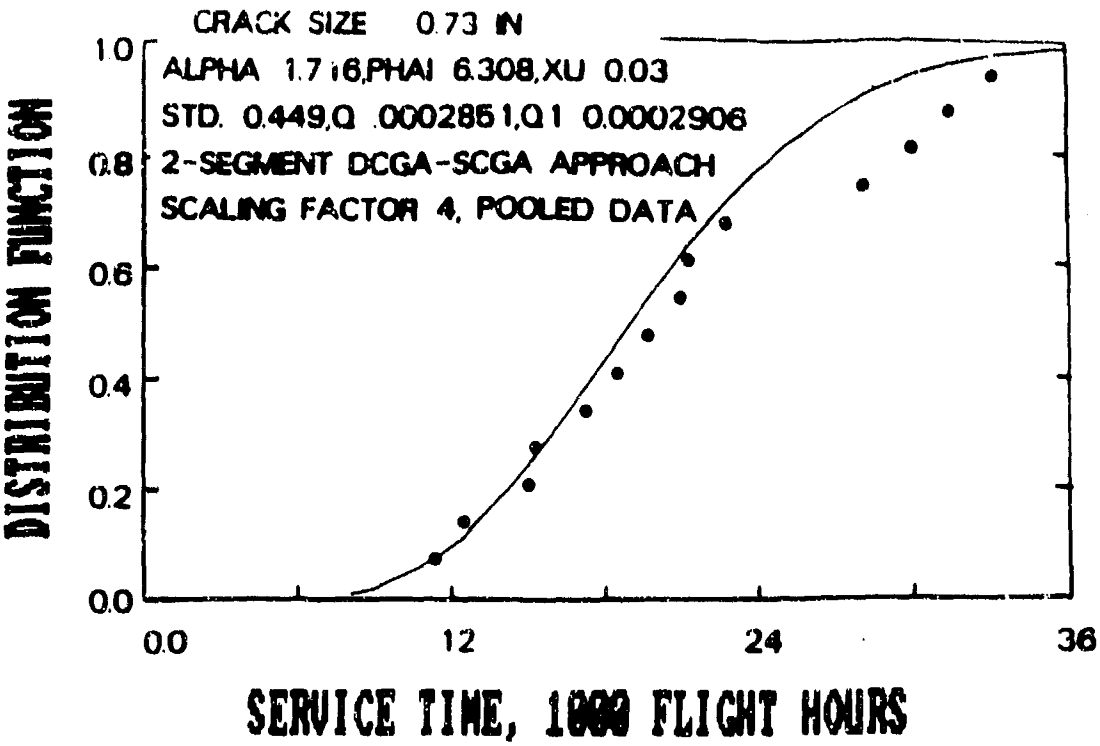

Figure 54. Correlations Between Theoretical Predictions and Experimental Results (WAFXMR4 Data Set) for Cumulative Distribution of Service Time to Reach Crack Size x_1 = .73" Based on DCGA-DCGA.

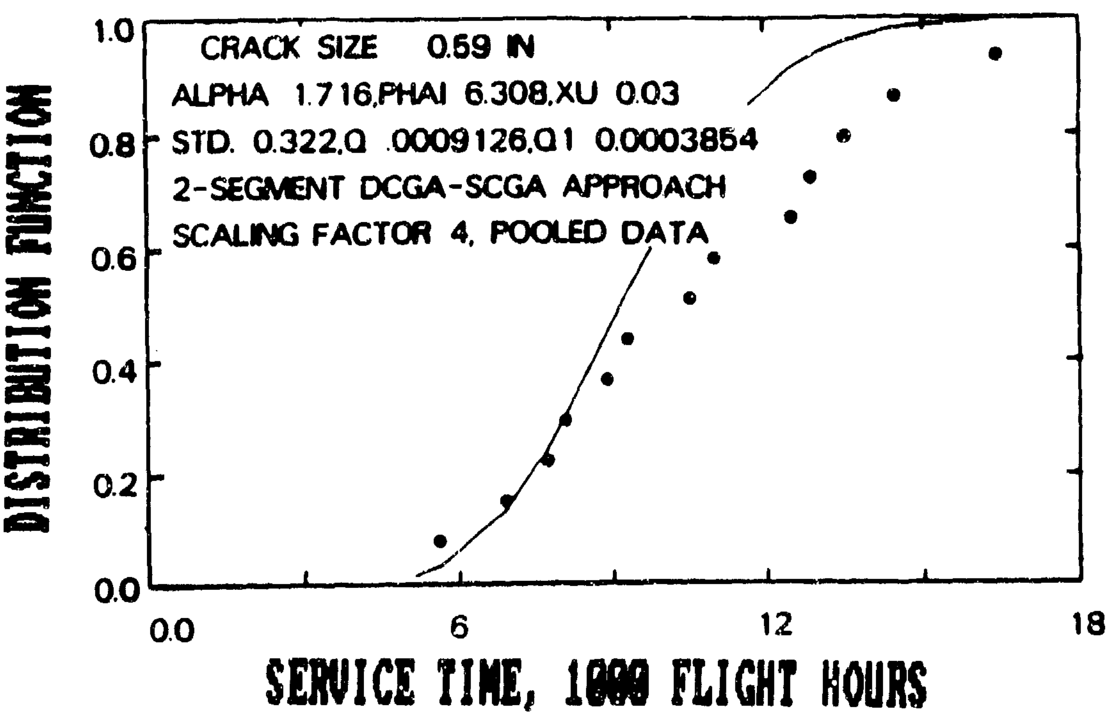

Figure 55. Correlations Between Theoretical Predictions and Experimental Results (WAFXHR4 Data Set) for Cumulative Distribution of Service Time to Reach Crack Size x_1 = .59" Based on DCGA-SCGA.

2. Excellent correlations were obtained for the WAFXMR4 and WAFXHR4 data sets for the DCGA-SCGA. In this case, better overall correlations were obtained using the DCGA-SCGA than the DCGA-DCGA.

3. The correlations for the WAFXMR4 data sets were slightly better than those for the WAFXHR4 data set for both the DCGA-DCGA and the DCGA-SCGA.

4.3.2 Straight-Bore Fastener Hole Specimens

The durability analysis extension for the DCGA-DCGA and the DCGA-SCGA are demonstrated for straight-bore clearance-fit fastener holes in 7475-T7357 aluminum herein. Procedures for the demonstration are given as follows.

1. The IFQ for straight-bore clearance-fit fastener holes is based on the Weibull-compatible EIFSD. Two narrow width (W = 1.5") specimen data sets (WPF and XWPF; see Figs. 4 and 5, respectively) and a data pooling procedure [1] were used to estimate the EIFSD parameters with the results: x_u = 0.03", α = 4.782 and ϕ = 4.658. These parameters are given in Table 11 under IFQ case 3 and they will be used for demonstration purposes herein. Details for estimating these parameters are given in Section 3.3.2.2.

2. The crack growth rate model of Eqs. 20 and 28 (with $b_1 = b_2 = 1$) and fractographic data for the WWPF data set are used to estimate the crack growth parameter Q_1 and Q_2 respectively, in the small and large crack size regions. In the present demonstrations, AL-AU = 0.01" - 0.05" is used for the small crack size region (i.e., "segment 1") and a_0 - AU' = 0.05" - 1" is used for the large crack size region (i.e., "segment 2"). Results for Q_1, Q_2 and σ_z for the WWPF data set are summarized in Table 14.

Table 14. Summary of Pooled Q and σ_z Values for WWPF Data Set.

DATA SET (1)	NO. SPECIMENS	SEGMENT 1 (3)	SEGMENT 2 (4)	
		$Q \times 10^{4}$ (1/HR.)	$Q \times 10^{4}$ (1/HR.)	σ_z
WWPF (2)	13	2.742	3.124	0.177

Notes: (1) Material: 7475-T7351 aluminum; straight-bore fastener holes with clearance-fit fasteners (NAS 6204-08)

(2) Ref. Fig. 2

(3) AL - AU = 0.01" - 0.05"

(4) a_0 - AU = 0.05" - 1"

(5) Ref. Eq. 32 (natural log basis)

3. Theoretical predictions for the probability of crack exceedance, $p(i,\tau)$, at service time τ = 18,400 flight hours, are shown in Figs. 56 and 57 for the DCGA-DCGA and the DCGA-SCGA, respectively. In both figures experimental results for the WWPF data set are plotted as plus signs (+) for comparison.

4. Theoretical predictions for the cumulative distribution of service time to reach a crack size x_1 = 0.5" are shown in Figs. 58 and 59 for the DCGA-DCGA and the DCGA-SCGA, respectively. Experimental results for the WWPF data set are plotted as plus signs (+) for comparison.

The following observations are based on the plots shown in Figs. 56 - 59 for the WWPF data set and the lessons learned under this program.

1. Excellent correlations were obtained between predictions for $p(i,\tau)$ and $F_{T(x_1)}(\tau)$ and experimental results for the WWPF data set for both the DCGA-DCGA and DCGA-SCGA (see Figs. 56 - 59).

2. A statistical scaling procedure was developed in Vol. 1 [1] so that fractographic results for specimens with a different number of holes per specimen could be used to estimate the EIFSD parameters in a global sense. IFQ case 3 (see Table 11) was used for the demonstration herein. The statistical scaling technique reflected in IFQ case 3 is recommended for durability analysis predictions. However, scaling the fractographic results for specimens with a different number of fastener holes involves complex issues, e.g., fatigue cracking interactions in fastener holes, bolt load transfer, assumption of independent cracking, etc. Further research on statistical scaling is needed to better understand the ef-

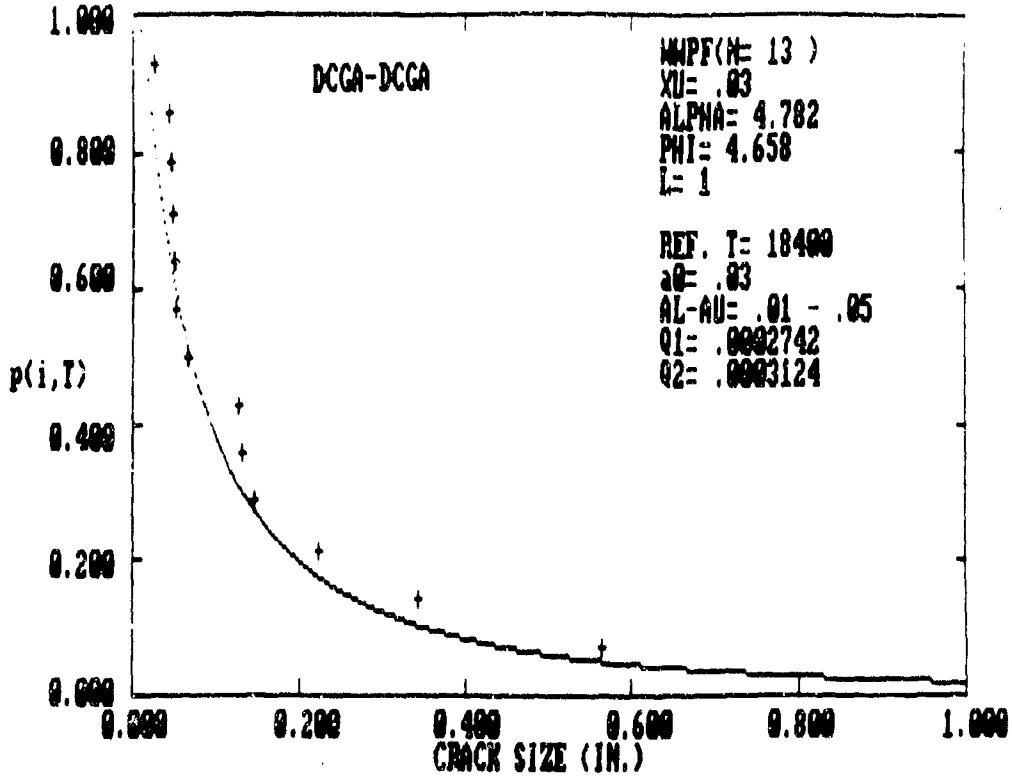

Figure 56. Correlations Between Theoretical Predictions and Experimental Results (WWPF Data Set) for Crack Exceedance Probability $p(i,\mathcal{T})$ at $\mathcal{T}$= 18400 Flight Hours Based on DCGA-DCGA.

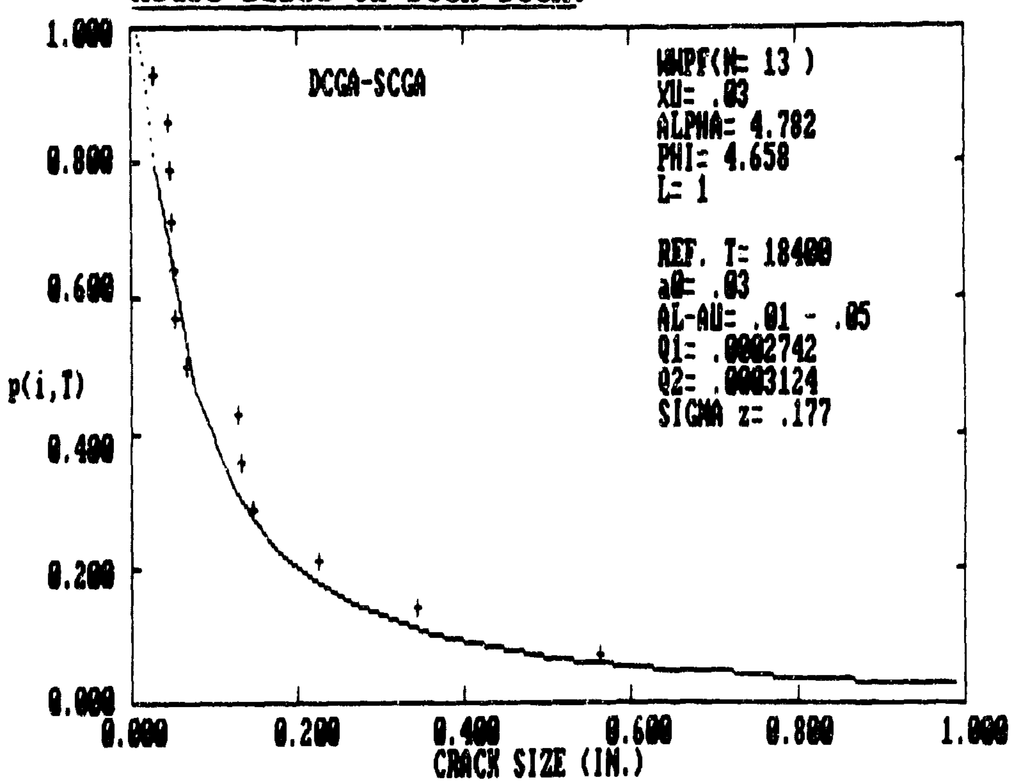

Figure 57. Correlations between Theoretical Predictions and Experimental Results (WWPF Data Set) for Crack Exceedance Probability $p(i,\mathcal{T})$ at $\mathcal{T}$= 18400 Flight Hours Based on DCGA-SCGA.

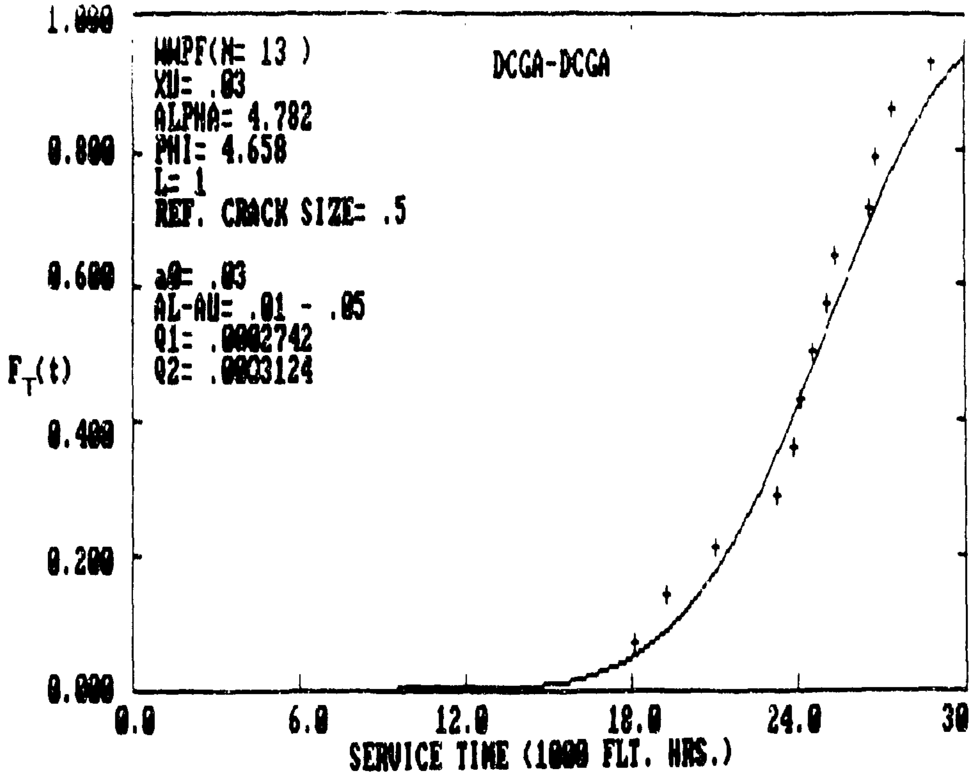

Figure 58. Correlations Between Theoretical Predictions and Experimental Results (WWPF Data Set) for Cumulative Distribution of Service Time to Reach Crack Size x_1 = 0.5" Based on DCGA-DCGA.

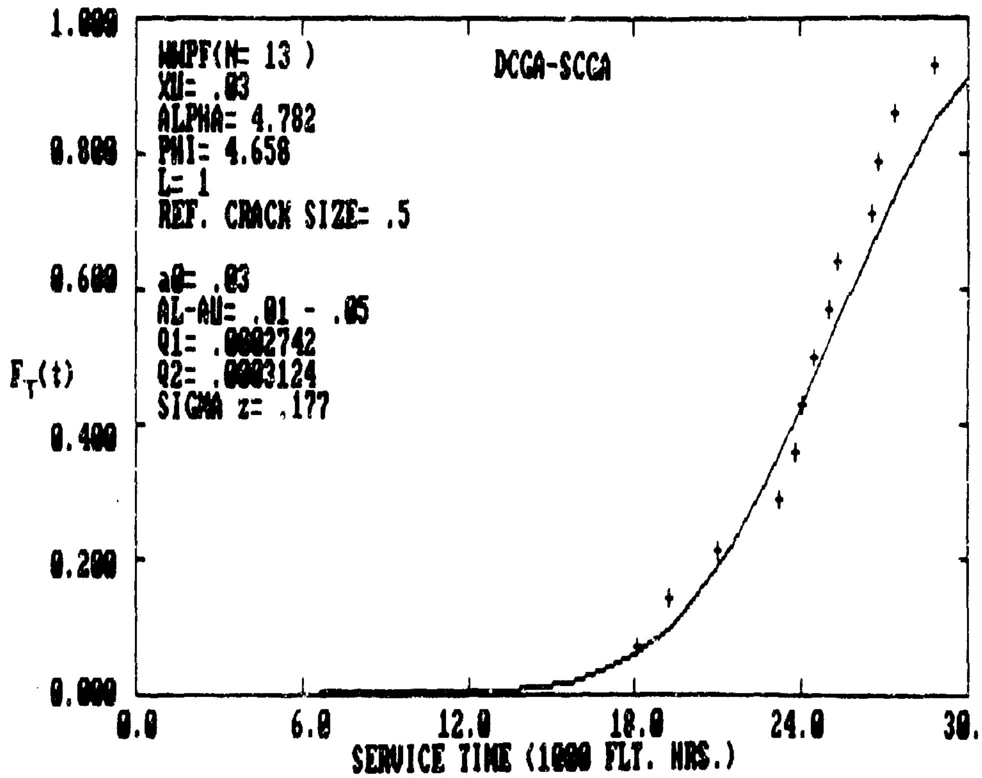

Figure 59. Correlations Between Theoretical Predictions and Experimental Results (WWPF Data Set) for Cumulative Distribution of Service Time to Reach Crack Size x_1 = 0.5" Based on DCGA-SCGA.

fects of scaling on the initial fatigue quality estimation and the accuracy for $p(i,\tau)$ and $F_{T(x_1)}(\tau)$ predictions.

3. Predictions for $p(i,\tau)$ and $F_{T(x_1)}(\tau)$ based on the DCGA-SCGA correlated slightly better than those based on the DCGA-DCGA, particularly in the large crack size region. Therefore, based on the results presented herein, the DCGA-SCGA is considered to be superior to the DCGA-DCGA.

4.4 DEMONSTRATION FOR THE F-16 LOWER WING SKINS

The two-segment DCGA-DCGA and DCGA-SCGA are demonstrated and evaluated in the following using the F-16 lower wing skin. Predictions will be correlated with results from the F-16 wing durability test articles. The F-16 wing box assembly is shown in Fig. 60 and stress regions for the lower wing skin are shown in Fig. 61.

A full-scale F-16 wing durability test was conducted using the F-16 1000 hour spectrum, consisting of two 500-hour blocks. After fatigue testing to 16,000 flight hours, a tear-down inspection was performed. All fastener holes in both lower wing skins (i.e., 3228 holes) were inspected using the eddy current technique. Each fastener hole with a crack indication was broken open and a fractographic analysis was performed. Tear-down inspection and fractographic results are documented in Ref. 4.

A durability analysis of the F-16 lower wing skins has been previously reported [8,9,11,20]. This analysis was concerned with relatively small fatigue cracks (e.g., $x_1 \leq 0.03"$) and reflected the one-segment DCGA [6,8].

The following procedures are used to demonstrate and

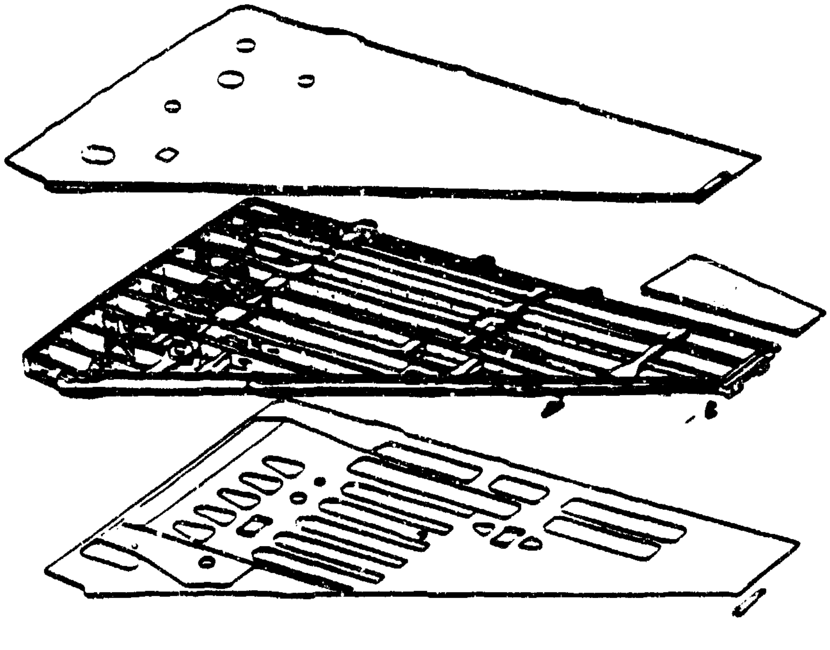

Figure 60. F-16 Wing Box Assembly.

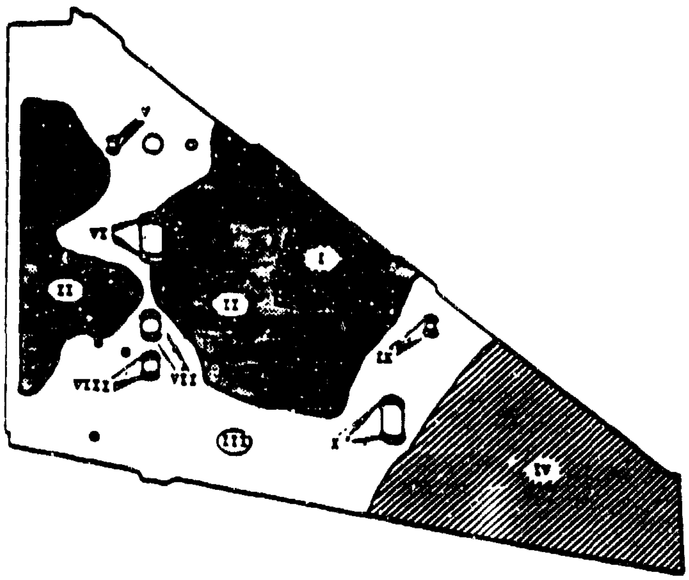

Figure 61. Stress Regions for F-16 Lower Wing Skin.

evaluate the two-segment DCGA-DCGA and DCGA-SCGA using the F-16 lower wing skins.

1. The IFQ is based on the fractographic results from AFXLR4, AFXMR4 and AFXHR4 data sets. A data pooling procedure based on the CLSSA is used to estimate the Weibull compatible EIFSD parameters; with the results used: $x_u = 0.03"$, $\alpha = 1.716$ and $\phi = 6.308$, see Table 13. These EIFSD parameters, based on the AL-AU = 0.01" - 0.05" and $\ell = 4$ for each of the three data sets, characterize the distribution of EIFS for a single hole population.

2. The F-16 lower wing skin is divided into 10 stress regions as shown in Fig. 61. The stress level and the number of fastener holes in each stress region are shown in Table 15.

3. The crack growth rate parameter, Q_1 for segment 1, in each stress region are determined using (1) the available pooled Q values from the AFXLR4, AFXMR4 and AFXHR4 data sets (see Table 13; AL-AU = 0.01" - 0.05"), and (2) the model for Q as a function of stress given by Eq. 43. Results of the model parameters C and V in Eq. 43 obtained from three data sets (AFXLR4, AFXMR4 and AFXHR4) are shown in Figs. 47 and 62(a).

4. The crack growth rate parameters, Q_2, for segment 2 in each stress region are determined using available wide specimen fractographic results of WAFXMR4 and WAFXHR4 in a_0 - AU' = 0.05" - 0.5" along with Eq. 43. The model parameters C and V obtained from WAFXMR4 and WAFXHR4 data sets are shown in Fig 62(b).

5. Prediction for $p(i,\tau)$ in each stress region using the two-segment DCGA-DCGA is computed from Eqs 22 - 26. Equations 33 - 38 are used to compute $p(i,\tau)$ in each stress region using the DCGA-SCGA.

Table 15. Stress Levels and Number of Fastener Holes for F-16 Lower Wing Skin

STRESS REGION	MAX. STRESS LEVEL (ksi)	NO. OF FASTENER HOLES
I	28.3	59
II	27.0	320
III	24.3	680
IV	16.7	469
V	28.4	8
VI	29.2	30
VII	32.4	8
VIII	26.2	8
IX	26.2	12
X	25.7	20
		1614

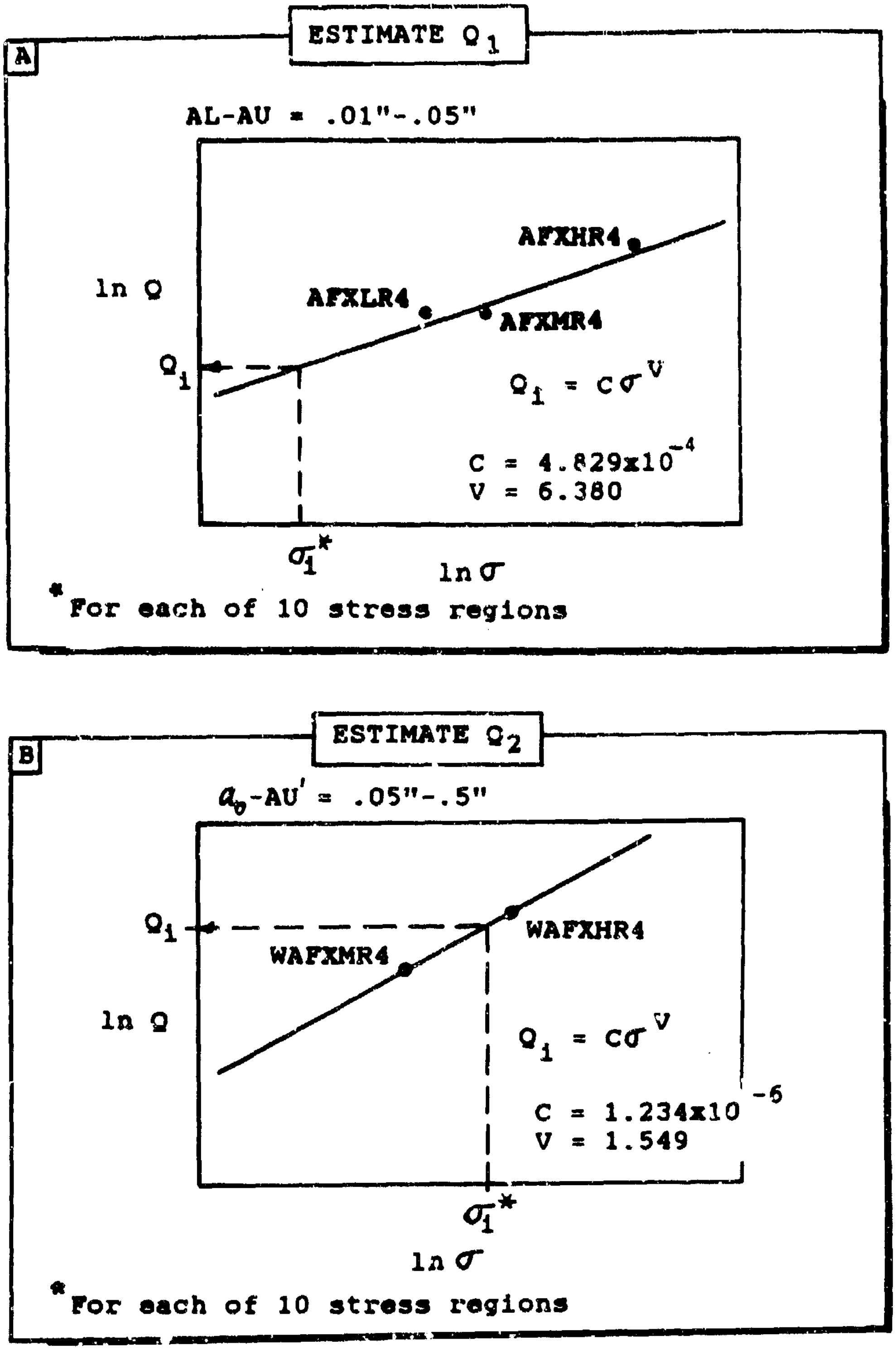

Figure 62. General Approach for Estimating Service Crack Growth Parameters Q_1 and Q_2.

6. From the predicted crack exceedance probability, $p(i, \tau)$, and the number of fastener holes in each stress region, the statistics for the number of cracks exceeding some crack sizes in the entire lower wing skin are computed using the Binomial distribution, Eqs. 39 - 42.

7. Theoretical predictions will be correlated with actual test results from the F-16 durability test articles. Results will be plotted in a useful format for evaluating the two-segment DCGA-DCGA and the DCGA-SCGA for durability analysis.

The same three fractographic data sets, i.e. AFXLR4, AFXMR4 and AFXHR4, were used to determine the EIFSD parameters in the previous [8] and present durability analyses for F-16 lower wing skin. However, different α and ϕ values for x_u = 0.03" are obtained in the present analysis due to different: (1) AL-AU ranges used, (2) fractographic data processing methods/screening considerations used. The resulting EIFSD parameter values are x_u = 0.03", α = 1.716 and ϕ = 6.308 (see Table 13).

In the previous durability analysis [8], experimental terminal crack size dimensions in fastener holes were based on initial measurements of the fracture. In the present durability analysis, however, terminal crack sizes were based on the fractography. The final crack dimensions based on the fractography are more accurate than the initial fracture surface measurements. There are small differences between the initial crack size dimensions and those based on the fractography. As a result of these differences, the experimental results for the average number of fastener holes/skin (for both wing skins) with a crack size 0.03" is 14.5 holes (fractography) versus 16.5 holes (initial measurements).

The F-16 durability test article was fatigue tested to 16,000 flight hours using the F-16 1,000 hour spectrum. This preliminary spectrum included two 500 hour blocks. The F-16 400 hour spectrum has been used extensively in recent years for General Dynamics IRAD and CRAD research programs. This spectrum is slightly more severe than the F-16 1,000 - hour spectrum but it doesn't apply to F-16 production aircraft. It is assumed for durability analysis purposes that the coupon fractographic results (i.e., AFXLR4, AFXMR4, AFXHR4, WAFXMR4 and WAFXHR4) based on the F-16 400 - hour spectrum directly can be applied to the prediction of the F-16 durability test article.

The F-16 lower wing skins contain several cutouts. However, the present durability analysis/correlation covers only fatigue cracks in fastener holes.

4.4.1 Estimation of Service Crack Growth Parameters

The service crack growth parameters Q_1 and Q_2 were estimated for the small (i.e., AL-AU =0.01" - 0.05") and large crack size region (i.e., a_0 - AU' = 0.05" - 0.5") for each of the ten stress regions. A general approach for estimating Q_1 and Q_2 is described in Fig. 62. In the small crack size region, Q_1 values for the AFXLR4, AFXMR4 and AFXHR4 data sets were obtained previously (Table 13 and Fig. 47). From these Q_1 values, the constants C and V in Eq. 43 were determined using a least-squares fit procedure (Fig. 47). Then, Q_1 values in each of the ten stress regions are computed from Eq. 43, and the results are shown in Table 16.

A similar approach to that described above was used for the large crack size region to estimate Q_2 for each of the ten stress regions. In this case, fractographic results of the WAFXMR4 and WAFXHR4 data sets (see Table 12) were used to estimate the constants C and V in Eq. 43. Results are shown in Table 16 and in Fig. 63.

In practice, suitable fractographic data may not be available to estimate Q_1 and Q_2. In such cases, an analytical crack growth program [e.g., 18,19] can be used to estimate the crack size versus time information needed to establish Q_1 and Q_2 for given durability analysis conditions (e.g., stress level, load spectrum, % bolt load transfer, etc.). (Refer to Vol. I [1] and the durability design handbook (2nd Edition) [21] for guidelines and procedures).

4.4.2 Theoretical/Experimental Correlations

Probability of crack exceedance predictions $p(i,\tau)$ at τ = 16,000flight hours for five different crack sizes (i.e., x_1 = 0.03", 0.05", 0.1", 0.2" and 0.3") are shown in Tables 17 and 18 for the two-segment DCGA-DCGA and the DCGA-SCGA, respectively. The average number of fastener holes in each stress region, $\bar{N}(i,\tau)$ with a crack size greater than x_1 at τ = 16,000 flight hours is also shown in these two tables. The analysis for the DCGA-SCGA was conducted using $\sigma_z = 0.3$ (natural log basis), which is quite reasonable for countersunk fastener holes in 7475-T7351 aluminum [21].

Predictions for the average number of fastener holes in the entire lower wing skin with a crack size > x_1 at 16,000 flight hours, $\bar{L}(\tau)$, and the standard deviation, $\sigma_L(\tau)$, are shown in Table 19 for both the DCGA-DCGA and the DCGA-SCGA. $\bar{L}(\tau)$ and $\sigma_L(\tau)$ values are computed based on the Binomial distribution, Eqs. 39 and 40. The tear-down inspection results based on the average of two lower wing skins are shown in the same table for comparison.

Theoretical predictions for the average number of fastener holes with a crack size > x_1 at τ= 16,000 flight hours

Table 16. Summary of Crack Growth Rate Parameters for Each Stress Region.

STRESS REGION	MAX. STRESS LEVEL (ksi)	NO. OF FASTENER HOLES	$Q_1 \times 10^4$ (1) (1/HR.)	$Q_2 \times 10^4$ (2) (1/HR.)
1	28.3	59	0.884	2.187
2	27.0	320	0.655	2.033
3	24.3	680	0.334	1.727
4	16.7	469	0.030	0.966
5	28.4	8	0.904	2.199
6	29.2	30	1.080	2.296
7	32.4	8	2 097	2.697
8	26.2	8	0.541	1.941
9	26.2	12	0.541	1.941
10	25.7	20	0.478	1.884
		1614		

Notes: (1) Segment 1: AL-AU = .01"-.05"
$C_1 = 4.829 \times 10^{-14}$; $V_1 = 6.380$
(2) Segment 2: AL-AU = .05"-.5"
$C_2 = 1.234 \times 10^{-6}$; $V_2 = 1.549$

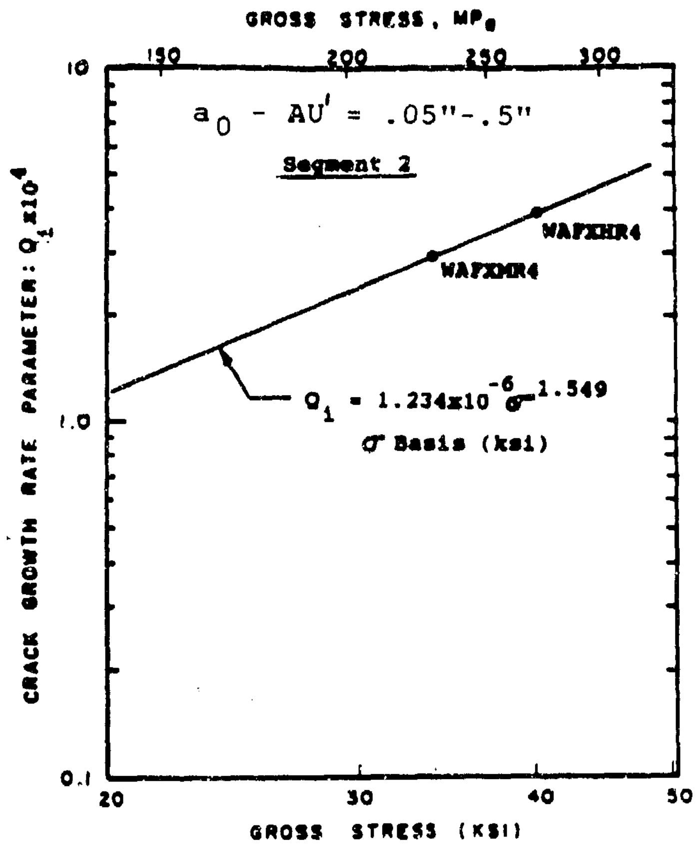

Figure 63. Crack Growth Rate Parameter Q Versus Gross Stress for Wide Specimen Data Sets (WAFXMR4 and WAFXHR4).

Table 17. Crack Exceedance Probability and Average Number of Fastener Holes with Crack Size Exceeding x_1 at $\mathcal{T}$ = 16000 Flight Hours in Each Stress Region Based on DCGA-DCGA

STRESS REGION	x_1 = 0.03"		x_1 = 0.05"		x_1 = 0.1"		x_1 = 0.2"		x_1 = 0.3"	
	$p(i,\mathcal{T})$	$\bar{N}(i,\mathcal{T})$	$p(i,\mathcal{T})$	$\bar{N}(i,\mathcal{T})$	$p(i,\mathcal{T})$	$\bar{N}(i,\mathcal{T})$	$p(i,\mathcal{T})$	$\bar{N}(i,\mathcal{T})$	$p(i,\mathcal{T})$	$\bar{N}(i,\mathcal{T})$
1	.0739	4.36	.035	2.07	.018	1.06	.00674	.39	.00222	.13
2	.0449	14.37	.0145	4.64	.0056	1.81	.000687	.22	----	--
3	.0144	9.79	.0000683	0.05	----	--	----	--	----	--
4	.00023	0.11	.0000065	0.00	----	--	----	--	----	--
5	.0768	0.61	.0371	0.29	.020	.16	.00752	.06	.00265	.02
6	.1027	3.08	.0576	1.73	.034	1.02	.0158	.47	.00782	.23
7	.2871	2.29	.2250	1.80	.16	1.28	.1065	.85	.0772	.62
8	.0326	0.26	.00714	0.06	.0019	.01	----	--	----	--
9	.0326	0.39	.00714	0.09	.0019	.02	----	--	----	--
10	.0264	0.53	.00403	0.08	.0005	.01	----	--	----	--
		35.79		10.81		5.37		1.99		1.00

Table 18. Crack Exceedance Probability and Average Number of Fastener Holes with Crack Size Exceeding x_1 at $\mathcal{T}$ = 16000 Flight Hours in Each Stress Region Based on DCGA-SCGA.

STRESS REGION	x_1 = 0.03"		x_1 = 0.05"		x_1 = 0.1"		x_1 = 0.2"		x_1 = 0.3"	
	$p(i,\mathcal{T})$	$\bar{N}(i,\mathcal{T})$	$p(i,\mathcal{T})$	$\bar{N}(i,\mathcal{T})$	$p(i,\mathcal{T})$	$\bar{N}(i,\mathcal{T})$	$p(i,\mathcal{T})$	$\bar{N}(i,\mathcal{T})$	$p(i,\mathcal{T})$	$\bar{N}(i,\mathcal{T})$
1	.0739	4.36	.0350	2.07	.0183	1.08	.0071	.42	.00348	.20
2	.0449	14.37	.0145	4.64	.00566	1.81	.00126	.40	.000419	.13
3	.0144	9.79	.0000683	.05	.0000066	.004	.0000066	.004	.0000066	.004
4	.000239	.11	.00	.00	.0000066	.003	.0000066	.003	.0000066	.003
5	.0768	.61	.0371	.29	.0196	.16	.00783	.06	.00392	.03
6	.103	3.09	.0577	1.73	.0335	1.00	.0158	.47	.00894	.27
7	.287	2.29	.225	1.80	.160	1.28	.104	.83	.0756	.60
8	.0326	.26	.00714	.06	.00187	.01	.000196	.002	.0000451	.00
9	.0326	.39	.00714	.09	.00187	.02	.000196	.002	.0000451	.00
10	.0264	.53	.00403	.08	.000621	.01	.000031	.001	.0000096	.00
		35.80		10.81		5.377		2.192		1.237

Table 19. **Statistics for Number of Fastener Holes with Crack Size Exceeding x_1 in F-16 Lower Wing Skin for Both DCGA-DCGA and DCGA-SCGA.**

x_1 (IN.)	DCGA-DCGA		DCGA-SCGA		EXPERIMENTAL RESULTS (AVE.)
	$L(\tau)$	$\sigma_L(\tau)$	$L(\tau)$	$\sigma_L(\tau)$	
0.03	35.80	5.800	35.80	5.800	14.5
0.05	10.81	3.185	10.81	3.185	9.5
0.1	5.37	2.258	5.38	2.262	7.0
0.2	1.99	1.379	2.19	1.450	1.0
0.3	1.00	0.977	1.24	1.097	0.5

in the entire lower wing skin are plotted in Fig. 64 for both of the two-segment crack growth approaches. In this figure, the results for the DCGA-DCGA and the DCGA-SCGA are depicted by a solid curve and a dashed curve, respectively. Results for both approaches are identical for the crack size $x_1 \leq 0.05"$ in the first crack growth segment. The tear-down inspection results are shown in Fig. 64 as solid circles for comparison. These results reflect the average extent of damage for a lower wing skin based on the total extent of damage for both lower wing skins combined.

The extent of damage estimate for an exceedance probability of P = 0.05 is also plotted in Fig. 64 as a solid-dashed-solid curve (—— —— ——). This curve represents the estimated upper bound limit for extent of damage for P = 0.05. It is computed from $\bar{L}(\tau) + 1.65\,\sigma_L(\tau)$ where $\bar{L}(\tau)$ and $\sigma_L(\tau)$ values are shown in Table 19 for the DCGA-SCGA. Since the number of details in each stress region is large, it is reasonable to approximate the binomial distribution by the normal distribution. Hence, the predicted mean extent of damage, $\bar{L}(\tau)$, corresponds to an exceedance probability of P = 0.5.

To illustrate the usefulness of the extent of damage concept consider, for example, the extent of damage at x_1 = 0.3" in Fig. 64. The (predicted) probability is 50% (i.e., P = 0.5) that 1.24 fastener holes will have a crack size exceeding x_1 = 0.03"; whereas, the probability is 5% (i.e., P = 0.05) that 3.05 fastener holes will have a crack size larger than x_1 = 0.03" at τ = 16,000 flight hours. Therefore, the durability analysis provides quantitative estimates of the extent of damage mean and upper bound limit. This type of information provides a physical description of the state of damage for a durability-critical component and a logical basis for estimating structural maintenance/repair requirements and costs.

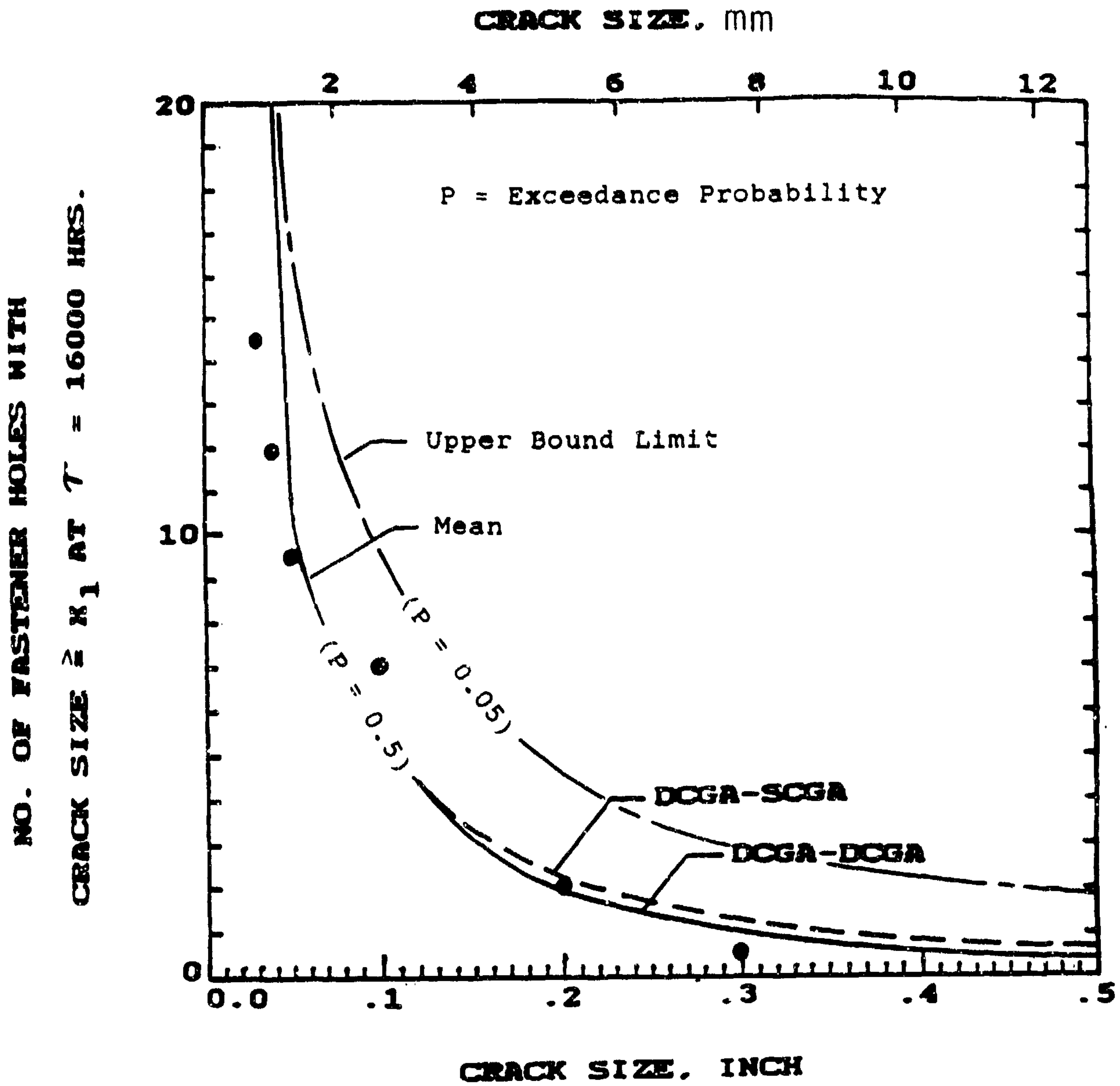

Figure 64. Correlations between Theoretical Predictions and Experimental Results for Fighter Lower Wing Skin for Extent of Damage at τ = 16000 Flight Hours.

4.4.3 Discussion of Results

Two different two-segment approaches (i.e., DCGA-DCGA and DCGA-SCGA) have been demonstrated and evaluated using fractographic results for both coupon specimens and lower wing skins from a fighter aircraft. Straight bore and countersunk fastener holes with clearance-fit fasteners were considered. Results for both two-segment approaches were compared for the lower wing skin demonstration. Both approaches are considered reasonable for evaluating functional impairment due to fuel leakage/ligament breakage in metallic aircraft structures. However, the DCGA-SCGA is recommended for durability analysis because predictions are more accurate and slightly more conservative than those based on the DCGA-DCGA.

The stress level for each stress region is important for crack growth predictions. Therefore, the stress analysis for durability-critical components should reflect appropriate finite element model grid sizes to obtain the desired stress analysis accuracy for each stress region.

SECTION V

DURABILITY ANALYSIS STUDIES

Numerous studies were conducted during this program to evaluate and refine durability analysis and data processing methods. These studies are documented in Appendices B-J. A brief description of the durability analysis software developed for this program is presented in Appendix A. A software user's guide is provided in Volume V [5].

SECTION VI

CONCLUSIONS AND RECOMMENDATIONS

6.1 CONCLUSIONS

1. A comprehensive probabilistic durability analysis approach has been developed for metallic aircraft structures. It applies to the crack growth accumulation in any type of structural detail (e.g., fastener holes, cutouts, fillets, etc.). The approach has been verified for clearance-fit fastener holes in 7475-T7351 aluminum at two levels: (1) coupon specimens and (2) full-scale aircraft structure. Very reasonable durability analysis results have been obtained, including damages due to both small cracks (e.g., $\leq$ 0.05") and large through-the-thickness cracks (e.g., $\geq$ 0.5").

2. It has been shown that the initial fatigue quality (IFQ) of both straight-bore and countersunk fastener holes with clearance-fit fasteners can be reasonably estimated using fractographic results from coupon specimens and that the IFQ can be represented by an equivalent initial flaw size distribution (EIFSD). Furthermore, it has been demonstrated that the IFQ of fastener holes in full-scale structures can be defined using coupon specimens.

3. The probabilistic durability analysis approach developed can be used to "quantify" structural durability in meaningful terms, such as: (1) probability of crack exceedance at any service time, (2) probability of functional impairment at any service time, (3) cumulative distribution of service time to reach any given crack size, (4) extent of damage and (5) structural wearout rate. Since the probabilistic approach developed accounts for the fatigue crack growth accumulation in each structural detail susceptible to fatigue cracking in service, it is referred to as a "quanti-

tative durability analysis approach." The extent of damage prediction at a given service time is defined by the statistics, such as the average and standard deviation, of the number of structural details expected to exceed functional impairment crack size limits. This quantitative prediction provides an effective basis for evaluating functional impairment, economic life and structural wearout, and trade-offs as a function of the design and service variables.

4. The probabilistic durability analysis approach is a powerful "durability design tool." It gives the user new durability analysis capabilities and features not provided by the existing deterministic crack growth approach based on the "worst case" detail within a group of details. The probabilistic durability analysis method is not intended to completely replace the deterministic crack growth approach in the durability design process. The deterministic crack growth approach will continue to be a valuable tool for durability analysis - primarily during the preliminary design process. Since a deterministic crack growth analysis provides information only for the "worst case" detail within a group of details, it cannot provide the "extent of damage" type information for the entire population of structural details.

5. Actual initial flaws in the bore of manufactured fastener holes in metallic aircraft structures usually consist of random scratches, burrs, microscopic imperfections, etc. Such flaws, except for gross manufacturing defects, cannot be reliably detected and quantified by NDE for production aircraft structures. In reality, the actual initial flaws in fastener holes produced by manufacturing and assembly are not physical "cracks" in the usual sense associated with the linear elastic fracture mechanics approach. Whatever the source of fatigue cracking may be, a practical method for representing the reality of the as-manufactured condition is needed for durability

analysis. This is taken care of by the equivalent initial flaw concept.

6. An equivalent initial flaw size (EIFS) is an artificial crack size which results in an actual crack size at an actual point in time when the equivalent initial flaw is grown forward. It is determined by back-extrapolating fractographic results and has the following characteristics: (1) An EIFS is an artificial crack assumed to represent the initial fatigue quality of a structural detail in the as-manufactured condition whatever the source of fatigue cracking may be, (2) no direct relationship to actual initial flaws in fastener holes such as scratches, burrs, microdefects, etc., and it cannot be verified by NDI, (3) it has a universal crack shape in which the crack size is measured in the direction of crack propagation, (4) EIFSs are in a fracture mechanics format but they are not subject to such laws and limitations as the "short crack effect," (5) it depends on the fractographic data used, the fractographic crack size range for the back-extrapolation and the crack growth rate model used, (6) it must be grown forward in a manner consistent with the basis for the EIFS, and (7) EIFSs are not unique - a different set is obtained for each crack growth law used for the back-extrapolation.

7. Equivalent initial flaw sizes (EIFSs) are determined by back-extrapolating fractographic results. Since the fractographic data depends on the testing conditions (e.g., load spectrum, fastener holes, cutout, etc.), EIFSs are not strictly "generic." However, EIFSD parameters can be estimated for different fractographic data sets using the data pooling and statistical scaling procedures. It has been conclusively shown that the EIFSD based on given fractographic data sets can be used to obtain very reasonable durability analysis predictions for the other data sets and full-scale aircraft structure for clearance-fit fastener holes (both

straight-bore and countersunk) in 7475-T7351 aluminum. It should be clear that an EIFSD does not necessarily contain the "rogue flaw."

8. When an EIFSD is grown forward to a selected service time, the service crack growth should be consistent with the "basis" for the EIFSs. Therefore, the analytical crack growth program used [e.g., 18,19] should be "tuned" or "curve fitted" to the EIFS master curves reflected in the EIFSD.

9. Probabilistic-based durability analysis methods [1, 14,16] are now sufficiently developed and demonstrated for immediate applications to metallic airframes. An updated durability design handbook [21] and software for an IBM or IBM-compatible PC are available for implementing the advanced durability analysis [5].

10. A "natural fatigue crack" data base for estimating the initial fatigue quality of structural details can be acquired as a part of the Aircraft Structural Integrity Program (ASIP) test plan. For example, by not preflawing structural details in test specimens, "natural fatigue crack" data can be obtained--thereby satisfying data requirements for both durability and damage tolerance. Additional testing and fractographic evaluations, beyond the normal ASIP effort, may be needed to define IFQ, depending on the desired confidence level and circumstances. IFQ data requirements can be readily incorporated into the ASIP test plan to minimize the cost and time for acquiring the requisite data base.

11. The stress level for each stress region is important for crack growth predictions. Therefore, the stress analysis for durability-critical components should reflect appropriate finite element grid sizes to obtain the desired stress analysis accuracy.

12. Probabilistic durability analysis methodologies developed can be extended to establish the optimal inspection/repair/replacement/proof test maintenance for life management of metallic aircraft structure. The extension can be made based on some fundamental research efforts appearing in the literature [e.g., 43-53].

6.2 RECOMMENDATIONS

1. The advanced durability analysis method developed under this program should be used for future durability analyses for metallic airframes. Structural durability can now be quantitatively accounted for in the durability design process.

2. Recommendations for durability analysis are as follows: (1) define the equivalent initial flaw size distribution (EIFSD) using fractographic data in the small crack size region (e.g., 0.01"-0.05"), (2) use fractographic data pooling procedure and statistical scaling technique to estimate the EIFSD parameters in a "global sense" for a "single hole population" basis, and (3) use the two-segment deterministic-stochastic crack growth approach (DCGA-SCGA) to predict the extent of damage in the entire durability critical component; the two-segment deterministic crack growth approach (DCGA-DCGA) is also reasonable but it is slightly less conservative than the DCGA-SCGA.

3. The recommended changes in Air Force philosophy and durability design requirements described in Volume IV [54] should be adopted. This will allow the full potential of the probabilistic durability analysis approach to be utilized in the design and analysis of future metallic aircraft structures.

4. The advanced durability analysis approach developed

under this program should be investigated for other structural details and considerations. For example, the life enhancement effects of fastener hole cold working, interference fit fasteners, press fit bushings, etc., on initial fatigue quality should be investigated. Similarly, the initial fatigue quality of structural details, such as cutouts, lugs, fillets, etc., should be investigated. Suitable test specimens should be developed and standardized for acquiring initial fatigue quality data for the key structural details to be included in the durability analysis.

5. Future ASIP test plans should be designed to provide data for initial fatigue quality, durability and damage tolerance. Selected fatigue tests should be conducted using specimens without intentional preflaws so that "natural fatigue crack" data can be obtained. This approach should be used to minimize cost and time for acquiring the requisite IFQ data base.

6. The meaning and limitations of EIFSs and an EIFSD must be emphasized. In particular, all EIFSs should be grown forward consistent with the basis for the EIFSD. The EIFSD should not be grown forward using an analytical crack growth program without tuning and considering the basis for the EIFS.

7. All aerospace contractors should use the same method to define EIFSs for different materials and structural details so that compatible EIFSs can be obtained. The "Qa(t) model" reflected in Eq. 4 is reasonable for determining EIFSs. This model or some other suitable model should be used to standardize the way EIFSs are determined. Then, for a given fractographic data set, fractographic crack size range (AL-AU) and the same analysis procedure, all contractors will obtain the same EIFSs. By standardizing the way EIFSs are determined, EIFSs from various sources can be di-

rectly compared -- thereby providing a means for cataloging and utilizing existing data from various sources to estimate the initial fatigue quality of structural details.

8. Initial fatigue quality should not be represented by the identical initial flaw size distribution irrespective of material, type of fastener hole, structural details, manufacturing processes, etc. For example, the statistical dispersion of EIFSD for countersunk holes is significantly larger than that of the EIFSD for straight-bore holes for clearance-fit fasteners in the same material in which the holes were drilled using comparable methods. Thus, if a single initial flaw size is selected for a given probability or percentile (e.g., 1/1000), and the deterministic approach is used for durability analysis, the initial flaw size for a countersunk fastener hole should be larger than that for a straight-bore fastener hole based on our investigation.

9. The probabilistic durability analysis approach should be investigated for discriminating "quality" at three levels: (1) material, (2) manufactured detail, and (3) component. Of particular interest is the following question: "How does improvement in initial material quality translate into improvement in life of actual aircraft components?" This research can be built on the advancements made under this program and the work conducted by ALCOA [e.g., 55,56].

REFERENCES

1. Manning, S. D., and Yang, J. N., "Advanced Durability Analysis, Volume I - Analytical Methods" AFWAL-TR-86-3017, Air Force Wright Aeronautical Laboratories, Wright-Patterson Air Force Base, OH, July 1987.

2. Gordon, D. E., et al, "Advanced Durability Analysis, Volume III - Fractographic Test Data," AFWAL-TR-86-3017, Air Force Wright Aeronautical Laboratories, Wright-Patterson Air Force Base, OH, August 1987.

3. Noronha, P. J., et al, "Fastener Hole Quality," AFFDL-TR-78-206, Vols. I and II, Dec. 1978.

4. Speaker, S. M., et al , "Durability Methods Development - Vol. VIII - Test and Fractography Data," AFFDL-TR-79-3118, Air Force Flight Dynamics Laboratory, Wright-Patterson Air Force Base, OH, Nov. 1982.

5. Manning, S. D., and Yang, J. N., "Advanced Durability Analysis, Volume V - Durability Analysis Software User's Guide," AFWAL-TR-86-3017, Air Force Wright Aeronautical Laboratories, Wright-Patterson Air Force Base, OH, August 1987.

6. Yang, J. N., Manning, S. D., and Garver, W. R., "Durability Methods Development, Vol. V - Durability Analysis Methodology, AFFDL-TR-79-3118, Air Force Flight Dynamics Lab., Wright-Patterson Air Force Base, OH, Sept. 1979.

7. Yang, J. N., and Manning, S. D., "Distribution of Equivalent Initial Flaw Size," 1980 Proceedings, Annual Reliability and Maintainability Symposium, San Francisco, CA, 22-24 Jan. 1980, pp. 112-120.

8. Manning, S. D., and Yang, J. N., "USAF Durability Design Handbook: Guidelines for the Analysis and Design of Durable Aircraft Structures," AFWAL-TR-83-3027, Air Force Wright Aeronautical Laboratories, Wright-Patterson Air Force Base, OH, Jan. 1984.

9. Rudd, J. L., Yang, J. N., Manning, S. D., and Yee, B. G. W., Probabilistic Fracture Mechanics Analysis Method for Structural Durability," Proceedings, Conference on the Behavior of Short Cracks in Airframe Components, AGARD-CP-328, Toronto, Canada, Sept. 1982, pp. 10-1 through 10-23.

10. Rudd, J. L., Yang, J. N., Manning, S. D., and Yee, B. G. W., "Damage Assessment of Mechanically Fastened Joints in the Small Crack Size Range," Proceedings on the Ninth U. S. National Congress of Applied Mechanics, 1982, pp. 329-338.

11. Manning, S. D., Yang, J. N., and Rudd, J. L., "Durability of Aircraft Structures," Probabilistic Fracture Mechanics and Reliability, Edited by J. W. Proven, Martinus Nijhoff Publishers, The Netherlands, 1987, pp. 213-268.

12. Yang, J. N., Manning S. D., Rudd, J. L., and Hsi, W. H., "Stochastic Crack Propagation in Fastener Holes," Journal of Aircraft, Vol. 22, No. 9, Sept. 1985, pp. 810-817.

13. Yang, J. N., Manning, S. D., and Rudd, J. L., "Evaluation of a Stochastic Initial Fatigue Quality Model for Fastener Holes," Fatigue in Mechanically Fastened Composite and Metallic Joints, ASTM STP 927, John M. Potter, Ed., American Society for Testing and Materials, Philadelphia, 1986, pp. 118-149.

14. Yang, J. N., Manning, S. D., Rudd, J. L., and Artley, M. E., "Probabilistic Durability Analysis Methods for Metallic Airframes," Journal of Probabilistic Engineering Mechanics, Vol. 1, No. 4, Dec. 1986.

15. Yang, J. N., Manning, S. D., Rudd, J. L., Artley, M. E., and Lincoln, J. W., "Stochastic Approach for Predicting Functional Impairment of Metallic Airframes," Proceedings of the 28th AIAA/ASME/ASCE/AHS Structures, Structural Dynamics and Materials Conference, Paper No. AIAA-87-0752-CP, Monterey, CA, April 1987.

16. Yang, J. N., Manning, S.D., Akbarpour, A. and Artley, M. E., "Demonstration of Probabilistic-Based Durability Analysis Method for Metallic Airframes," AIAA Paper No. 88-2421, Paper presented at the 29th AIAA/ASME/ASCE/AHS Structure, Structural Dynamics and Materials Conference, Williamsburg, VA, 18-20 April 1988.

17. Yang, J. N., Hsi, W. H., Manning, S. D., and Rudd, J. L., "Stochastic Crack Growth Models for Application to Aircraft Structures," Chapter IV, Probabilistic Fracture Mechanics and Reliability, Edited by J. W. Provan, Martinus Nijhoff Publishers, The Netherlands, 1987, pp. 171-211.

18. Roach, G. R., McComb, T. H., and Chung, J. H., "ADAMSys Users Manual," Structures and Design Department, General Dynamics, Fort Worth Division, July 1987.

19. Engle, R. M., and Wead, J. A., "CRACKS-PD, A Computer Program for Crack Growth Analysis Using the Tektronix 4051 Graphics System," Air Force Flight Dynamics Laboratory, Wright-Patterson AFB, OH, AFFDL-TM-79-63-FBE, June 1979.

20. Manning, S. D., Yang, J. N., Shinozuka, M., Gordon, D. E., and Speaker, S. M., "Durability Methods Development - Vol. VII - Phase II Documentation," AFFDL-TR-79-3118, Air Force Flight Dynamics Lab., Wright-Patterson Air Force Base, OH, Nov. 1982.

21. Manning, S. D., and Yang, J. N., "USAF Durability Design Handbook: Guidelines for the Analysis and Design of Durable Aircraft Structures," AFWAL-TR-83-3027, Second Edition, Air Force Wright Aeronautical Laboratories, WrightPatterson Air Force Base, OH, August 1988.

22. Benjamin, J. R., and Cornell, C. A., <u>Probability, Statistics and Decision of Civil Engineers</u>, New York: McGraw-Hill Book Company, 1970.

23. Rudd, J. L., Yang, J. N., Manning, S. D., and Garver, W. R., "Durability Design Requirements and Analysis for Metallic Airframe," <u>Design of Fatigue and Fracture Resistant Structures</u>, ASTM STP 761, P. R. Abelkis and C. M. Hudson, Eds., American Society for Testing and Materials, 1982, pp. 133-151.

24. Forness, S. D., "Fracture Mechanics Methodology Update," General Dynamics, Fort Worth Division, Report ERR-FW2219 (Proprietary), Dec. 1981.

25. Walker, K., "The Effects of Stress Ratio During Crack Propagation and Fatigue for 2024-T3 and 7075-T6 Aluminum," <u>Effects of Environment and Complex Load History on Fatigue Life</u>, ASTM-STP 462, American Society for Testing and Materials, 1970, pp. 1-14.

26. Gallagher, J. P., and Huges, T. F., "Influence of Yield Strength on Overload Affected Fatigue Crack Growth Behavior in 4340 Steel," AFFDL-TR-74-27, Air Force Flight Dynamics Laboratory, Wright-Patterson Air Force Base, OH, July 1974.

27. Virkler, D.A., Hillberry, B. M., and Goel, P. K., "The Statistical Nature of Fatigue Crack Propagation," AFFDL-TR-78-43, Air Force Flight Dynamics Laboratory, April 1978.

28. "Standard Test Method for Measurement of Fatigue Crack Growth Rates," ASTM Standard E647-86a, <u>1987 Annual Book of ASTM Standards</u>, Section 3, "Metals Test Methods and Analytical Procedures," pp. 899-926.

29. Ostergaard, D. F., Thomas, J. R., and Hillberry, B. M., "Effect of a-Increment on Calculating da/dN from a versus N Data," Fatigue Crack Growth Measurement and Data Analysis, ASTM-STP 738, S. J. Hodak, Jr., and R. J. Bucci, Eds., American Society for Testing and Materials, 1981, pp. 194-204.

30. Fong, J. T., and Dowling, N. E., "Analysis of Fatigue Crack Growth Rate Data from Different Laboratories," Fatigue Crack Growth Measurement and Data Analysis, ASTM-STP 738, S. J. Hudak, Jr., and R. J. Bucci, Eds., American Society for Testing and Materials, 1981, pp. 171-193.

31. Anon., "Military Specification Aircraft Structures General Specification For," MIL-A-87221 (USAF), Air Force Aeronautical Systems Division, Wright-Patterson Air Force Base, OH, Feb. 28, 1985.

32. Pearson, S., "Initiation of Fatigue Cracks in Commercial Aluminum Alloys and the Subsequent Propagation of Very Short Cracks," Engineering Fracture Mechanics, Vol. 7, 1975, pp. 235-247.

33. Cruse, T. A., "Fracture Mechanics Problems for Gas Turbine Engine Structures," Fracture Mechanics, Proceedings of the 2nd International Symposium on Fracture Mechanics, the University Press of Virginia, Sept. 1978, pp. 399-420.

34. Hudak, S. J., "Small Crack Behavior and the Prediction of Fatigue Life", Journal of Engineering Materials and Technology, Vol. 103, 1981, pp. 26-35.

35. Lankford, J., "The Growth of Small Fatigue Cracks in 7075-T6 Aluminum," Fatigue Eng. Mat. Struct., Vol. 5, 1982, pp. 233-248.

36. Miller, K. J., "The Short Crack Problem," Fatigue of Engineering Materials and Structures, Vol. 5, No. 3, 1982, pp. 223-232.

37. Smith, R. A., "Short Fatigue Cracks," Fatigue Mechanisms: Advances in Quantitative Measurement of Physical Damage, American Society for Testing and Materials, ASTM STP 811, 1983, pp. 269-279.

38. Chan, K. S., Lankford, J., and Davidson, D. L., "A Comparison of Crack-Tip Field Parameters for Large and Small Fatigue Cracks," Transactions of the ASME, Journal of Engineering Materials and Technology, Vol. 10B, July 1986, pp. 206-213.

39. Yang, J. N., and Donath, R. C., "Statistical Fatigue Crack Propagation in Fastener Holes Under Spectrum Loading," Journal of Aircraft, AIAA, Vol. 20, No. 12, Dec. 1983, pp. 1028-1032.

40. Yang, J. N., Salivar, G. C., and Annis, C. G., "Statistical Modeling of Fatigue Crack Growth in a Nickel-Based Superalloy," Journal of Engineering Fracture Mechanics, Vol. 18, No. 2, June 1983, pp. 257-270.

41. Yang, J. N., "Statistical Estimation of Service Cracks and Maintenance Costs for Aircraft Structures," Journal of Aircraft, AIAA, Vol. 13, No. 12, Dec. 1976, pp. 929-937.

42. Manning, S. D. and Yang, J. N., Unpublished Research, 1984-1987.

43. Yang, J. N., "Statistical Estimation of Economic Life for Aircraft Structures," Proc. AIAA/ASME/ASCE/AHS 20th Structures, Structural Dynamics, and Materials Conference, April 4-6, 1979, St. Louis, Mo., pp. 240-248; Journal of Aircraft, AIAA, Vol. 17, No. 7, 1980, pp. 528-535.

44. Yang, J. N., and Chen, S., "Fatigue Reliability of Gas Turbine Engine Components Under Schedule Inspection Maintenance," Journal of Aircraft, AIAA, Vol. 22, No. 5, May 1985, pp. 415-422.

45. Yang, J. N., and Chen, S., "An Exploratory Study of Retirement-for-Cause for Gas Turbine Engine Components," Journal of Propulsion and Power, AIAA, Vol. 2, No. 1, January 1986, pp. 38-49.

46. Yang, J. N., and Trapp, W. J., "Reliability Analysis of Fatigue-Sensitive Aircraft Structures Under Random Loading and Periodic Inspection," Air Force Materials Laboratory Technical Report, AFML-TR-74-2, Wright-Patterson Air Force Base, February 1974.

47. Yang, J. N., and Trapp, W. J., "Reliability Analysis of Aircraft Structures Under Random Loading and Periodic Inspection," AIAA Journal, Vol. 12, No. 12, 1974, pp. 1623-1630.

48. Yang, J. N., and Trapp, W. J., "Inspection Frequency Optimization for Aircraft Structures Based on Reliability Analysis," Journal of Aircraft, AIAA, Vol. 12, No. 5, 1975, pp. 494-496.

49. Yang, J. N., "Reliability Analysis of Structures Under Periodic Proof Test In Service," AIAA Journal, Vol. 14, No. 9, Sept. 1976, pp. 1225-1234.

50. Yang, J. N., "Optimal Periodic Proof Test Based on Cost-Effective and Reliability Criteria," AIAA Journal, Vol. 15, No. 3, March 1977, pp. 402-409.

51. Yang, J. N., and Chen, S., "Fatigue Reliability of Structural Components Under Scheduled Inspection and Repair Maintenance," Probabilistic Methods in Mechanics of Solids and Structures, edited by S. Eggwertz and N. C. Lind, Springer-Verlag, Berlin, Jan. 1985, pp. 559-568.

52. Heer, E., and Yang, J. N., "Structural Optimization Based on Fracture Mechanics and Reliability Criteria," AIAA Journal, Vol. 9, No. 5, April 1971, pp. 621-628.

53. Lincoln, J. W., "Risk Assessment of an Aging Military Aircraft," J. Aircraft, Vol. 22, No. 8, Aug. 1985, pp. 687-691.

54. Manning, S. D. and Yang, J. N., "Advanced Durability Analysis, Volume IV - Executive Summary," AFWAL-TR-86-3017, Air Force Wright Aeronautical Laboratories, Wright-Patterson Air Force Base, OH, September 1987.

55. Bucci, R. J., Brazill, R. L., and Brockenbrough, J. R., "Assessing Growth of Small Flaws from Residual Strength Data," Small Fatigue Cracks, Edited by R. O. Ritchie and J. Lankford, The Metallurgical Society of AIME, 1986, pp. 541-556.

56. Owen, C. R., Bucci, R. J., and Kegarise, R. J., "An Aluminum Quality Breakthrough for Aircraft Structural Reliability," Alcoa Laboratories Technical Report No. 57-87-20, October 19, 1987.

DEFINITIONS

The technical terms defined herein supercede those given in Volume I [1]. New terms have been added and selected Volume I terms have been revised. Should any questions arise, the definitions herein should be used.

DEFINITIONS

1. Combined Least Square Sums Approach (CLSSA) - the least square sums for individual fractographic data sets are combined to estimate the EIFSD parameters in a "global sense." This approach is used in conjunction with the data pooling philosophy.

2. Compatible Equivalent Initial Flaw Size Distribution Function - this is a distribution function for equivalent initial flaw sizes (EIFS) which is derived using a physically meaningful cumulative distribution of time-to-crack initiation (TTCI) function and a suitable deterministic crack growth law.

3. Crack Size - is the length of a crack in a structural detail in the direction of crack propagation.

4. Cumulative Distribution of Service Time ($F_{T(x_1)}(\tau)$) - is defined as the probability that the service time $T(x_1)$ to reach a crack size x_1 is shorter than τ. It is equal to the probability that the crack size $a(\tau)$ at service life τ will exceed x_1, which is simply the probability of crack exceedance, i.e.,

$$F_{T(x_1)}(\tau) = P[T(x_1) \leq \tau] = P[a(\tau) \leq x_1] = p(i,\tau)$$

5. Data Pooling - is a concept for estimating the EIFSD parameters using one or more fractographic data sets in a "global sense." A data pooling procedure is used to increase the sample size for determining the EIFSD parameters.

6. Deterministic Crack Growth Approach (DCGA) -- Crack growth parameters are treated as deterministic values resulting in a single value prediction for crack length.

7. Durability - is a quantitative measure of the structural resistance to fatigue cracking under specified service conditions. Structural durability is concerned with the prevention of functional impairments due to (1) excessive cracking and (2) fuel leakage/ligament breakage. Excessive cracking is concerned with relatively small subcritical crack sizes (e.g., $\leq$ 0.05") which affect functional impairment, structural maintenance requirement and life-cycle-costs. Such cracks may not pose an immediate safety problem. However, if the structural details containing such cracks are not repaired, economical repairs cannot be made when these cracks exceed a limiting crack size. Functional impairment due to fuel leakage/ligament breakage is typically concerned with large through-the-thickness cracks (e.g., 0.50"-0.75"). Although such cracks are usually subcritical, they affect the residual strength, fleet readiness, and may require increased maintenance action.

8. Durability Analysis - is concerned with quantifying the extent of structural damage due to fatigue cracking for structural details (e.g., fastener hole, fillet, cutout, lug, etc.) as a function of service time. Results are used to ensure design compliance with Air Force's durability design requirements.

9. Economic Life - is that point in time when an aircraft structure's damage state due to fatigue, accidental damage and/or environmental deterioration reaches a point where operational readiness goals cannot be preserved by economically acceptable maintenance action.

10. <u>Economic Life Criteria</u> - are guidelines and formats for defining quantitative economic life requirements for aircraft structure to satisfy U. S. Air Force Durability design requirements. The economic life criterion provides the basis for analytically and experimentally ensuring design compliance of aircraft structure with durability design requirements. Two recommended formats for economic life criteria are:

- o probability of crack exceedance
- o cost ratio: repair cost/replacement cost

11. <u>Economic Repair Limit</u> - is the maximum damage size that can be economically repaired (e.g., repair 0.03"-0.05" radial crack in fastener holes by reaming hole to next size).

12. <u>Equivalent Initial Flaw Size (EIFS)</u> - is an artificial crack size which results in an actual crack size at an actual point in time when the initial flaw is grown forward. It is determined by back-extrapolating fractographic results. It has the following characteristics: (1) an EIFS is an artificial crack assumed to represent the initial fatigue quality of a structural detail in the as-manufactured condition whatever the source of fatigue cracking may be, (2) no direct relationship to actual initial flaws in fastener holes such as scratches, burrs, microdefects, etc., and it cannot be verified by NDI, (3) a universal crack shape in which the crack size is measured in the direction of crack propagation, (4) it's in a fracture mechanics format but EIFSs are not subject to linear elastic fracture mechanics (LEFM) laws or limitations, such as the "short crack effect" [e.g., 32-38], (5) it depends on the fractographic data, the fractographic crack size range for the back extrapolation, and the crack

growth rate model used, (6) it must be grown forward in a manner consistent with the basis for the EIFS, and (7) EIFSs are not unique - a different set is obtained for each crack growth law used for the back- extrapolation.

13. Equivalent Initial Flaw Size Distribution (EIFSD) - is used to represent the initial fatigue quality variation of a structural detail. An EIFS is a random variable, and the EIFSD statistically describes the EIFS population. The EIFSD does not necessarily contain the "rogue flaw."

14. EIFS Master Curve - is a curve (e.g., equation, tabulation of a(t) vs. t or curve without prescribed functional form) used to determine the EIFS value at t=0 corresponding to a given TTCI value at a specified crack size. Such a curve is needed to determine the EIFS distribution. The EIFS master curve depends on several factors, such as the fractographic data base, the fractographic crack size range used, the functional form of the crack growth equation used in the curve fit, etc. (Ref. EIFS).

15. Extent of Damage - is a quantitative measure of structural durability at a given service time. For example, the number of structural details (e.g., fastener holes, cutouts, fillets, etc.) or percentage of details exceeding specified crack size limits with a certain probability. Crack length is the fundamental measure for structural damage. The predicted extent of damage is compared with the specified economic life criterion for ensuring design compliance with U. S. Air Force durability requirements.

16. Generic EIFS Distribution - An EIFS distribution is "generic" if it depends only on the material and manufacturing/fabrication processes. An EIFSD is not strictly "generic" because it is based on fractographic results which reflect given conditions (e.g., load spectra). For durability analysis, an EIFSD is established using the fractographic results for one or more data sets, and the resulting EIFSD is justified for a different set of conditions.

17. Initial Fatigue Quality (IFQ) - characterizes the initial manufactured state of a structural detail or details with respect to initial flaws in a part, component, or airframe prior to service. Actual initial flaws in a fastener hole are typically random scratches, burrs, microscopic imperfections, etc. Such flaws are not cracks per se like those associated with linear elastic fracture mechanics. The IFQ is represented by an equivalent initial flaw size distribution (EIFSD).

18. Probability of Crack Exceedance ($p(i,\tau)$) - refers to the probability that a crack in the ith stress region will exceed a specified crack size, x_1, at a given service time, τ. It can be used to quantify the extent of damage due to fatigue cracking in fastener holes, cutouts, fillets, lugs, etc.

19. Reference Crack Size (a_0) - This is the specified crack size in a detail used to reference TTCIs.

20. <u>Service Crack Growth Master Curve (SCGMC)</u> - SCGMC is a curve, expressed by equation or tabulation of a(t) versus t, used to grow EIFSs forward in order to determine the crack size distribution at any service time. The SCGMC must be consistent with the basis for the EIFS distribution.

21. <u>Service Time to Reach Any Crack Size x_1</u> - This term describes the time, $T(x_1)$, to reach any specified crack size x_1. In this context, the crack size x_1 can be associated with either the "crack initiation" or the "crack propagation" process. The time-to-crack-initiation (TTCI) term is restricted to crack sizes associated with the crack initiation process, where $x_1 = a_0$ (reference crack size for TTCIs).

22. <u>Statistical Scaling</u> - is used to account for the inhomogeneous fractographic data, in particular fractographic data associated with the largest flaw per specimen with holes.

23. <u>Stochastic Crack Growth Approach (SCGA)</u> - an approach which directly accounts for the crack growth rate dispersion in the durability analysis.

24. <u>Structural Detail</u> - is any element in a metallic structure susceptible to fatigue cracking (e.g., fastener hole, fillet, cutout, lug, etc.).

25. <u>Time-To-Crack-Initiation (TTCI)</u> - is the time or service hours required to initiate a specified (observable) fatigue crack size, a_0, in a structural detail (with no initial flaws intentionally introduced).

26. <u>TTCI Lower Bound Limit (ϵ)</u> - is a minimum value for time-to-crack initiation with a reference crack size a_0. It depends on the reference crck size a_0 for TTCI; the larger a_0, the larger ϵ.

27. <u>Upper Bound EIFS Limit (x_u)</u> - defines the largest EIFS in the initial fatigue quality distribution. Constraints on x_u for fatigue holes: largest EIFS in data set $\leq x_u$ (e.g., 0.03"-0.05").

ACRONYMS

ADA	=	Advanced Durability Analysis
ASIP	=	Aircraft Structural Integrity Program
CLSSA	=	Combined Least Square Sums Approach
DADTA	=	Durability and Damage Tolerance Assessment
DCGA	=	Deterministic Crack Growth Approach
EIFS	=	Equivalent Initial Flaw Size
EIFSD	=	Equivalent Initial Flaw Size Distribution
FHQ	=	Fastener Hole Quality
HEIFS	=	Homogeneous EIFS
IFQ	=	Initial Fatigue Quality
LEFM	=	Linear Elastic Fracture Mechanics
LT	=	Load Transfer Through the Fastener
MM	=	Method of Moments
NDE	=	Non Destructive Evaluation
NDI	=	Non Destructive Inspection
NLT	=	No Load Transfer Through the Fastener
SCGA	=	Stochastic Crack Growth Approach
SCGMC	=	Service crack growth master curve
SSE	=	Sum Squared Error
TSE	=	Total Standard Error
TTCI	=	Time-to-Crack Initiation

LIST OF SYMBOLS

a	=	Crack Size
a_0	=	Reference crack size for given TTCIs
$a(0)$	=	EIFS = Crack size at t=0
$a(t)$	=	Crack size at any service time t
$a(t)$, $a(t_1)$, $a(t_2)$	=	Crack size at time t, t_1 and t_2, respectively
$a(T)$	=	Crack size at service time T
$a(\tau)$	=	Crack size at any service time τ
AL, AU	=	Lower and upper bound fractographic crack size, respectively, used to define the EIFSD parameters. Also used in conjunction with the SCGMC to define crack size limits for the small crack size region.
AU'	=	Upper bound crack size limit for the large crack size region
b, Q	=	Crack growth parameters in the equation $\frac{da(t)}{dt}=Q[a(t)]^b$. Used in conjunction with the IFQ model.
b_1, Q_2	=	Service crack growth rate parameters in the equation $da/dt = Q_1(a)^{b_1}$ associated with the one-segment DCGA or 1st segment of the two-segment approach.

b_2, Q_2	=	Service crack growth rate parameters in the equation $da/dt = Q_2(a)^{b_2}$ for segment two of the two-segment DCGA.
c	=	b - 1; Used in conjunction with the IFQ model when the crack growth law, $\frac{da(t)}{dt} = Q[a(t)]^b$ is used and $b > 1.0$.
$\frac{da(t)}{dt}$	=	Crack growth rate as a function of time
$f_X(u)$	=	Probability density function of X.
$F_{a(0)}(x)$	=	EIFS cumulative distribution function for a "single hole population."
$F_{a_\ell(0)}(x)$	=	Cumulative distribution of EIFS based on the largest fatigue crack per test specimen with ℓ holes.
$F_{a_{\ell_i}(0)}(x_{ij})$	=	Subscripted notation used for $F_{a_\ell(0)}(x)$ in conjunction with data pooling, where: j denotes the jth crack in the ith data set.
$F_{a(t)}(x)$	=	Cumulative distribution of crack size a(t) at any service time t.
$F_{a_\ell(t)}(x)$	=	Cumulative distribution of crack size $a_\ell(t)$ at any service time t for the largest fatigue crack per test specimen with ℓ holes.

$F_T(t)$	=	TTCI cumulative distribution function
$F_{T_{\ell_i}}(t)$	=	Cumulative distribution of minimum TTCIs based on the largest fatigue crack per test specimen with ℓ_i holes.
$F_{T_{\ell_i}}(t_{ij})$	=	Subscripted notation used for $F_{T_\ell}(t)$ in conjunction with data pooling, where: j = jth TTCI value in the ith data set.
$F_{T(x_1)}(\tau)$	=	Cumulative Distribution of service time $T(x_1)$ to reach a crack size x_1.
$G(x_1;\tau \mid X=u)$	=	Initial flaw size corresponding to crack size x_1 at time τ with X = u.
ℓ	=	No. of fastener holes per test specimen.
$L(\tau)$, $\bar{L}(\tau)$	=	Total and average number of details, respectively, in the entire component having a crack size $\geq x_1$ at any service time τ.
LT	=	Load transfer through the fastener.
m	=	Number of stress regions (or total number of fatigue cracks in a data set, Eqs. 3-33, 3-34).
M	=	Total number of EIFS data sets used to estimate the EIFSD parameters.
N_i	=	Number of TTCI or EIFS values for the ith data set used in conjunction with the combined least square sums approach.

$N(i,\tau)$, $\bar{N}(i,\tau)$	=	Total and average number of details, respectively, having a crack size exceeding x_1 at any service time τ
$p(i,\tau)$	=	Probability that a detail in the ith stress region will have a crack size $>x_1$ at the service time τ
Q_i	=	Crack growth rate parameter (see Eq. 3-6) for the ith fractographic data set or "pooled Q" value. It is used to determine EIFSs.
Q_j	=	Crack growth rate parameter (see Eq. 3-5) for the jth fatigue crack in a fractographic data set.
t, t_1, t_2	=	Flight hours at t, t_1, t_2, respectively.
T, TTCI	=	Time-to-crack-initiation
$T(x_1)$	=	Service time to reach any crack size x_1.
u	=	A particular value of X (lognormal random variable).
x	=	Crack size
x_1	=	Crack size used for $p(i,\tau)$ predictions or reference crack size for $F_{T(x_1)}(\tau)$ predictions.

x_u	= Upper bound limit for EIFS
X	= Lognormal random variable with a median of 1.0.
X_{ij}	= $\ln \ln(x_u/x_{ij})$
$y_{1i}(\tau)$	= An EIFS value in the EIFSD corresponding to a crack size x_1 at time τ in the ith stress region.
Y_{ij}	= $\ln\{-(1/\alpha_i)\ln[\frac{j}{N_i+1}]\}$
Z	= Log X
$\Gamma(\ )$	= Gamma function
C, V	= Empirical constants in the equation: $Q_i = C\sigma_i^V$, where σ_i = stress
σ_z	= Standard deviation of Z = Log X.
τ	= A particular service time
α, ϕ	= Weibull compatible shape and scale EIFSD parameters, respectively
γ	= Q_1/Q_2

APPENDIX A

DURABILITY ANALYSIS SOFTWARE

Software is available for implementing the advanced durability analysis method described in this Volume (II) and in Volume I [1]. A comprehensive software user's guide is given in Volume V [5].

A.1 SOFTWARE DESCRIPTION

The advanced durability analysis software includes six programs in "GWBASIC". The purpose of each program is described in Table A.1. All programs can be implemented on an IBM or IBM-compatible personal computer.

Software is available for plotting the fractographic data for any crack size or time range and/or durability analysis results for $F_{T(x_1)}(\tau)$, $p(i,\tau)$ or $F_{a(t)}(x)$. A plotting capability is available for the following durability analysis options: (1) DCGA, (2) DCGA-DCGA and (3) DCGA-SCGA. Plots can be obtained with or without correlating data. Typical example plots are shown in Fig. A.1

A.2 SYSTEM REQUIREMENTS

Minimum system requirements are as follows:

Memory:	640K RAM
Operating System:	MS-DOS Version 2.0 or Later
Graphics Monitor:	Monochrome or Color
Disk Drive:	1 Double Sided Disk Drive
Printer:	IBM or IBM-Compatible Graphics Printer
Graphics Program:	Need Special "GRAPHICS" Program for Doing Screen Prints of Graphic Display

TABLE A.1. Description of Durability Analysis Software.

PROGRAM FILENAME	PURPOSE
"FRACT"	Save or read/print out fractographic data on 5 1/4" floppy disk
"SCREEN"	Study the character and quality of a fractographic data set (tabulate data and plot fractography)
"QSZAT"	Compute pooled Q and σ_z for a given fractographic data set
"WCIFQ"	Estimate EIFSD parameters for Weibull compatible distribution function
"PLOT"	Plot fractographic data and/or durability analysis results
"ANAL"	Make durability analysis predictions

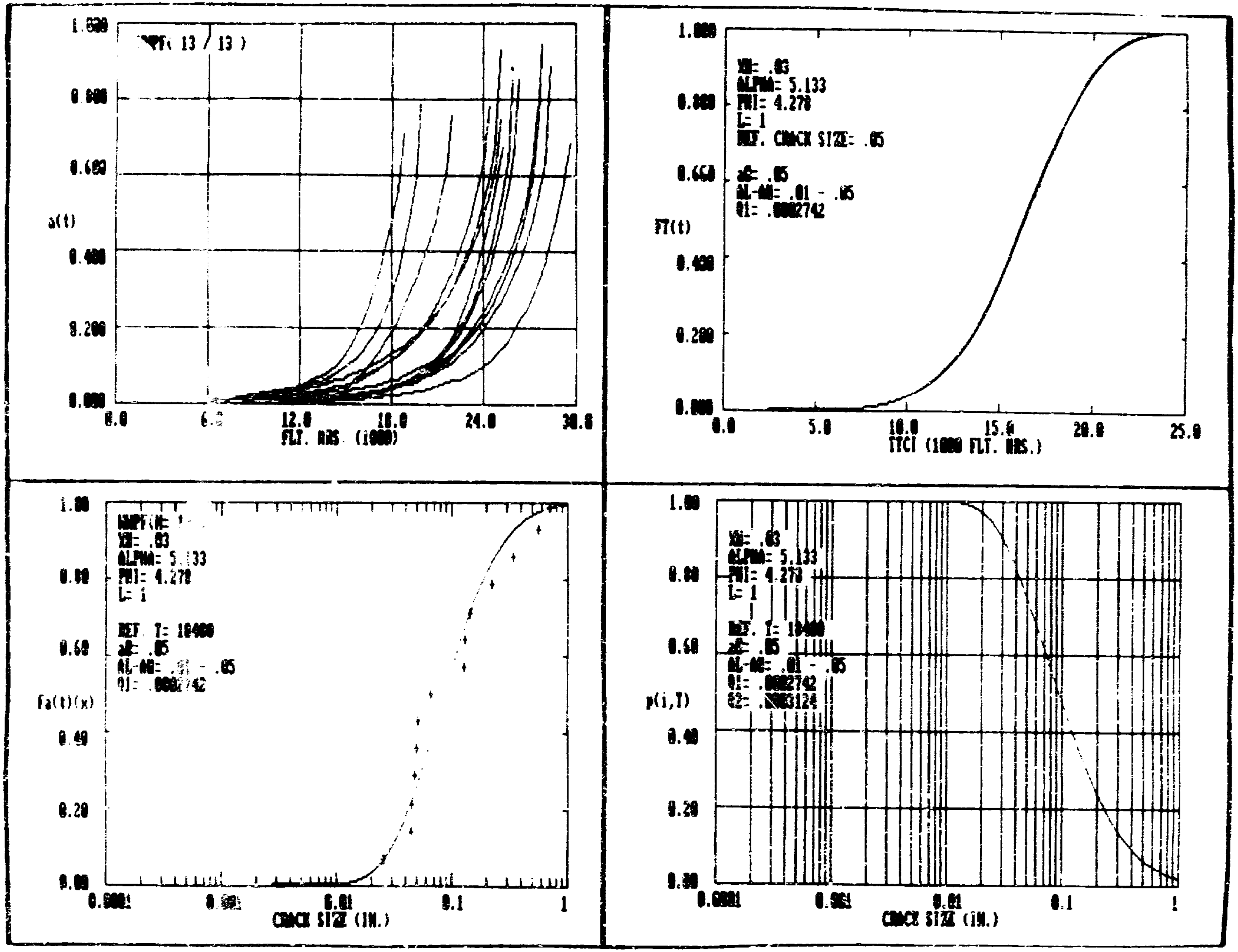

Figure A.1. Example Plots for Durability Analysis Software "PLOT".

APPENDIX B

FRACTOGRAPHIC DATA SCREENING/PROCESSING

B.1 INTRODUCTION

The purpose of this section is to review fractographic data screening and processing considerations for durability analysis. This aspect is particularly important because fractographic data is used to determine (1) pooled Q values for individual data sets, (2) the initial fatigue quality (IFQ) or EIFSD parameters for fastener holes, (3) the TTCIs for a given reference crack size (a_0), and (4) the crack sizes, a(t), at a given reference time. Fractographic data considerations, data screening and plotting are considered in the following.

B.2 FRACTOGRAPHIC DATA CONSIDERATIONS

Fractographic data are used to estimate the IFQ of structural details for the durability analysis. The IFQ depends on the fractographic data and crack size range, AL-AU, used. Ideally, the fractographic data should be homogeneous and cover the desired AL-AU range (i.e., AL $\leq$ a(t) $\leq$ AU) for defining the EIFSD parameters. Realistically, the fractographic data may not be perfectly homogeneous.

The following fractographic data considerations will be made: (1) data sparsity, (2) fatigue crack origins, (3) extrapolations, and (4) survivors/failures.

"Data sparsity" occurs when all the fractographic data in a data set do not uniformly cover the desired AL-AU range that is to be used to define the IFQ. For example, there may be little data (i.e., a(t) versus t) in the desired AL-AU range for a particular crack. Hence, some data may have to be extrapolated to "cover" the AL-AU range. If extrapolations are made care should be taken for extrapolations far beyond the limits of the actual (a(t), t) data.

Fastener holes in durability test specimens are not intentionally preflawed so that natural fatigue cracks can occur. Fatigue cracks usually originate in the bore of the hole. There may be multiple crack origins and crack branching in the microstructure. Eventually, the individual micro-cracks tend to merge into a single crack front. Microcracking is a very complex process. Sometimes, for various reasons, fatigue cracks may originate on the surface of mating parts instead of the bore of the hole. Pooled Q, σ_z and the EIFSD parameters should be defined using fractographic data for similar crack origins. For example, don't mix cracks with origins in the bore of the hole with those with origins on the surface.

The fractographic data may be based on fatigue tests to a specified time or failure - whichever comes first. Specimens tested to failure are called "failures;" otherwise, specimens are called "runouts" or "survivors." The fractographic data processing and data rankings for a given data set should recognize whether a specimen is a failure or a runout.

B.3 FRACTOGRAPHIC DATA SCREENING AND PLOTTING

Fractographic data should be screened and plotted before using it for any durability analysis purpose. Software for an IBM or IBM-compatible PC is available in Volume V [5] for screening and plotting fractographic data. Screening involves a physical description of fractographic data limits and a display of the actual fractographic data for visual observation.

A physical survey of each fractographic data set acquired under this program is given in Tables B.1 through B.11. Survey results for data sets AFXHR4, AFXLR4 and AFXMR4 [4] are shown in Tables B.12, B.13, and B.14, respectively. These tables provide the following information for each crack in the data set: (1) crack I.D., (2) minimum and maximum a(t), (3) minimum and maximum TTCI, (4) number of (a(t), t) fractographic readings, and (5) type of data (i.e., F = failure and S = survivor). Also, the minimum critical crack size, largest initial time fractography reading, minimum time to failure, and the common crack size range, AL-AU, for all cracks are defined for each data set. The above information provides an overall description of the fractographic data.

Plots of the fractographic data (i.e., a(t) versus t) are given in Figs. B.1 through B.18 for selected data sets from the current program. Other plots are also shown for AFXLR4, AFXMR4 or AFXHR4 in Figs. B.21 through B.24. Two crack size ranges are plotted: (1) full range (use all the data) and (2) AL-AU = 0 - 0.5" range. Such plots are convenient for assessing data sparsity, variability and abnormal crack growth behavior. For example, in Fig. B.19 the abnormal crack growth behavior of crack number 8 is observed. Also note in Fig. B.20 that some cracks cover the AL-AU = .01" - .05" range; whereas others do not.

TABLE B.1 FRACTOGRAPHIC DATA SURVEY FOR WWPF DATA SET

CRACK I.D.	a(t) MIN.	a(t) MAX.	TTCI MIN.	TTCI MAX.	NC(I)	TYPE
1	.0035	.69	12000	29616	46	F
2	.0069	.712	6000	18806	33	F
3	.0154	.76	10000	24435	37	F
4	.0037	.578	10800	25232	37	F
5	.0089	.05	10000	25931	41	F
6	.0058	.85	11600	26336	38	F
7	.0094	.78	12000	27551	40	F
8	.0095	.89	12400	28355	41	F
9	.0104	.79	6000	19884	36	F
10	8.999999E-03	.76	10800	21880	39	F
11	.0098	.95	11600	27827	42	F
12	.0073	.93	8400	25120	43	F
13	8.000001E-03	.75	7200	25150	46	F

CONSTRAINTS DUE TO FAILURE(S) IN DATA SET

MAX. AO(REF.)= .578 MAX. TAU= 18806

LARGEST INITIAL TIME/DATA SET= 12400

LARGEST COMMON CRACK SIZE RANGE/DATA SET= .0154 - .578

TABLE B.2 FRACTOGRAPHIC DATA SURVEY FOR WWPB DATA SET

CRACK I.D.	a(t) MIN.	a(t) MAX.	TTCI MIN.	TTCI MAX.	NC(I)	TYPE
1	.0016	.8316	12656	29858	18	F
2	.0071	.8050001	10547	34889	25	F
3	.0028	.8499999	10547	34910	25	F
4	.0057	.69	18773	39656	21	F
5	.0018	.7909	21937	36492	15	F
6	.0019	.9080999	10547	26051	18	F
7	9.599999E-03	.6737	27000	38596	12	F
8	.0036	.8043	28055	40494	13	F
9	.0087	.8474999	21937	35432	14	F
10	.0069	.6365	27000	38596	12	F
11	.0037	.8091	26156	43664	18	F
12	.0052	.7839	25101	40494	16	F

CONSTRAINTS DUE TO FAILURE(S) IN DATA SET

MAX. AO(REF.)= .6737 MAX. TAU= 26051

LARGEST INITIAL TIME/DATA SET= 28055

LARGEST COMMON CRACK SIZE RANGE/DATA SET= 9.599999E-03 - .6737

TABLE B.3 FRACTOGRAPHIC DATA SURVEY FOR WAFXMR4 DATA SET

CRACK I.D.	a(t) MIN.	a(t) MAX.	TTCI MIN.	TTCI MAX.	NC(I)	TYPE
1	.0016	.915	12800	21208	22	F
2	.0004	.8337	14800	28436	35	F
3	.1475	.758	20800	33208	32	F
4	.0086	.7855	10000	22836	33	F
5	.0262	.7388	7200	17236	26	F
6	.0156	.9895	4400	11608	19	F
7	.0019	.7916	3200	19637	43	F
8	.0054	.7677	14800	30036	39	F
9	.0136	.9341	3600	12808	24	F
10	.0046	.9875	6800	15208	22	F
11	.0028	.7304	8000	18436	27	F
12	.0114	1.2976	14800	21792	19	F
13	8.999999E-03	.9037	10800	15304	13	F
14	.0199	.8949	24400	31636	19	F

CONSTRAINTS DUE TO FAILURE(S) IN DATA SET

MAX. A0(REF.)= .7304 MAX. TAU= 11608

LARGEST INITIAL TIME/DATA SET= 24400

LARGEST COMMON CRACK SIZE RANGE/DATA SET= .1475 - .7304

TABLE B.4 FRACTOGRAPHIC DATA SURVEY FOR WAFXHR4 DATA SET

CRACK I.D.	a(t) MIN.	a(t) MAX.	TTCI MIN.	TTCI MAX.	NC(I)	TYPE
1	.0048	.76	2000	7297	14	F
2	.0092	.85	1600	5616	12	F
3	.0051	.79	4800	12968	22	F
4	.0086	.79	1200	9323	22	F
5	.0089	.68	400	8108	21	F
6	8.000001E-03	.65	4400	14589	27	F
7	.0067	.88	2000	13649	31	F
8	9.100001E-03	.63	800	10567	26	F
9	.0132	.88	1200	9537	22	F
10	.0097	.59	2000	10973	24	F
11	.0123	.678	1200	12592	30	F
12	.0031	.72	2000	16643	38	F
13	.0149	.6137	1600	7732	17	F

CONSTRAINTS DUE TO FAILURE(S) IN DATA SET

MAX. A0(REF.)= .59 MAX. TAU= 5616

LARGEST INITIAL TIME/DATA SET= 4800

LARGEST COMMON CRACK SIZE RANGE/DATA SET= .0149 - .59

TABLE B.5 FRACTOGRAPHIC DATA SURVEY FOR WWPCL DATA SET

CRACK I.D.	a(t) MIN.	a(t) MAX.	TTCI MIN.	TTCI MAX.	NC(I)	TYPE
1	.0033	.9115	36400	55192	48	F
2	.0697	.9866999	40800	59252	48	F
3	.0129	1.0224	30800	45992	39	F
4	.0158	.7356	28000	38792	28	F

CONSTRAINTS DUE TO FAILURE(S) IN DATA SET

MAX. A0(REF.)= .7356 MAX. TAU= 38792

LARGEST INITIAL TIME/DATA SET= 40800

LARGEST COMMON CRACK SIZE RANGE/DATA SET= .0697 - .7356

TABLE B.6 FRACTOGRAPHIC DATA SURVEY FOR WWPCH DATA SET

CRACK I.D.	a(t) MIN.	a(t) MAX.	TTCI MIN.	TTCI MAX.	NC(I)	TYPE
1	.0127	.7144	24800	33652	24	F
2	.0106	.9641999	12000	21112	24	F
3	.0119	.9281	18800	24700	16	F
4	.1449	.9522999	18400	24980	18	F
5	8.599998E-03	.7561	24000	31252	20	F
6	.0087	.8176	15600	24924	24	F

CONSTRAINTS DUE TO FAILURE(S) IN DATA SET

MAX. A0(REF.)= .7144 MAX. TAU= 21112

LARGEST INITIAL TIME/DATA SET= 24800

LARGEST COMMON CRACK SIZE RANGE/DATA SET= .1449 - .7144

TABLE B.7 FRACTOGRAPHIC DATA SURVEY FOR WFI DATA SET

CRACK I.D.	a(t) MIN.	a(t) MAX.	TTCI MIN.	TTCI MAX.	NC(I)	TYPE
1	.0072	.77	12400	31200	48	F
2	.0087	.72	8000	27200	49	F
3	.0061	.7820001	3600	23600	51	F
4	.003	.7454	6000	30400	62	F
5	.0044	.71	11200	30800	50	F
6	.0087	.71	5600	17600	31	F
7	8.999999E-03	.94	2400	16400	36	F
8	.0089	1.02	8400	28000	50	F
9	9.599999E-03	1.06	12000	36480	63	F
10	.0079	.823	6800	30000	59	F
11	.0087	.8599999	6800	20400	35	F
12	.0088	.8560001	11200	32400	54	F
13	.0093	1.03	5600	29360	61	F
14	.0094	.758	12800	33600	53	F

CONSTRAINTS DUE TO FAILURE(S) IN DATA SET

MAX. A0(REF.)= .71　　MAX. TAU= 16400

LARGEST INITIAL TIME/DATA SET= 12800

LARGEST COMMON CRACK SIZE RANGE/DATA SET= 9.599999E-03 - .71

TABLE B.8 FRACTOGRAPHIC DATA SURVEY FOR WBI DATA SET

CRACK I.D.	a(t) MIN.	a(t) MAX.	TTCI MIN.	TTCI MAX.	NC(I)	TYPE
1	.0197	.8264	28055	41449	14	F
2	.0102	.0858	39656	44739	6	S
3	.0134	.8983999	31219	43200	13	F
4	.0103	.7704	45773	58050	13	F
5	.0075	.7159	35437	51975	17	F
6	.0046	.891	37547	54601	18	F
7	.0083	.7161	26156	37979	13	F
8	.0084	.9030999	46828	58020	13	F
9	8.499999E-03	.743	25101	39129	15	F
10	.0103	.8015	25101	40078	16	F
11	.0067	.2611	51047	57659	8	S
12	.012	.8764	32273	49655	18	F

CONSTRAINTS DUE TO FAILURE(S) IN DATA SET

MAX. A0(REF.)= .7159　　MAX. TAU= 37979

LARGEST INITIAL TIME/DATA SET= 51047

LARGEST COMMON CRACK SIZE RANGE/DATA SET= .0197 - .0858

TABLE B.9 FRACTOGRAPHIC DATA SURVEY FOR WXWPB DATA SET

CRACK I.D.	a(t) MIN.	a(t) MAX.	TTCI MIN.	TTCI MAX.	NC(I)	TYPE
1	.0083	.9745999	15609	27830	13	F
2	.0043	.8178	19828	39644	20	F
3	.0045	.8427999	14555	30470	17	F
4	.0057	.919	18773	42595	24	F
5	.0098	.9224999	24047	40698	18	F
6	.0081	.7423	25101	42595	18	F
7	.0044	1	33328	55677	23	F
8	.0147	1.1	18773	40784	23	F
9	.0037	1.0614	30164	51352	22	F
10	.0076	.8990999	27000	55571	29	F
11	.0179	.95	18773	36743	19	F
12	9.099999E-03	1.0249	19828	47870	28	F
13	.0041	.9048999	17719	38798	22	F
14	.0036	1.1447	27000	53832	27	F
15	.0013	.9501999	25101	46815	22	F

CONSTRAINTS DUE TO FAILURE(S) IN DATA SET

MAX. A0(REF.)= .7423 MAX. TAU= 27830

LARGEST INITIAL TIME/DATA SET= 33328

LARGEST COMMON CRACK SIZE RANGE/DATA SET= .0179 - .7423

TABLE B.10 FRACTOGRAPHIC DATA SURVEY FOR WABXHR4 DATA SET

CRACK I.D.	a(t) MIN.	a(t) MAX.	TTCI MIN.	TTCI MAX.	NC(I)	TYPE
1	[illegible]	.6935	2109	15385	14	F
2	.0035	.9138999	2109	17389	16	F
3	.009[illegible]	.5828	4219	19815	16	F
4	.006[illegible]	.739	1055	12644	12	F
5	.004[illegible]	.8008	2109	16650	15	F
6	.0076	.6531	2109	19815	18	F
7	.0055	.4411	1055	12643	12	F
8	.0156	.5523	4219	11589	8	F
9	.006[illegible]	.8328	3164	15808	14	F
10	.0088	.5702	5273	15595	11	F
11	.0069	.9536	1055	11875	12	F
12	.0042	.7463	4219	13700	11	F
13	.0077	.7026	2109	14540	13	F
14	.0069	.7616	3164	13277	11	F
15	.0084	.8211	2109	11486	10	F

CONSTRAINTS DUE TO FAILURE(S) IN DATA SET

MAX. A0(REF.)= .4411 MAX. TAU= 11486

LARGEST INITIAL TIME/DATA SET= 5273

LARGEST COMMON CRACK SIZE RANGE/DATA SET= .0156 - .4411

TABLE B.11 FRACTOGRAPHIC DATA SURVEY FOR WWPFO DATA SET

CRACK I.D.	a(t) MIN.	a(t) MAX.	TTCI MIN.	TTCI MAX.	NC(I)	TYPE
1	.0068	.8882	14800	22348	20	F
2	.0057	.8552	3600	15478	31	F
3	8.499999E-03	.6317	14000	19635	15	F
4	.004	.7789	15200	24406	24	F
5	.0125	.7558	15600	26806	29	F
6	.0046	.9410001	16800	26006	24	F
7	.0043	.7726	16400	27235	28	F
8	.0074	.8193	14800	22806	21	F
9	.0026	.7831	12000	23606	30	F
10	.004	.6601	11200	20435	24	F
11	.006	.6979	15200	23606	22	F
12	.0032	.8523	12800	24000	29	F
13	.0064	.6854	10800	20035	24	F
14	.0057	.7966	8000	21206	34	F

CONSTRAINTS DUE TO FAILURE(S) IN DATA SET

MAX. A0(REF.)= .6317   MAX. TAU= 15478

LARGEST INITIAL TIME/DATA SET= 16800

LARGEST COMMON CRACK SIZE RANGE/DATA SET= .0125 - .6317

TABLE B.12 FRACTOGRAPHIC DATA SURVEY FOR AFXHR4 DATA SET

CRACK I.D.	a(t) MIN.	a(t) MAX.	TTCI MIN.	TTCI MAX.	NC(I)	TYPE
1	.0125	.4681	1200	9871	23	F
2	.0158	.3527	4800	13073	21	F
3	.014	.3087	4800	12806	21	F
4	.0084	.2664	2400	6900	13	F
5	.0093	.2543	6400	16000	25	S
6	.0339	.3091	4000	8035	12	F
7	.0252	.274	2000	4807	9	F
8	.0187	.3254	2000	5206	10	F
9	.0181	.3292	6000	12435	18	F
10	.0155	.5777	1600	7075	15	F

CONSTRAINTS DUE TO FAILURE(S) IN DATA SET

MAX. A0(REF.)= .2664   MAX. TAU= 4807

LARGEST INITIAL TIME/DATA SET= 6400

LARGEST COMMON CRACK SIZE RANGE/DATA SET= .0339 - .2543

TABLE B.13 FRACTOGRAPHIC DATA SURVEY FOR AFXLR4 DATA SET

CRACK I.D.	a(t) MIN.	a(t) MAX.	TTCI MIN.	TTCI MAX.	NC(I)	TYPE
1	.0166	.1821	8000	16000	21	S
2	.0245	.4332	4000	10407	18	F
3	.0296	.437	12000	25235	35	F
4	.0205	.4008	5200	23235	46	F
5	.0089	.4616	6800	24806	47	F
6	.0191	.1343	9600	31606	56	F
7	.0097	.1817	10000	32000	56	S
8	.0698	.1335	11600	32000	52	S
9	.0177	.199	20000	30808	28	F
10	.0299	.1801	8800	19206	27	F
11	.015	.4324	5600	11606	17	F

CONSTRAINTS DUE TO FAILURE(S) IN DATA SET

MAX. A0(REF.)= .1343 MAX. TAU= 10407

LARGEST INITIAL TIME/DATA SET= 20000

LARGEST COMMON CRACK SIZE RANGE/DATA SET= .0698 - .1335

TABLE B.14 FRACTOGRAPHIC DATA SURVEY FOR AFXMR4 DATA SET

CRACK I.D.	a(t) MIN.	a(t) MAX.	TTCI MIN.	TTCI MAX.	NC(I)	TYPE
1	.0229	.0709	4000	16000	31	S
2	.0099	.3526	3600	11255	20	F
3	.0017	.0764	6000	16000	26	S
4	.0223	.0777	7200	16000	23	S
5	.0239	.3008	4000	16000	31	S
6	.0217	.5372	4400	12806	22	F
7	.0041	.0504	6800	16000	24	S
8	.0312	.5572	5200	16000	28	S
9	.0181	.3786	2400	6006	11	F

CONSTRAINTS DUE TO FAILURE(S) IN DATA SET

MAX. A0(REF.)= .3526 MAX. TAU= 6006

LARGEST INITIAL TIME/DATA SET= 7200

LARGEST COMMON CRACK SIZE RANGE/DATA SET= .0312 - .0504

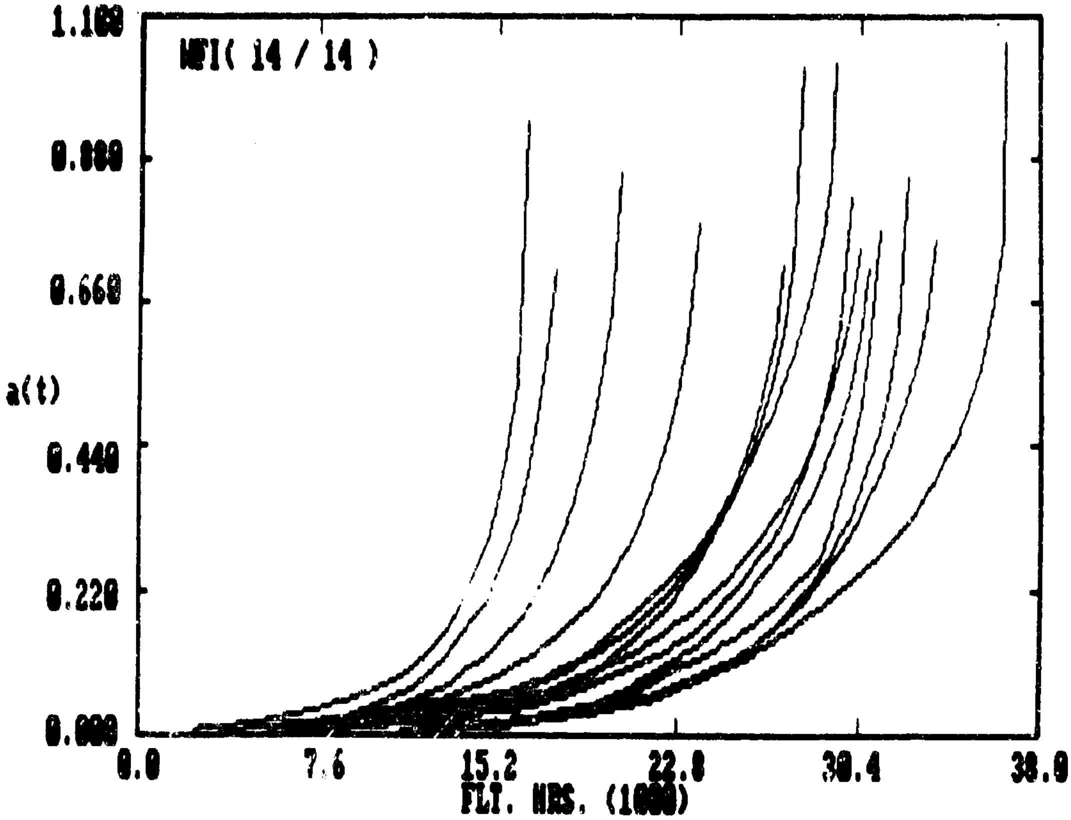

Figure B.1. a(t) VERSUS t FRACTOGRAPHIC DATA FOR WFI DATA SET (FULL RANGE).

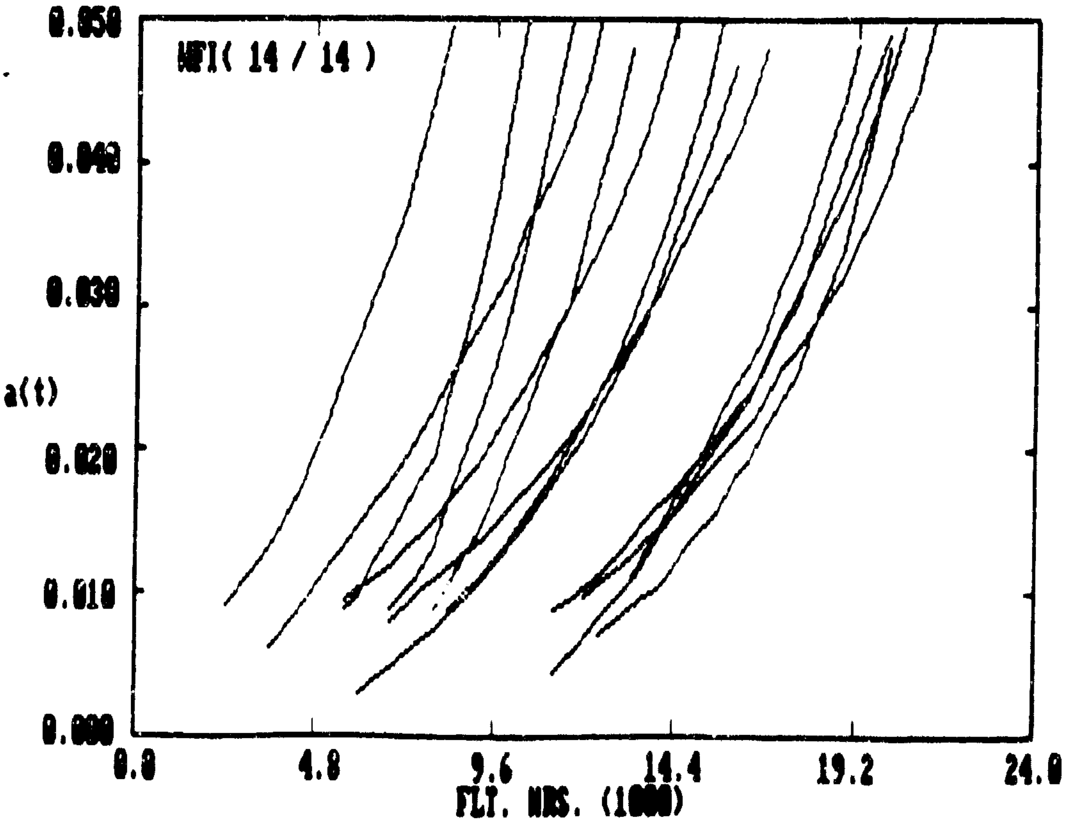

Figure B.2. a(t) VERSUS t FRACTOGRAPHIC DATA FOR WFI DATA SET (AL-AU = 0 - .05").

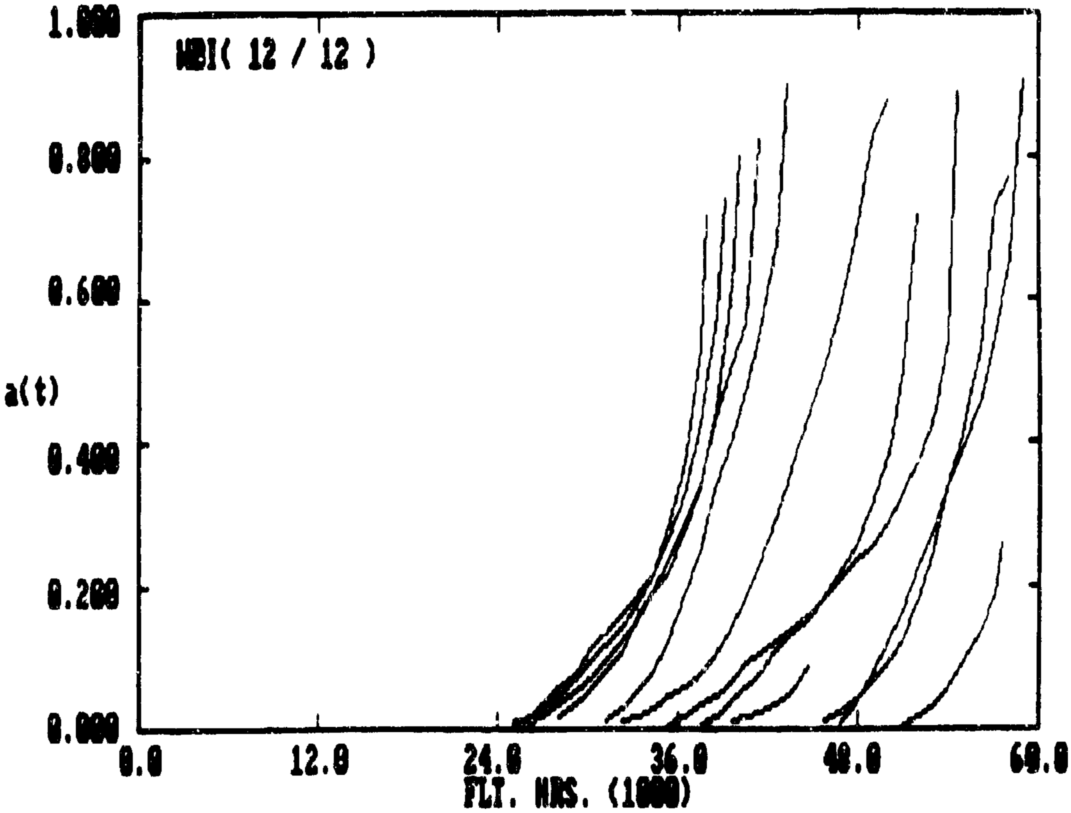

Figure B.3. a(t) VERSUS t FRACTOGRAPHIC DATA FOR WBI DATA SET (FULL RANGE).

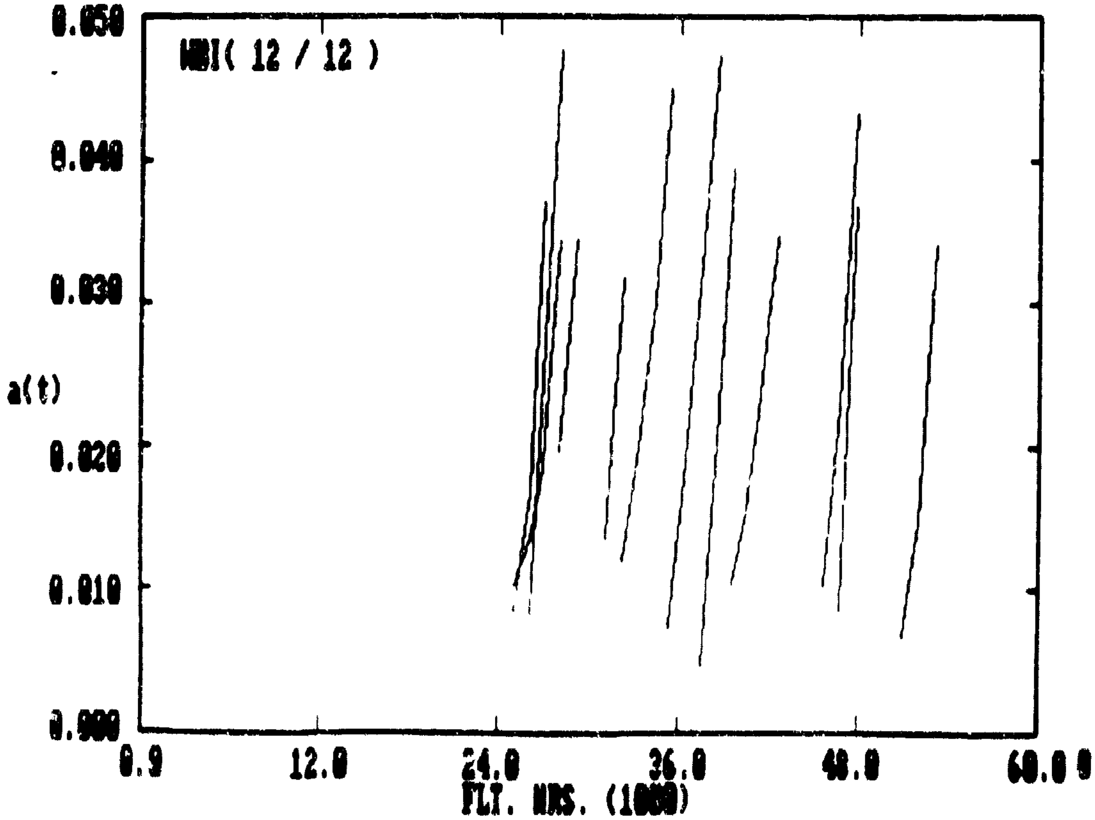

Figure B.4. a(t) VERSUS t FRACTOGRAPHIC DATA FOR WBI DATA SET (AL-AU = 0 -.05")

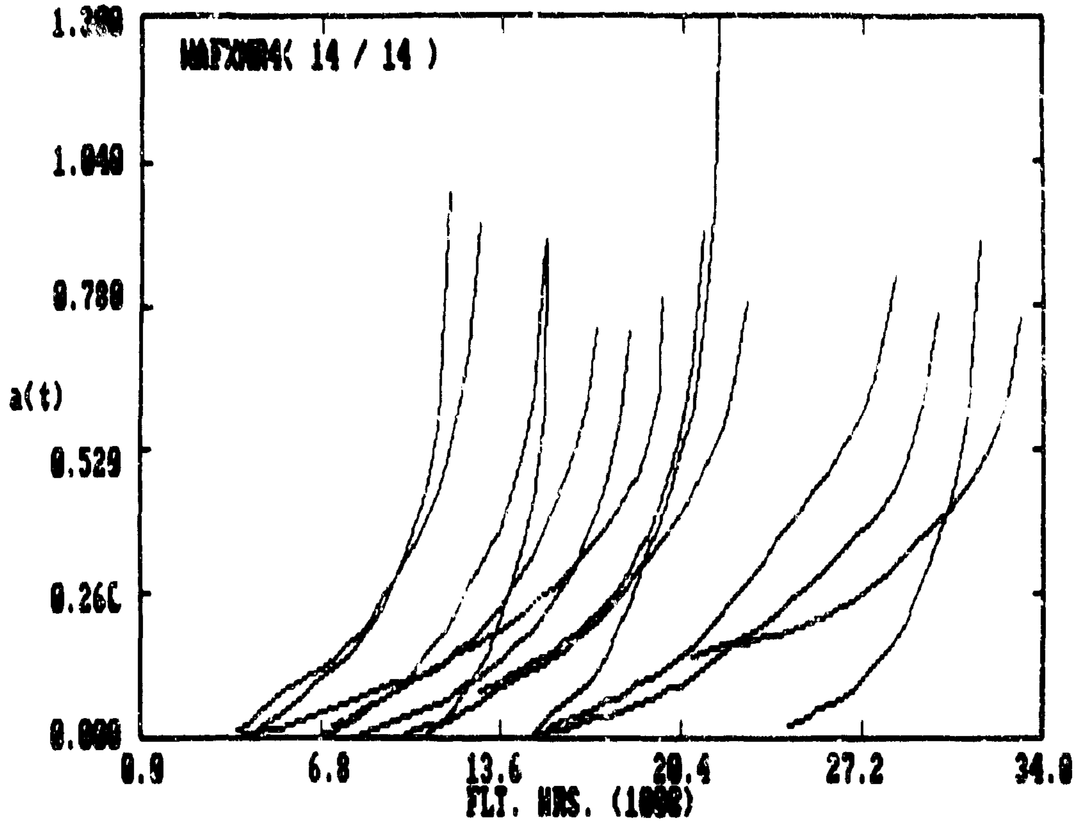

Figure B.5. a(t) VERSUS t FRACTOGRAPHIC DATA FOR WAFXMR4 DATA SET (FULL RANGE).

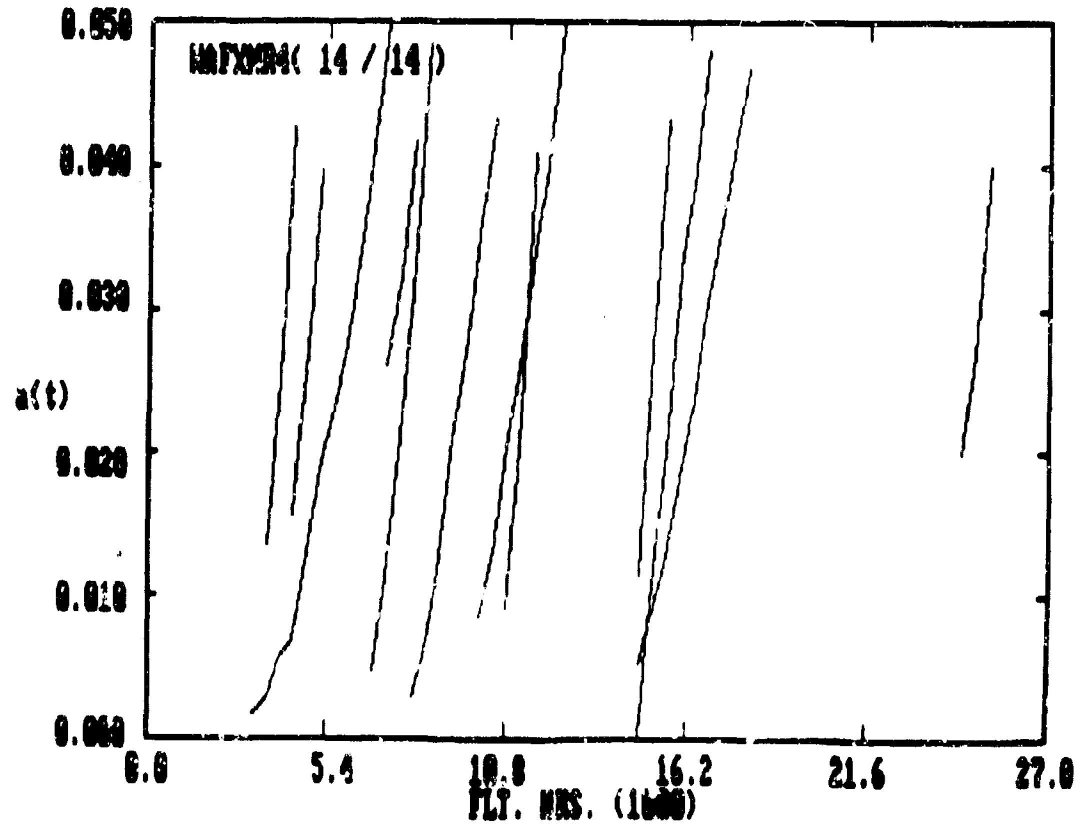

Figure B.6. a(t) VERSUS t FRACTOGRAPHIC DATA FOR WAFXMR4 DATA SET (AL-AU = 0 - .05").

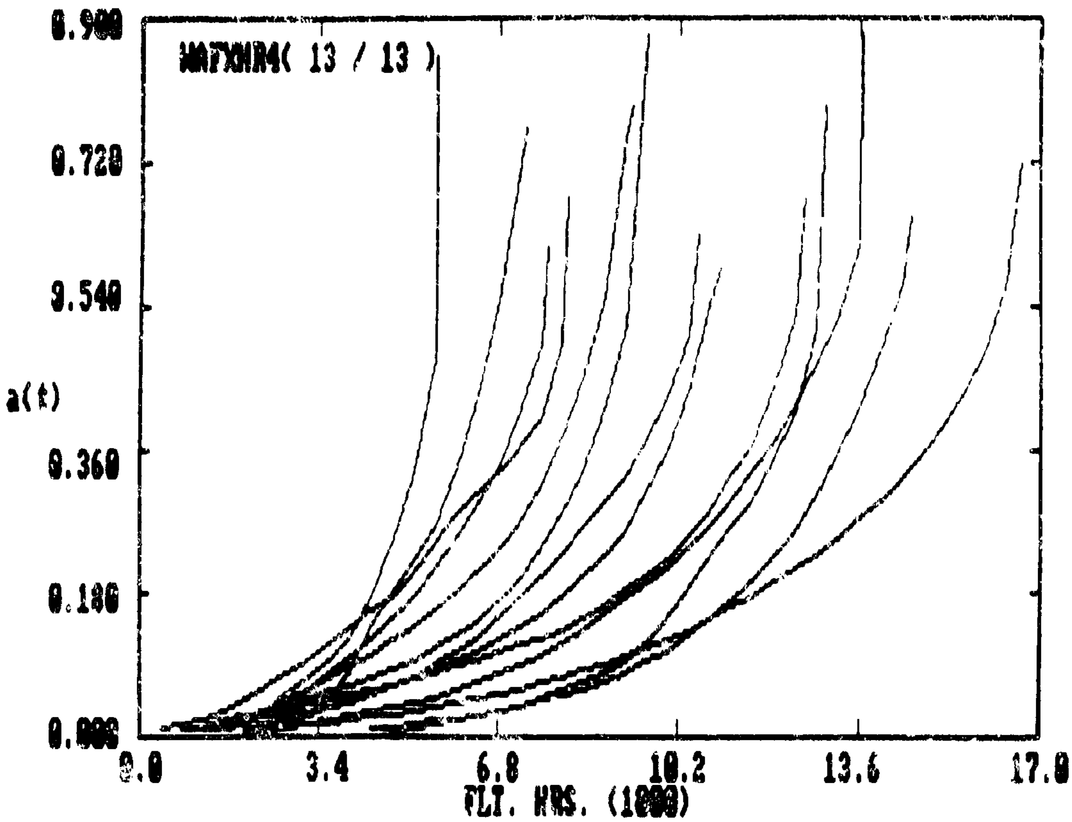

Figure B.7. a(t) VERSUS t FRACTOGRAPHIC DATA FOR WAFXHR4 DATA SET (FULL RANGE).

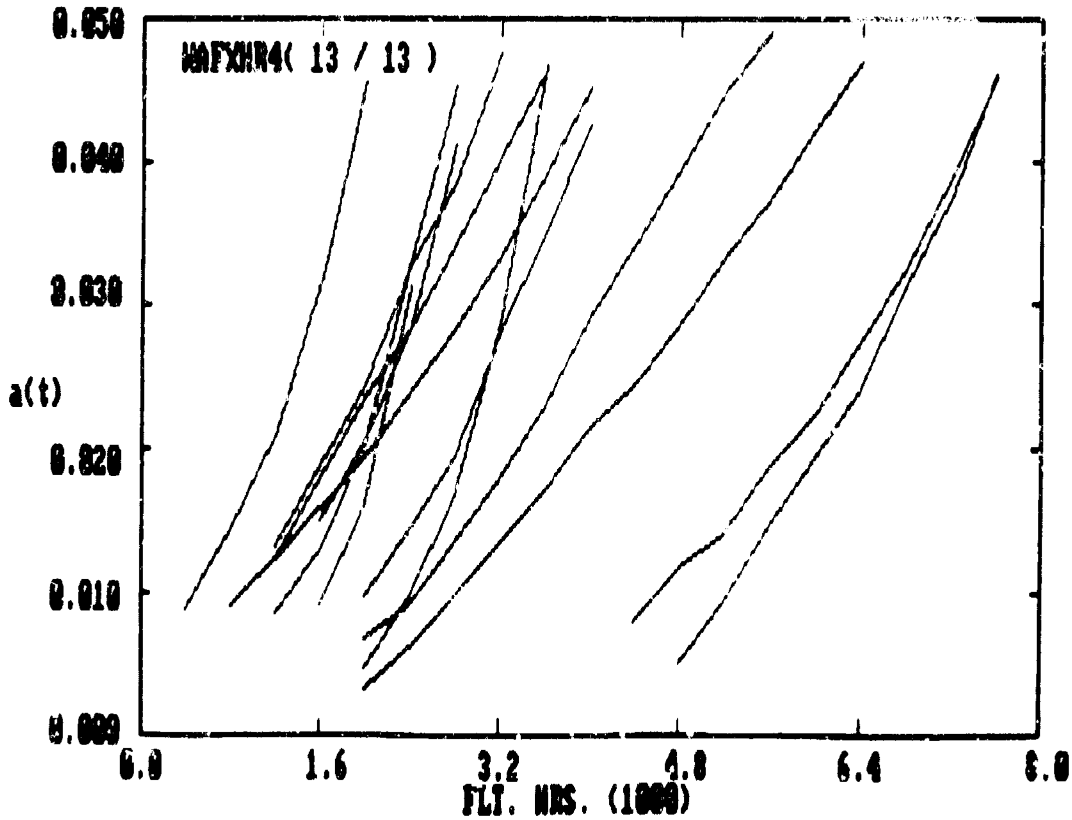

Figure B.8. a(t) VERSUS t FRACTOGRAPHIC DATA FOR WAFXHR4 DATA SET (AL-AU = 0 - .05").

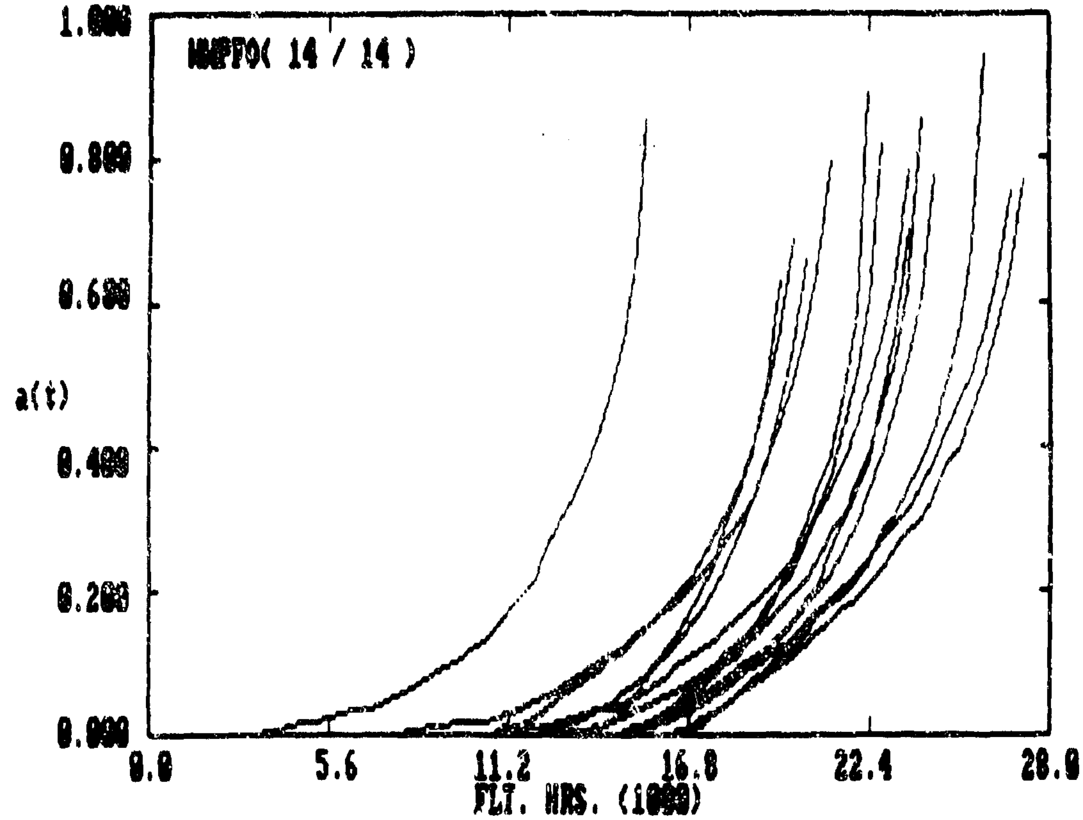

Figure B.9. a(t) VERSUS t FRACTOGRAPHIC DATA FOR WWPFO DATA SET (FULL RANGE).

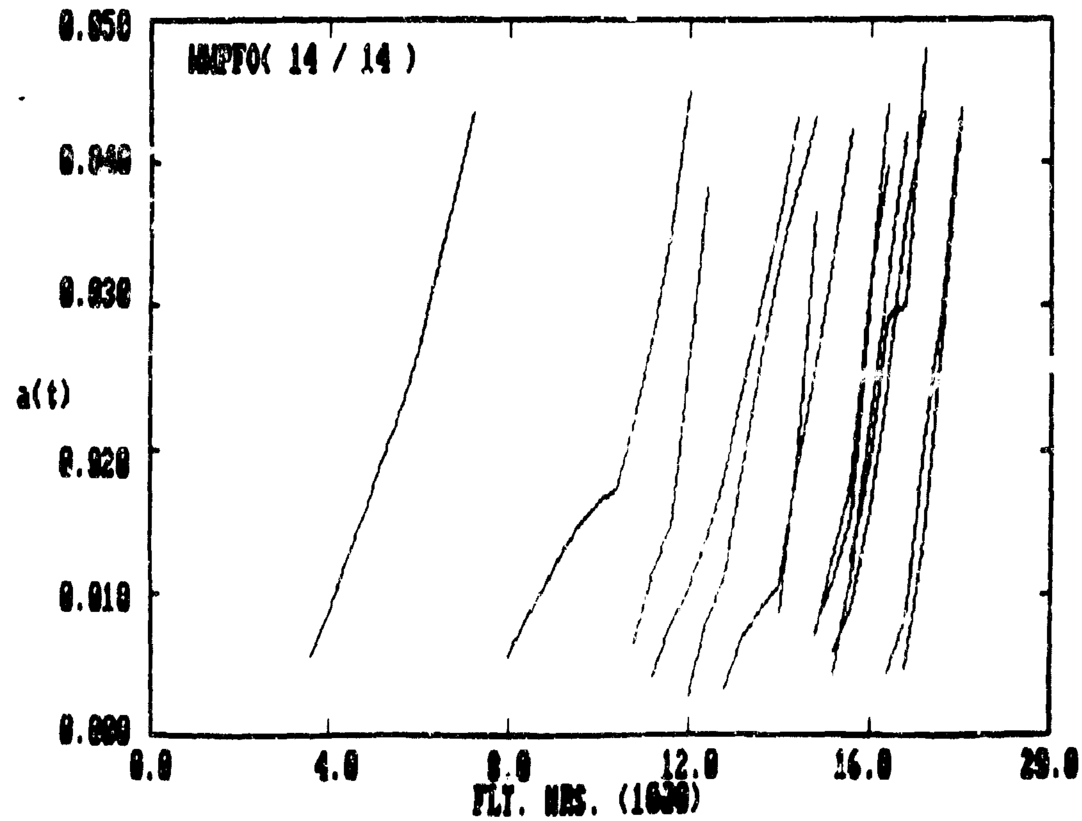

Figure B.10. a(t) VERSUS t FRACTOGRAPHIC DATA FOR WWPFO DATA SET (AL-AU = 0 - .05").

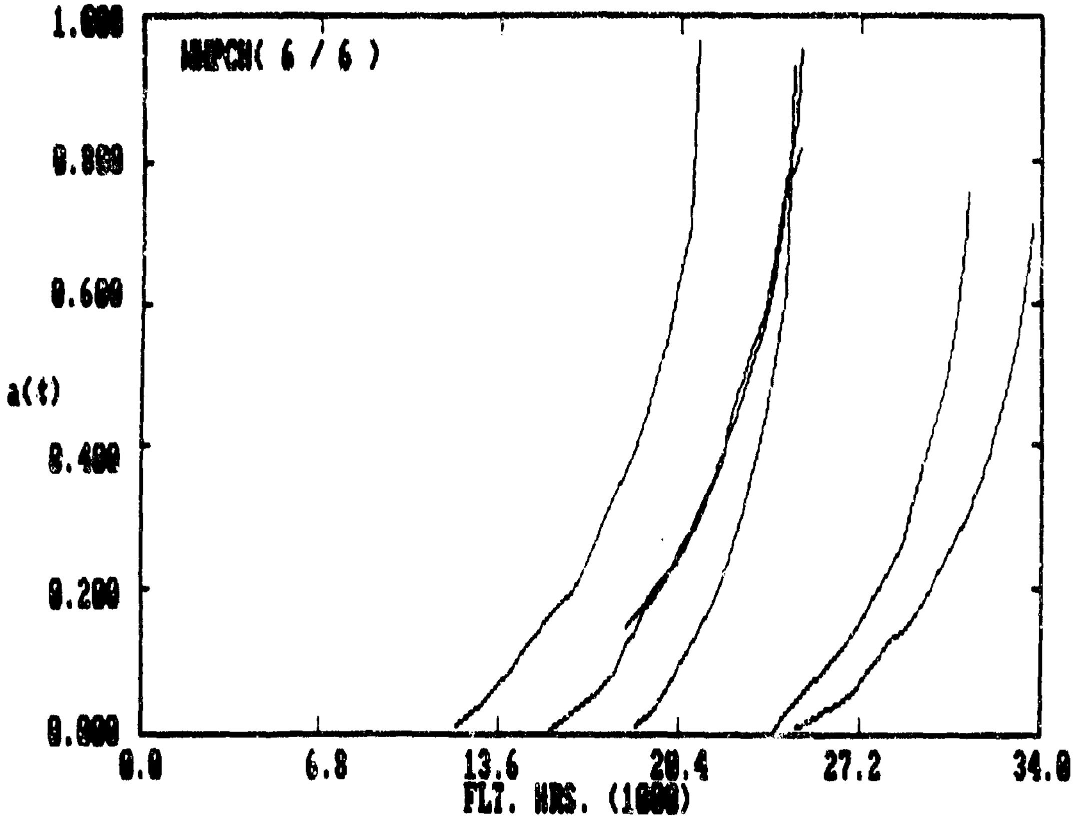

Figure B.11. a(t) VERSUS t FRACTOGRAPHIC DATA FOR WWPCH DATA SET (FULL RANGE).

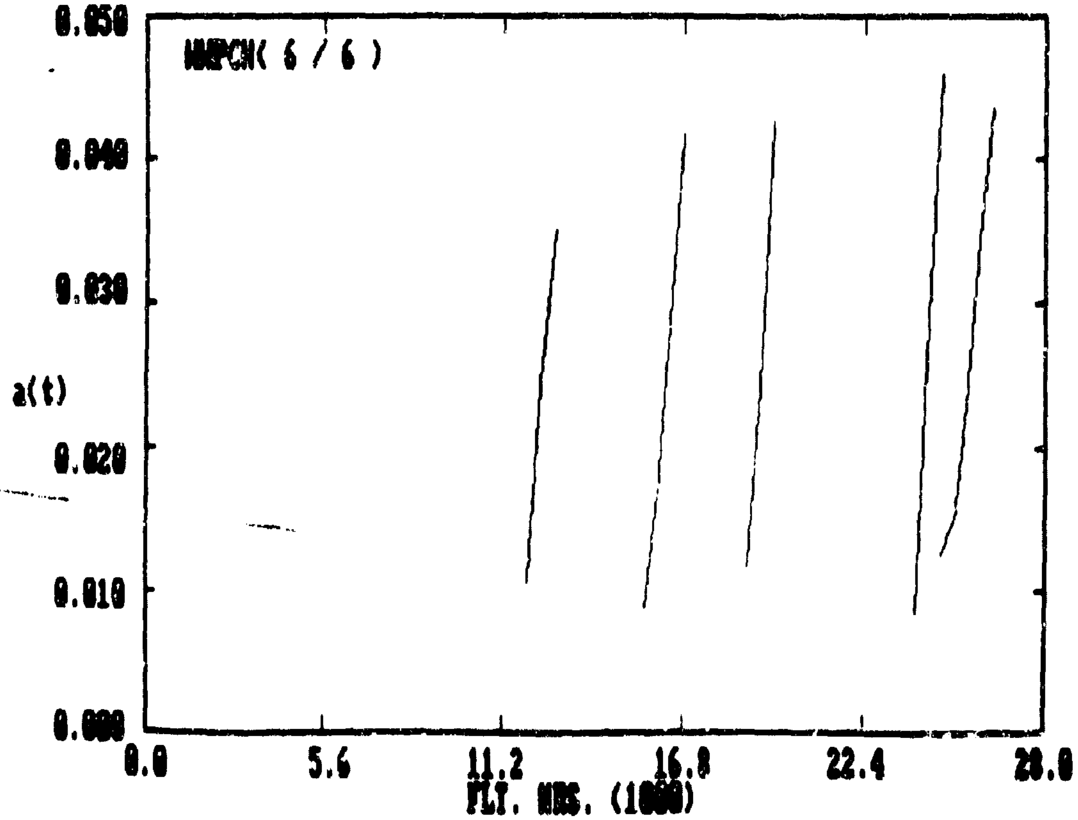

Figure B.12. a(t) VERSUS t FRACTOGRAPHIC DATA FOR WWPCH DATA SET (AL-AU = 0 - .05").

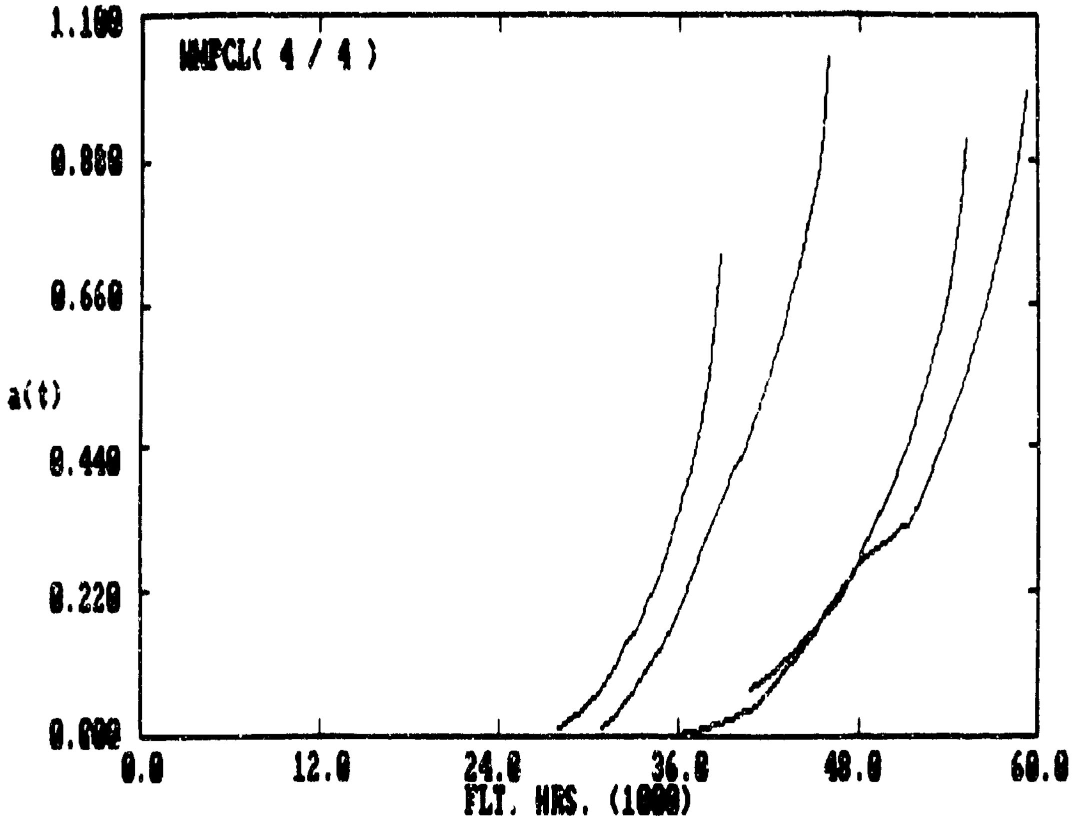

Figure B.13. a(t) VERSUS t FRACTOGRAPHIC DATA FOR WWPCL DATA SET (FULL RANGE).

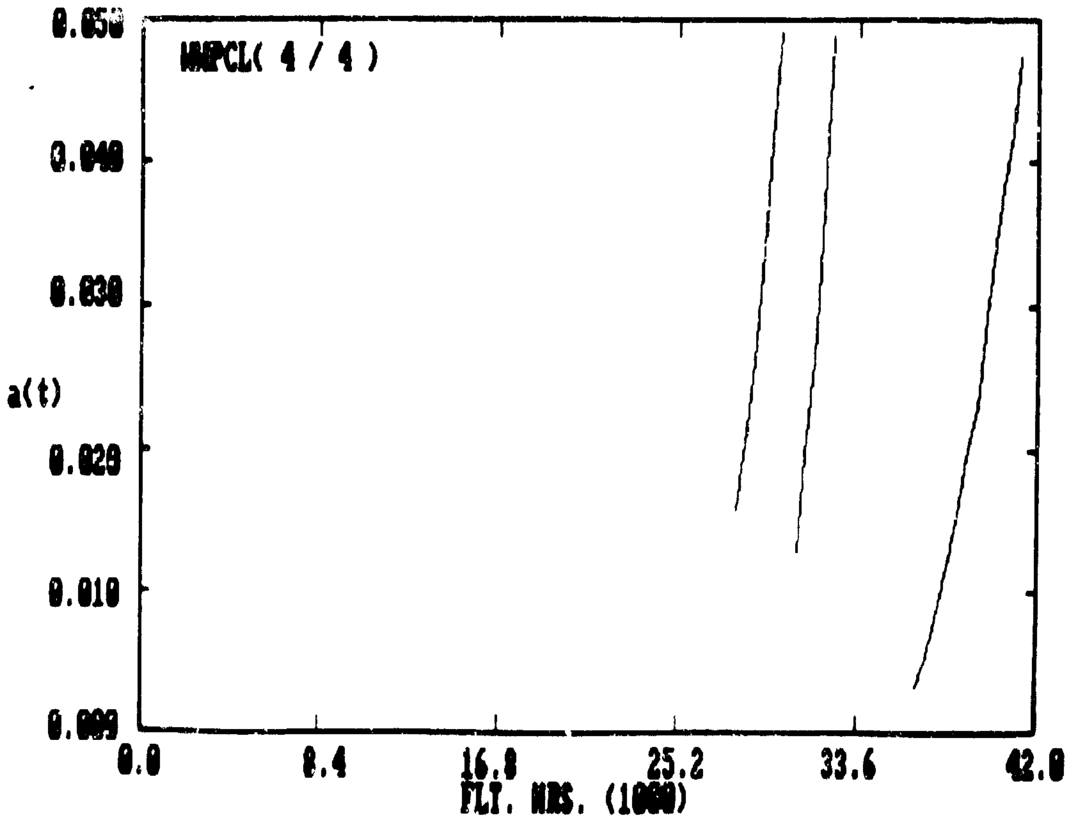

Figure B.14. a(t) VERSUS t FRACTOGRAPHIC DATA FOR WWPCL DATA SET (AL-AU = 0 - .05").

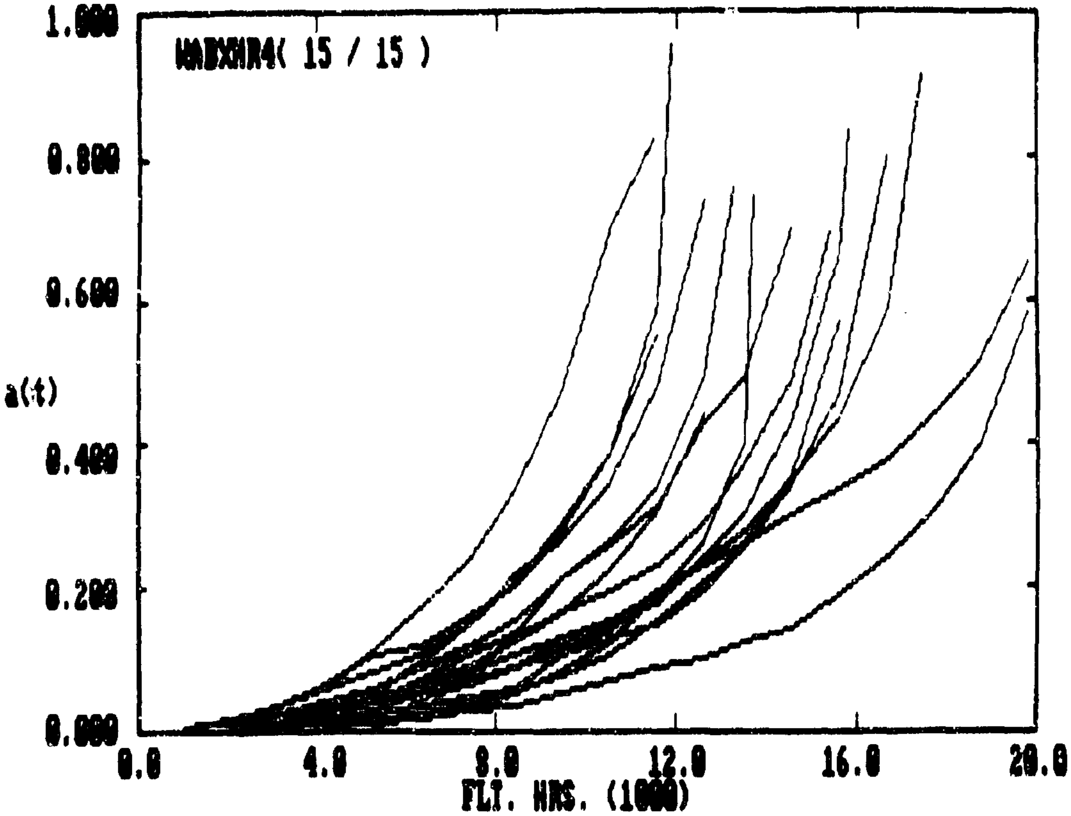

Figure B.15. a(t) VERSUS t FRACTOGRAPHIC DATA FOR WABXHR4 DATA SET (FULL RANGE).

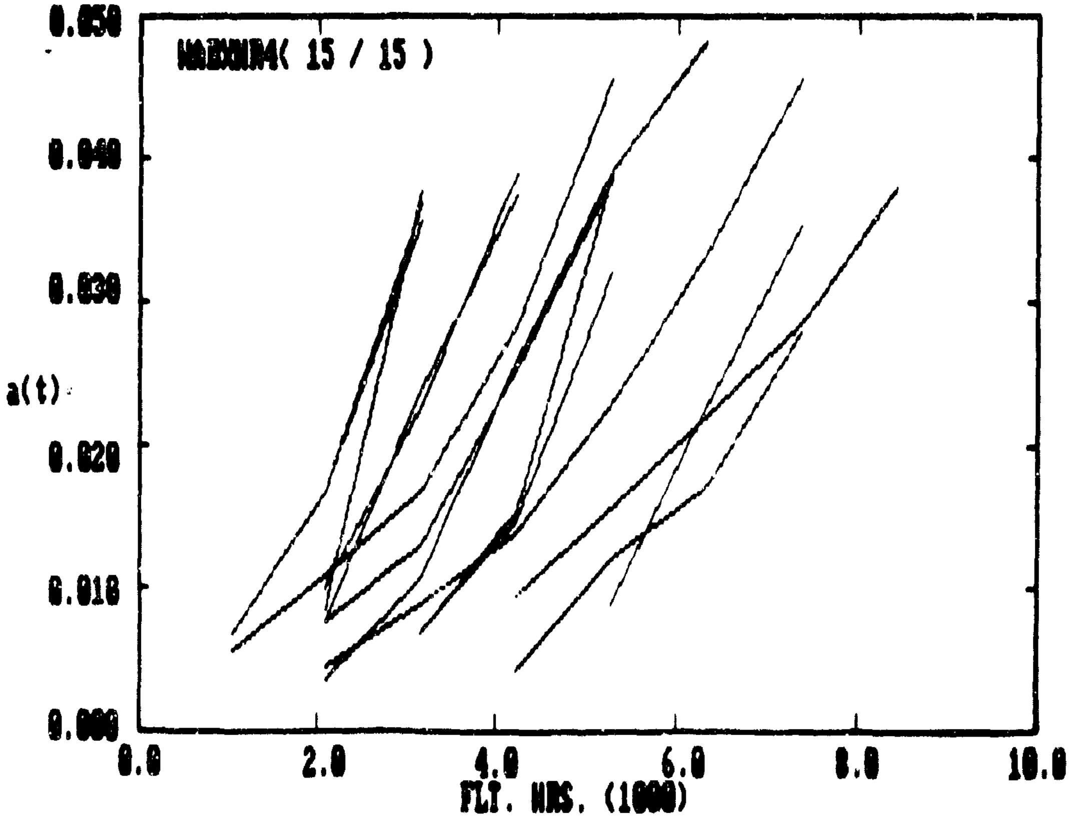

Figure B.16. a(t) VERSUS t FRACTOGRAPHIC DATA FOR WABXHR4 DATA SET (AL-AU = 0 - .05")

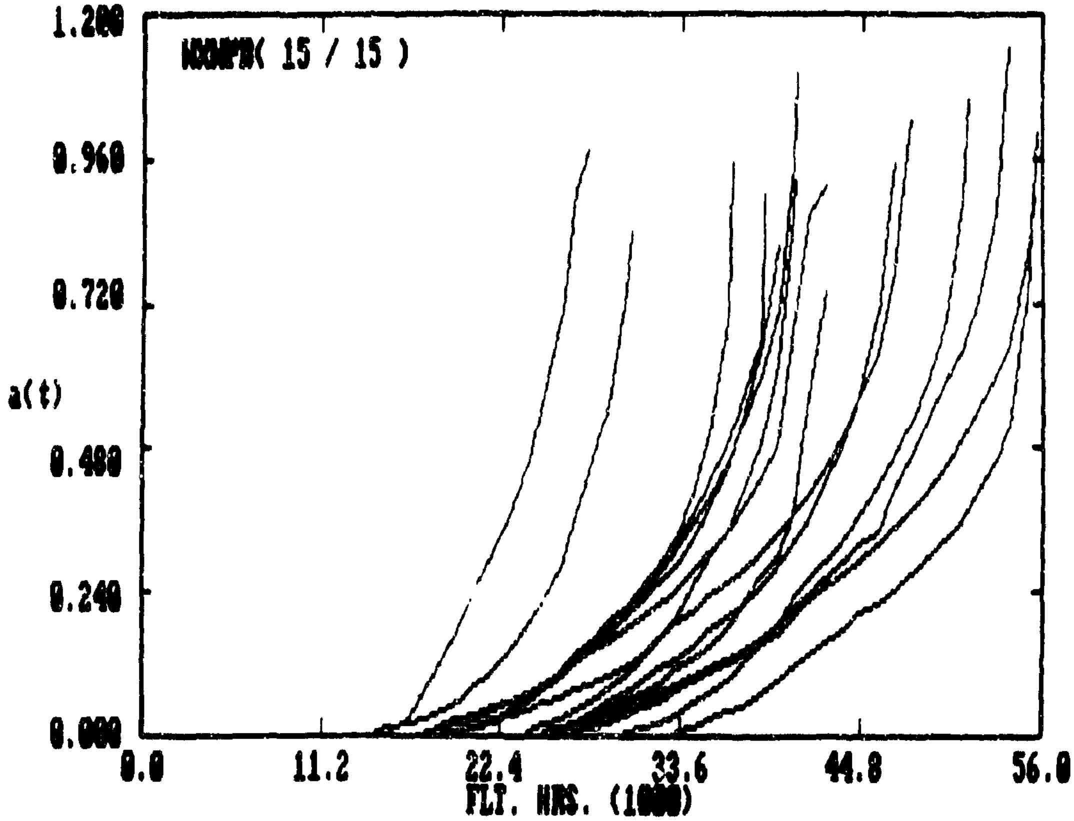

Figure B.17. a(t) VERSUS t FRACTOGRAPHIC DATA FOR WXWPB DATA SET (FULL RANGE).

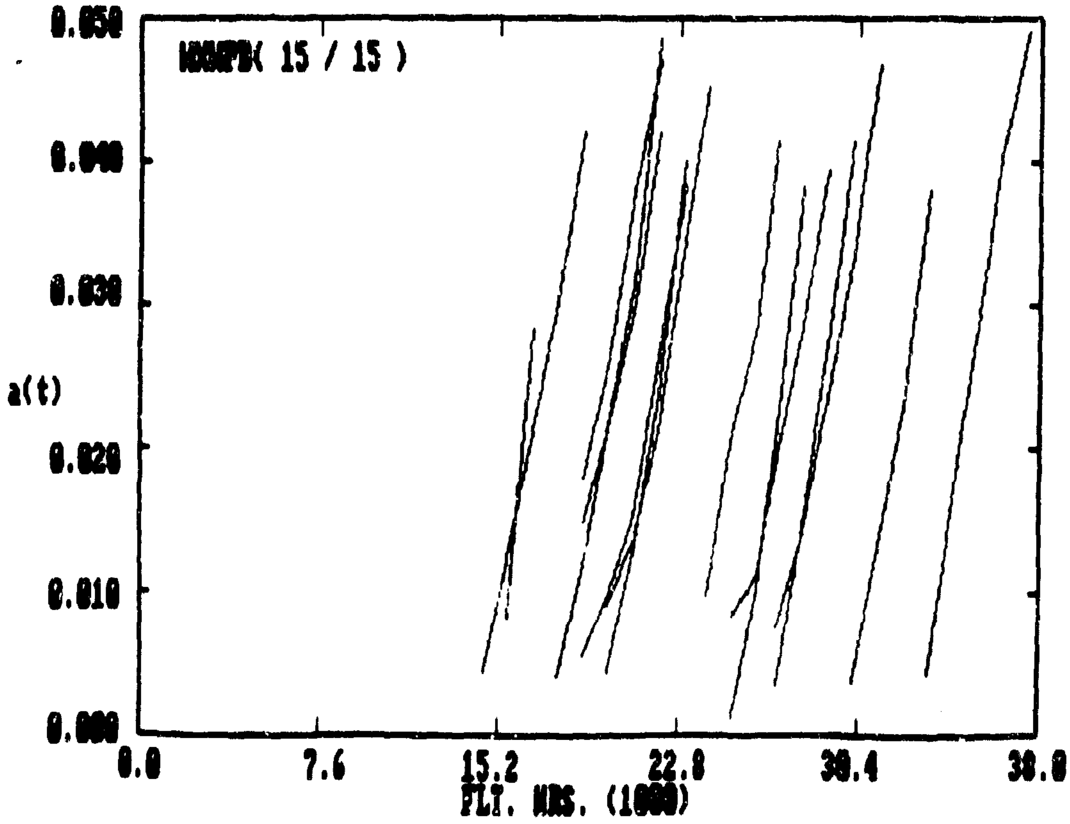

Figure B.18. a(t) VERSUS t FRACTOGRAPHIC DATA FOR WXWPB DATA SET (AL-AU = 0 - .05").

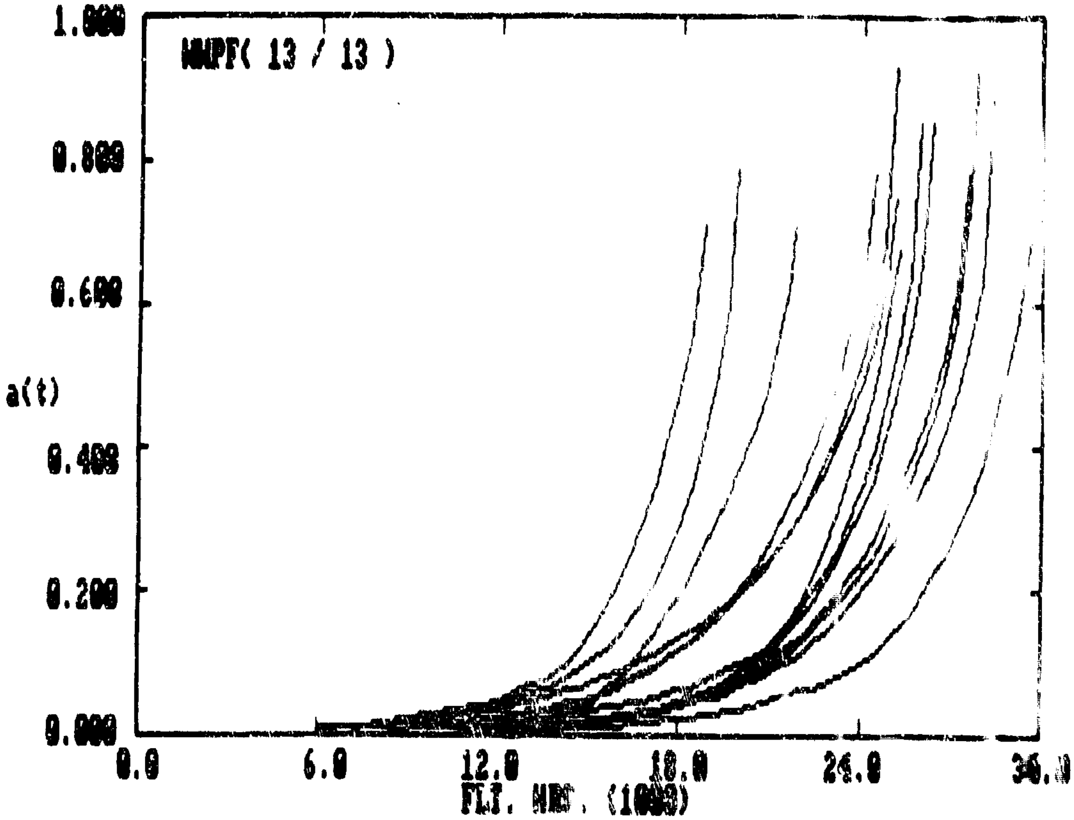

Figure B.19. a(t) VERSUS t FRACTOGRAPHIC DATA FOR WWPF DATA SET (FULL RANGE).

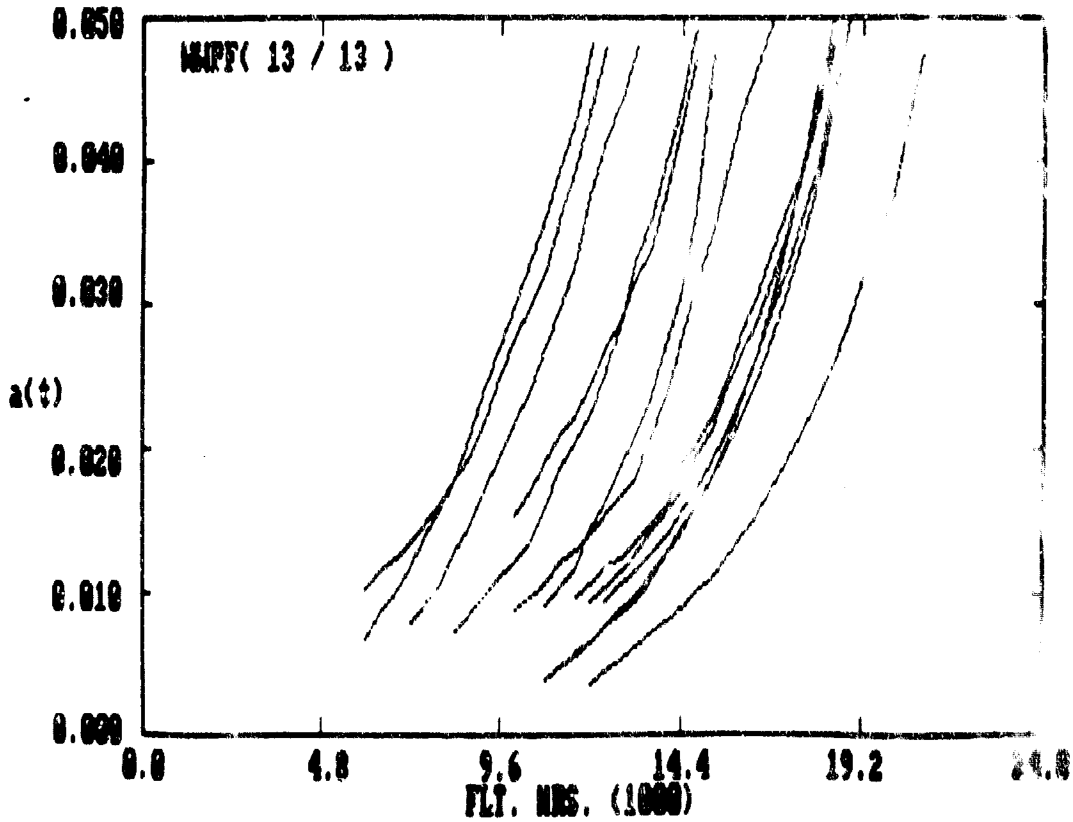

Figure B.20. a(t) VERSUS t FRACTOGRAPHIC DATA FOR WWPF DATA SET (AL-AU = 0 - .05").

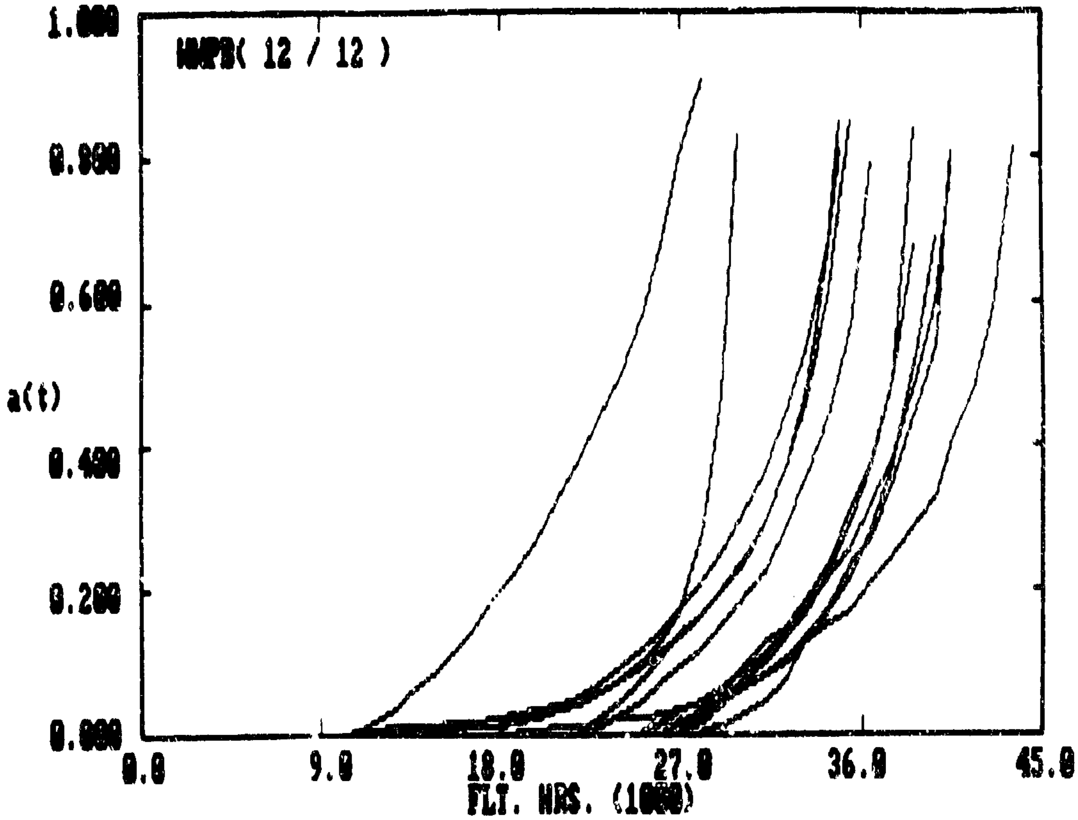

Figure B.21. a(t) VERSUS t FRACTOGRAPHIC DATA FOR WWPB DATA SET (FULL RANGE).

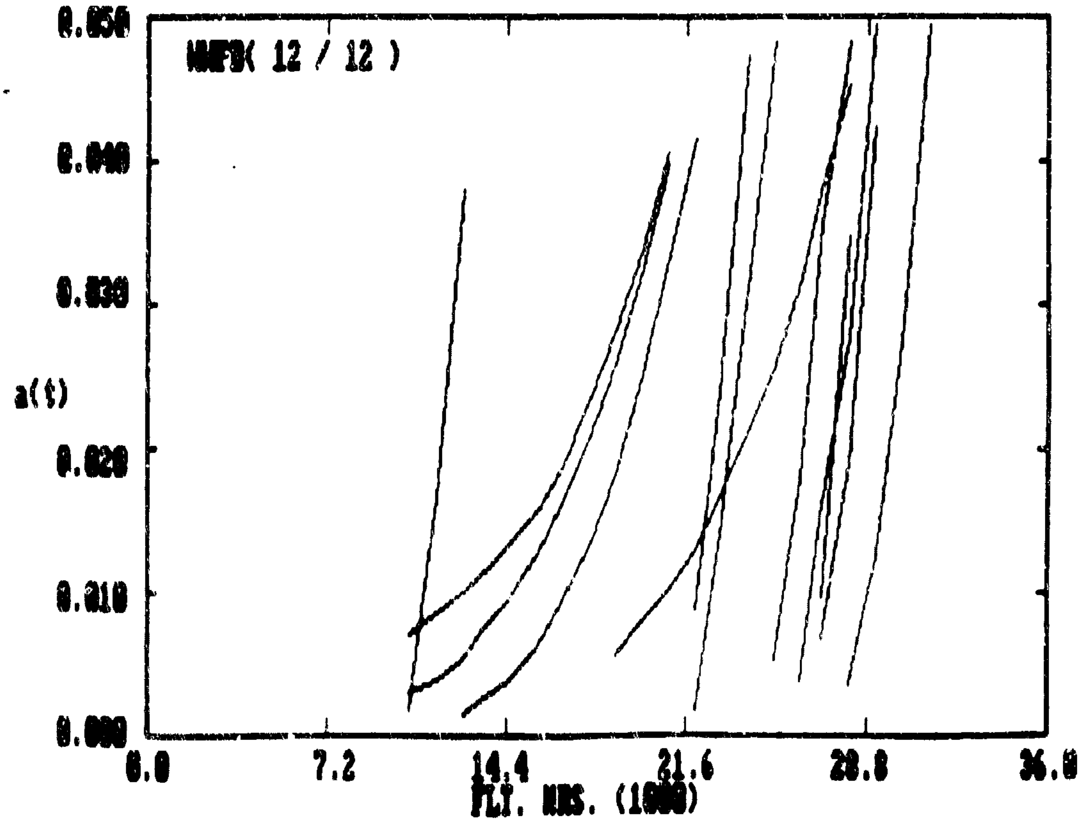

Figure B.22. a(t) VERSUS t FRACTOGRAPHIC DATA FOR WWPB DATA SET (AL-AU = 0 - .05").

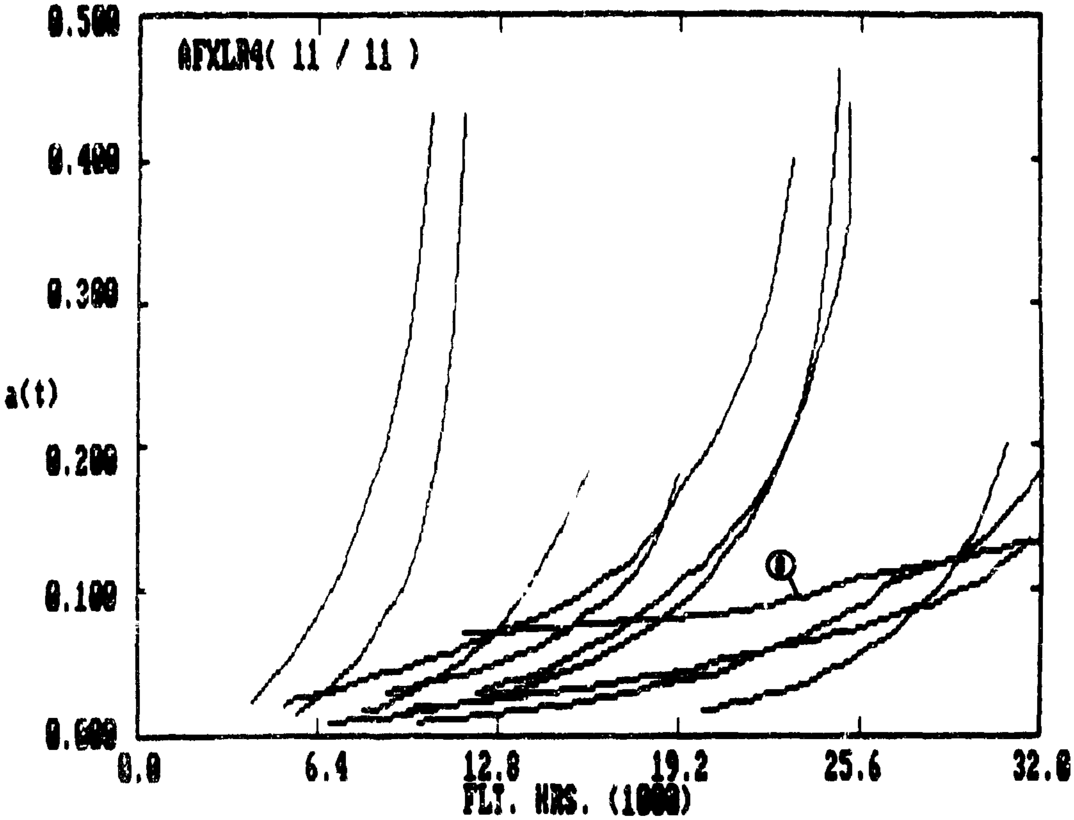

Figure B.23. a(t) VERSUS t FRACTOGRAPHIC DATA FOR AFXLR4 DATA SET (FULL RANGE).

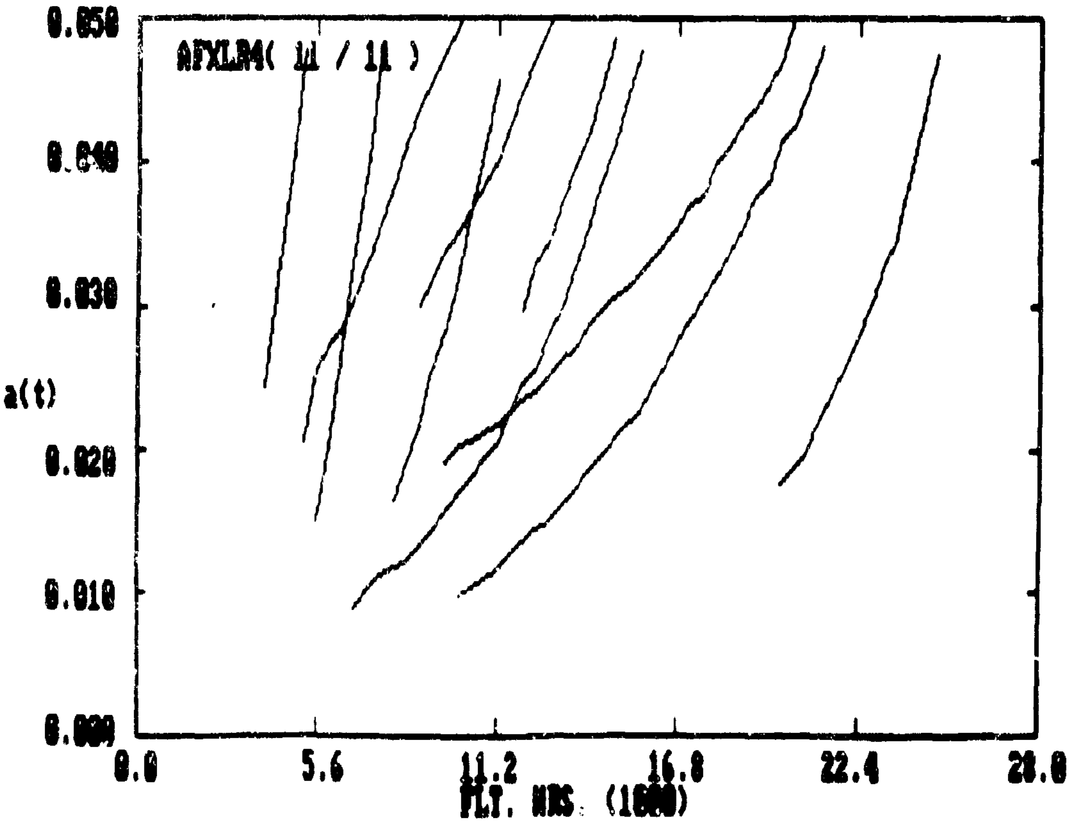

Figure B.24. a(t) VERSUS t FRACTOGRAPHIC DATA FOR AFXLR4 DATA SET (AL-AU = 0 - .05").

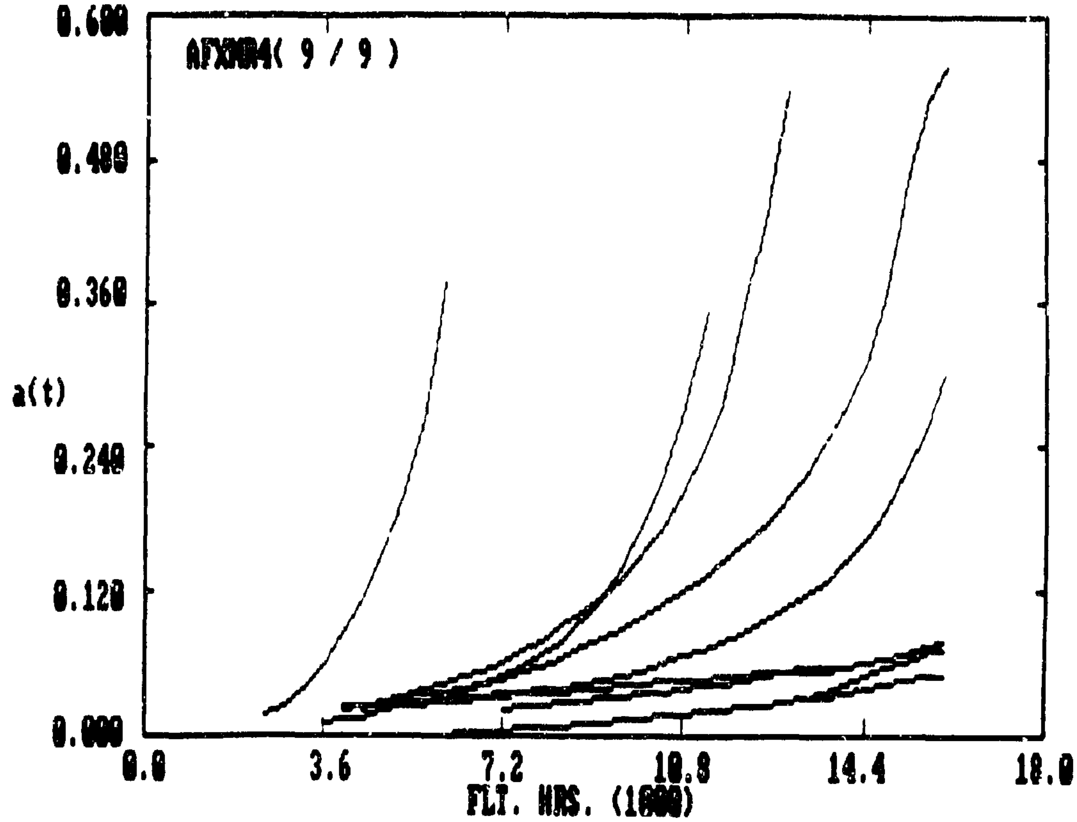

Figure B.25. a(t) VERSUS t FRACTOGRAPHIC DATA FOR AFXMR4 DATA SET (FULL RANGE).

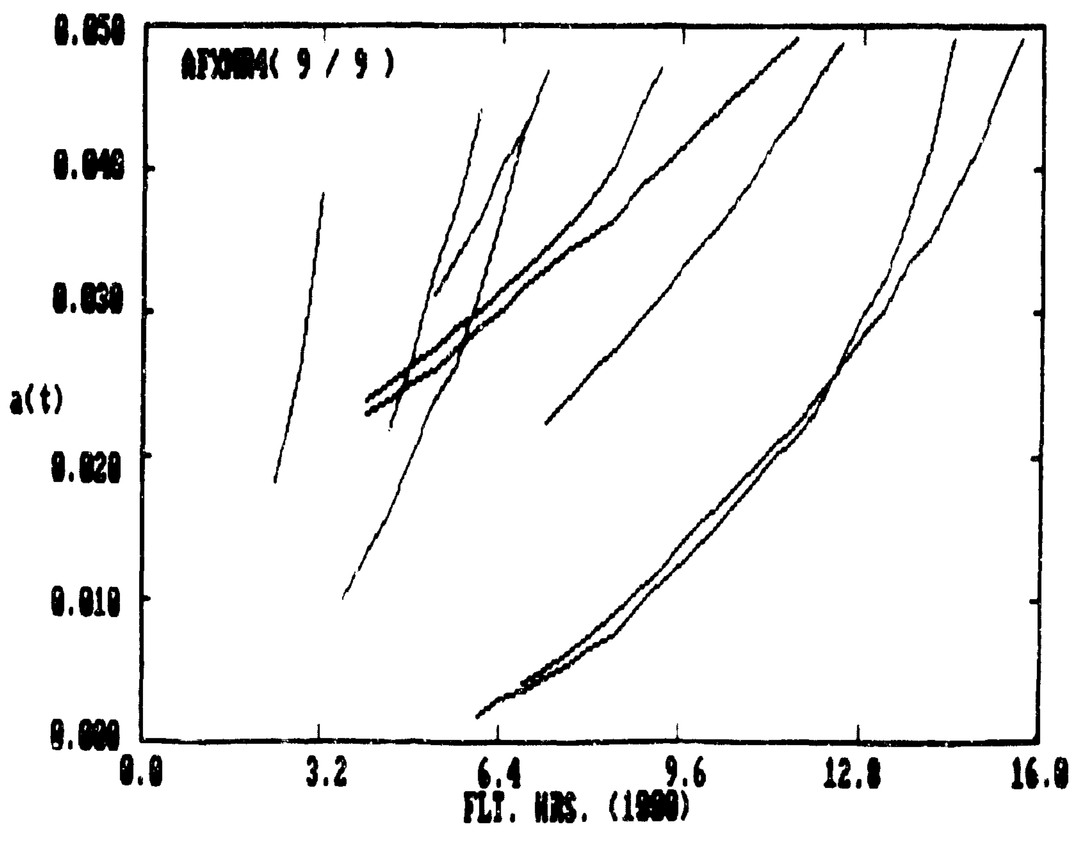

Figure B.26. a(t) VERSUS t FRACTOGRAPHIC DATA FOR AFXMR4 DATA SET (AL-AU = 0 - .05").

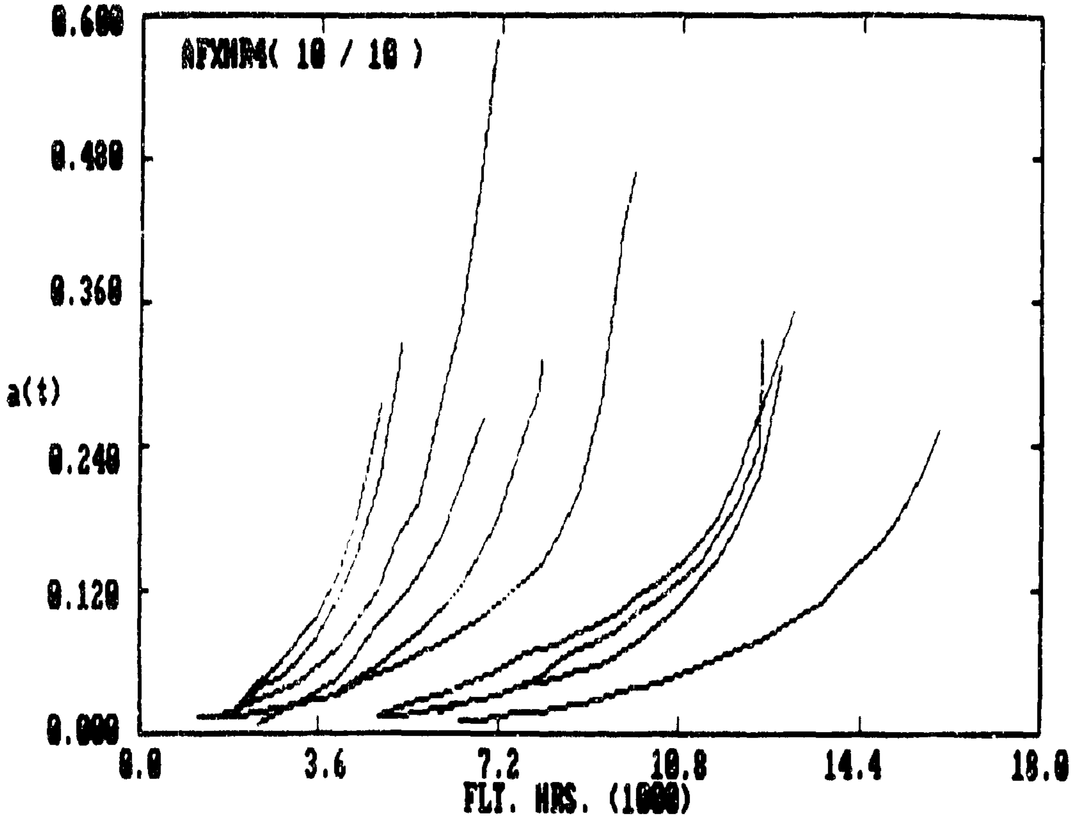

Figure B.27. a(t) VERSUS t FRACTOGRAPHIC DATA FOR AFXHR4 DATA SET (FULL RANGE).

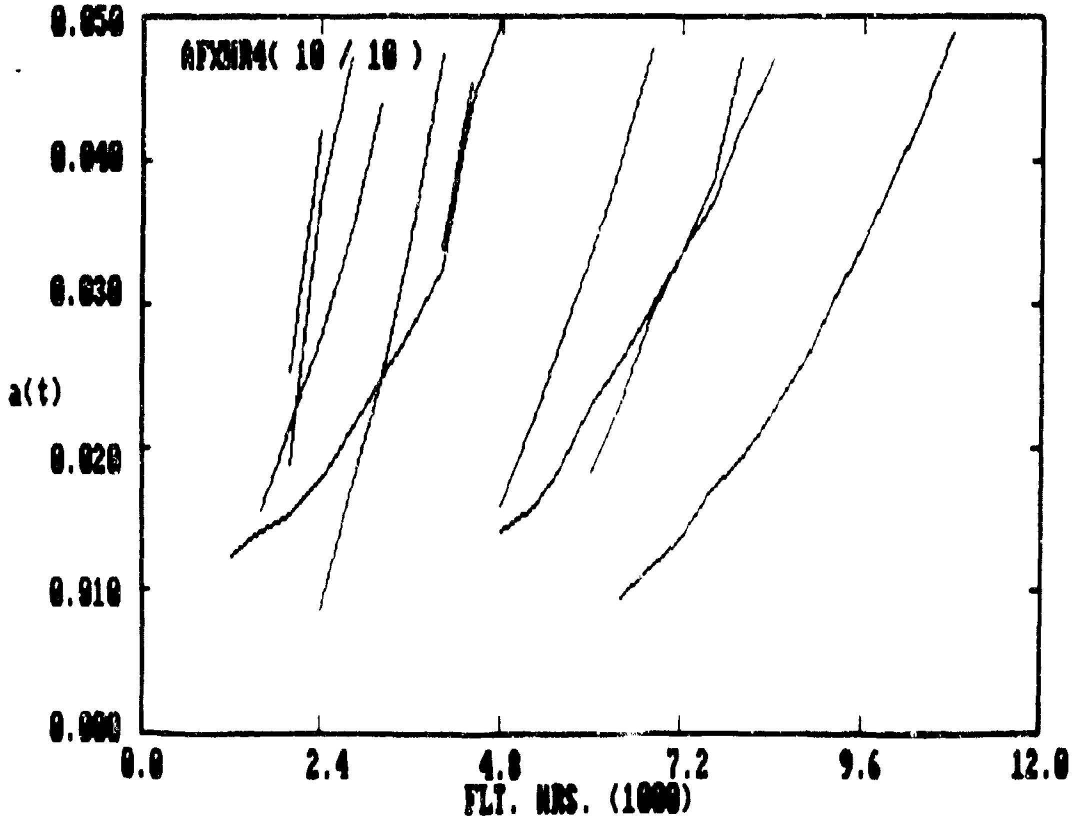

Figure B.28. a(t) VERSUS t FRACTOGRAPHIC DATA FOR AFXHR4 DATA SET (AL-AU = 0 - .05").

APPENDIX C

EVALUATION OF STATISTICAL SCALING METHOD

C.1 INTRODUCTION

The purpose of this section is to evaluate the statistical scaling method described in Volume I [1]. This method can be applied to obtain the EIFSD for fastener holes on a "single hole basis" using only the fractographic data for the largest crack in ℓ holes per specimen. Fractographic results from Volume III [2] will be used.

The initial fatigue quality of fastener holes is "single hole population basis." This means that the fatigue cracking resistance of each fastener hole in each specimen should be accounted for. If fractographic readings are available for the largest fatigue crack in each hole of each specimen, and these results are used to define the IFQ, the resulting IFQ will automatically reflect a single hole population basis. However, if fractographic results are available only for the largest fatigue crack per specimen with ℓ holes, a method is needed for "scaling" the fractographic results to obtain the EIFD on a single hole population basis. Such a method has been developed in Volume I [1].

C.2 EVALUATION PLAN

The plan for evaluating the statistical scaling method described in Volume I [1] is conceptually described in Fig. C.1. A brief overview of the plan is described below and details are provided later.

1. The statistical scaling method is evaluated using the durability analysis methods developed in Volume I [1] and the "WFI" fractographic data set from Volume III [3]. The

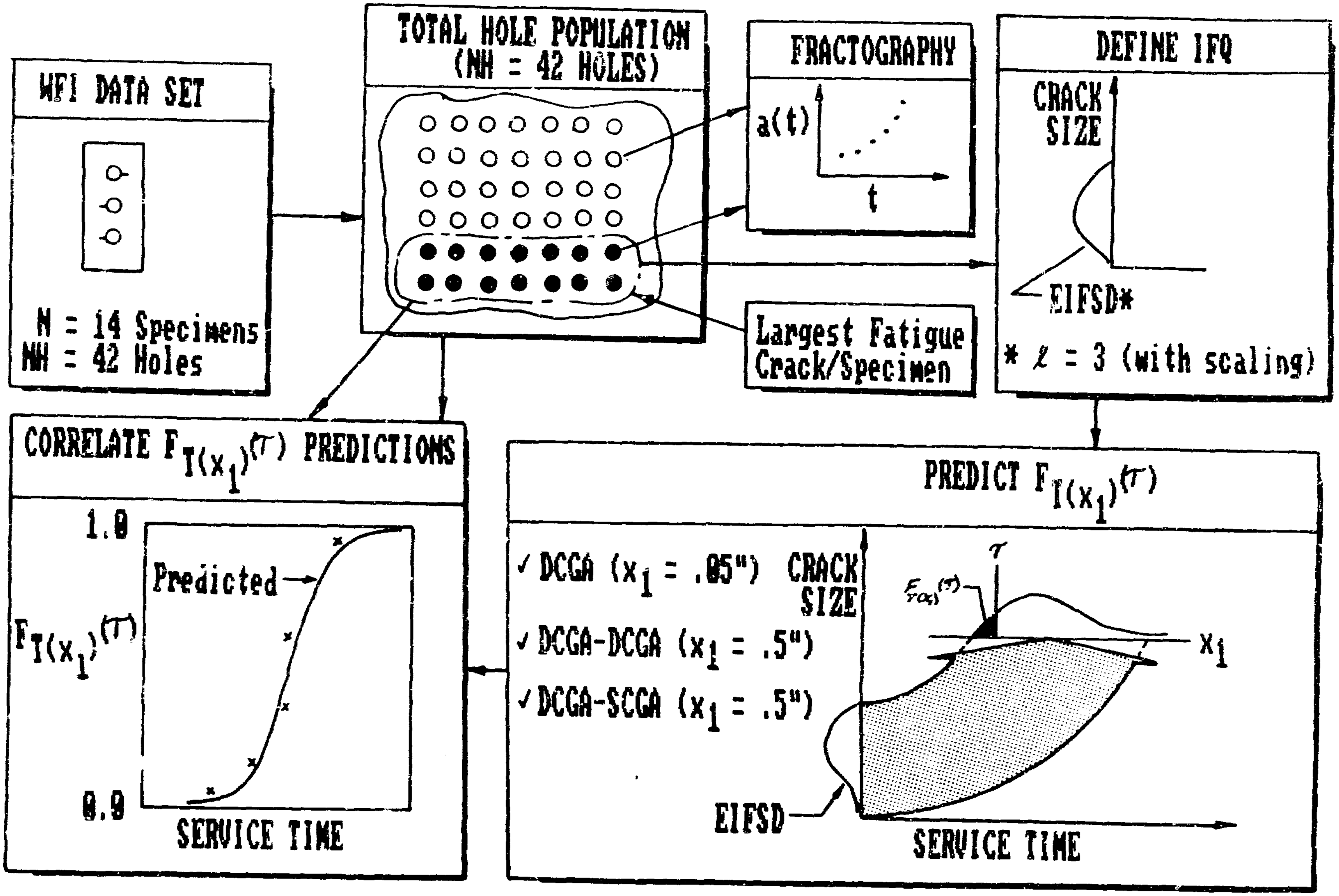

Figure C.1. Study Plan for Evaluating Statistical Scaling Method.

WFI data set is described in Table C.1 and specimen details are shown in Fig. 1.

2. The initial fatigue quality of the 42 fastener holes in the WFI data set is estimated using (1) fractographic results for only 14 fastener holes (i.e., the largest fatigue crack in each of 14 specimens), (2) the Weibull compatible distribution function (Eq. 1), (3) statistical scaling, (4) combined least square sums approach (CLSSA), and (5) an "EIFS fit A fractographic crack size range of AL-AU = .01"-.05" and x_u = .03" is used to estimate the EIFSD parameters (i.e., α and ϕ). The EIFSD parameter ϕ is also estimated using $\ell = 1$ (no scaling) and $\ell = 3$ (with scaling) for later evaluation and comparison.

3. Predictions for the cumulative distribution of service time, $F_{T(x_1)}(\tau)$, to reach x_1 = .05" based on the one segment DCGA, are correlated with experimental results for WFI data set. Results are evaluated for the following: (1) largest fatigue crack per specimen (NH = 14), (2) total fastener hole population (NH = 42 fastener holes).

4. Statistical scaling is also evaluated for $F_{T(x_1)}(\tau)$ predictions in the large crack size region (e.g., x_1 = .5"). In this case two different two-segment crack growth approaches are considered (i.e., DCGA-DCGA and DCGA-SCGA). The IFQ based on $\ell = 3$ is used to make $F_{T(x_1)}(\tau)$ predictions for x_1 = .5". Predictions are correlated with experimental results for the WFI data set (i.e., largest fatigue crack per specimen data).

C.3 WFI DATA SET DETAILS/DATA

The WFI data set, described in Table C.1 and in Fig. 1, includes 15 specimens fatigue tested to failure. Fractographic results for only 14 specimens are used in the

TABLE C.1 Description of WFI Data Set

Material: 7475-T7351 Aluminum (1/2" plate)

No. Specimens: 14

Fastener Type: MS-90353-08 (1/4") Blind Pull Through Rivet (csk)

Specimen With: 3.00"

Test Spectrum: F-16 400 Hour

Maximum Gross Stress: 34 ksi

No. of Holes/Specimen: 3

Percent of Load Transfer: 0%

evaluation herein because specimen WFI-12 was not tested properly. Each specimen in the WFI data set included 3 countersunk fastener holes with no load transfer and MS90353 rivets installed. Therefore, there are 42 fastener holes in the 14 specimens from the WFI data set.

The time-to-failure (TTF) for each specimen in the WFI data set and the service time to reach a crack size x_1 = .05" are summarized in Table C.2. Fastener holes are identified as "A", "B", and "C". Fractographic results were acquired [3] for the largest fatigue crack per specimen. Where possible, fractographic results were also acquired for the largest fatigue crack in the other two holes. In some cases, fractographic results could not be acquired for some fastener holes for various reasons (e.g., cracks too small and complex, damaged fracture surfaces, etc.). For ranking purposes, service times to reach a crack size x_1 = .05" in some fastener holes are shown as less than or greater than the TTF in Table C.2.

Service times for the largest fatigue crack per specimen (NH = 14 holes) to reach x_1 = .05" are summarized in Table C.3 for the WFI data set. These results are used later to correlate $F_{T(x_1)}(\tau)$ predictions.

Ranked service times to reach x_1 = .05" and .5" are summarized in Table C.4 for the WFI data set total hole population (i.e., NH = 42 holes). These results are used later to evaluate $F_{T(x_1)}(\tau)$ predictions.

C.4 COMPUTATION OF Q AND σ_z

The crack growth rate parameter Q in Eq. 10 and the standard deviation σ_z in Eq. 30 are needed to conduct the analysis described in Fig. C.1 and they are estimated using the fractographic results for the largest fatigue crack per specimen (NH = 14 holes) in the WFI data set. Pooled Q are obtained (i.e., AL-AU = .01"-.05" and .05"-.5") using Eqs. 4 and

Table C.2. Summary of Service Times to Reach x_1 = .05" for Each Hole in Each Specimen of the WFI Data Set.

WFI HOLE I.D. (1)	TTF (FLT. HRS.) (2)	SERVICE TIME (FLT. HRS.) (7)		
		A	B	C
-1	31200	>31200	20191	28200
-2	27200	22776	17867	13451
-3	23600 (3)	12747	12411	<23600
-4	30400	16302	22540	25167
-5	30800	19376	>30800	21892
-6	17600	10400	>17600	16428
-7	16400	8445	12092	>16400
-8	28000	>28000	15634	<28000
-9	36480	21235	(30800)	27843
-10	30000	19200	22000	17000
-11	20400	11617	16989	<20400
-12	30240 (4)	<30240	24240	<30240
-13	32400	<32400	20218	>32400
-14	29360	17421	14440	25512
-15	33600	20472	>33600	>33600

NOTES:
(1) Material: 7475-T7351 Aluminum; Ref. Fig. 1
(2) TTF = Time-To-Failure
(3) Specimen failed when disk drive was disconnected from computer system
(4) Specimen bent in compression due to load cell malfunction
(5)

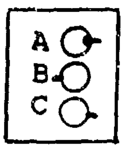

(6) (xxx) = Value extrapolated from fractographic results
(7) Ref. 2

Table C.3. Summary of Service Times to Reach x_1 for Largest Fatigue Crack/Specimen Basis (NH=14).

I	SERVICE TIME (FLT. HRS.)	
	(x_1 = .05")	(x_1 = .50")
1	8445	15860
2	10400	16938
3	11617	19342
4	12411	22683
5	13451	26255
6	14440	26509
7	15634	26864
8	16302	28939
9	17000	28994
10	19376	29782
11	20191	30445
12	20218	31423
13	20472	32230
14	21235	34950

Table C.4. Summary of Ranked Service Times for Lower Tail for WFI Data Set.

I	I/(N+1)	SERVICE TIME (FLT. HRS.)	
		(x_1 = .05")	(x_1 = .5")
1	.023	8445	15860
2	.047	10400	16400
3	.069	11617	>16400
4	.093	12092	¦
5	.116	12411	¦
6	.139	12747	¦
7	.163	13451	¦
8	.186	14440	¦
9	.209	>14440	¦
¦	¦	¦	¦
42	.977	>14400	>16400

32, respectively. The IBM-compatible software of Volume V [5] and filename = "QSZAT" were used to determine pooled Q and σ_z values. Results are summarized in Table C.5.

C.5 ESTIMATE EIFSD PARAMETERS

EIFSD parameters for the Weibull compatible distribution function, Eq. 1, were estimated for x_u=.03" using: (1) fractographic results for the largest fatigue crack per specimen in the WFI data set, (2) the CLSSA, (3) an "EIFS fit", and (4) statistical scaling (i.e., $\ell = 1$ (no scaling) and $\ell = 3$ (with scaling)). IBM-compatible PC software from Volume V [5] and filename = "WCIFQ" were used. The resulting EIFSD parameters without scaling ($\ell = 1$) and with scaling ($\ell = 3$) are summarized in Table C.6.

C.6 $F_{T(x_1)}(\tau)$ PREDICTIONS AND CORRELATIONS

$F_{T(x_1)}(\tau)$ predictions for x_1 = .05" based on the one segment DCGA, are correlated with experimental results for the WFI data set in Figs. C.2 through C.4.

In Fig. C.2, predicted service times to reach x_1 = 0.05", $F_{T(x_1)}(\tau)$, for the largest fatigue crack per specimen (NH = 14) in the WFI data set, based on the EIFSD established with scaling ($\ell = 3$), are plotted as a solid curve. The experimental results are shown in the figure as a plus sign (+) for comparison. The same predictions and correlations are displayed in Fig. C.3 when the EIFSD is established without scaling ($\ell = 1$).

Theoretical predictions for $F_{T(x_1)}(\tau)$ for the total hole population (NH = 42) of the WFI data set, based on the EIFSD established without scaling ($\ell = 1$), are displayed in Fig. C.4 as a solid curve. The ranked experimental results for the 8 smallest values out of 42 holes are shown as a plus sign (+) for comparison. Similar predictions and correlations are given in Fig. C.4 when the EIFSD is established with scaling

Table C.5. Summary of Pooled Q and σ_z Values for Different Crack Size Ranges for WFI Data Set.

CRACK SIZE RANGE	$Qx10^4$ (1/HR.)	σ_z
.01" - .05"	2.329	.247
.05" - .5"	2.114	.212

Table C.6. Summary of EIFSD Parameters for Weibull Compatible Distribution Function for WFI Data Set.

CASE	AL - AU	$Qx10^4$	a_0	ℓ	x_u	α	ϕ
I	.01" - .05"	2.329	.05"	1	.03"	3.045	3.565
II	.01" - .05"	2.329	.05	3	.03"	3.045	5.113

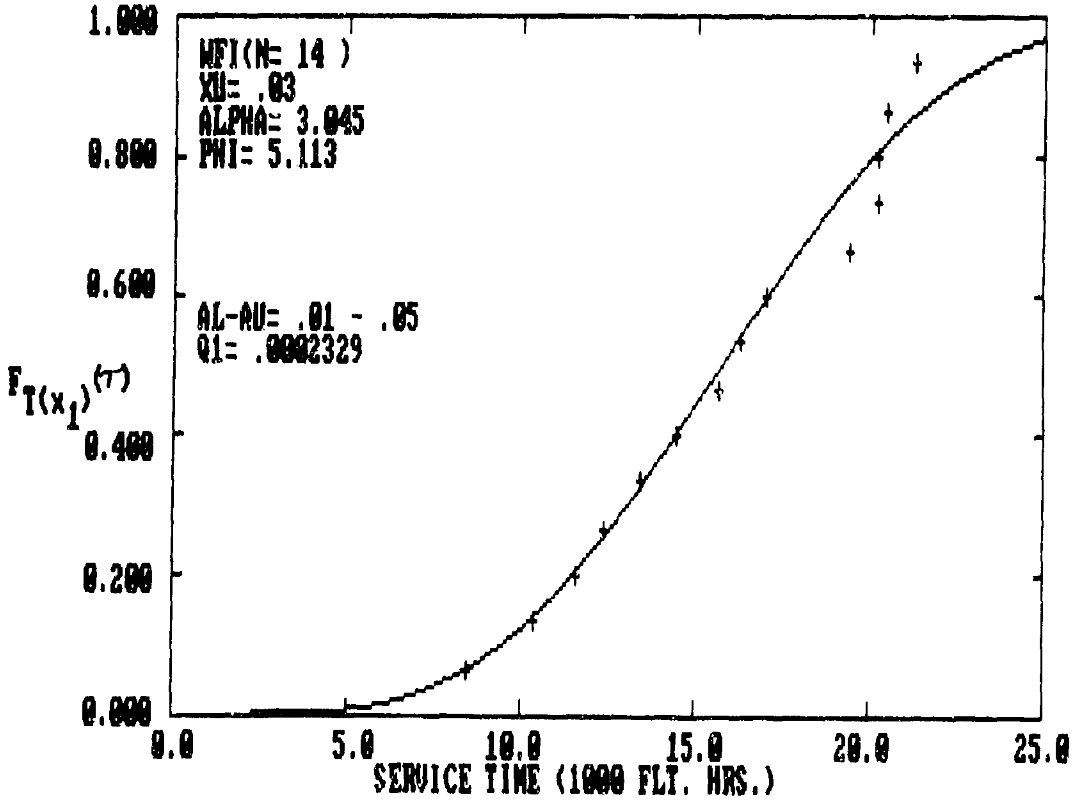

Figure C.2. Predicted Service Time to Reach x_1 = .05" for the Largest Fatigue Crack Per Specimen (NH = 14) in the WFI Data Set Based on EIFSD With Scaling (ℓ = 3).

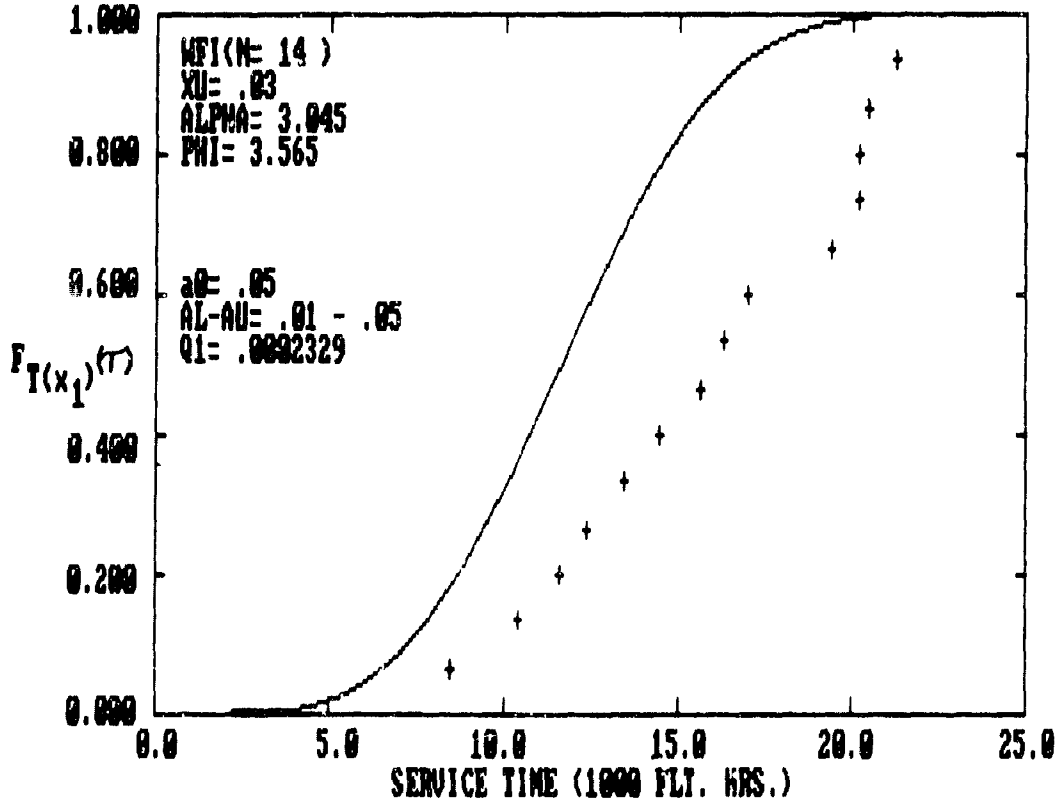

Figure C.3. Predicted Service Time to Reach x_1 = .05" for the Largest Fatigue Crack Per Specimen (NH = 14) in the WFI Data Set Based on EIFSD Without Scaling (ℓ = 1).

(ℓ = 3). The ranked service times for x_1 = .05" reflected in Figs. C.2 through C.5 are shown in Tables C.3 and C.4.

Data for the service time to reach a large crack size of x_1 = 0.5" for the total hole population can not be analyzed and ranked meaningfully. This is because when a specimen fails, most of the cracks in the other two holes have not reached 0.5" yet. However, service data to reach x_1 = 0.5" for the crack population consisting of the largest fatigue crack per specimen (NH = 14) are available. Consequently, correlations and predictions will be made for such a crack population using EIFSD established with (ℓ = 3) and without (ℓ = 1) scaling. $F_{T(x_1)}(\tau)$ predictions for x_1 = 0.5" using the two-segment DCGA-DCGA are plotted as a solid curve in Fig. C.6. The predicted results are based on the EIFSD with scaling of ℓ = 3. For comparison, the ranked test results are depicted as a plus sign (+) in the same figure. Similar predictions and correlations are displayed in Fig. C.7 using the two-segment DCGA-SCGA.

C.7 DISCUSSIONS AND CONCLUSIONS

The statistical scaling technique developed in Volume I [1] has been evaluated herein using fractographic results for coupon specimens containing three fastener holes per specimen. Theoretical predictions for $F_{T(x_1)}(\tau)$ at x_1 = .05", based on the one-segment DCGA and ℓ = 3, correlated very well with ranked service times for NH = 14 holes (Fig. C.2) and NH = 42 holes (Fig. C.5). The effects of "scaling" can be clearly shown by comparing the results of Fig. C.2 (ℓ = 1) with Fig. C.3 (ℓ = 3) as well as the results of Fig. C.4 (ℓ = 1) with Fig. C.5 (ℓ = 3). It is clear that the fatigue cracking resistance of each fastener hole in a test specimen should be accounted for when defining the IFQ of fastener holes.

$F_{T(x_1)}(\tau)$ predictions for the largest fatigue crack per specimen (NH = 14) with x_1 = .5", based on the DCGA-DCGA and the DCGA-SCGA, are shown in Figs. C.6 and C.7, respectively.

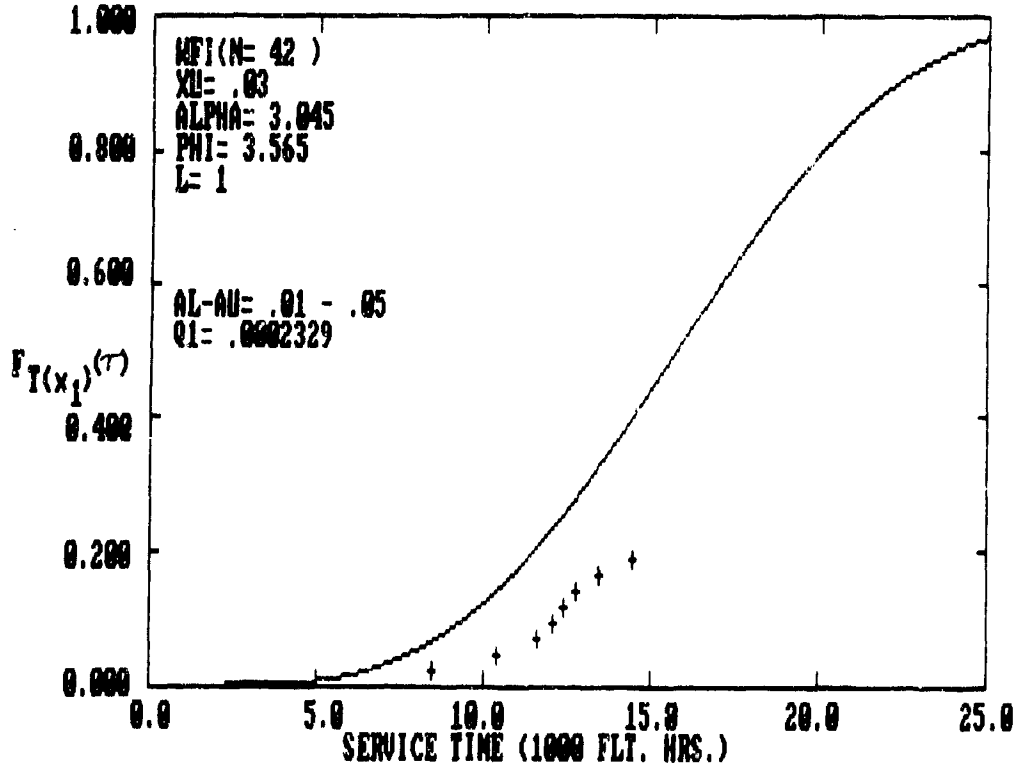

Figure C.4. Predicted Service Time to Reach x_1 = .05" for the Total Hole Population (NH = 42) of the WFI Data Set Based on EIFSD Parameters With No Scaling (ℓ = 1).

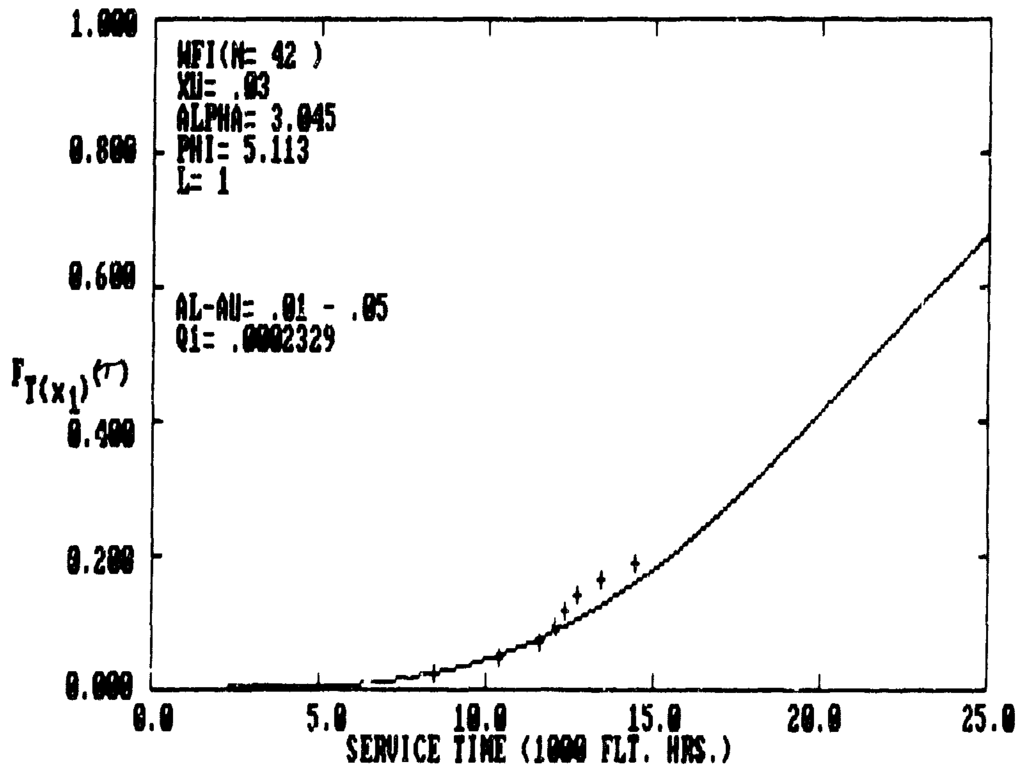

Figure C.5. Predicted Service Time to Reach x_1 = .05" for the Total Hole Population (NH = 42) of the WFI Data Set Based on EIFSD Parameters With Scaling (ℓ = 3).

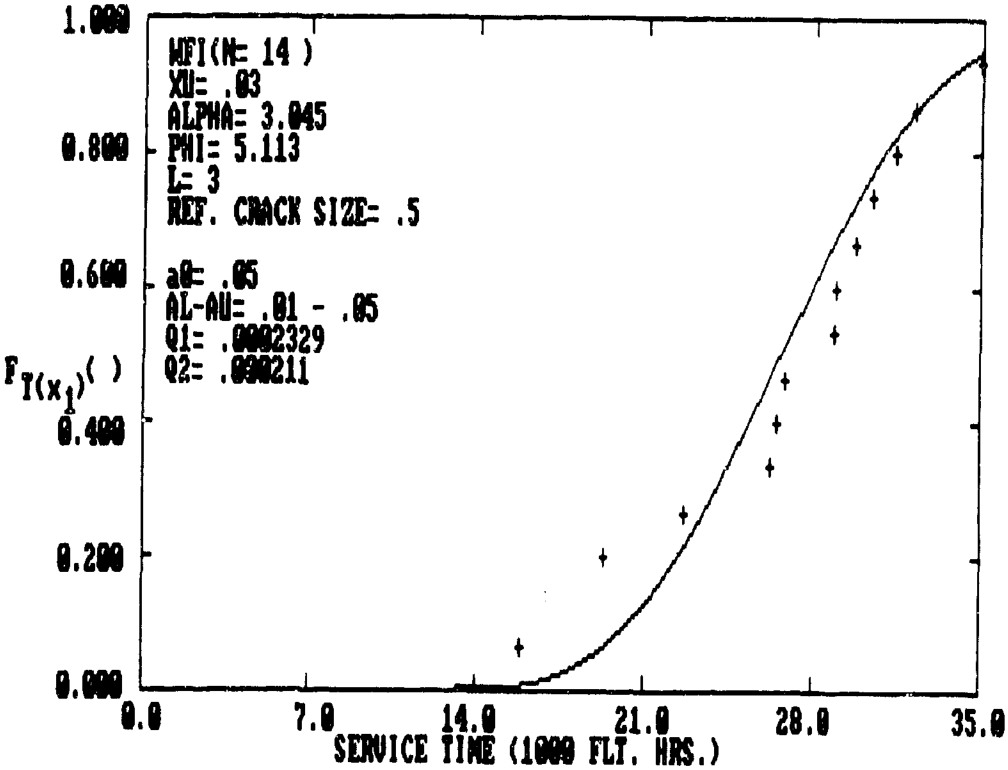

Figure C.6. Predicted Service Time to Reach x_1 = .5" for the Largest Fatigue Crack Per Specimen (NH = 14) in the WFI Data Set Based on EIFSD Parameters With Scaling (ℓ = 3); DCGA-DCGA.

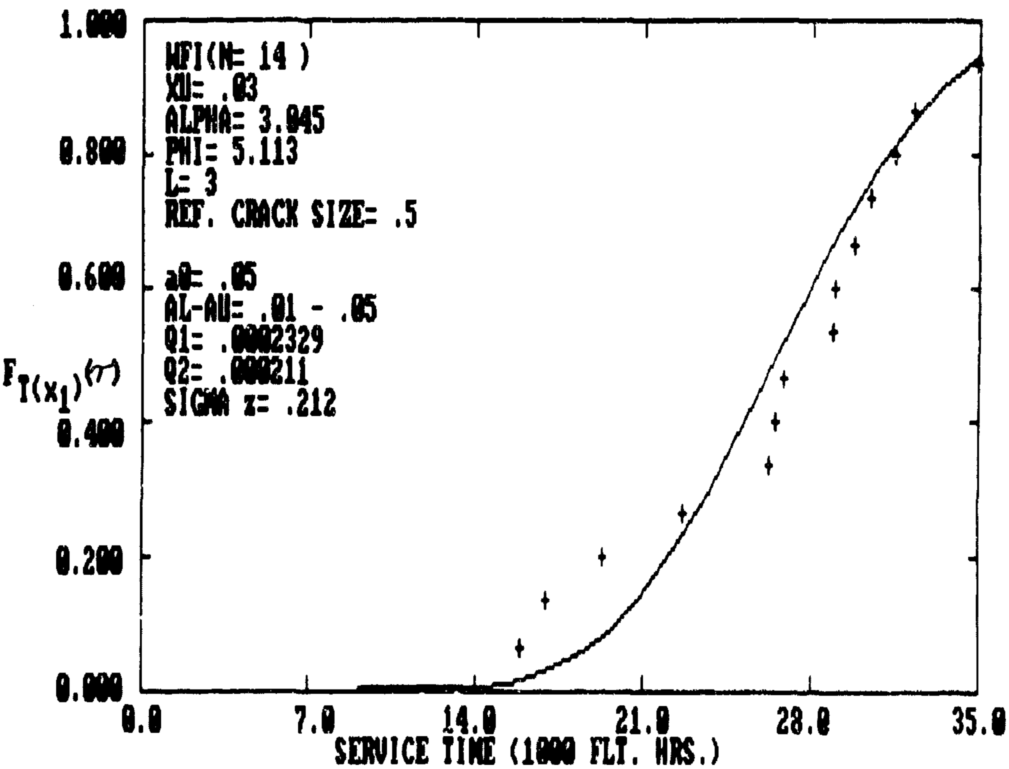

Figure C.7. Predicted Service Time to Reach x_1 = .5" for the Largest Fatigue Crack Per Specimen (NH = 14) in the WFI Data Set Based on EIFSD Parameters With Scaling (ℓ = 3); DCGA-SCGA.

These results reflect a scaling factor of $\ell = 3$ used for establishing EIFSD. Theoretical predictions in both cases correlated reasonably well with ranked service times to reach $x_1 = .5''$. No significant difference in the theoretical predictions for either the DCGA-DCGA or the DCGA-SCGA were observed in this case.

The statistical scaling technique has also been demonstrated using the F-16 lower wing skins in Section 4.4 of this volume (II). Very reasonable durability analysis predictions were obtained using the statistical scaling technique developed.

APPENDIX D
SERVICE CRACK GROWTH MASTER CURVE TUNING STUDY

D.1 INTRODUCTION

A service crack growth master curve (SCGMC) and an equivalent initial flaw size distribution (EIFSD) are needed to predict the probability of crack exceedance at any service time for desired service conditions (e.g., load spectrum, stress level, % bolt load transfer, etc.). SCGMCs can be determined using either fractographic results (if available) or a suitable LEFM analytical crack growth program [e.g., 24]. For consistent durability analysis, the SCGMC should be compatible with the basis for EIFSD. When a LEFM analytical crack growth program is used to define the SCGMC, the crack growth program should be "tuned" or "curve fitted" to the EIFSD data base.

A study was performed to illustrate how SCGMCs can be determined by "curve fitting" an analytical crack growth program to the EIFSD data base. Details of the study, including methods, results and conclusions are presented in this section.

D.2 DETAILS OF THE SCGMC TUNING STUDY

A SCGMC tuning study was performed using eight fractographic data sets from the "Fastener Hole Quality" program [3]. The data sets used are described in Table D.1.

Based on Eq. D-1, an EIFS master curve was defined for each fractographic data set.

$$a(0) = a(t) \exp(-Qt) \qquad \text{(D-1)}$$

Table D.1 Description of Fractographic Data Sets Used in the SCGMC Study

Fractographic Data Set [3]	Material	% Bolt Load Transfer	Load Specrum	Max. Stress (Gross) (ksi)	Fastener I.D.
WPF	7475-T7351	0	F-16 400 Hrs	34	*NAS-6402 (1/4" Dia)
XWPF		15		34	
HYWPF		15		40.8	
LYWPF		15		30.6	
WPB		0	B-1 Bomber	34	
XWPB		15		34	
HYWPB		15		40.8	
LYWPB		15		30.6	

*Straight shank fastener installed in a straight-bore hole drilled with a Modified Winslow Specematic drill.

in which $a(0)$ = EIFS, $a(t)$ = crack size at time t, and Q = "pooled Q" value for a data set. Equation D-1 is based on the crack growth rate model of Eq. D-2 (Refer to Volume I for details [1]).

$$da(t)/dt = Q*a(t) \tag{D-2}$$

Pooled Q values for each of the eight fractographic data sets were determined using a fractographic crack size range of AL-AU = 0.01" - 0.05". Results are summarized in Table D.2. The pooled Q values are based on a preliminary method developed early in the program. For example, Q values were based directly on Eq. D-2 instead of Eq. D-1, that is now recommended for use. Also, this study was conducted without any prior screening or plotting of the fractographic data. Fractographic results for a few surface cracks were combined with results for fatigue cracking in the bore of the fastener hole. The pooled Q values used in this study, however, have the same order of magnitude as those values based on the refined method. For illustrative purposes, it is not critical if the pooled Q values used are identical to those based on the refined methods with fractographic data screening. The main goal of this section is to illustrate "curve fitting" the analytical crack growth program to the EIFSD data base in order to obtain the desired SCGMC(s).

The SCGMC tuning study was based on the following: (1) RXN analytical crack growth program [24], (2) Walker- ΔK crack growth rate model [25], and (3) Modified Willenborg retardation model [26]. Different parameter values were used in the SCGMC tuning study (see Table D.3 for summary).

The Walker ΔK equation [25], given in Eq. D-3, was used to model the crack growth rate in the RXN analytical crack growth program. In Eq. D-3, a = half crack length, N =

Table D.2 Summary of EIFS Master Curve Parameters Used in the SCGMC Tuning Study

Fractographic Data Set [3]	Load Spectrum	Crack Size Range Used	Q_i*x10^4 (1/HR)	a(0)* (In)
WPF	F-16 400 Hr	0.01"-0.05"	2.731	0.005"
XWPF	↓	↓	3.437	↓
HYWPF	↓	↓	8.316	↓
LYWPF	↓	↓	2.210	↓
WPB	B-1 Bomber	↓	1.258	↓
XWPB	↓	↓	2.368	↓
HYWPB	↓	↓	4.375	↓
LYWPB	↓	↓	1.550	↓

*Initial flaw size at t= 0

TABLE D.3 Summary of Parameters Used in The SCGMC Tuning Study

FRACTOGRAPHIC DATA SET [3]	LOAD SPECTRUM	[1] WALKER-ΔK PARAMETERS			GENERALIZED WILLENBORG		RXH CRACK GROWTH ANALYSIS INPUT					
		$C \times 10^{10}$	M	N	$(K_{max})_{TH}$ (2)	S (3)	K_{Ic} (ksi-$\sqrt{in}$)	YIELD STR. (ksi)	HOLE DIA. (In)	STRESS LEVEL (ksi)	% LT (5)	INITIAL FLAW SIZE
WPF	F-16 400 HR	9.3	3.544	0.60	1.50	2.00 2.50 2.55 2.65 3.00 2.55	35	59.5	0.25	34	0	0.005-[4]
XWPF											0 3.0 4.0 5.0 7.0	
HYWPF										40.8	3.0 4.0 5.0 7.0	
LYWPF										30.6	5.0	
WPB	B-1 Bomber					2.00 2.65 3.00 4.00 4.75 5.00 5.25 4.75				34	0	
XWPB											4.0 5.0 6.0 7.0 8.0	
HYWPB										40.8	6.0	
LWYPB										30.6	6.0	

Notes: (1) Based on GD/FWD Data for 7475-T7351 Aluminum
(2) Threshold Max. Stress-Intensity Factor
(3) Overload Shutoff Ratio
(4) Corner Flaw
(5) % Bolt Load Transfer

number of cycles of loading, ΔK = stress intensity factor range, R = stress ratio, and C, m and n = empirical constants. The constants C, m and n were determined using GD/FWD data for 7475-T7351 aluminum.

$$da/dN = C\left[\frac{\Delta K}{(1-R)^{1-m}}\right]^n \qquad \text{(D-3)}$$

For reference purposes, the key equations of the Generalized Willenborg retardation model [26] are summarized below (D-4 through D-10).

$$(\Delta K)_{eff} = (K_{max})_{eff} - (K_{min})_{eff} \qquad \text{(D-4)}$$

$$R_{eff} = \frac{(K_{min})_{eff}}{(K_{max})_{eff}} \qquad \text{(D-5)}$$

The effective values of K_{max} and K_{min} are defined in the following manner:

$$(K_{max})_{eff} = (K_{max})_{\infty} - \phi\left[K_{max}^{OL}\left[1 - \frac{\Delta a}{Z_{OL}}\right]^{1/2} - (K_{max})_{\infty}\right] \qquad \text{(D-6)}$$

$$(K_{min})_{eff} = (K_{min})_{\infty} - \phi\left[K_{max}^{OL}\left[1 - \frac{\Delta a}{Z_{OL}}\right]^{1/2} - (K_{max})_{\infty}\right] \qquad \text{(D-7)}$$

in which

$$\phi = \frac{1 - [(K_{max})_{TH}/(K_{max})_{\infty}]}{S - 1} \qquad \text{(D-8)}$$

$$S = \frac{K_{max}^{OL}}{(K_{max})_{\infty}} \qquad \text{(D-9)}$$

$$Z_{OL} = \frac{1}{2\pi}\left[\frac{(K_{max}^{OL})_{\infty}}{\sigma_{ty}}\right]^2 \text{ (plane stress)} \qquad \text{(D-10)}$$

where

(K_{max}) = maximum remote stress-intensity factor of current cycle,

K_{max}^{OL} = maximum remote stress-intensity factor of overload cycle,

a = incremental growth following overload,

Z_{OL} = load interaction zone size created by overload,

(K_{min}) = minimum remote stress-intensity factor of current cycle,

$(K_{max})_{TH}$ = threshold maximum stress-intensity factor for no fatigue growth at R = 0,

S = overload shut-off ratio that produced no fatigue growth, and

$_{ty}$ = tensile yield strength.

The three-step procedure below was used to "tune" the RXN analytical crack growth program [24] to the selected fractographic data sets:

1. Select a baseline fractographic data set with no bolt load transfer to perform the initial tuning (e.g., WPF and/or WPB in Table D.1).

2. For a given maximum stress intensity threshold, $(K_{max})_{TH}$, determine by trial and error, using the RXN program, the corresponding overload shutoff ratio (S) that will give a reasonable "curve fit" to the EIFS master curve for the baseline specimen geometry/configuration. In our case we used $(K_{max})_{TH}$=1.5 ksi-$\sqrt{in.}$ and varied S as indicated in Table D.3.

3. The overload shutoff ratio (S) and corresponding $(K_{max})_{TH}$ for the baseline specimen geometry/configuration was then used to "curve fit" the EIFS master curve for a bolt load transfer case. By trial and error, the % bolt load

transfer was varied in the RXN program to accomplish the curve fitting. The bolt load transfer specimen used (e.g., XWPF), a double- reversed dog-bone specimen, was designed for a particular % bolt load transfer, but due to the clearance fit between the fasteners and holes, the actual % bolt load transfer varies depending on applied load level to the specimen. A strain survey is presented in Appendix G. This step is important because a "transfer function" is developed for scaling the % load transfer in the crack growth analysis to the % load transfer data base.

Once the theoretical-to-test % load transfer relationship has been determined, the crack growth analysis parameter developed in steps 1-3 (i.e., S, $(K_{max})_{TH}$ and % bolt load transfer) can be used to obtain SCGMCs for other % bolt load transfers and stress levels.

D.3 RESULTS

Results of the SCGMC tuning study are shown in Figs. D.1 - D.8 for the eight data sets shown in Table D.1. Figs. D.1 and D.5 show step one of the procedure while Figs. D.2 and D.6 show step two. The remaining figures are representative of step three. For both the fighter and bomber load spectra, approximately a 6% bolt load transfer was required to obtain a reasonable "curve fit" for the "15% bolt load transfer" cases. The 6% bolt load transfer agrees very well with the results from the strain survey at the 100% load level (see Appendix G).

D.4 CONCLUSIONS

The conclusions of this study are:

1. The procedure illustrated in this study for tuning the analytical crack growth program to the EIFSD data base is reasonable for determining the SCGMC needed for durability analysis.

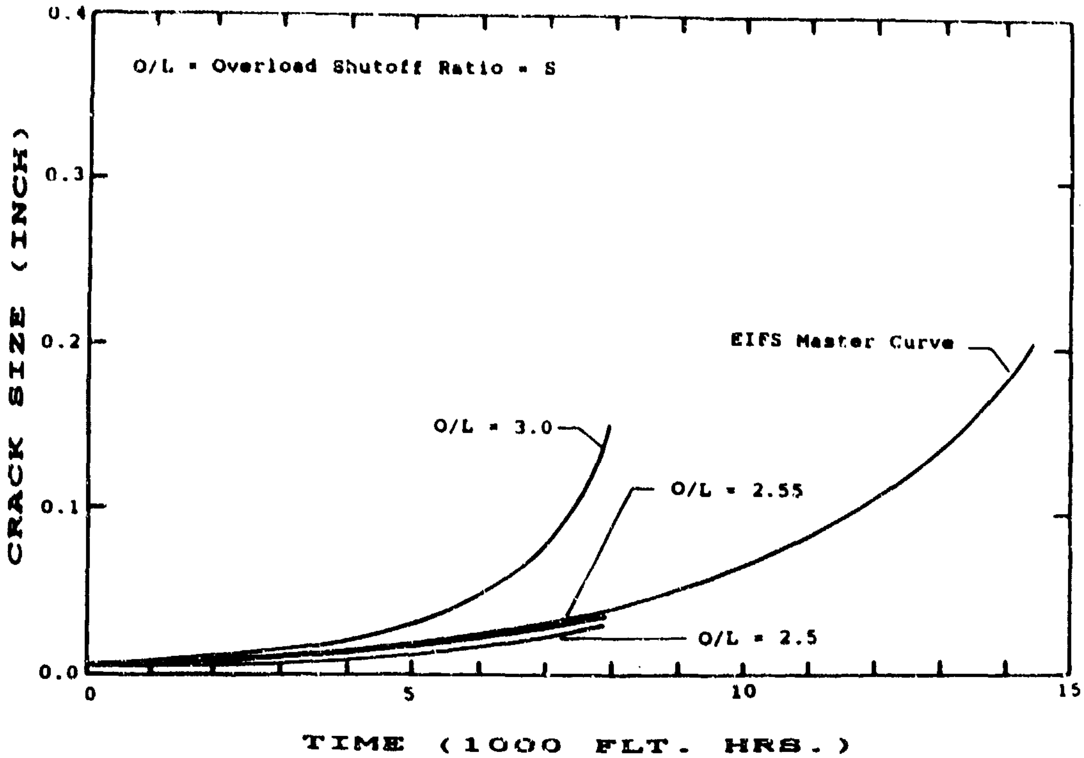

Figure D.1. Tuning the SCGMC to the WPF Data Set $((K_{max})_{TH}$ = 1.5 ksi-$\sqrt{in.}$ Vary S).

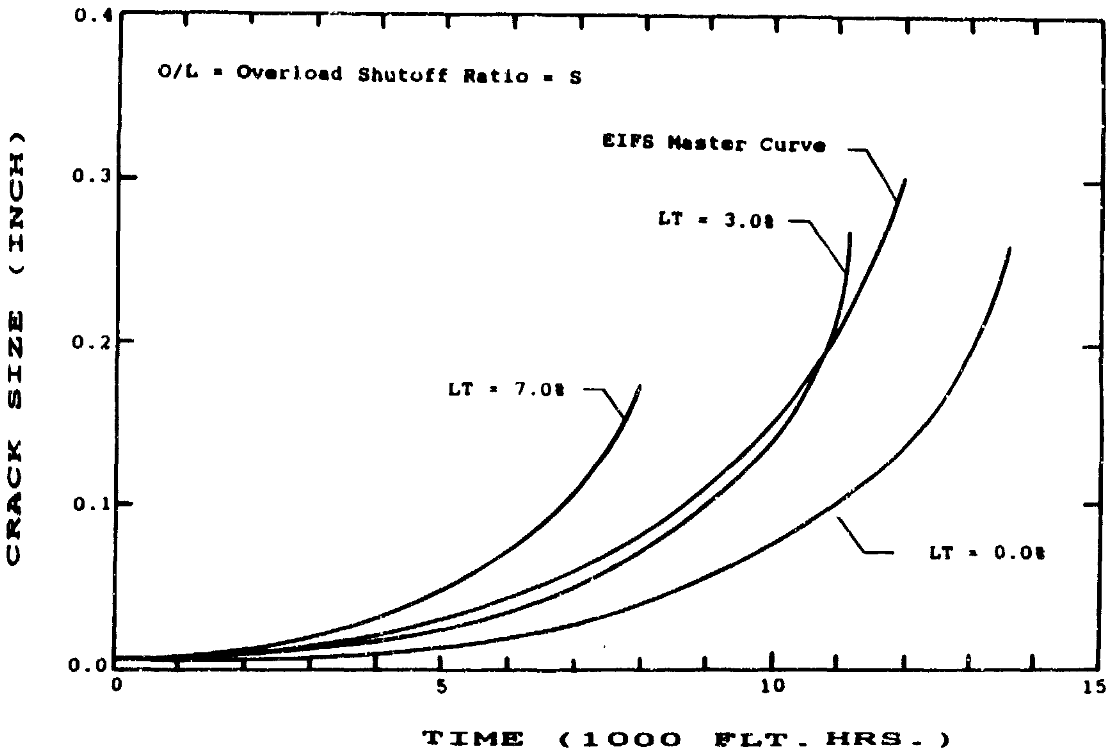

Figure D.2. Tuning the SCGMC to the XWPF Data Set $((K_{max})_{TH}$ = 1.5 ksi-$\sqrt{in.}$, S = 2.55; Vary % Load Transfer).

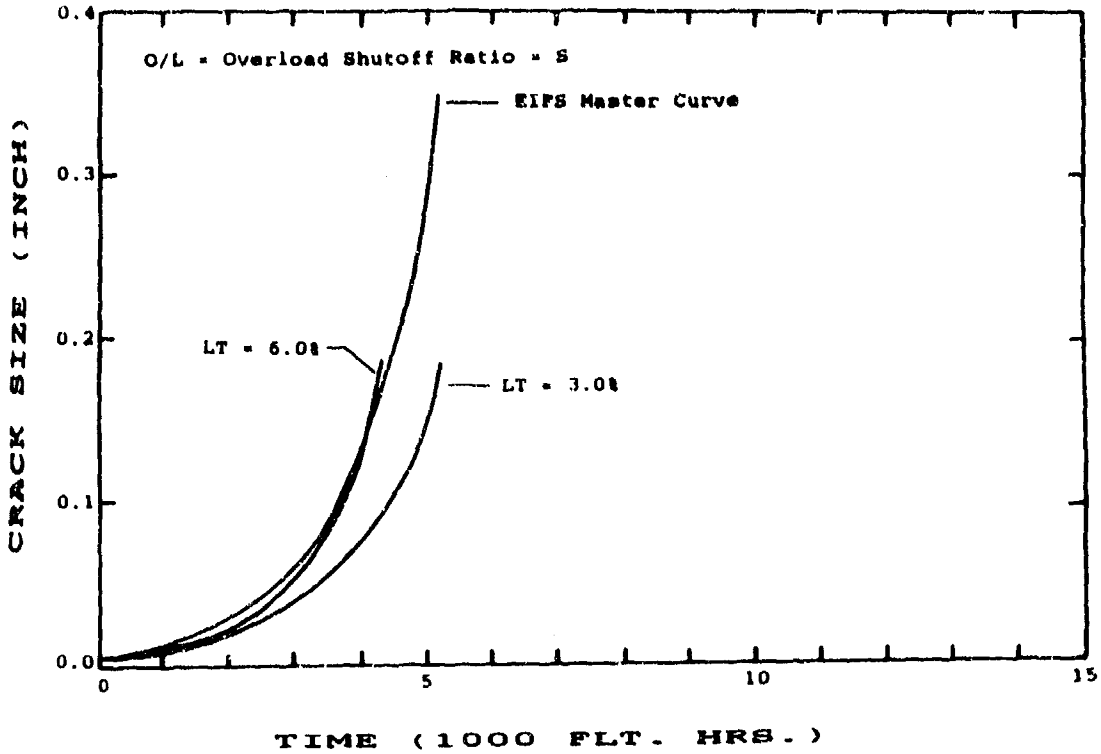

Figure D.3. Tuning the SCGMC to the HYWPF Data Set $((K_{max})_{TH}$ = 1.5 ksi-$\sqrt{in.}$, S = 2.55; Vary % Load Transfer).

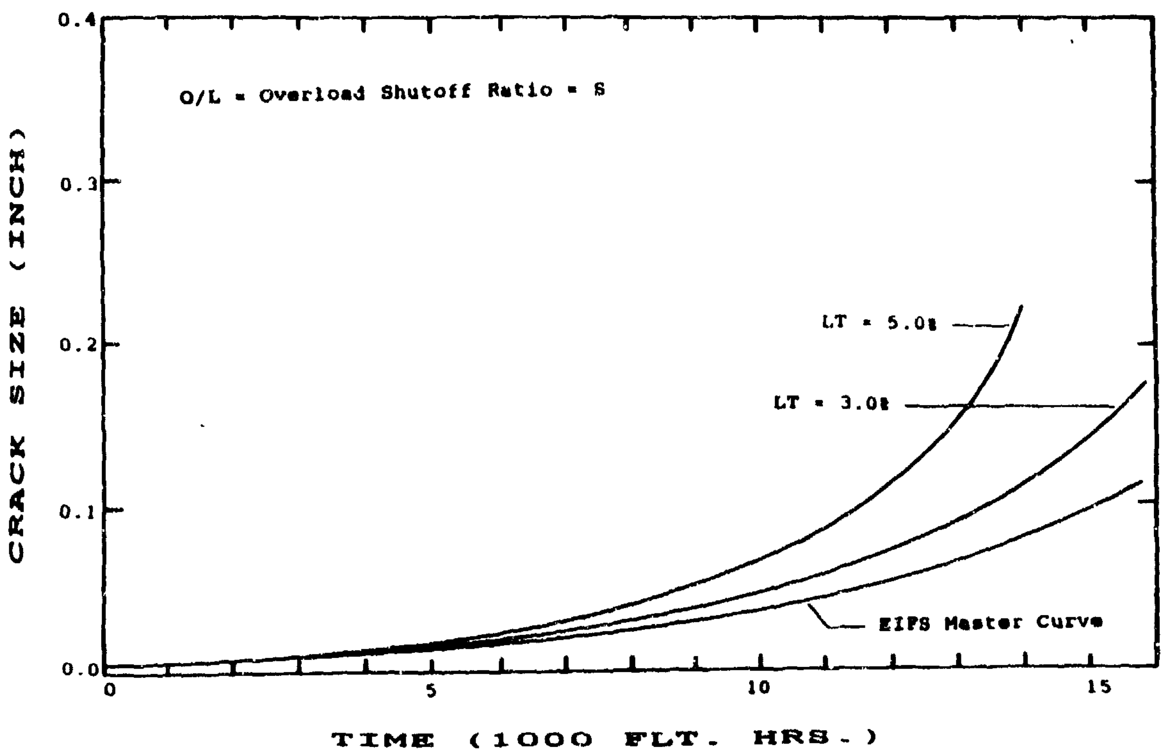

Figure D.4. Tuning the SCGMC to the LYWPF Data Set $((K_{max})_{TH}$ = 1.5 ksi-$\sqrt{in.}$, S =2.55; Vary % Load Transfer).

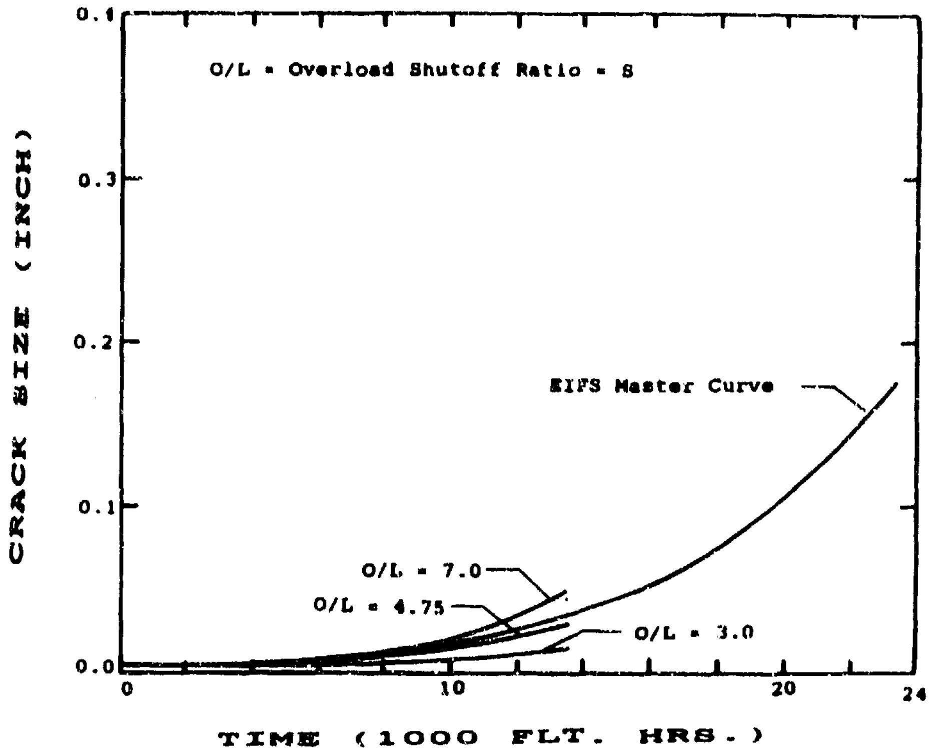

Figure D.5. Tuning the SCGMC to the WPB Data Set ($(K_{max})_{TH}$ = 1.5 ksi-$\sqrt{in.}$, Vary S).

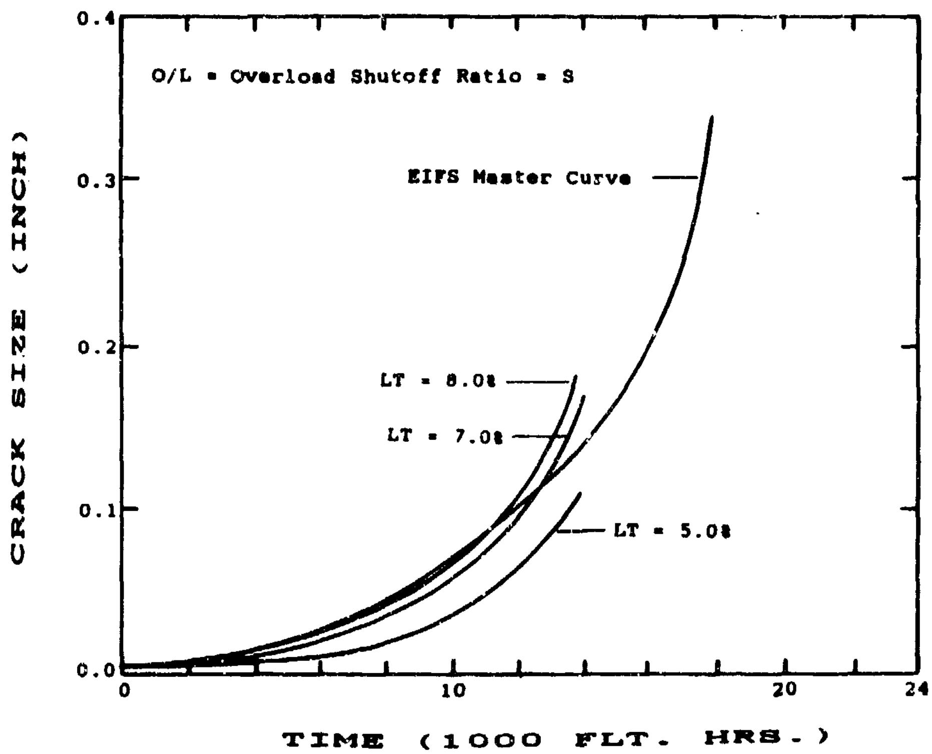

Figure D.6. Tuning the SCGMC to the XWPB DAta Set ($(K_{max})_{TH}$ = 1.5 ksi-$\sqrt{in.}$, S = 4.75; Vary % Load Transfer).

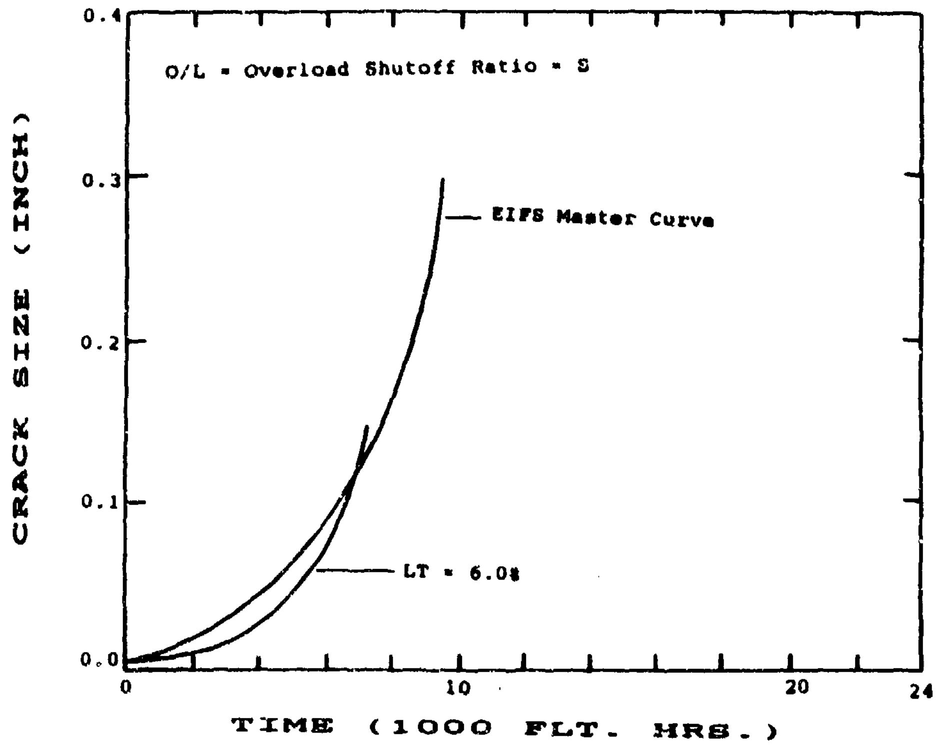

Figure D.7. Tuning the SCGMC to the HYWPB Data Set ($(K_{max})_{TH}$ = 1.5 ksi-$\sqrt{in.}$, S = 4.75; Vary % Load Transfer).

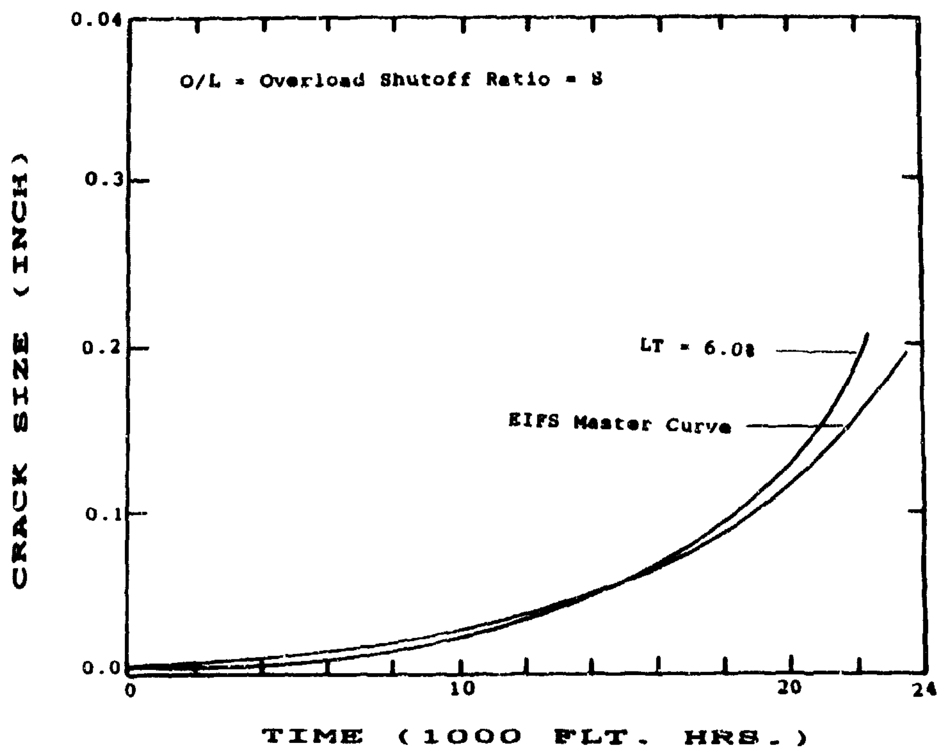

Figure D.8. Tuning the SCGMC to the LYWPB Data Set ($(K_{max})_{TH}$ = 1.5 ksi-$\sqrt{in.}$, s = 4.75; Vary % Load Transfer).

2. When applicable fractographic data is limited or not available for a direct determination of the SCGMC, an analytical crack growth program can be used to estimate the SCGMC. In this case, the user has to make assumptions, judgements and adapt available data to the crack growth conditions. This situation is no different than a "damage tolerance" type crack growth analysis required for specified conditions (e.g., material load spectrum, stress level, percent bolt load transfer, flaw shape and geometry).

3. An initial flaw size of a(0) = 0.005" was used to plot the baseline EIFS master curves used in this investigation. The maximum crack size reflected in the EIFS master curve plot was arbitrarily selected. Also, the analytical crack growth program was loosely "curve fitted" to an unspecified crack size range. In practice, the analytical crack growth program should be "curve fitted" to the same AL-AU crack size range (e.g., 0.01" - 0.05") that is used to define the EIFSD parameters.

4. One or more crack growth segments may be required to define a SCGMC for durability analysis in the large crack size region (e.g., crack size > 0.50"). The same curve fitting concept used in this section can also be used to determine the SCGMC for desired AL-AU ranges. In any case, the SCGMC is determined for a specified AL-AU crack size range. A two-segment SCGMC is discussed in Volume I [1].

5. A SCGMC can be determined for the small crack size region without violating LEFM principles. For example, the analytical crack growth program is curve fitted to the EIFS master curve for a crack size range of AL-AU = 0.01" - 0.05". Since the analytical crack growth program is used as a "curve fitting tool" and is limited to a minimum crack size of AL = 0.01". LEFM principles apply and "short crack effects" do not have to be accounted for.

APPENDIX E

INITIAL FATIGUE QUALITY STUDIES FOR FASTENER HOLES IN 7475-T7351 ALUMINUM

E.1 INTRODUCTION

A comprehensive investigation was conducted to evaluate and refine the initial fatigue quality methods developed under this program. Also, the sensitivity of various factors on the initial fatigue quality (IFQ) results was investigated. This effort was extensive but the results are too voluminous to present herein [42]. The purpose of this section is to briefly describe the overall investigation conducted, to discuss the key issues and to summarize our overall conclusions and recommendations. The studies described herein were a part of the "learning process" for developing and refining the methods and procedures for defining IFQ. Durability analysis methods and equations are developed in Volume I [1].

E.2 INVESTIGATION SUMMARY

The investigation included numerous studies with overlapping aspects. These studies are loosely grouped into four parts as follows: (1) evaluation of methods for determining Q, (2) evaluation of EIFSD parameters, (3) sensitivity of IFQ parameters, and (4) estimation of initial flaw sizes. All studies were conducted using fractographic data for fastener holes in dog-bone specimens of 7475-T7351 aluminum [2-4]. Both straight-bore and countersunk fastener holes (clearance-fit) were considered. Studies are briefly described in the following and sample results are presented.

E.2.1 Evaluation of Methods for Determining Q

The crack growth rate parameter Q in Eq. 2 for a data set, referred to as the pooled Q is needed to implement the durability analysis method developed. Pooled Q for a given fractographic data set can be estimated using either Eq. 2 or Eq. 3 and a least squares fit procedure as follows. Suppose the ith fractographic data set contains a total of m fatigue cracks, where each fatigue crack is denoted by j = 1,2,....,m. The jth fatigue crack has a total of N_j pairs of fractographic data in the AL-AU crack size range. Q can be determined from Eq. 2 using the following least squares fit expression,

$$Q = \exp\left\{ \frac{\sum_{j=1}^{m}\sum_{k=1}^{N_j} \ln(da(t)/dt)_{jk} - \sum_{j=1}^{m}\sum_{k=1}^{N_j} \ln a_j(t_k)}{\sum_{j=1}^{m} N_j} \right\} \tag{E-1}$$

where, N_j = number of pairs of $[(da(t)/dt)_{jk}, a_j(t_k)]$ values in the AL-AU range (i.e., $k = 1,2,\ldots,N_j$) and $(da(t)/dt)_{jk}$ = kth crack growth rate for the jth fatigue crack at service time t_k, denoted by $a_j(t_k)$. Q can also be determined from Eq. 3 using the least squares fit expression as follows,

$$Q = \frac{N\sum_{j=1}^{m}\sum_{k=1}^{N_j} X_{jk}Y_{jk} - \left(\sum_{j=1}^{m}\sum_{k=1}^{N_j} X_{jk}\right)\left(\sum_{j=1}^{m}\sum_{k=1}^{N_j} Y_{jk}\right)}{\sum_{j=1}^{m}\sum_{k=1}^{N_j} X_{jk}^2 - \left(\sum_{j=1}^{m}\sum_{k=1}^{N_j} X_{jk}\right)^2} \tag{E-2}$$

where, $X_{jk} = t_{jk}$ (i.e., kth service time for the jth fatigue crack denoted by $a_j(t_k)$), $Y_{jk} = \ln a_j(t_k)$ and N = total number of $[X_{jk}, Y_{jk}]$ pairs in the AL-AU range $= \sum_{j=1}^{m} N_j$. Eqs. E-1 and E-2 were derived in Volume I [1].

Studies were conducted to evaluate pooled Q based on Eq. E-1 and E-2. Various data processing methods for computing pooled Q using fractographic results for both straight-bore and countersunk fastener holes were investigated. The modified secant method [27] and the five-point incremental polynomial method [28] were used to estimate $(da(t)/dt)_{jk}$ values for computing pooled Q values based on Eq. E-1.

The following effects on pooled Q values were also investigated: (1) fractographic crack size range (i.e., AL-AU), (2) equalizing or not equalizing the number of a(t)s for each fatigue crack in the selected AL-AU range, and (3) fractographic data censoring.

Pooled Q value for each data set results from the study, based on Eqs. E-1 and E-2, are shown in Table E.1 for three different fractographic data sets. These results were based on fractographic data for straight-bore fastener holes with clearance-fit fasteners.

E.2.2 Evaluation of EIFSD Parameters

Three different distribution functions were considered for representing the EIFSD: (1) Weibull compatible distribution proposed by Yang and Manning [6,7], (2) two-parameter Weibull, and (3) lognormal. Both the homogeneous EIFS approach (HEIFS) and the combined least square sums approach (CLSSA) for estimating the EIFSD parameters were investigated. These approaches are described in Volume I [1].

EIFSD parameters were also determined using the data pooling procedure and statistical scaling technique described in Volume I. The CLSSA for estimating EIFSD parameters was evaluated using a "EIFS fit" [1] and a "TTCI fit" [1]. The following methods for estimating the EIFSD parameters were also considered: (1) non-linear least squares fit [1], (2) method of moments, and (3) maximum likelihood estmation (MLE). Single and double precision accuracy were considered in the evaluation of the linear and non linear least square fit methods.

Sample results from this study are shown in Table E.2 for selected fractographic data sets. These data sets were used to demonstrate and evaluate the durability analysis extension given in Section IV of this Volume (II). Similar results were obtained for numerous other data sets and for different fractographic data pooling combinations.

Table E.1. SUMMARY OF COMPUTED Q VALUES FOR SELECTED FRACTOGRAPHIC DATA SETS

DATA SET (1)	No. Cracks Used	% LT	GROSS STRESS (KSI)	TEST SPECTRUM	(7) AL-AU	$Qx10^4$ (1/HR) (5) MS	(6) 5PP	Eq. E-2
WPF (2)	31/33	0	34	F-16 400 HR	.01"-.05"	2.394	2.397	2.393
WWPF (3)	13/13	0	34	F-16 400 HR	.01"-.05"	2.739	2.742	2.742
XWPF (4)	33/33	15	34	F-16 400 hr	.01"-.05"	3.812	3.816	3.851

NOTES: (1) Specimen Material: 7475-T7351 Aluminum

(2) Ref. Fig. 4

(3) Ref. Fig. 2

(4) Ref. Fig. 5

(5) MS - Modified Secant Method [27]

(6) 5PP = Five point incremental polynomial [28]

(7) AL-AU = Fractographic crack size range used

Table E.2. Summary of EIFSD Parameters and Initial Flaw Size Percentile Results for Weibull-Compatible Distribution Function for Countersunk and Straight-Bore Fastener Holes.

DATA SET (1)	TYPE HOLE	σ (ksi)	Cracks Used	AL-AU	Pooled $Q \times 10^4$	x_u	α	ϕ	ℓ	INITIAL FLAW SIZE (7) a(1/1000)	INITIAL FLAW SIZE (7) a(1/10000)	Approach
AFXLR4 (2)	CSK (6)	32	10/11	.01"-.05"	2.101	.03"	1.960	5.708	4	.0254"	.0285"	CLSSA
						.05"	2.450	5.918	4	.0351"	.0436"	CLSSA
AFXMR4 (2)		34	9/9		2.514	.03"	1.960	4.355	4	.0264"	.0288"	CLSSA
						.05"	2.545	4.646	4	.0368"	.0441"	CLSSA
AFXHR4 (2)		38	10/10		6.062	.03"	1.870	6.857	4	.0253"	.0285"	CLSSA
						.05"	2.240	7.108	4	.0361"	.0445"	CLSSA
{AFXLR4, AFXMR4, AFXHR4} (3)		{32, 34, 38}	{10/11, 9/9, 10/10}		{2.101, 2.514, 6.062}	.03"	1.716	6.308	{4, 4, 4}	.0268"	.0291"	CLSSA
						.05"	2.132	6.453		.0388"	.0459"	CLSSA
												CLSSA
WPF (4)	SB (6)	34	31/33	.01"-.05"	2.329	.03"	6.920	3.808	1	.0074"	.0109"	CLSSA
XWPF (5)		34	31/33		3.671	.03"	5.136	5.440	4	.0073"	.0121"	CLSSA
{WPF, XWPF} (3)		{34, 34}	{31/33, 31/33}		{2.329, 3.671}	.03"	4.782	4.658	{1, 4}			CLSSA
										.0099"	.0152"	CLSSA
{WPF, WJPF} (3)		{34, 34}	{31/33, 13/13}		{2.329, 2.742}	.03"	6.390	3.964	{1, 1}	.0078"	.0117"	HEIFS
						.03"	5.740	3.990		.0091"	.0135"	CLSSA
						.05"	7.280	4.480	{1, 1}	.0088"	.0141"	HEIFS
						.05"	6.536	4.507		.0104"	.0166"	CLSSA

NOTES:
(1) Specimen material: 7475-T7351 aluminum
(2) Individual data set; Ref. 6 for specimen geometry
(3) Pooled fractographic data sets
(4) Individual data set; Ref. 4 for specimen geometry
(5) Individual data set; Ref. 5 for specimen geometry
(6) CSK = countersunk; SB = straight bore
(7) a(1/1000), a(1/10000) = Initial flaw size for upper percentiles P = .001 and P = .0001, respectively

In Table E.2, the bracketed ( ) data sets indicate that the data pooling procedure with statistical scaling [1] was used. The sample results in Table E.2 are for the Weibull compatible EIFSD function. Parameters α and ϕ, for a given x_u (i.e., 0.03" or 0.05"), are based on an "EIFS fit" and either the CLSSA or the HEIFS approach. Initial flaw sizes for 0.1 and 0.01 percentiles are shown in Table E.2 for each EIFSD case.

E.2.3 Sensitivity of Initial Fatigue Quality Parameters

The effects and sensitivity of various factors on the resulting IFQ of fastener holes were evaluated. For example, the effects of the following factors on IFQ were investigated: (1) fractographic crack size range used (i.e., AL-AU), (2) fractographic data censoring, (3) fractographic data pooling and statistical scaling, and (4) EIFS upper bound limit (x_u). Typical results for this investigation, shown in Table E.2, will be discussed later.

E.2.4 EIFS UPPER TAIL FIT

The EIFSD is established previously by fitting the distribution function to all EIFS values computed from available fractographic results. This procedure is referred to as the "total EIFS population fit". When the crack exceedance probability of practical concern is small, the upper tail portion of the EIFSD is critical to the prediction. Hence, the upper tail portion of the EIFSD should be determined with sufficient accuracy. For the total EIFS population fit, however, the EIFSD tends to fit the majority of EIFS values in the central portion, thus sacrificing the accuracy of fitting the upper tail. To overcome such a difficulty, the EIFSD may be established by fitting the distribution function to only upper q% of EIFS values, e.g., upper 30% of EIFS values. Such a procedure is referred to as the "upper tail fit".

EIFSD parameters will be obtained based on both the "total EIFS population fit" and the "upper tail fit". These parameters will be compared and evaluated. Both the Weibull compatible and two-parameter Weibull distribution functions will be considered for EIFDS. In the case of the upper tail fit, only the upper 30% of EIFS values will be used.

The Weibull compatible and two-parameter Weibull distribution functions are shown in Eq. 1 and E-3, respectively.

$$F_{a(o)}(x) = 1 - exp\{-(x/\beta)^{\alpha}\}; \; x \geq 0 \qquad \text{(E-3)}$$

In Eq. E-3, α and β are the Weibull shape and scale parameters, respectively.

Equations 1 and E-3 can be transformed into a linear least squares fit form as shown in Eqs. E-4 and E-5 respectively.

$$ln\{-ln F_{a(o)}(x)\} = \alpha \, ln \, ln(x_u/x) - \alpha \, ln \phi \qquad \text{(E-4)}$$

$$ln\{-ln[1 - F_{a(o)}(x)]\} = \alpha \, ln \, x - \alpha \, ln \beta \qquad \text{(E-5)}$$

In Fig. E.1, the ranked EIFS values x_j ($j = 1, 2, \ldots, N$) for WPF data set are plotted in terms of $ln(-lnF_{a(o)}(X_j))$ versus $ln(ln(x_u/x))$ with $X_u = 0.03''$, where $F_{a(o)}(x_j) = j/(N+1)$. The least square fit line for the total EIFS population fit is shown in Fig. E.1 by a solid line whereas the result from the upper tail fit is denoted by a semi-dashed line. A similar plot for the two-parameter Weibull distribution is shown in Fig. E.2. the EIFSD parameters thus obtained are summarized in Table E.3.

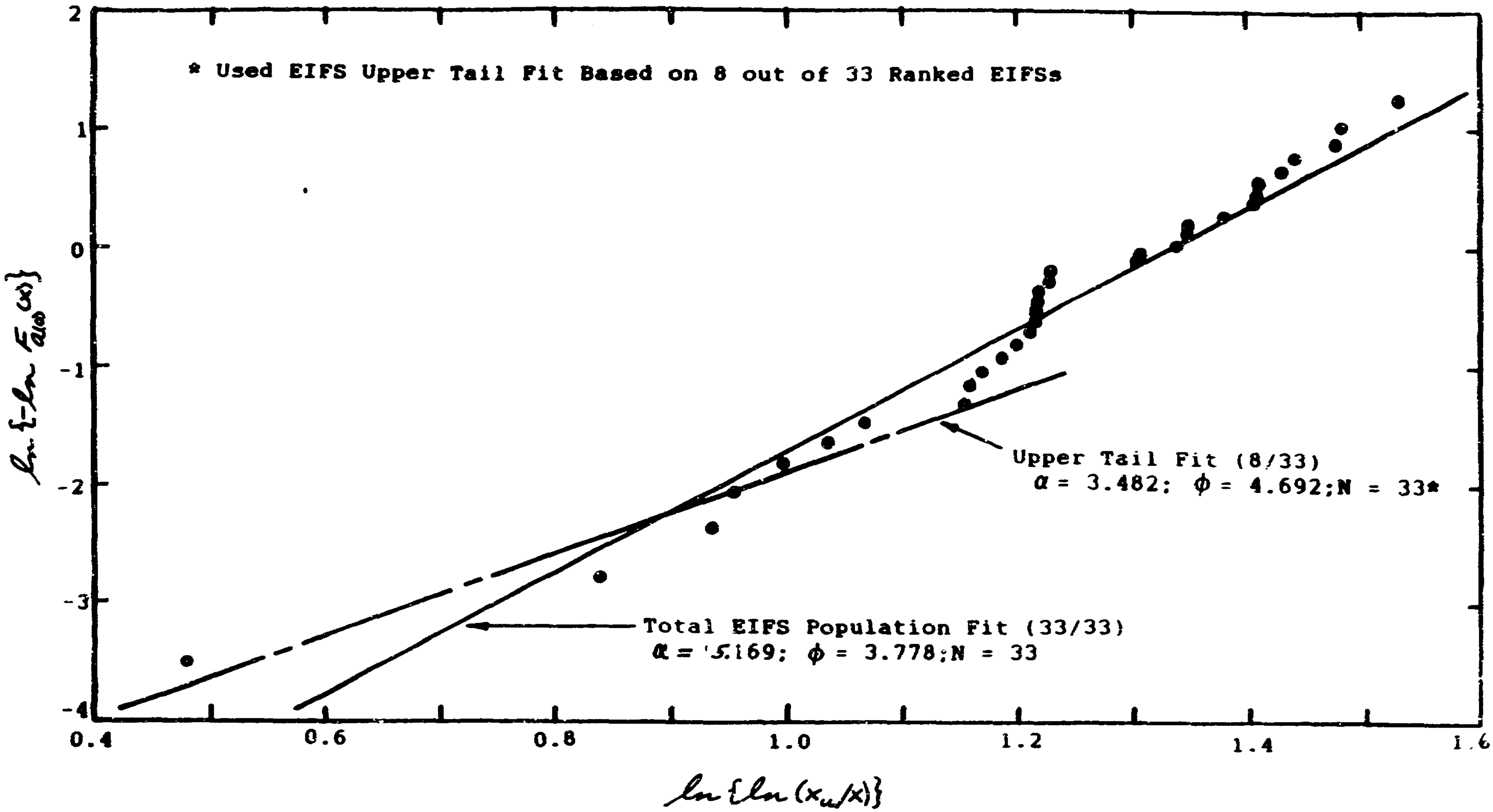

Figure E.1. $\ln\{-\ln F_{a(0)}(x)\}$ Versus $\ln\{\ln(x_u/x)\}$ for WPF Data Set and Weibull Compatible Fit for EIFSD Parameters.

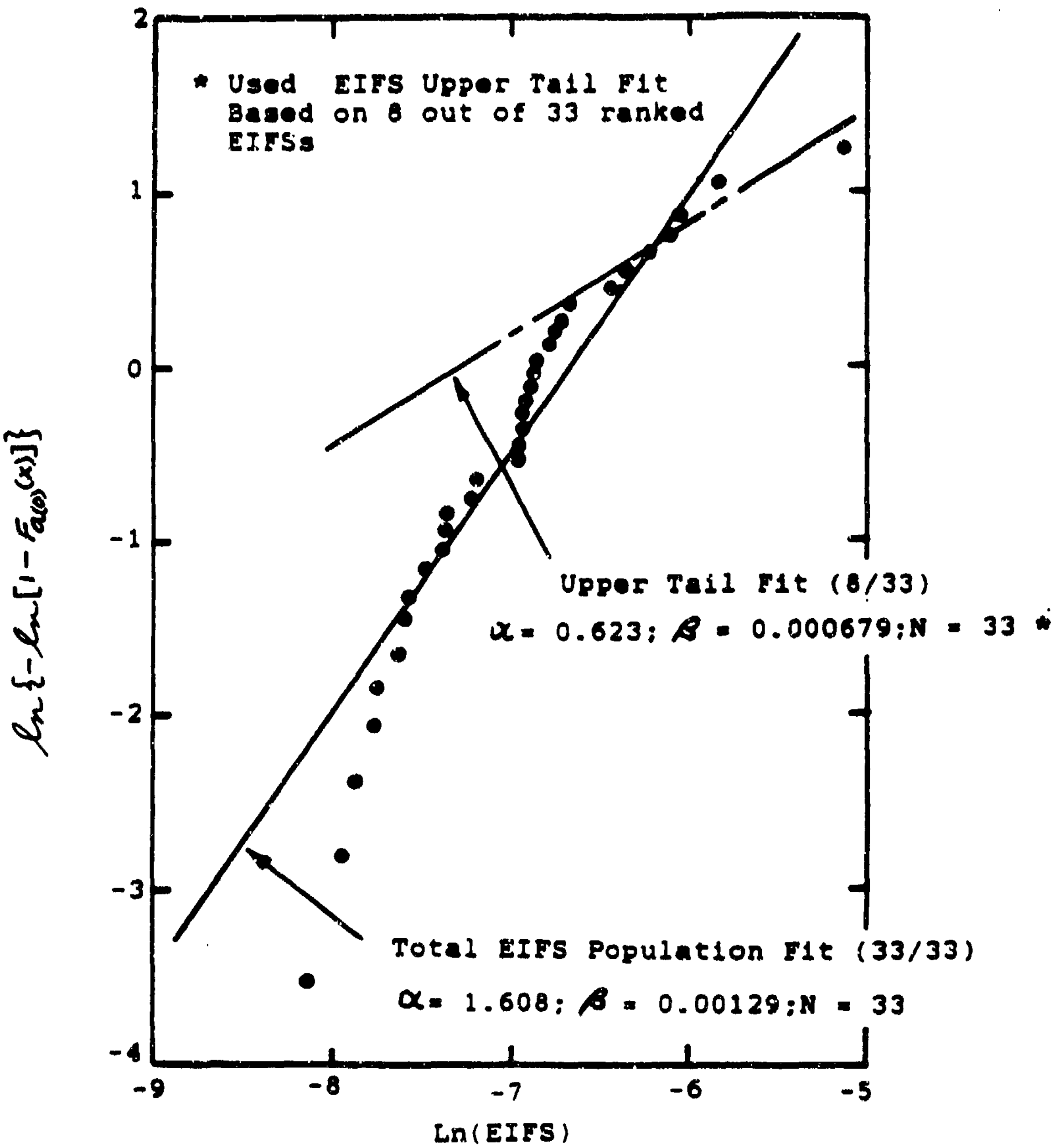

Figure E.2. $\ln\{-\ln[1-F_{a(0)}(x)]\}$ Versus Ln(EIFS) for WPF Data Set and Two-Parameter Weibull Fit for EIFSD Parameters.

Table E.3. Comparison of EIFSD Parameters for the Weibull-Compatible and Two-Parameter Weibull Distribution Functions Based on Total Population Fit and Upper Tail Fit (WPF Data Set).

DISTRIBUTION FUNCTION	EIFSD PARAMETERS (2)	
	TOTAL POP. FIT	UPPER TAIL FIT
Weibull-Compatible	x_u = 0.03"	x_u = 0.03"
	α = 5.169	α = 3.482
	ϕ = 3.778	ϕ = 4.692
Two Parameter Weibull	α = 1.608	α = 0.623
	β = 0.00129	β = 0.000679

NOTES: (1) 7475-T7351 aluminum; straight-bore fastener holes with NAS 6204-08 bolt installed (clearance-fit)

(2) Least squares fit; 50% confidence

The α value in both the Weibull compatible and two-parameter the statistical variability. On the other hand, β and ϕ in the respective EIFS distribution function denote the central tendency of the EIFS. For the Weibull compatible distribution function the average EIFS decreases as ϕ increases; whereas for the two parameter Weibull distribution function the average EIFS increases as β increases. It is observed from Table E.3 that with the upper tail fit, the α value decreases indicating that the statistical dispersion increases. However, ϕ increases for the Weibull compatible distribution whereas β decreases for the two-parameter Weibull distribution.

E.3 CONCLUSIONS AND RECOMMENDATIONS

1. As shown in Table E.1, the pooled Q values can be determined using either Eq. E-1 or E-2. Also, no significant differences in the pooled Q values were found using either the modified secant or the five-point incremental polynomial method. Therefore, since Eqs. E-1 and E-2 yield the same pooled Q value, Eq. E-2 is recommended for durability analysis because it is simpler to implement.

2. The value of the crack growth rate parameter Q (pooled) in Eq. 2 depends on the fractographic data used as well as the fractographic crack size range (i.e., AL-AU) used.

3. All fractographic data should be screened and censored for any durability analysis purpose. In particular, data sparsity should be examined (i.e. scrutinize data outside the desired AL-AU range for the durability analysis). Screening can be accomplished using the durability analysis software of Volume V [5].

4. EIFSD parameters based on the Weibull compatible distribution function are shown in Table E.2 for selected data sets. The following conclusions and recommendations are based on the extensive investigation conducted [42]:

(1) The CLSSA is effective for estimating the EIFSD parameters for individual or pooled fractographic data sets. It provides a rational approach for statistically scaling fractographic results to a common baseline.

(2) It is interesting to note in Table E.2 that α values for a given x_u based on the HEIFS approach are slightly larger than those based on the CLSSA. The same ϕ value, however, is obtained using either approach.

(3) α for the Weibull compatible EIFSD increases as x_u increases. The α value characterizes the variability of the EIFSD. For example, the variability decreases as α increases. It is observed that higher α values were obtained for straight-bore fastener holes than for countersunk fastener holes.

(4) The Weibull compatible distribution function or other suitable "compatible type" distribution functions (e.g., lognormal compatible, etc.) are recommended for defining IFQ. With a compatible type EIFSD function an upper bound EIFS limit is imposed (refer to Vol. I [1], Section H.3). The selected upper bound limit, x_u, involves a subjective decision. However, reasonable limits can be selected based on considerations for the economical repair limit and/or NDI. For fastener holes an upper bound limit of x_u = 0.03" - 0.05" is recommended.

(5) Initial flaw sizes for different upper percentiles (i.e., P = .001 and P = .0001) are shown in Table E.2. It is seen that the upper percentile initial flaw size values for the countersunk and straight-bore fastener hole data sets are very consistent for individual and/or pooled data sets.

(6) Larger upper percentile initial flaw sizes were obtained for countersunk fastener holes than are currently used for a deterministic-based durability analysis. For example, in Table E.2 for (AFXLR4+AFXMR4+AFXHR4) and x_u = .03" the initial flaw sizes are .0268" and .0291" for P = .001 and .0001, respectively. For x_u = .05", the initial flaw sizes are .0388" and .0459", for P = .001 and .0001, respectively. If an EIFS is selected from the EIFSD for a given upper percentile, the resulting EIFS should be grown forward consistent with the basis for the EIFS distribution (see Vol. I [1]).

(7) A fractographic crack size range of AL-AU = .0" - .05" is considered reasonable for determining the EIFSD parameters for clearance-fit fastener holes. In any case, all durability analysis applications should be consistent with the basis for the IFQ results. For example, fatigue cracks should be grown backwards and forwards in a consistent manner.

(8) The reference crack size, a_0, should fall within the AL-AU range used (e.g., AL $\geq a_0 \geq$ AU). a_0 = AU is recommended for clearance-fit fastener holes.

(9) EIFSD parameters for the Weibull compatible distribution function were estimated using linear and nonlinear least square fit methods [42]. For a given x_u, no significant differences in α and ϕ were observed using either approach. Therefore, the linear least square fit method, reflected in the CLSSA, is recommended for estimating EIFSD parameters.

5. EIFS values, based on the total EIFS population fit and the upper tail fit are shown in Table E.3 for the Weibull compatible and two-parameter Weibull distribution functions. In this case, the initial flaw size values are of the same order of magnitude. Note that larger initial flaw sizes are obtained using the upper tail fit than the total population

fit. For durability analysis, initial flaw size should be based on a total EIFS population fit since we are concerned with the total flaw population - not just the extreme values. For damage tolerance analysis, however, the upper tail fit is considered reasonable. Once again, we emphasize the importance of growing EIFSs forward in the same manner as EIFSs were defined.

APPENDIX F

EVALUATION AND SENSITIVITY OF Q AND σ_z FOR STRAIGHT-BORE AND COUNTERSUNK FASTENER HOLES IN 7475-T7351 ALUMINUM

F.1 INTRODUCTION

The objectives of this section are to (1) evaluate and compare preliminary and refined methods for computing the crack growth parameter, Q, and the standard deviation, σ_z of Z = lnX using fractographic data, (2) evaluate the sensitivity of Q, and σ_z with respect to various analysis considerations (e.g., data processing, fractographic crack size range (AL-AU, data censoring, etc.).

This investigation was divided into two parts as follows. Part I was concerned with the determination of Q, and σ_z for selected uncensored fractographic data sets and the sensitivity of the results with respect to: (1) fractographic crack size range (AL-AU), (2) equalizing or not equalizing the number of data points in the selected AL-AU range, and (3) method for computing crack growth rate, (i.e., modified secant [27] and five-point incremental polynomial [28]). In Part II we investigated the effects of fractographic data censoring, crack size range, and/or fractographic extrapolations, on Q, σ_z mean TTCI and mean EIFS.

Both straight-bore and countersunk fastener hole data sets were considered in Part I. Fractograhic data sets from the "Fastener Hole Quality" (FHQ) [3] and the "Advanced Durability Analysis" (ADA) programs [2] were utilized. Only straight-bore fastener hole fractographic data sets were considered in Part II. All the fractographic data sets used in this investigation are described in Tables F.1 and F.2. Specimen details are shown in Figs. 1-5. Details of the investigation, including methods, results, observations and

TABLE F.1. Description of Fastener Hole Quality (FHQ) Fractographic Data Sets.

(1) DATA SET	NO. SPECIMEN	% LT	(KSI) (2)	WIDTH (IN.)	LOAD SPECTRUM	TYPE HOLE	SPECIMEN DETAILS
WPF	33	0	34	1.5	F-16 400 HR.	SB(3)	Fig. 4
LYWPF	7	15	30.6				Fig. 5
XWPF	33	15	34				
HYWPF	10	15	40.8				
WPB	32	0	33		B-1 BOMBER		Fig. 4
LYWPB	10	15	29.7				Fig. 5
XWPB	31	15	33				
HYWPB	10	15	39.6				

Notes: (1) 7475-T7351 Aluminum
(2) Maximum gross stress due to peak load in spectrum
(3) SB = straight-bore; NAS6204-08(1/4" Dia.)
(4) FHQ fractographic data in Ref. 3

TABLE F.2. Description of Advanced Durability Analysis (ADA) Fractographic Data Sets.

(1) DATA SET	NO. SPECIMEN	% LT	σ (KSI) (2)	WIDTH (IN.)	LOAD SPECTRUM	TYPE HOLE	SPECIMEN DETAILS
WWPF	13	0	34	3.0	F-16 400 HR.	SB(3)	Fig. 2
WWPB	12	0	34		B-1 Bomber		
WWPCL	4	0	34		F-16 C/D		
WWPCH	5	0	40.8		F-15 C/D		
WWPFO	14	0	34		F-16 400 HR.	(6)	
WPF	15	15	34		F-16 400 HR.	CSK(4)	Fig.1
WPB	13	15	36		B-1 BOMBER		
WAFXMR4	14	15	34		F-16 400 HR.		Fig.3
WAFXMR4	14	15	40.8		F-16 400 HR.		
WXWPB	15	15	34		B-1 BOMBER		

Notes: (1) 7475-T7351 Aluminum
(2) Maximum gross stress due to peak load in spectrum
(3) SB = straight-bore; NAS6204-08 (1/4" Dia.)
(4) MS 90353-08 Pull-Through Rivet
(5) ADA fractographic data in Volume III [3]
(6) Open hole

conclusions, are presented in the following.

F.2 PART I - EVALUATION OF PRELIMINARY AND REFINED METHODS USING UNCENSORED DATA SETS

Fractographic data for selected data sets in Tables F.1 and F.2 were used to evaluate Q, and σ_z. Preliminary and refined methods for computing Q and σ_z are documented in Volume I [1]. The preliminary method for computing Q and σ_z was thoroughly evaluated and refined to obtain the recommended method. This was definitely a "learning process" in which many variations in data processing and analysis were considered. Applicable equations for computing Q and σ_z for the preliminary and refined methods are summarized in the following.

The simple crack growth rate model given in Eq. F-1 is useful for representing one segment of the service crack growth master curve (SCGMC).

$$da(t)/dt = Qa(t) \qquad \text{(F-1)}$$

In Eq. F-1, $da(t)/dt$ = crack growth rate, Q = crack growth rate parameter, and $a(t)$ = crack size at any time t. The Q in Eq. F-1 can be determined for a single fatigue crack or pooled fatigue cracks. For a single fatigue crack, Eq. F-1 is rewritten as

$$da(t)/dt = Q_j a(t) \qquad \text{(F-2)}$$

where, Q_j = crack growth rate constant for the jth fatigue crack in a fractographic data set and the other terms are the same as those defined for Eq. F-1. For pooled fatigue cracks, Q can be approximated by a lognormal random variable. The Q value evaluated in Eqs. F-5 and F-8 represents the median value; whereas the standard deviation of lnQ, denoted by σ_z, are evaluated in Eqs. F-7 and F-10. Note that the stochastic crack growth rate equation presented in Vol. I is expressed as da(t)/dt = XQa(t), where X is a lognormal random variable. The Q value in such an equation is also evaluated from Eqs. F-5 and F-8; whereas the standard deviation of lnX is equal to σ_z, that is determined from Eqs. F-7 and F-10. In what follows, the Q values obtained from Eqs. F-5 and F-8 are referred to as the "pooled Q" values for a data set.

Equations F-1 and F-2 can be transformed into Eq. F-3 and F-4, respectively.

$$\ln da(t)/dt = \ln Q + \ln a(t) \qquad \text{(F-3)}$$

$$\ln da(t)/dt = \ln Q_j + \ln a(t) \qquad \text{(F-4)}$$

A preliminary method for determining pooled Q and Q_j, based on a least square fit procedure using [da(t)/dt, a(t)] data is described in Volume I [1]. A subscript "i" is added to Q (i.e., Q_i) to denote the "pooled Q" value for the ith fractographic data set. In the following, either Q or Q_i is used. The resulting equations for Q_i and Q_j are shown in Eqs. F-5 and F-6, respectively.

$$Q = Q_i = \exp\left\{\frac{\sum_{j=1}^{m}\sum_{k=1}^{N_j} \ln\left[da(t)/dt\right]_{jk} - \sum_{j=1}^{m}\sum_{k=1}^{N_j} \ln a_j(t_k)}{\sum_{j=1}^{m} N_j}\right\} \qquad \text{(F-5)}$$

$$Q_j = \frac{N_j \sum_{k=1}^{N_j} X_k Y_k - \sum_{k=1}^{N_j} X_k \sum_{k=1}^{N_j} Y_k}{\sum_{k=1}^{N_j} X_k^2 - \left(\sum_{k=1}^{N_j} X_k\right)^2} \tag{F-6}$$

In Eqs. F-5 and F-6, m = total number of fatigue cracks in the data set, N_j = number of a(t)s for the jth fatigue crack, $[da(t)/dt]_{jk}$ = ith crack growth rate for the jth fatigue crack, and $a_j(t_k)$ = kth a(t) value for the jth fatigue crack. An expression for determining the standard deviation, σ_z, is given in Eq. F-7.

$$\sigma_z = \sqrt{\frac{\sum_{j=1}^{m} \sum_{k=1}^{N_j} \left\{ \ln [da(t)/dt]_{jk} - \ln Q - \ln a_j(t_k) \right\}^2}{\sum_{j=1}^{m} N_j}} \tag{F-7}$$

All terms in Eq. F-7 have already been defined in Eq. F-5. σ_z is needed to implement the stochastic crack growth approach (SCGA), but it is not needed for the deterministic crack growth approach (DCGA).

Two methods for determining $[da(t)/dt]_{jk}$ in Eqs. F-5 through F-7 were investigated: (1) modified secant method [27] and (2) five-point incremental polynomial method [28].

The refined method for computing pooled Q_i, Q_j and σ_z is described in Volume I [1]. Applicable expressions for pooled Q_i, Q_j and σ_z are given in Eqs. F-8, F-9, and F-10, respectively.

$$Q = Q_i = \exp\left\{ \frac{1}{m} \sum_{j=1}^{m} \ln Q_j \right\} \tag{F-8}$$

$$Q_j = \frac{N_j \sum_{k=1}^{N_j} X_k Y_k - \sum_{k=1}^{N_j} X_k \sum_{k=1}^{N_j} Y_k}{N_j \sum_{k=1}^{N_j} X_k^2 - \left(\sum_{k=1}^{N_j} X_k\right)^2} \tag{F-9}$$

$$\sigma_z = \sqrt{\frac{\sum_{j=1}^{m}\left[\ln(Q_j/Q)\right]^2}{m}} \tag{F-10}$$

In Eqs. F-8 through F-10, m = number of fatigue cracks in the data set, N_j = number of a(t)s for the jth fatigue crack; X_k and Y_k are defined in Eq. F-11.

$$X_k = t_k$$
$$Y_k = \ln a_j(t_k) \tag{F-11}$$

In Eq. F-11, t_k = kth time for the jth fatigue crack and $a_j(t_k)$ = kth a(t) value for the jth fatigue crack.

The primary objective of the Part I investigation was to justify the refined methods for computing pooled Q and σ_z and to study the effects of various data processing considerations on the resulting pooled Q and σ_z values.

Results for pooled Q and σ_z, based on the modified secant and five-point incremental polynomial method for computing the da(t)/dts, are shown in Tables F.3 and F.4, respectively. These results were based on uncensored fractographic data sets. In this case, the effect of the following on pooled Q, and σ_z values will be examined: (1) fractographic crack size range (AL-AU), (2) unequal number of a(t)s for each fatigue crack in the AL-AU range, and (3) modified secant versus five-point incremental polynomial method for computing da(t)/dt data. The pooled Q and σ_z values shown in Tables F.3 and F.4 were based on Eqs. F-5 and F-7, respectively. Two different fractographic crack size ranges were considered, i.e., AL-AU = 0.01"-0.05" and all the data with no AL-AU restriction.

TABLE F.3. Summary of Q and σ_z Based on Modified Secant Method for da/dts (With and Without Equalizing the Number of a(t)s in AL-AU Range).

(1) DATA SET	LOAD SPECTRUM	MAX (KSI)	NO. CRACKS (1)	AL-AU	da/dt FILE (3)	EQUALIZE NO. a(t)s? (7)	(5) $Qx10^4$ (1/HR) (4)	(6) σ_z (4)
WPF	F16 -400 HR	34	33	.01"-.05"	"DAWFS"	YES NO	2.395 2.305	0.215 0.217
				ALL (2)		YES NO	2.541 2.588	0.369 0.391
XWPF	F16 -400 HR	34	33	.01"-.05"	"DAXFS"	YES NO	3.831 3.467	0.431 0.338
				ALL (2)		YES NO	3.674 3.373	0.452 0.407
LYWPF	F16 -400 HR	30.6	7	.01"-.05"	"DALFS"	YES NO	2.257 2.172	0.383 0.289
				ALL (2)		YES NO	2.103 2.177	0.367 0.385
HYWPF	F16 -400 HR	40.8	18	.01"-.05"	"DAHFS"	YES NO	9.175 8.577	0.318 0.367
				ALL (2)		YES NO	8.432 8.478	0.506 0.571

Notes:
(1) Uncensored data set
(2) Use all the a(t), ts with no AL-AU restriction
(3) Filename for da/dts
(4) Based on program filename = "EIFS17" (Digital "Rainbow" PC)
(5) "Pooled Q" for data set based on da/dt = Qa(t) fit ;Ref. Eq. F-5
(6) Standard deviation; ln da/dt versus ln a(t);Ref. Eq. F-7
(7) Artifically equalized the number of a(t)s for each fatigue crack in the data set for selected AL-AU range (yes or no)
(8) Deterministic crack growth approach used

TABLE F.4. Summary of Q and σ_z Based on Five-Point Incremental Polynomial Method for da/dts (With and Without Equalizing the Number of a(t)s in AL-AU Range).

DATA SET	LOAD SPECTRUM	MAX (KSI)	NO. CRACKS (1)	AL-AU	da/dt FILENAME (3)	EQUALIZE NO. a(t)s ? (7)	(5) $Q \times 10^4$ (1/HR)	(6) σ_z (4)
WPF	F-16 400	34	33	.01"-.05"	"DAWPFP"	YES	2.398	0.212
						NO	2.300	0.214
				ALL (2)		YES	2.538	0.359
						NO	2.570	0.345
HWPF	↓	34	33	.01"-.05"	"DAHWPFP"	YES	3.837	0.427
						NO	3.477	0.336
				ALL (2)		YES	3.735	0.424
						NO	3.374	0.393
LYWPF	↓	30.6	7	.01"-.05"	"DALYWPFP"	YES	2.260	0.301
						NO	2.178	0.287
				ALL (2)		YES	2.269	0.346
						NO	2.186	0.366
HYWPF	↓	40.8	10	.01"-.05	"DAHYWPFP"	YES	9.224	0.316
						NO	8.690	0.360
				ALL (2)		YES	8.519	0.506
						NO	8.569	0.573

Notes:
(1) Uncensored data set
(2) Use all the a(t). ts with no AL-AU restriction
(3) Filename for da/dts
(4) Based on program filename = "EIFS17" (Digital "Rainbow" PC)
(5) "Pooled Q" for data set based on da/dt = Qa(t) fit ;Ref. Eq. F-5
(6) Standard deviation; ln da/dt versus ln a(t);Ref. Eq. F-7
(7) Yes = a(t)s in AL-AU range artifically equalized for each fatigue crack in data set; No = actual a(t)s in AL-AU range used
(8) Deterministic crack growth approach used

Note that Q_j varies from specimen (crack) to specimen (crack) in a data set. As a result, the mean value, standard deviation and coefficient of variation for Q_j in a data set can be computed. These quantities are referred to as the Q_j statistics.

The refined method was used to compute pooled Q, σ_z and Q_j statistics for selected FHQ program [3] and "Advanced Durability Analysis" (ADA) program [2] data sets. In this case, pooled Q and σ_z values were determined using Eqs. F-8 and F-10, respectively. Different AL-AU ranges were considered. In some cases, crack growth data outside the given AL-AU range were used because some fatigue cracks either had no data or insufficient data in the AL-AU range to carry out the computations. A default crack size range, DL-DU was used only for those fatigue cracks with insufficient data in the AL-AU range. Q_j values for individual fatigue cracks were determined using Eq. F-9. The mean, standard deviation and coefficient of variation for Q_j was determined using standard statistical anlaysis methods [e.g., 22].

Pooled Q, σ_z and Q_j statistics for selected FHQ fighter and bomber load spectra data sets are shown in Tables F.5 and F.6, respectively. Results for the ADA data sets are shown for straight-bore and countersunk data sets in Table F.7 and F.8, respectively. These results are discussed in Section F.4.

F.3 PART II - STUDY OF REFINED METHOD AND EFFECTS OF DATA CENSORING ON POOLED Q, σ_z, MEAN TTCI AND MEAN EIFS

The purpose of the Part II study was to investigate the effects of fractographic data censoring, crack size range (AL-AU) and/or fractographic extrapolations on pooled Q, σ_z, mean TTCI and mean EIFS.

Table F.5. Summary of Pooled Q, σ_z, and Q Statistics for Different AL-AU Crack SIZE Ranges Based on Recommended Methods (FHQ -- Fighter Data Sets)

DATA SET (1)	LOAD SPECTRUM	σ MAX. (ksi) (2)	NO. CRACKS (3)	AL-AU	DL-DU (4)	$Q \times 10^4$ (1/HR.) (5)	σ_z (6)	Q_j STATISTICS: (MEAN)$\times 10^4$ (1/HR.)	Q_j STATISTICS: STD. DEV. $\times 10^4$	Q_j STATISTICS: COV
WPF	F16 -400 HR	34	33	.01"-.05"	AL-AU	2.393	0.166	2.429	0.464	0.191
				.01"-.10"		2.364	0.159	2.396	0.422	0.176
				.01"-1"		2.364	0.162	2.398	0.440	0.183
				ALL		2.528	0.150	2.559	0.420	0.164
XWPF		34	32 (8)	.01"-.05"		3.651	0.262	3.776	0.962	0.255
				.01"-.10"		3.387	0.280	3.521	0.978	0.278
				.01"-1"		3.231	0.267	3.351	0.935	0.279
				ALL		3.351	0.234	3.445	0.822	0.239
LYWPF		30.6	7	.01"-.05"		2.330	0.247	2.408	0.664	0.276
				.01"-.10"		2.185	0.214	2.241	0.562	0.250
				.01"-1"		2.120	0.176	2.156	0.429	0.199
				ALL		2.253	0.249	2.322	0.555	0.239
HYWPF		40.8	10	.01"-.05"	.005"-.2"	9.304	0.293	9.682	2.529	0.261
				.01"-.10"	.005"-.2"	8.452	0.254	8.721	2.144	0.246
				.01"-1"	.005"-.2"	7.965	0.229	8.177	1.893	0.231
				ALL	AL-AU	8.805	0.249	9.057	1.904	0.219

Notes: (1) 7475-T7351 Al.;straight bore holes with NAS 6204-08 (1/4" Dia.) bolts installed
(2) Maximum gross stress at peak spectrum load
(3) Uncensored data set
(4) Default range used when data does not exist or is insufficient in the AL-AU range for required computations
(5) Ref. Eq. F-8
(6) Ref. Eq. F-10
(7) Deterministic crack growth approach used
(8) One surface fatigue crack not used

Table F.6. Summary of Pooled Q, σ_Z, and Q Statistics for Different AL-AU Crack Size Ranges Based on Recommended Methods (FHQ -- Bomber Data Sets)

DATA SET (1)	LOAD SPECTRUM	σ MAX. (ksi) (2)	NO. CRACKS (3)	AL-AU	DL-DU (4)	$Q\times10^4$ (1/HR.) (5)	σ_Z (6)	Q_j STATISTICS (MEAN)$\times10^4$ (1/HR)	STD. DEV. $\times10^4$	COV
WPB	B-1 Bomber	33	32	.01"-.05"	AL-AU	1.401	0.139	1.415	0.197	0.139
				.01"-.10"		1.425	0.149	1.441	0.219	0.152
				.01"-1"		1.449	0.166	1.469	0.256	0.174
				ALL		1.509	0.141	1.524	0.218	0.143
NWPB		33	31	.01"-.05"		2.469	0.233	2.534	0.564	0.222
				.01"-.10"		2.464	0.225	2.525	0.544	0.215
				.01"-1"		2.473	0.228	2.538	0.580	0.229
				ALL		2.493	0.213	2.550	0.547	0.214
LYWPB		29.7	16	.01"-.05"		1.596	0.249	1.647	0.423	0.256
				.01"-.10"		1.667	0.213	1.706	0.384	0.225
				.01"-1"		1.724	0.202	1.760	0.371	0.210
				ALL		1.562	0.150	1.579	0.231	0.146
HYWPB		39.6	16	.01"-.05"		4.410	0.229	4.527	1.036	0.229
				.01"-.10"		4.226	0.216	4.328	0.974	0.225
				.01"-1"		4.338	0.151	4.389	0.673	0.153
				ALL		4.835	0.144	4.886	0.712	0.146

Notes: (1) 7475-T7351 Al.;straight bore holes with NAS 6204-08 (1/4" Dia.) bolts installed
(2) Maximum gross stress at peak spectrum load
(3) Uncensored data set
(4) DL-DU same as AL-AU range to compute the crack growth parameter Q for a give crack or cracks in the data set
(5) Ref. Eq. F-8
(6) Ref. Eq. F-10
(7) Deterministic crack growth approach used

Table F.7. Summary of Pooled Q, σ_z, and Q Statistics for Straight-Bore Fastener Holes Based on Recommended Methods.

(1) DATA SET	LOAD SPECTRUM	σ MAX. (ksi) (2)	NO. CRACKS (3)	AL-AU	(4) DL-DU	(5) $Q \times 10^4$ (1/HR)	(6) σ_z	Q_j STATISTICS (MEAN)$\times 10^4$ (1/HR.)	STD. DEV. $\times 10^4$	COV
WWPF	F-16 400 HR	34	13	.01"-.05"	AL-AU	2.742	0.119	2.762	0.340	0.123
				.01"-.10"		2.750	0.146	2.782	0.450	0.165
				.01"-2"		2.924	0.153	2.959	0.479	0.162
				.05"-2"		3.123	0.177	3.172	0.555	0.175
				.10"-2"		3.248	0.185	3.300	0.599	0.181
				ALL		2.918	0.147	2.951	0.462	0.156
WWPB	B-1 BOMBER	34	12	.01"-.05"	.005"-.10"	4.458	0.538	5.054	2.228	0.452
				.01"-.10"	AL-AU	3.655	0.400	3.936	1.402	0.356
				.01"-2"		2.452	0.176	2.492	0.452	0.182
				.05"-2"		2.259	0.197	2.307	0.509	0.221
				.10"-2"		2.240	0.246	2.317	0.684	0.295
				ALL		2.733	0.201	2.789	0.553	0.198
WWPCL	F-16 C/D	34	4	.01"-.05"	.005"-.10"	4.579	0.479	5.092	2.193	0.431
				.01"-.10"	AL-AU	4.178	0.411	4.520	1.667	0.373
				.01"-2"		2.185	0.331	2.300	0.695	0.302
				.05"-2"		1.879	0.271	1.950	0.535	0.274
				.10"-2"		1.752	0.260	1.813	0.486	0.268
				ALL		2.239	0.337	2.359	0.700	0.297
WWPCH		40.8	6	.01"-.05"	.005"-.20"	9.638	0.556	10.884	4.723	0.434
				.01"-.10"	.005"-.20"	7.387	0.442	8.039	3.227	0.401
				.01"-2"	AL-AU	4.056	0.234	4.172	1.124	0.269
				.05"-2"		3.526	0.187	3.591	0.793	0.221
				.10"-2"		3.323	0.199	3.394	0.812	0.239
				ALL		4.192	0.239	4.312	1.129	0.262
WWPFO	F-16 400 HR	34	14	.01"-.05"	AL-AU	8.606	0.379	9.213	3.431	0.372
				.01"-.10"		6.624	0.279	6.895	2.049	0.297
				.01"-2"		3.994	0.197	4.075	0.836	0.205
				.05"-2"		3.460	0.204	3.534	0.742	0.209
				.10"-2"		3.388	0.208	3.462	0.724	0.209
				ALL		4.346	0.199	4.436	0.918	0.207

Ref. Table F.9 for notes.

Table F.8. Summary of Pooled Q, σ_z, and Q Statistics for Countersunk Fastener Holes Based on Recommended Methods.

DATA SET (1)	LOAD SPECTRUM	σ MAX. (ksi) (2)	NO. CRACKS (3)	AL-AU	(4) DL-DU	(5) $Q \times 10^4$ (1/HR.)	(6) σ_z	Q_j STATISTICS (MEAN)$\times 10^4$ (1/HR)	STD. DEV. $\times 10^4$	COV
WFI	F-16 400 HR	34	14	.01"-.05"	AL-AU	2.329	.247	2.404	.654	.272
				.01"-.10"		2.228	.221	2.287	.576	.252
				.01"-2"		2.167	.205	2.237	.531	.237
				.05"-2"		2.216	.224	2.276	.583	.256
				.10"-2"		2.334	.262	2.421	.731	.302
				ALL		2.216	.204	2.227	.530	.234
MBI	B-1 BOMBER	36	12	.01"-.05"	.01"-.20"	5.709	.284	5.949	1.806	.304
				.01"-.10"	AL-AU	4.699	.206	4.803	1.082	.225
				.01"-2"		2.747	.268	2.852	.863	.302
				.05"-2"	.05"-2"	2.402	.288	2.519	.837	.332
				.10"-2"	AL-AU	2.309	.313	2.435	.904	.371
				ALL		2.941	.248	3.039	.866	.291
WAFXMR4	F-16 400 HR	34	14	.01"-.05"	.01"-.20"	6.955	.825	8.835	5.066	.573
				.01"-.10"	.01"-.20"	5.108	.706	6.135	3.159	.515
				.01"-2"	AL-AU	3.335	.449	3.679	1.716	.467
				.05"-2"		2.970	.441	3.274	1.551	.474
				.10"-2"		2.906	.446	3.209	1.538	.479
				ALL		3.543	.447	3.901	1.814	.465
WAFXHB4		40.8	13	.01"-.05"	AL-AU	6.980	.429	7.698	3.791	.492
				.01"-.10"		5.804	.427	6.393	3.109	.486
				.01"-2"		4.446	.347	4.743	1.933	.407
				.05"-2"		4.018	.328	4.259	1.673	.393
				.10"-2"		4.087	.343	4.369	1.928	.441
				ALL		4.655	.357	4.989	2.135	.429
WXWPB	B-1 BOMBER	34	15	.01"-.05"	.01"-.20"	4.277	0.209	4.376	0.981	0.224
				.01"-.10"	AL-AU	3.413	0.337	3.694	1.774	0.480
				.01"-2"	AL-AU	1.799	0.228	1.848	0.434	0.235
				.05"-2"		1.553	0.245	1.601	0.406	0.254
				.10"-2"		1.487	0.259	1.539	0.425	0.276
				ALL		1.968	0.239	2.026	0.507	0.250

Ref. Table F.9 for notes.

TABLE F.9. Notes for Tables F.7 and F.8.

Notes:
(1) 7475-T7351 Al.
(2) Maximum gross stress at peak spectrum load
(3) Uncensored data set
(4) Default range used when data does not exist or is insufficient in the AL-AU range for required computations
(5) Ref. Eq. F-8
(6) Ref. Eq. F-10
(7) Deterministic crack growth approach

The investigation was conducted as follows: Five fractographic data sets (straight-bore holes) from Tables F.1 and F.2 were used (i.e. WPF, XWPF, HYWPF, LYWPF, and WWPF). First, the fractographic results for the largest fatigue crack per specimen were screened. The number of fatigue cracks with factographic data covering selected AL-AU ranges was determined for each data set. Also, the maximum common Al-AU range for each data was determined. Some non typical fatigue cracks were deleted from the data set for analysis purposes. Results of this survey are shown in Table F.10.

Software is available for screening fractographic results for a given data set using an IBM or IBM-compatible PC [5]. This software can be used to plot the fractographic results for selected crack size ranges and/or flight hour ranges. Plots of the fractographic data (i.e. a(t) versus flight hours) for the five data sets considered in Part II are shown in Figs. F.1-F.10. Data for the full range as well as for AL-AU = 0.01" - 0.05" range are shown in these plots.

The following values were computed using censored and uncensored data sets: Pooled Q, σ_z, TTCI (mean and COV), and mean EIFS (two different methods). Results are summarized in Tables F.11 and F.12. In Table F.11 the TTCI values were determined for the reference crack size, a_0, that was selected so that all TTCIs could be determined by interpolation with no extrapolations. In Table F.11 two numbers are shown for the number of cracks used. The first number denotes the number of fatigue cracks used for the analysis and the second number, separated by a slash (/), denotes the total number of fatigue cracks (i.e. largest fatigue crack per specimen) in the data set.

Mean EIFS values, obtained with and without TTCI extrapolations, are summarized in Table F.12 for the same data

TABLE F.10. Crack Size Range Survey for Straight-Bore Hole Data Sets.

Data	No. Cracks in AL-AU Range	Common AL-AU Range	Remarks
WPF	27	.01"-.02"	Delete #6, 19, 20, 21, 23, 29
	21	.01 - .03	Delete #6, 13, 19, 20, 21, 23, 24, 29, 30, 31, 32, 33
	18	.01 - .04	Delete #6, 13, 17, 19, 20, 21, 22, 23, 24, 26, 29, 30, 31, 32, 33
	6	.01 - .05	Delete #5, 6, 7, 8, 9, 11, 12, 13, 15, 16, 17, 18, 19, 20, 21, 22, 23, 24, 25, 26-33
	32	.0085-.0129	Delete #6
XWPF	30	.01"-.02"	Delete #2, 16, 31
	30	.01-.03	Delete #2, 16, 31
	30	.01-.04	Delete #2, 16, 31
	30	.01-.05	Delete #2, 16, 31
	32	.0141"-.0299"	Delete #16
HYWPF	7	.01"-.02"	Delete #5
	5	.01-.03	Delete #4, 5, 7
	5	.01-.04	Delete #4, 5, 7
	5	.01-.05	Delete #4, 5, 7
	8	.0026-.0163	Use all
LYWPF	6	.01"-.02"	Use all
	5	.01-.03	Delete #1
	5	.01-.04	Delete #1
	5	.01-.05	Delete #1
	6	.01008-.02181	Use all
WWPF	12	.01"-.02"	Delete #3
	12	.01-.03	Delete #3
	12	.01-.04	Delete #3
	12	.01-.05	Delete #3
	13	.0154-.678	Use all

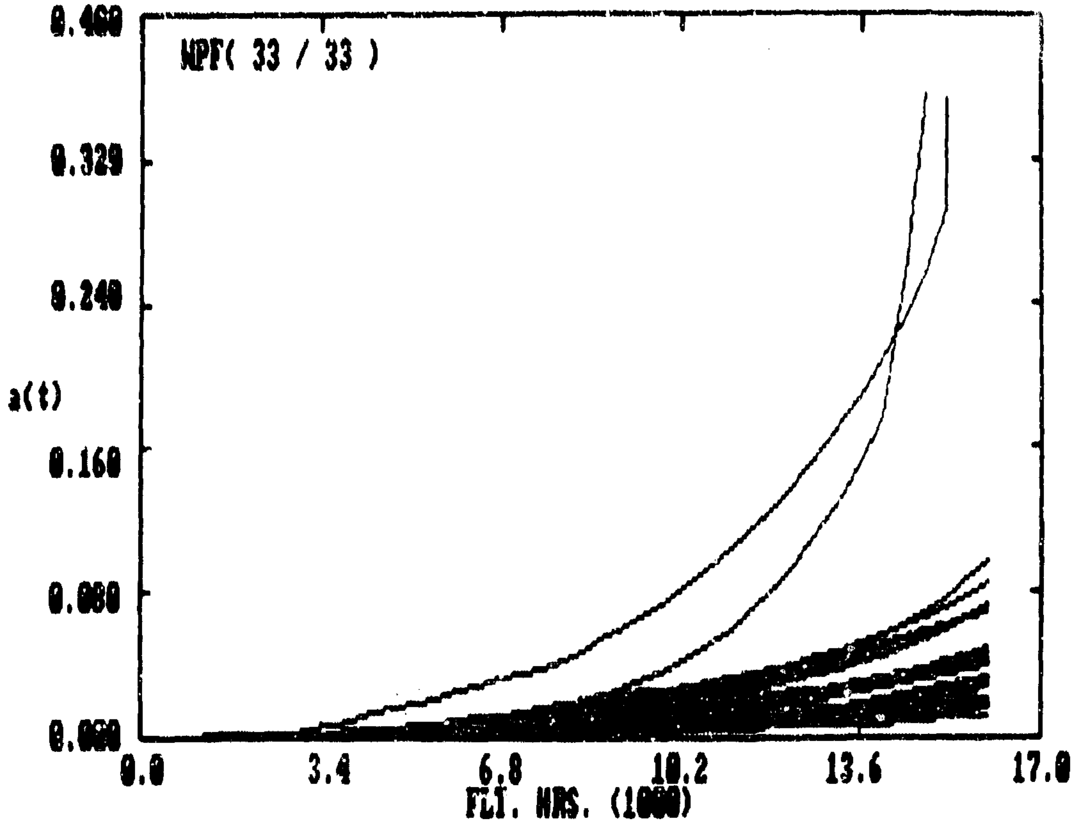

Figure F.1. a(t) Versus Flt. Hrs. for WPF Data Set (all the data).

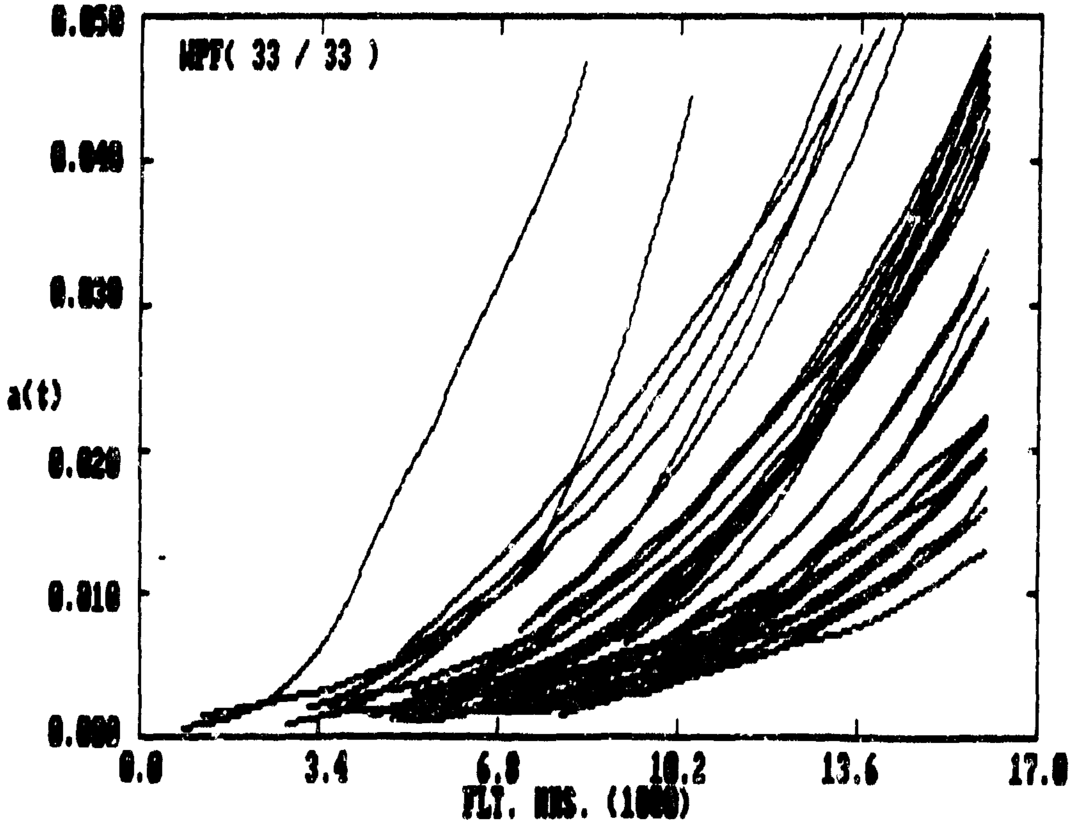

Figure F.2. a(t) Versus Flt. Hrs. for WPF Data Set (AL-AU = 0.0"-0.05").

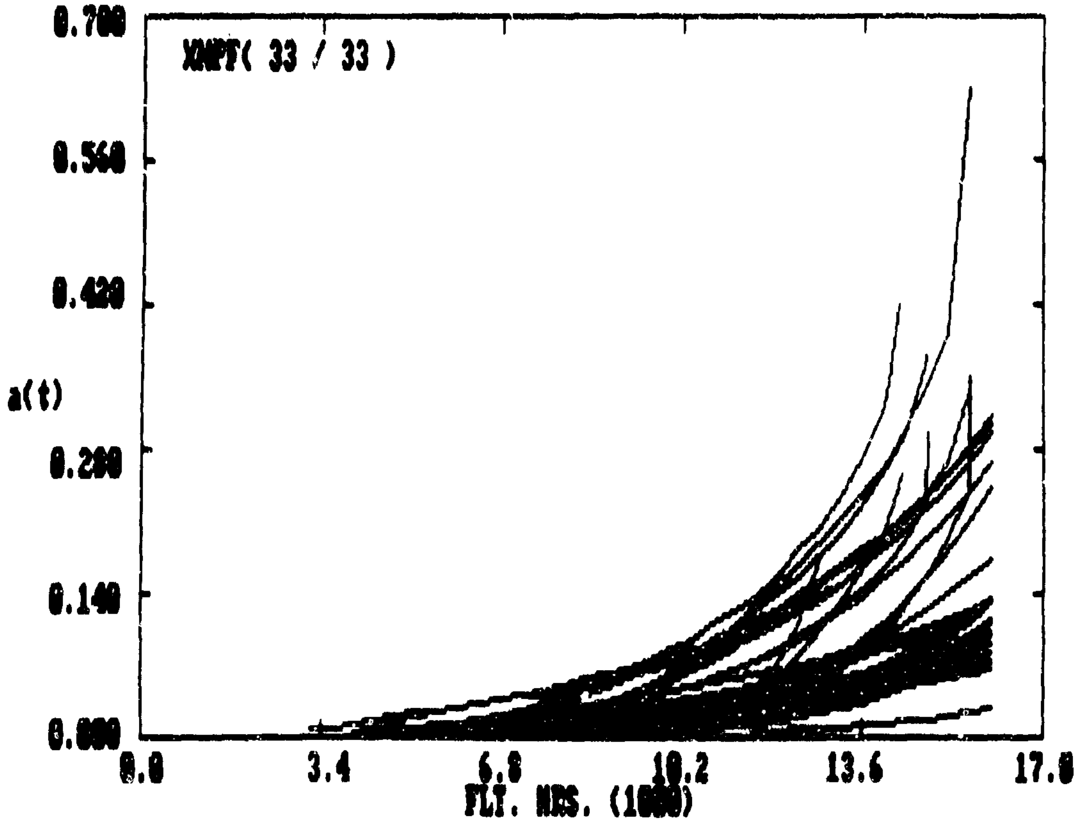

Figure F.3. a(t) Versus Flt. Hrs. for XWPF Data Set (all the data).

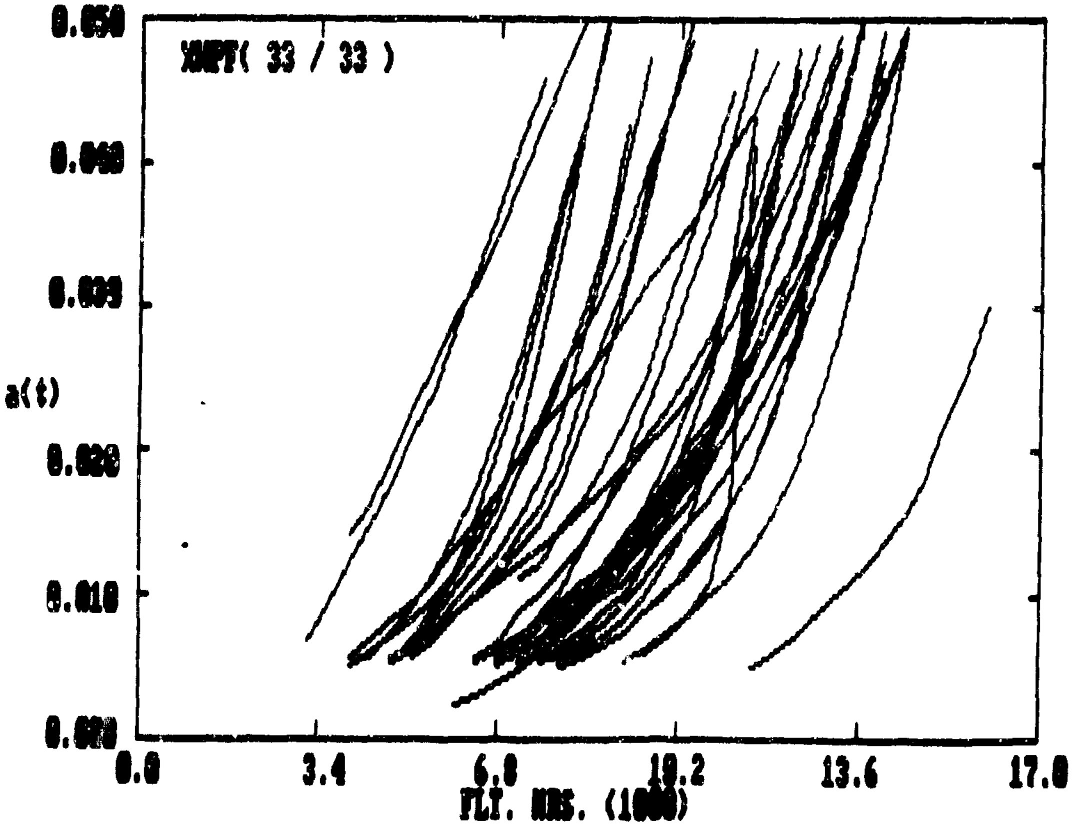

Figure F.4. a(t) Versus Flt. Hrs. for XWPF Data Set (AL-AU = 0.0"-0.05").

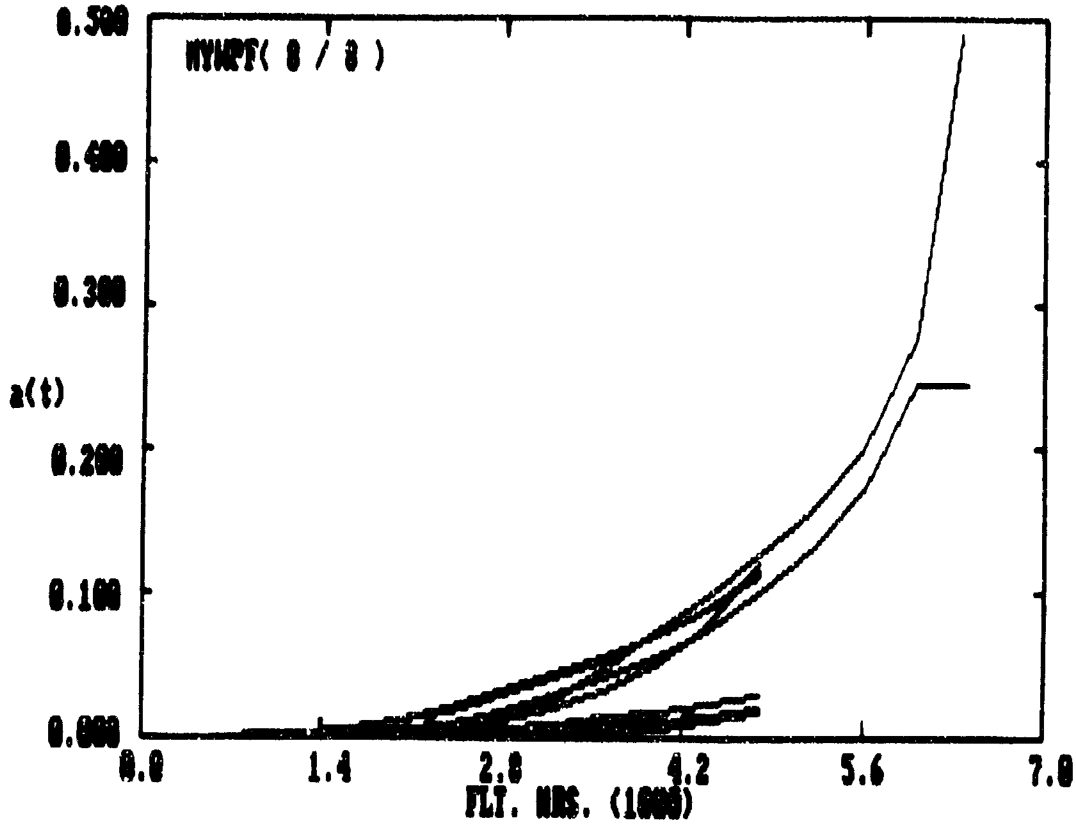

Figure F.5. a(t) Versus Flt. Hrs. for HYWPF Data Set (all the data).

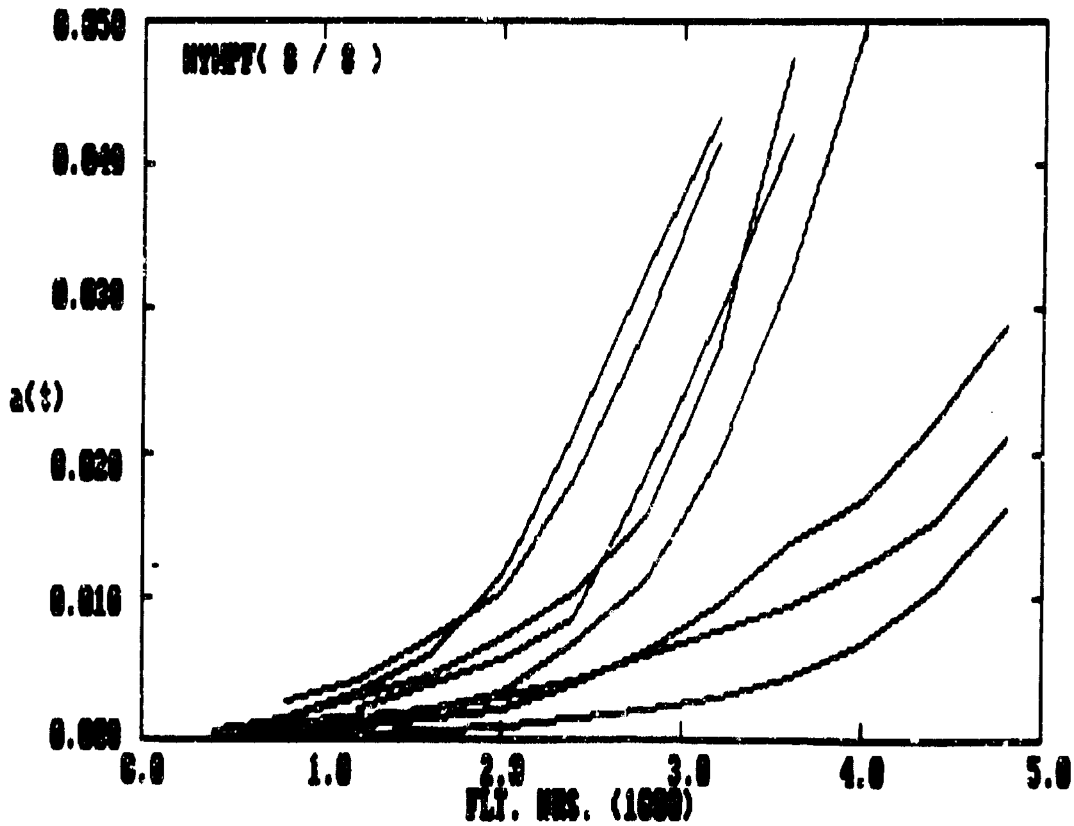

Figure F.6. a(t) Versus Flt. Hrs. for HYWPF Data Set (AL-AU = 0.0"-0.05").

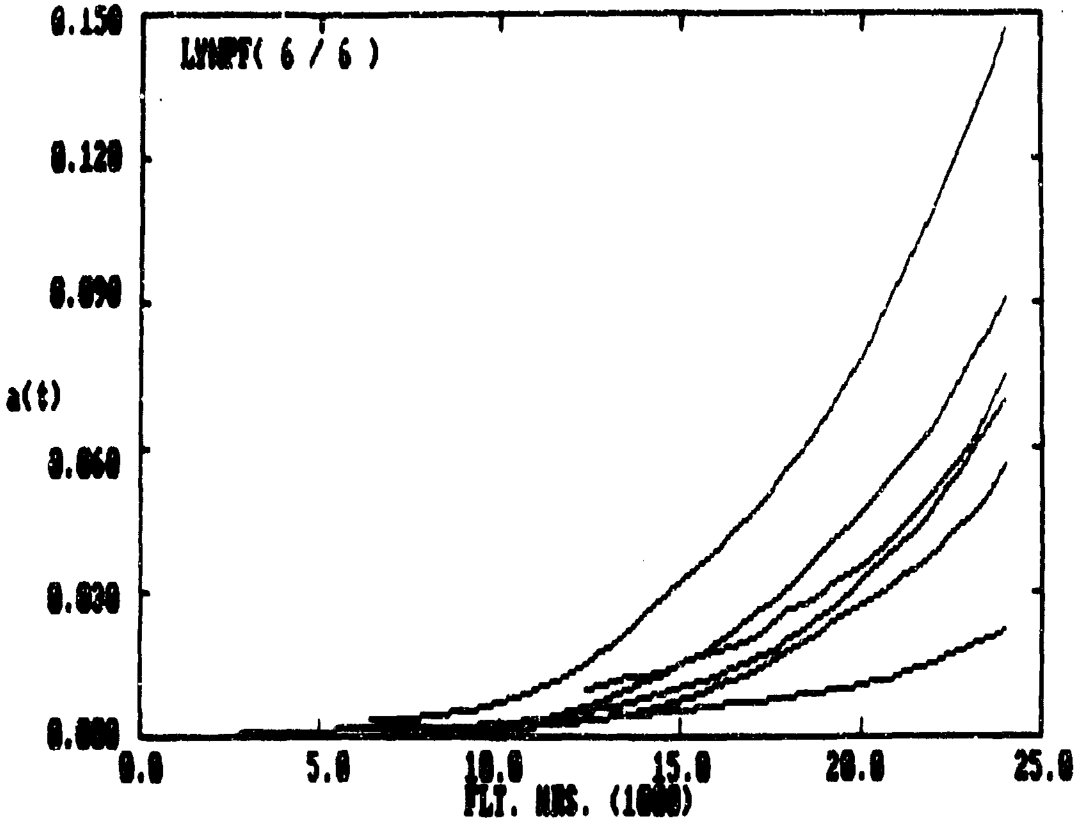

Figure F.7. a(t) Versus Flt. Hrs. for LYWPF Data Set (all the data).

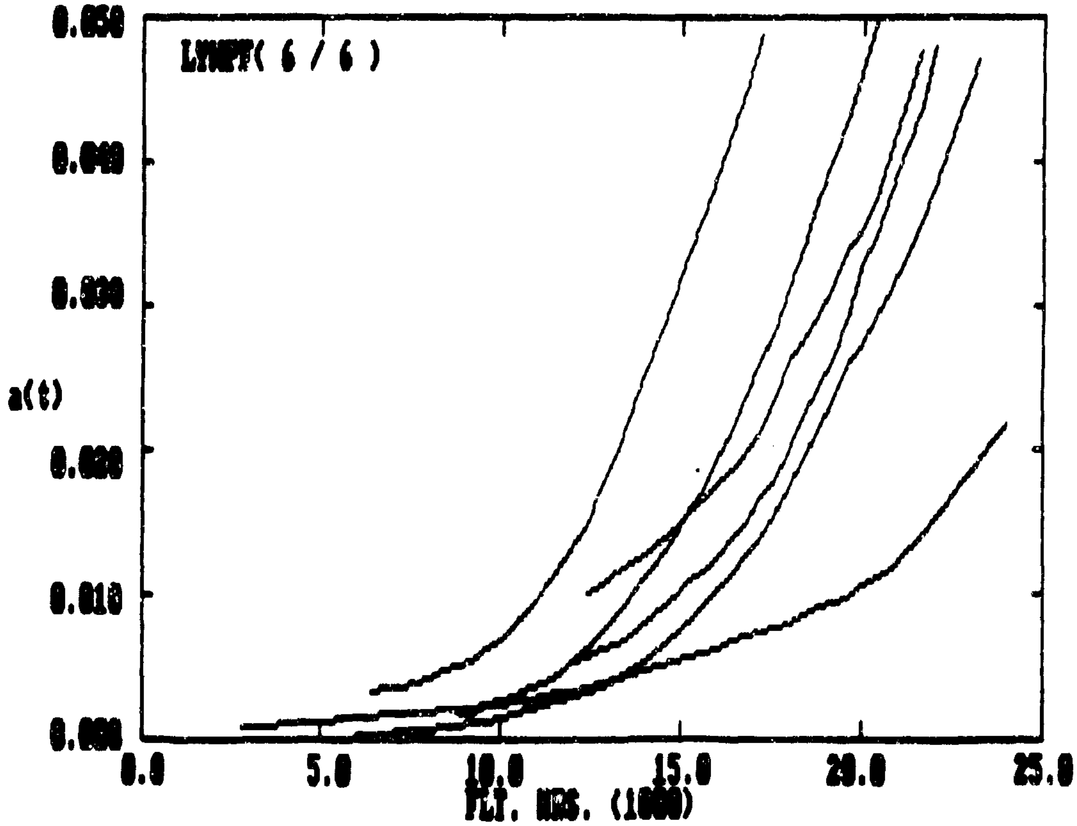

Figure F.8. a(t) Versus Flt. Hrs. for LYWPF Data Set (AL-AU = 0.0"-0.05").

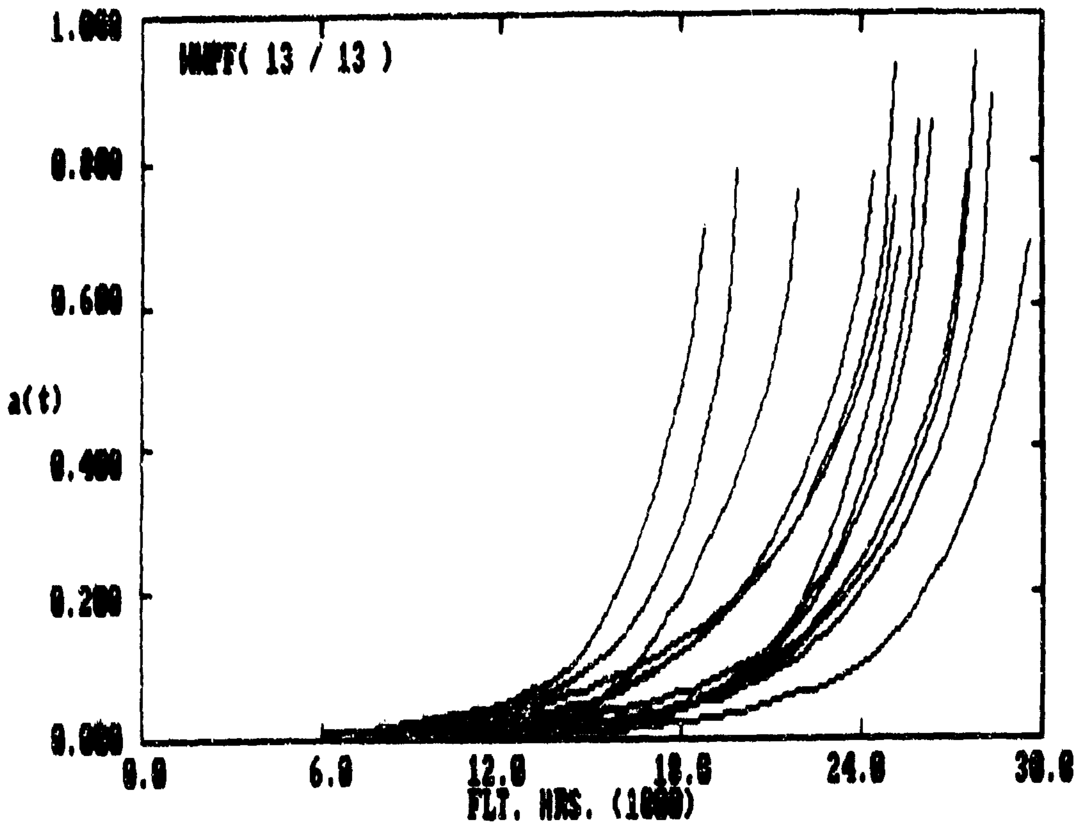

Figure F.9. a(t) Versus Flt. Hrs. for WWPF Data Set (all the data).

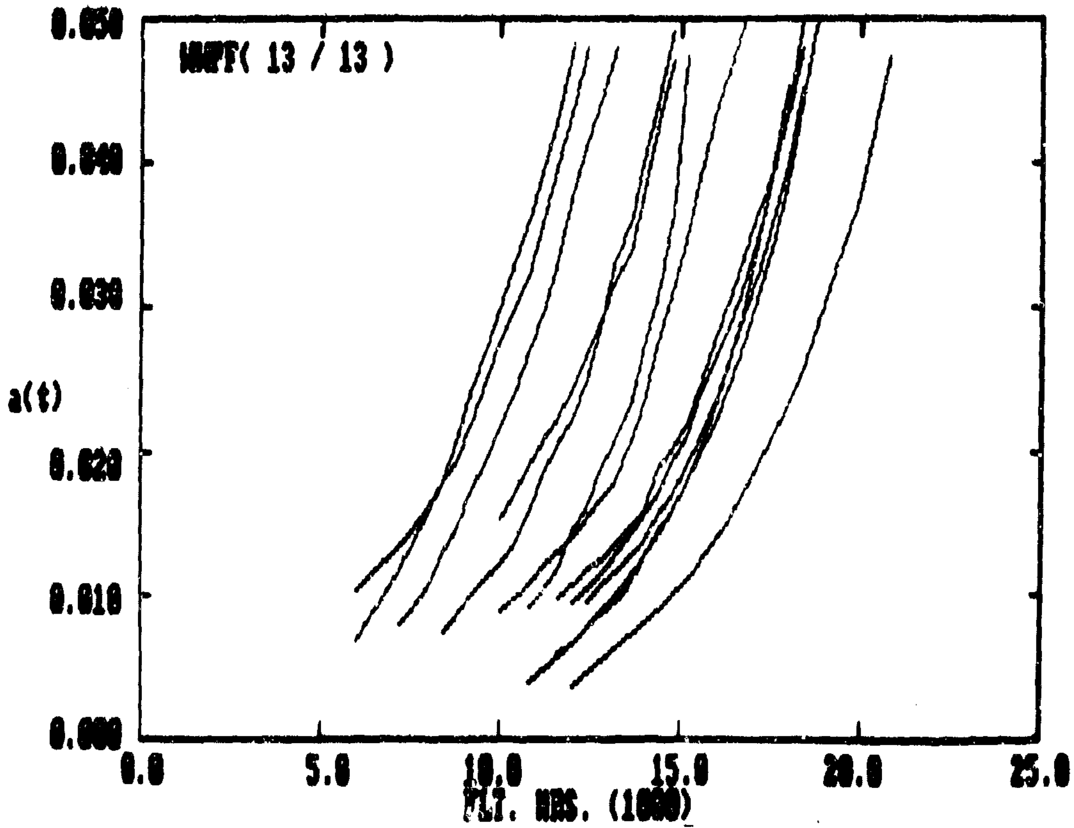

Figure F.10. a(t) Versus Flt. Hrs. for WWPF Data Set (AL-AU = 0.0"-0.05").

Table F.11. Sensitivity of Pooled Q, σ_z, Mean TTCI and Mean EIFS to AL-AU Range and Censored Data.

DATA SET	β	NO. CRACKS USED	AL-AU	DL-DU	Pooled Qx10^4	σ_z	a_0	MEAN TTCI	COV TTCI	① MEAN EIFS x 10^4	② MEAN EIFS x 10^4
NPF	1.0	32/33	.0085 - .0129	AL-AU	2.902	.143	.0129"	11364	.208	5.997	4.768
		32/33	0 - .0129	AL-AU	3.262	.232	.0129"	11364	.208	4.309	3.208
		27/33	.01 - .02	AL-AU	2.731	.182	.0129"	10717	.183	7.994	6.910
		28/33	.01 - .03	AL-AU	2.642	.178	.0129"	9903	.160	10.309	9.426
		18/33	.01 - .04	AL-AU	2.476	.184	.0129"	9611	.144	12.709	11.943
		6/33	.01 - .05	AL-AU	2.614	.264	.0129"	7873	.0929	16.774	16.474
		32/33	.01 - .05	AL-AU	2.376	.164	.0129"	11364	.208	10.125	8.669
KNPF	1.0	32/33	.0141 - .0299	.01 - .03	3.947	.337	.0299"	10431	.190	6.864	4.871
		32/33	0 - .0299	AL-AU	4.045	.218	.0299"	10431	.190	6.305	4.396
		30/33	.01 - .02	AL-AU	4.017	.279	.0299"	10592	.178	5.844	4.244
		30/33	.01 - .03	AL-AU	3.964	.305	.0299"	10592	.178	6.130	4.409
		30/33	.01 - .04	AL-AU	3.985	.312	.0299"	10592	.178	6.464	4.779
		30/33	.01 - .05	AL-AU	3.891	.371	.0299"	10592	.178	6.547	4.851
		32/33	.01 - .05	AL-AU	3.848	.363	.0299"	10431	.190	7.478	5.401
WNPF	1.0	13/13	.0154 - .03	AL-AU	2.795	.109	.03"	14539	.189	6.919	5.156
		13/13	.0154 - .04	AL-AU	2.749	.119	.03"	14539	.189	7.329	5.512
		13/13	.0154 - .05	AL-AU	2.726	.123	.03"	14539	.189	7.544	5.699
		13/13	.01 - .05	AL-AU	2.742	.119	.03"	14539	.189	7.394	5.569
		12/13	.01 - .02	AL-AU	2.819	.197	.03"	14674	.192	6.625	4.793
		12/13	.01 - .03	AL-AU	2.817	.124	.03"	14674	.192	6.638	4.887
		12/13	.01 - .04	AL-AU	2.806	.108	.03"	14674	.192	6.729	4.885
		12/13	.01 - .05	AL-AU	2.787	.109	.03"	14674	.192	6.890	5.024
		13/13	.01 - .05	AL-AU	2.742	.119	.03"	14539	.192	7.395	5.569
LYWPF	1.0	6/6	.01005 - .02181	AL-AU	2.329	.249	.02181"	10081	.175	4.886	3.234
		6/6	0 - .02181	AL-AU	2.345	.320	.02181"	10081	.175	3.982	3.142
		6/6	.01 - .02	AL-AU	2.331	.252	.02181"	10081	.175	4.073	3.223
		5/6	.01 - .03	AL-AU	2.404	.211	.02181"	16898	.112	4.207	3.753
		5/6	.01 - .04	AL-AU	2.293	.175	.02181"	16898	.112	5.021	4.528
		5/6	.01 - .05	AL-AU	2.191	.144	.02181"	16898	.112	5.910	5.379
		6/6	.01 - .05	AL-AU	2.140	.142	.02181"	10081	.112	5.558	4.552
HYWPF	1.0	8/8	.0026 - .0163	AL-AU	16.901	.244	.0163"	3286	.282	6.632	4.402
		8/8	0 - .0163	AL-AU	12.157	.210	.0163"	3286	.282	4.883	3.001
		7/8	.01 - .02	.01 - .03	10.135	.424	.0163"	3070	.254	9.336	7.259
		5/8	.01 - .03	AL-AU	13.220	.101	.0163"	2616	.123	5.595	5.121
		5/8	.01 - .04	AL-AU	12.625	.0453	.0163"	2616	.123	6.500	5.956
		5/8	.01 - .05	AL-AU	11.626	.0798	.0163"	2616	.123	8.339	7.786
		8/8	.01 - .05	AL-AU	9.969	.249	.0163"	3286	.123	8.705	6.159

TABLE F.12. Sensitivity of Mean EIFS to Data Censoring, AL-AU Range and Use of TTCI Extrapolations.

Data Set	β	No. Cracks Used	AL-AU	BL-BU	Pooled $\bar{Q}$ x10[4]	σ_z	w/Extrapolations: a_0 = .05** Mean EIFS x10[4]	No Extrapolations: a_0	No Extrapolations: MEAN EIFS x 10[4]	Crack No. Deleted
WPF	1.0	32/33	.0065-.0129	AL-AU	2.902	.143	4.315	.0129*	5.997	#6
		32/33	0 - .0129		3.242	.232	2.589		4.309	#6
		27/33	.01-.02		2.731	.182	6.396		7.994	#6, 19, 20, 21, 23, 29
		20/33	.01-.03		2.642	.178	8.930		10.309	#6, 13, 19, 20-24, 29-33
		18/33	.01-.04		2.476	.184	12.003		12.709	#6, 13, 17, 19-24, 26, 29-33
		6/33	.01-.05		2.614	.264	16.184		16.774	#5-9, 11-13, 15-33
		32/33	.01-.05		2.376	.164	9.699		10.125	#6
XWPF	1.0	32/33	.0141-.0299	.01-.03	3.947	.337	6.215	.0299*	6.864	#16
		32/33	0-.0299	AL-AU	4.045	.218	5.621		6.305	#16
		30/33	.01-.02		4.017	.279	5.432		5.844	#2, 16, 31
		30/33	.01-.03		3.964	.305	5.741		6.130	#2, 16, 31
		30/33	.01-.04		3.905	.312	6.106		6.464	#2, 16, 31
		30/33	.01-.05		3.891	.371	6.199		6.547	#2, 16, 31
		32/33	.01-.05		3.848	.363	6.881		7.478	#16
WWPF	1.0	13/13	.0154-.03	AL-AU	2.795	.109	6.822	.03**	6.919	Use all
		13/13	.0154-.04		2.749	.119	7.081		7.329	Use all
		13/13	.0154-.05		2.726	.123	7.323		7.544	Use all
		13/13	.01-.05		2.742	.119	7.154		7.394	Use all
		12/13	.01-.02		2.819	.197	6.321		6.625	#3
		12/13	.01-.03		2.817	.124	6.335		6.638	#3
		12/13	.01-.04		2.806	.108	6.437		6.729	#3
		12/13	.01-.05		2.787	.109	6.617		6.890	#3
		13/13	.01-.05		2.742	.119	7.155		7.395	Use all
LYWPF	1.0	6/6	.01005-.02181	AL-AU	2.329	.249	3.608	.02181	4.086	Use all
		6/6	0-.02181		2.345	.320	3.595		3.982	Use all
		6/6	.01-.02		2.331	.252	3.595		4.073	Use all
		5/6	.01-.03		2.404	.211	3.639		4.207	#1
		5/6	.01-.04		2.293	.175	4.638		5.021	#1
		5/6	.01-.05		2.191	.144	5.558		5.910	#1
		6/6	.01-.05		2.160	.142	5.287		5.558	Use all
XYWPF	1.0	8/8	.0026-.0163	AL-AU	10.991	.244	5.894	.0163**	6.632	Use all
		8/8	0-.0163	"	12.157	.210	3.833		4.883	Use all
		7/8	.01-.02	.01-.03	10.135	.424	9.121		9.336	#5
		5/8	.01-.03	AL-AU	13.228	.101	4.060		5.595	#4, 5, 7
		5/8	.01-.04		12.625	.0453	5.048		6.500	#4, 5, 7
		5/8	.01-.05		11.626	.0798	7.244		8.339	#4, 5, 7
		8/8	.01-.05		9.969	.249	8.621		8.705	Use all

sets and conditions shown in Table F.11. In one case, TTCI values were determined for $a_0 = 0.05"$ by either interpolation or extrapolation. In the other case, TTCI values were determined by interpolation for a selected reference crack size which "sliced through" all the data. Method 1, described in Fig. F.11, was used in this case.

The results for Part II are discussed in Section F.4, including comparisons with the results for Part I.

F.4 DISCUSSION

1. There's no significant difference in the resulting pooled Q, σ_z, and EIFS values based on either the modified secant or five-point incremental polynomial method for the uncensored FHQ data sets in the .01"-.05" crack size range considered, see results in Tables F.3 and F.4.

2. In most cases, equalizing or not equalizing the number of a(t)s in the AL-AU range does not significantly change the pooled Q and σ_z values. Larger differences are noted when all the data are used, as observed from Tables F.3 and F.4.

3. The AL-AU crack size range affects the pooled Q and σ_z values. For some data sets the effect of the AL-AU range on pooled Q and σ_z seems to be greater than others. In any case pooled Q and σ_z should be defined for a specified AL-AU range, see Table F.5.

4. Pooled Q and σ_z values computed using the preliminary method (based on da(t)/dts) were approximately the same as those based on the refined methods. For example, compare the results in Tables F.3 and F.4 with those results for the same AL-AU range in Table F.5. Since the refined method is simpler and more straight forward than the preliminary method

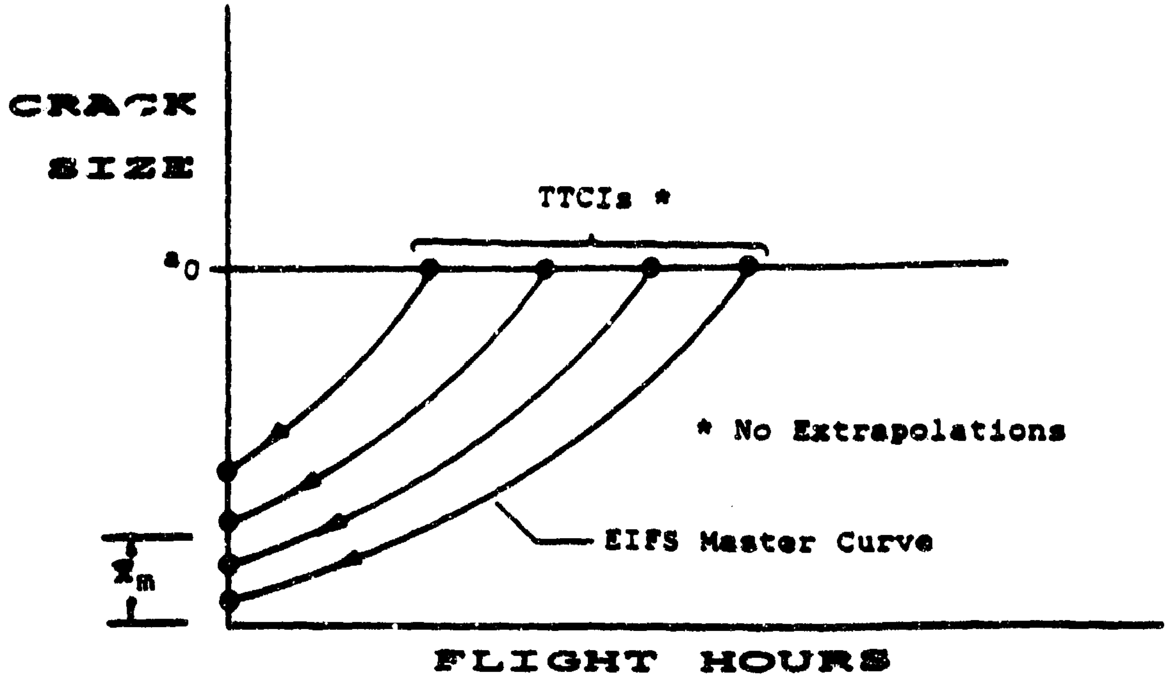

(a) Method 1--Use No TTCI Extrapolations and EIFS Master Curve

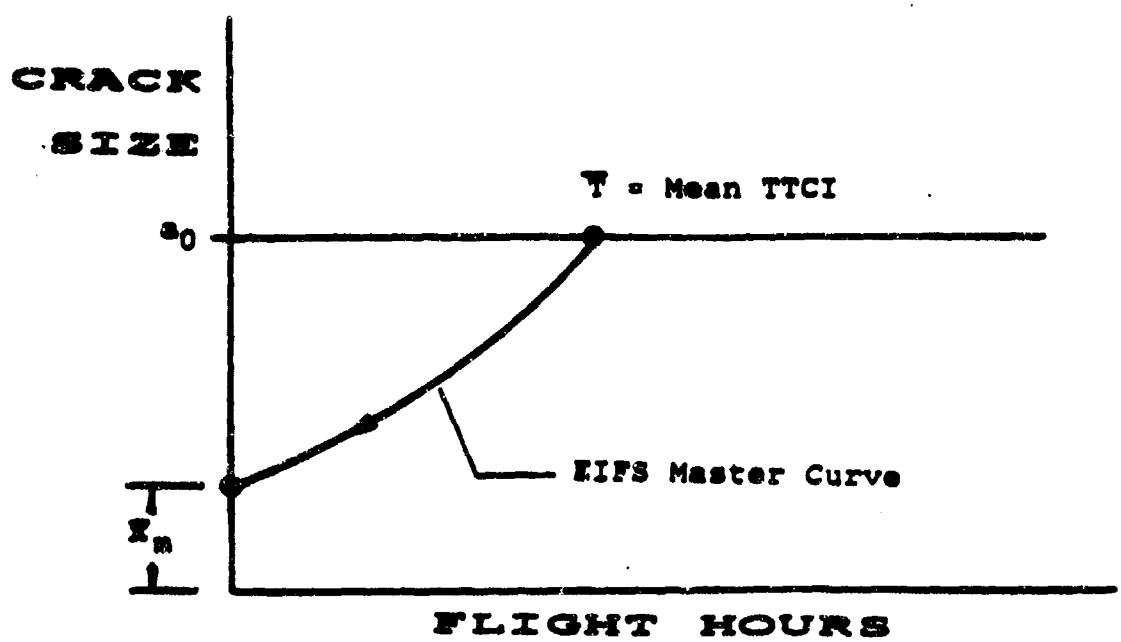

(b) Method 2--Use Mean TTCI and EIFS Master Curve

Figure F.11. Methods Considered for Determining the Mean EIFS for a Fractographic Data Set.

based on da(t)/dt data, it is recommended for durability analysis.

5. Pooled Q, σ_z, and Q_j statistics are shown in Tables F.7 and F.8 for the ADA data sets. Pooled Q and σ_z depend on the fractographic crack size range used. In particular, it appears that the AL-AU range has a bigger influence on σ_z than on pooled Q.

6. In Table F.10 the five fractographic data sets were surveyed to determine which cracks covered the selected AL-AU ranges. By far, the WPF data set contained more specimens with cracks that did not cover the designated AL-AU range than any of the other four data sets. For example, the WPF data set had only 6 specimens out of 33 that "covered" the .01"-.05" crack size range (i.e. .01"< a(t) > .05"). The other four data sets had the following number of specimens that covered the AL-AU = range: XWPF (30 out of 33), HYWPF (5 out of 8), LYWPF (5 out of 6) and WWPF (12 out of 13).

7. The fractographic plots shown in Fig. F.1 and F.10 are useful for quickly examining the character or behavior of the fractographic data sets. The durability software filename = "PLOT" can be effectively used to "zoom in" and study the fractographic data in desired crack size ranges. This tool should be used to screen fractographic results before being used in the durability analysis. Further details about the plotting tool are given in Volume V [5].

8. Conclusions about the sensitivity study summarized in Tables F.11 and F.12 are (1) the fractographic crack size range used (i.e. AL-AU) affects significantly pooled Q and σ_z values, (2) the variation in pooled Q and σ_z for different AL-AU ranges was greatest for the WPF data set, followed by the HYWPF data set, (3) "mixing and matching"

interpolated and extrapolated fractographic data can have a significant effect on the mean EIFS for a given data set (e.g., refer to results for the WPF data set), and (4) deleting fractographic results for an "abnormal fatigue cracks" can affect pooled Q, and the mean EIFS for a data set. It is important not to accept all fractographic results for durability analysis without screening the data first.

9. Mean EIFS values obtained using two different methods are summarized in Table F.12 for selected crack size ranges for five data sets. Conclusions are (1) Methods 1 and 2 do not give the same mean EIFS, (2) in all cases, mean EIFS values based on Method 1 were larger than those based on Method 2, (3) the mean EIFS is sensitive to the AL-AU crack size range used, and (4) the coefficient of variation for TTCI is fairly consistent for the selected AL-AU range for all five data sets.

APPENDIX G

STRAIN SURVEY FOR EVALUATING % BOLT LOAD TRANSFER

A strain survey was performed to determine the % bolt load transfer as a function of % load level for a double-reverse, dog-bone specimen (Fig. G.1). Experimental results from the strain survey are presented, evaluated, and discussed in this section. Objectives of the survey were to (1) estimate the actual % bolt load transfer and variations for a so-called "15% load transfer test specimen" and (2) provide a basis for comparing the predicted % bolt load transfer based on the service crack growth master curve (SCGMC) tuning studies (see Appendix D).

Two axial-type strain gages were mounted on the outer surface of the dog-bone specimen (i.e., Durability specimen #120), as shown in Fig. G.1. Gage Number 1 was located on the surface along the centerline of the specimen on the "big lug side". In a similar manner, Gage Number 2 was located on the "small lug side". Durability Specimen #120 dimensions were: width = 3.0085 in and total thickness of specimen (two pieces) = 0.3912".

The strain survey was conducted using a maximum ram load of 45.9K (100% load). Strain readings were taken in 20% load increments, starting at 0% up to a 100% load level. Following the strain gage readings at the 100% load level, the ram load was reduced to zero and the strain gages were read. Strain gage readings are summarized in Table G.1.

The strain survey results were used to determine the amount of bolt load transfer -- defined as the ratio of the bolt load (P_s) and the input load to the joint. Using this definition, two different bolt load transfers can be obtained, depending on which side of the specimen is considered.

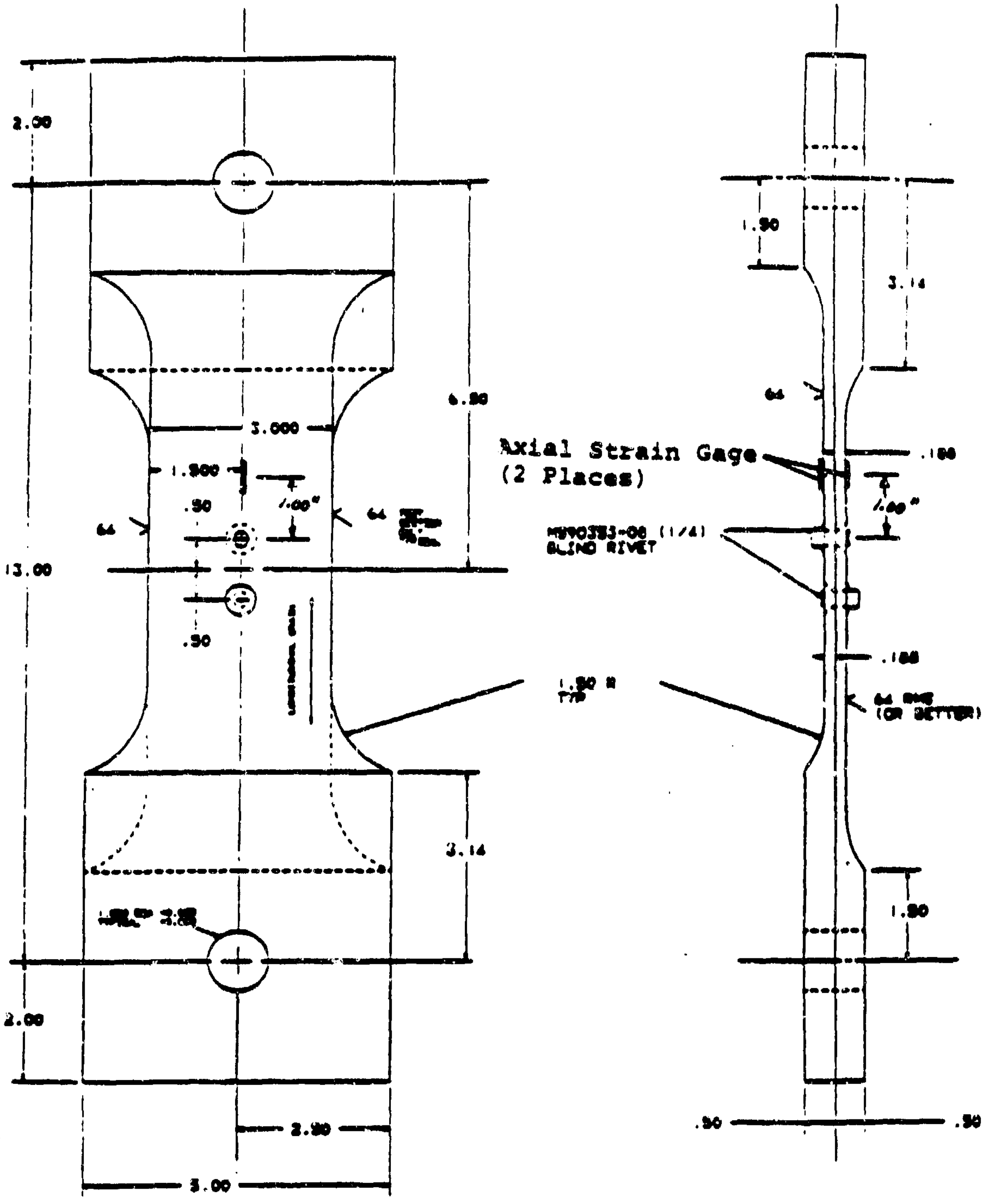

1. Material: 7475-T7351 Aluminum
2. Match drill holes using modified Winslow Spacematic drill without deburring
3. Drill and install MS90353-08 rivets per M198.

Figure G.1. Double-Reverse Dog-Bone Specimen (15% Bolt Load Transfer) with 3.00" Width.

TABLE G.1. Summary of Strain Survey Readings for Durability Specimen 120.

% LOAD	STRAIN READINGS (μ IN.)	
	ϵ_1	ϵ_2
0	0	0
20	845	594
40	1656	1228
60	2434	1910
80	3174	2620
100	3968	3417
0	0	0

For example, refer to the specimen freebodies shown in Fig. G.2 (detail "A" and "B"). For this reason, the amount of bolt load transfer was determined three ways: (1) based on detail "A" (P_s/P_1), (2) based on detail "B" ($2P_S/P_T$), and (3) based on results for detail "A" and "B".

Results of the bolt load transfer analysis, including the basic equations used, are summarized in Table G-2. Plots of the bolt load transfer variations as a function of the total applied load as shown in Fig. G.3. Three plots are shown in Fig. G.3, i.e., for the large and small lug side and the average result.

In Fig. G.3 it is interesting to note that the amount of bolt load transfer (based on the strain survey results): (1) varies depending on the total applied load to the specimen, (2) decreases as the total applied is increased, and (3) compares very well with the "15% LT speciman design" at the small % total specimen load level. Intuitively, it was expected, due to fastener hole-fit variations, that the amount of bolt load transfer would increase as the total applied load was increased.

The % bolt load transfer versus % total specimen load, shown in Fig. G.3, is based on a single specimen. To assess the variation in the % bolt load transfer, as a function of the % total specimen load, several "replicate specimens" would have to be tested. In any case, the % bolt load transfer for the "15% load transfer specimen" is expected to vary depending on fastener hole-fit, geometric variations and applied load level.

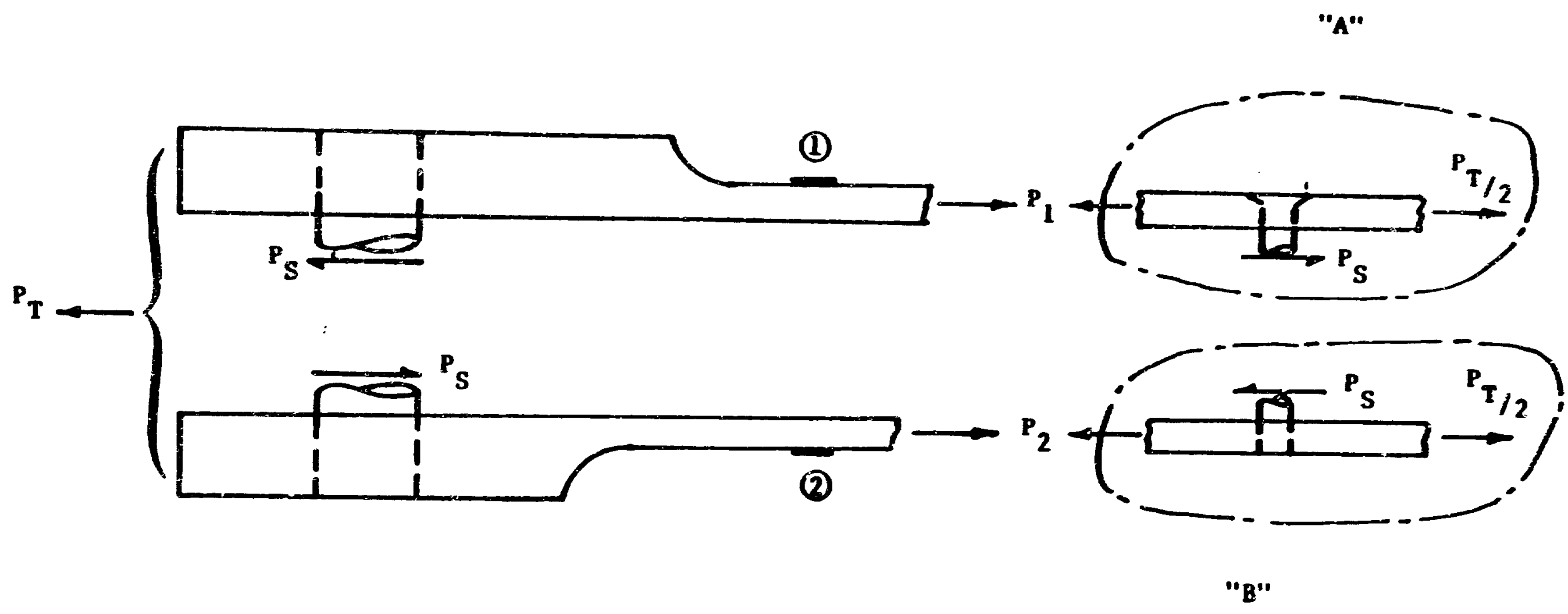

Figure G.2. **Freebodies for Double-Reverse Dog-Bone Type Specimen.**

TABLE G.2. Summary of Strain Survey Results and Evaluation of Bolt Load Transfer.

% LOAD	ϵ_1	ϵ_2	P_T	P_1 (1)	P_2 (2)	P_S (3)	P_S/P_1 (4)	$2P_S/P_T$ (5)	(6) AVE LT
	(μIN.)		(KIPS)						
0	0	0	0	0	0	0	--	--	--
20	845	594	9.18	5.39	3.79	± 0.8	0.148	0.174	0.161
40	1656	1228	18.36	10.54	7.82	± 1.36	0.129	0.148	0.139
60	2434	1910	27.54	15.43	12.11	± 1.66	0.108	0.120	0.114
80	3174	2620	36.72	20.12	16.60	± 1.76	0.087	0.096	0.092
100	3968	3417	45.9	24.66	21.24	± 1.71	0.069	0.074	0.072
0	0	0	0	0	0	0	--	--	--

Notes:

(1) $P_1 = P_T\left(\frac{\epsilon_1}{\epsilon_1 + \epsilon_2}\right)$

(2) $P_2 = P_T - P_1$

(3) $\left\{ \begin{array}{l} P_S = P_1 - P_{T/2} = P_{T/2} - P_2 \\ P_S = P_{T/2}\left(\frac{\epsilon_1 - \epsilon_2}{\epsilon_1 + \epsilon_2}\right) \end{array} \right.$

(4) $P_{S/P_1} = \frac{\epsilon_1 - \epsilon_2}{2\,\epsilon_1}$ (Ref. Fig. G.2; Detail "A")

(5) $2P_{S/P_T} = \frac{\epsilon_1 - \epsilon_2}{\epsilon_1 + \epsilon_2}$ (Ref. Fig. G.2; Detail "B")

(6) AVE LT $= \frac{1}{2}\left(P_{S/P_1} + 2P_{S/P_T}\right) = P_S\,(P_T + 2P_1)/2P_1\,P_T$

$$= \frac{(\epsilon_1 - \epsilon_2)(3\epsilon_1 + \epsilon_2)}{4\epsilon_1\,(\epsilon_1 + \epsilon_2)}$$

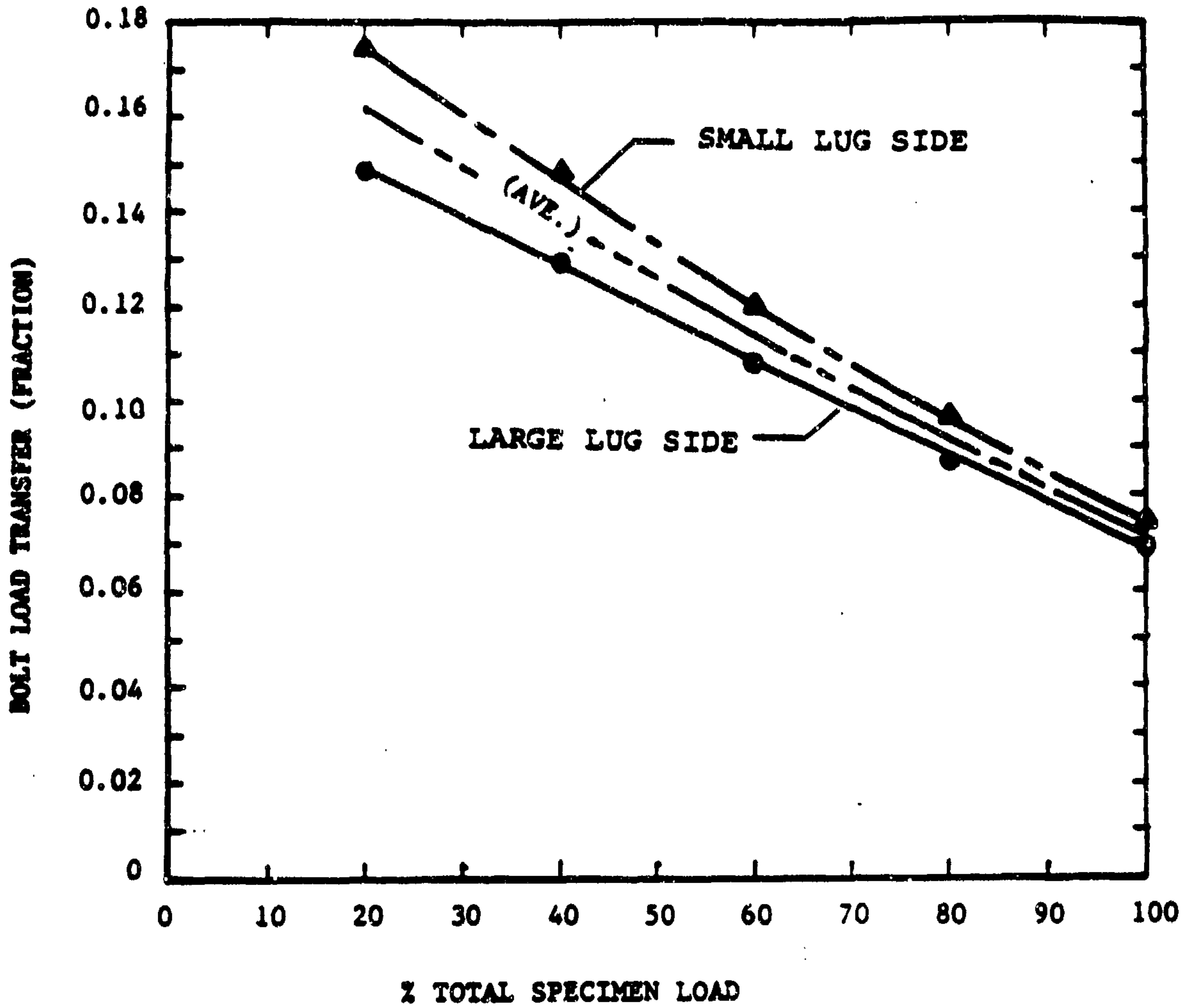

Figure G.3. Bolt Load Transfer (Fraction) Versus Specimen % Load.

APPENDIX H

TIME-TO-GIVEN-CRACK-SIZE (TTGCS) AND TIME-TO-FAILURE (TTF) STATISTICS

TTGSC and TTF statistics for the 3.0" wide specimens tested under this program (Volume III) are summarized in this section. All specimens considered were made from 7475-T7351 aluminum (1/2" plate).

The following information is presented for each data set:

	TTGSC or TTF
o Mean	
o Standard deviation	
o Coefficient of variation	
o Maximum and minimum values in data set	
o No. specimen reflected in the analysis	

The above statistics for TTGSC and TTF are summarized in Tables H.1 and H.2 for fighter and bomber load spectra, respectively. Given crack sizes of x_1 = 0.01", 0.03", 0.05", 0.1", 0.5", 0.75" and 1.0" are considered for the TTGSC.

The results shown in Tables H.1 and H.2 are based on the durability analysis software (filename = "QSZAT") documented in Volume V [5]. Fractographic data was extrapolated if necessary to obtain the TTGSC value for the selected given crack size, x_1. The fractographic data was not screened prior to the statistical analysis.

Coefficient of Variation (COV) values for comparable fighter and bomber data sets (i.e., same specimen configuration and type fastener hole) are summarized in H.3 for six data sets. COV values based on TTGCS for three different crack sizes (i.e., x_1 = 0.05", 0.1" and 0.5") are shown as

Table H.1. Summary of TTGCS and TTF Statistics for Advanced Durability Data Sets (Fighter Load Spectra)

DATA SETS	ITEM	TTGCS STATISTICS (4) GIVEN CRACK SIZE x_i .01"	.03"	.05"	.1"	.5"	.75"	1.0"	(4),(5) TTF STATISTICS
[illegible]	MEAN (FLT. HRS)	10580	14536	16452	18915	24143	25086	25697	25086
	STD. DEV.	2678	2745	2678	2768	3016	3079	3062	3092
	COV	.253	.189	.163	.146	.125	.123	.119	.123
	MAX. (FLT. HRS)	14800	18986	21058	24040	28825	29834	30546	29516
	MIN. (FLT. HRS)	5809	10000	12091	14372	18112	18969	19606	19884
	NO. SPECIMEN	23							
[illegible]	MEAN (FLT. HRS)	31933	34412	35777	37702	46372	48773	50137	49807
	STD. DEV.	3714	4256	4679	5007	7017	7546	7788	7970
	COV	.116	.124	.131	.133	.151	.155	.155	.160
	MAX. (FLT. HRS)	37501	39738	41401	42886	54432	57493	59170	59282
	MIN. (FLT. HRS)	27274	28999	30018	31632	37700	38851	39466	38792
	NO. SPECIMEN	4							
[illegible]	MEAN (FLT. HRS)	16265	17759	18579	19897	24510	25609	26220	25849
	STD. DEV.	6372	5989	5933	5870	6139	6205	6260	6123
	COV	.392	.337	.319	.295	.250	.242	.239	.237
	MAX. (FLT. HRS)	24605	25835	26677	27778	32910	33815	34455	33632
	MIN. (FLT. HRS)	5860	7683	8476	9780	13004	13805	14080	[illegible]
	NO. SPECIMEN	8							
[illegible]	MEAN (FLT. HRS)	13346	14539	15335	16815	21814	22712	23320	22686
	STD. DEV.	3381	2962	2805	2680	2926	2997	3049	3056
	COV	.253	.204	.183	.159	.134	.132	.131	.131
	MAX. (FLT. HRS)	17047	17661	18191	19773	26645	27173	27970	27235
	MIN. (FLT. HRS)	4146	6194	7490	9519	14541	15365	15863	15678
	NO. SPECIMEN	14							
[illegible]	MEAN (FLT. HRS)	9401	13944	16365	19651	27464	28711	29420	27880
	STD. DEV.	3776	4204	4404	4624	6447	6924	7256	5906
	COV	.402	.302	.269	.235	.235	.241	.246	.211
	MAX. (FLT. HRS)	16836	21837	24232	27547	40645	44345	46487	36480
	MIN. (FLT. HRS)	2739	6275	8448	11503	15874	16403	16606	16400
	NO. SPECIMEN	15							13 (6)
[illegible]	MEAN (FLT. HRS)	(7)	10723	11900	13977	20302	[illegible]	21877	21385
	STD. DEV.	(7)	5577	5421	5523	6560	6773	6937	6788
	COV	(7)	.520	.456	.395	.323	.318	.317	.317
	MAX. (FLT. HRS)	(7)	24854	25544	27085	31721	33196	34220	33208
	MIN. (FLT. HRS)	(7)	4107	4595	5957	10958	11613	11766	11606
	NO. SPECIMEN	14							
[illegible]	MEAN (FLT. HRS)	(7)	3369	4163	6047	10406	11006	11445	10799
	STD. DEV.	(7)	1589	1883	2100	2883	3002	3048	2981
	COV	(7)	.472	.452	.347	.277	.273	.266	.276
	MAX. (FLT. HRS)	(7)	6721	7892	9781	16031	16856	17485	16643
	MIN. (FLT. HRS)	(7)	1551	1562	3283	5649	5763	5993	5616
	NO. SPECIMEN	14							

Notes:
(1) Data Sets described in Section II.
(2) 7475-T7351 aluminum
(3) Fractographic Data from Ref. 2.
(4) Fractographic results were extrapolated (where necessary to obtain TTGCS values for the selected crack size, x_i . Such extrapolations were made without considering the time-to-failure (TTF) limitations.
(5) Some TTGCS statistics for larger x_i values are not compatible with the TTF results because of (4).
(6) All specimens tested were used to obtain TTGCS statistics but two specimens in this data set were not tested to failure due to testing problems.
(7) Statistics not computed for this x_i
(8) Used fractographic results for the largest fatigue crack per specimen.

Table H.2. Summary of TTGCS and TTF Statistics for Advanced Durability Data Sets (Bomber Load Spectra)

DATA SET	ITEM	TTGCS STATISTICS (4) GIVEN CRACK SIZE x_1							TTF Statistics
		.01"	.03"	.05"	.1"	.5"	.75"	1.0"	
WWPB	MEAN (FLT. HRS)	21347	23847	25320	27703	35154	36623	37740	36761
	STD. DEV.	5887	4972	4619	4798	4723	4626	4563	4310
	COV	.276	.209	.190	.173	.134	.126	.121	.117
	MAX. (FLT. HRS)	28916	30299	31248	32663	41824	43499	44826	43664
	MIN. (FLT. HRS)	11169	12291	13156	15241	24047	26542	28568	28051
	NO. SPECIMEN	12							
WB1	MEAN (FLT. HRS)	33606	35899	37194	39445	47047	48662	49825	47242
	STD. DEV.	10108	9056	8685	8191	7495	7436	7511	7961
	COV	.301	.252	.234	.208	.159	.154	.151	.159
	MAX. (FLT. HRS)	51520	52964	53718	55217	59596	60687	61460	59020
	MIN. (FLT. HRS)	14386	23079	27158	29781	37410	38341	39153	36408
	NO. SPECIMEN	13							
WWNPB	MEAN (FLT. HRS)	22694	24062	26335	29347	40517	42631	43776	43418
	STD. DEV.	5528	5363	5506	5684	7648	8126	8082	8194
	COV	.244	.216	.209	.194	.189	.191	.185	.189
	MAX. (FLT. HRS)	33822	35514	37608	39990	53773	55122	56302	55677
	MIN. (FLT. HRS)	15298	16698	17107	18180	24516	26119	27758	27830
	NO. SPECIMEN	15							
WABO3R4	MEAN (FLT. HRS)	3039	4002	5980	7940	14137	15246	16133	14814
	STD. DEV.	1167	1538	1670	1997	2635	2811	2942	2648
	COV	.384	.320	.279	.252	.186	.184	.182	.179
	MAX. (FLT. HRS)	5359	7580	9236	12475	19492	20863	22415	19815
	MIN. (FLT. HRS)	1425	2814	3764	5055	9550	10868	11956	11486
	NO. SPECIMEN	15							

NOTES:
(1) **Data sets described in Section II**
(2) 7475-T7351 Aluminum.
(3) Ref. AFWAL-TR-86-3017, Vol. III (Fractographic Test Data)
(4) Fractographic results were extrapolated (where necessary) to obtain TTCI Values for the selected ref. crack size, a_0. Such extrapolations were made without considering the time-to-failure (TTF) limitations.
(5) Some TTCI statistics for larger a_0 values are not compatible with the TTF results because of (4).
(6) All specimens tested were used to obtain TTCI statistics but 2 specimens in this data set were not tested to failure due to testing problems.
(7) Statistics not computed for this a_0.
(8) Used fractographic results for the largest fatigue crack per specimen.

TABLE H.3. Coefficient of Variation (COV) Comparisons for Fighter and Bomber Data Sets.

DATA SET	NO. SPECIMENS	COEFFICIENT OF VARIATION (COV)				FASTENER HOLE	σ (ksi)	% LT
		TTGSC			TTF			
		x_0 = .05"	x_1 = .1"	x_1 = .5"				
WWPF	13	.163	.146	.125	.123	SB	34	0
WWPB	12	.190	.173	.134	.117	SB	34	0
WFI	15	.269	.235	.235	.211	CSK	34	0
WBI	13	.234	.208	.159	.159	CSK	36	0
WAFXHR4	14	.452	.347	.277	.276	CSK	40.8	15
WABXHR4	15	.279	.252	.186	.179	CSK	40.8	15

well as COVs based on the time-to-failure (TTF). These results were obtained from Tables H.1 and H.2.

In Table H.3 it is interesting to note that (1) the COVs are very consistent for comparable fighter and bomber data sets for the same fastener hole type, (2) the COV values, based on TTGCS, decrease as x_1 increases, (3) as x_1 increases, the resulting COV values approach the COV values based on TTF, (4) COVs are smaller for straight-bore fastener holes than for countersunk fastener holes, (5) COVs are larger for 15% bolt load transfer specimens than for no load transfer type specimens, and (6) larger differences in the COVs are observed for the 15% bolt load transfer specimens for fighter and bomber data sets than for comparable no load transfer type specimens.

APPENDIX I

EVALUATION OF DETERMINISTIC AND STOCHASTIC-BASED EIFSs FOR STRAIGHT-BORE FASTENER HOLES

The purpose of this section is to (1) demonstrate three variations of a deterministic crack growth method and one stochastic crack growth method for determining EIFSs, (2) compute deterministic and stochastic-based EIFSs and EIFS statistics for a selected straight-bore hole fractographic data set, and (3) compare and discuss the EIFS results.

The investigation was conducted as follows: Fractographic results for the "WPF" data set from the "Fastener Hole Quality" (FHQ) program [3] was used to determine the deterministic and stochastic-based EIFSs. The WPF data set is described in Table F.1 and specimen details are shown in Fig. 4. Clearance-fit bolts (i.e., NAS 6204-08) were installed in the fastener hole of each specimen.

Methods for determining deterministic and/or stochastic-based EIFSs are given in Appendix E of Volume I [1]. Three methods for determining deterministic-based EIFSs are described in Fig. I.1. The method used to determine the stochastic-based EIFSs is conceptually described in Fig. I.2. Essential equations for computing EIFS, denoted by a(0), are summarized in the following.

Expressions for three different method variations for determining a deterministic-based EIFS for a given fatigue crack are given in Eqs. I-1 through I-3. The following notations are used: $a_j(0)$ = EIFS for the jth fatigue crack in a fractographic data set, $a_j(t_k)$ = kth crack size for the jth fatigue crack at service time t_k in the AL-AU crack size range, Q = "pooled Q" or Q_i value for the ith fractographic data set (see Eq. 6), a_0 = reference crack size for TTCIs, τ = service time to reach crack size a_0, $X_k = t_k$, $Y_k = \ln a_j(t_k)$

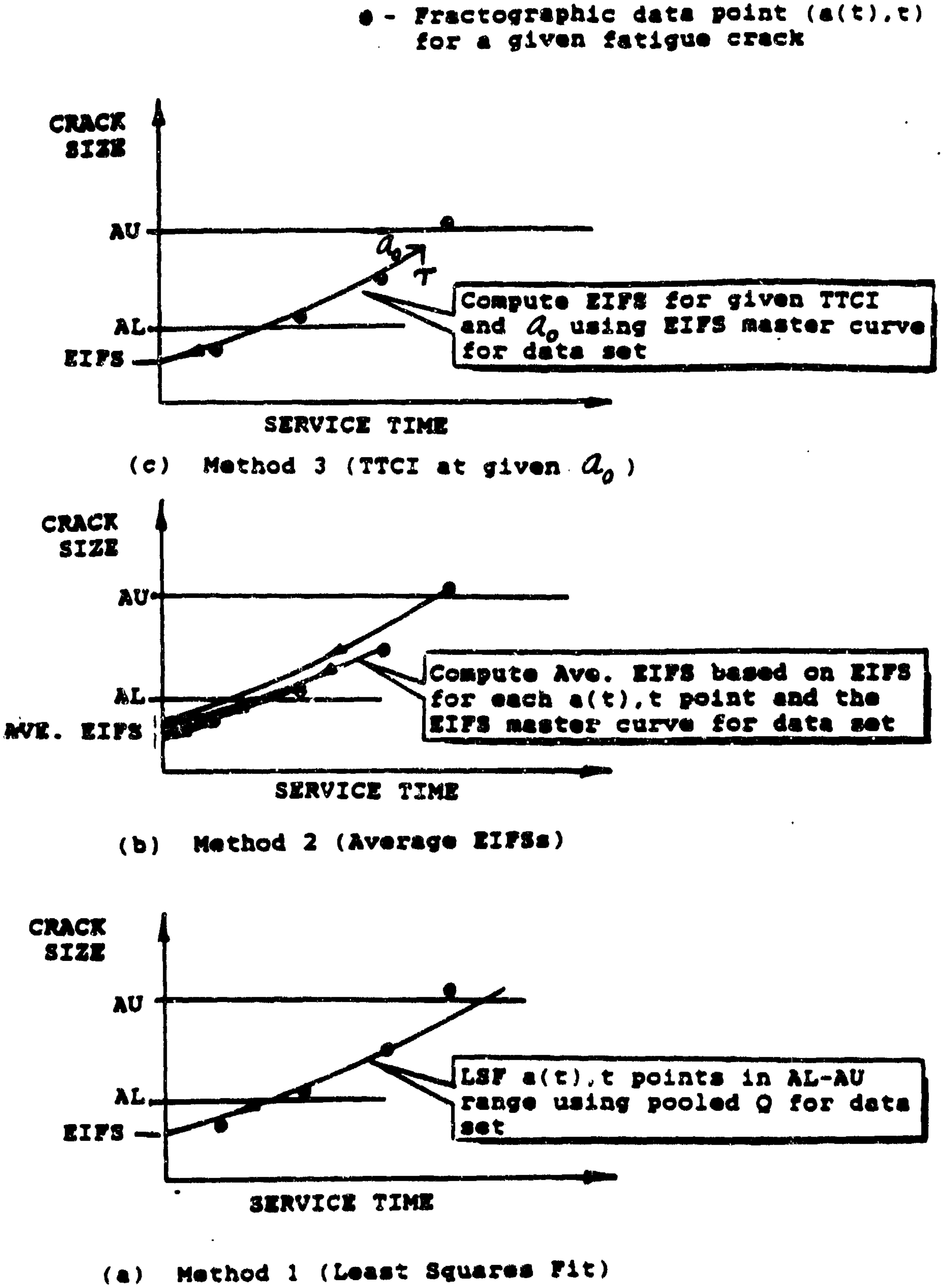

Figure I.1. Different Methods for Computing Deterministic-Based EIFSs.

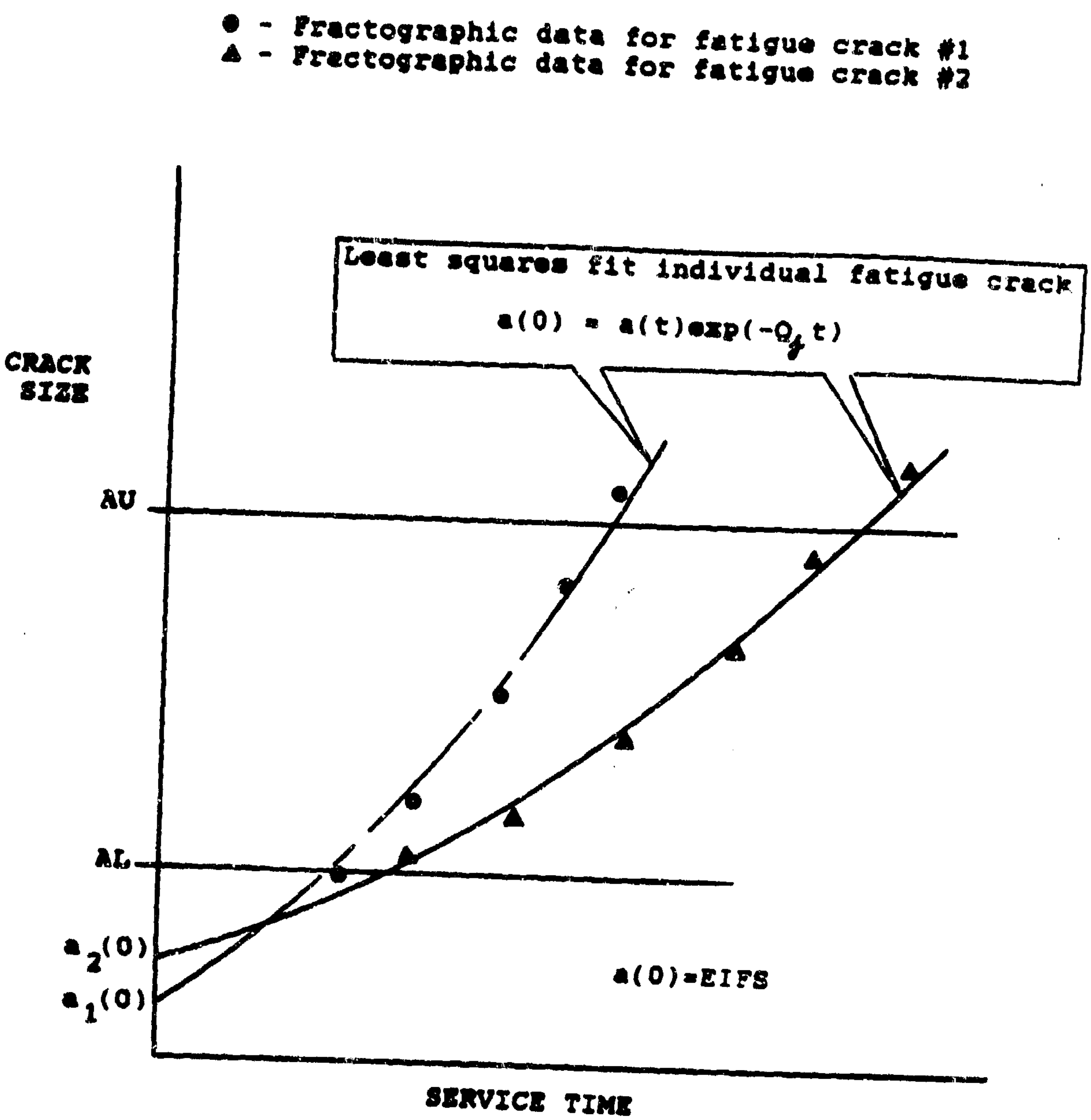

Figure I.2. Method for Computing Stochastic-Based EIFSs.

and N_j = number of pairs $[a_j(t_k), t_k]$ in the AL-AU range. These notations are slightly different than those used in the original derivation in Volume I [1]. Notations were changed herein to further clarify the terms used and to be consistent with the notations reflected in the durability design handbook [21].

Method 1 (Least Squares Fit)

$$a_j(0) = \text{EIFS} = \exp\left\{\frac{\sum_{k=1}^{N_j} Y_k - Q\sum_{k=1}^{N_j} X_k}{N_j}\right\} \tag{I-1}$$

Method 2 (Average EIFS)

$$a_j(0) = \text{EIFS} = \frac{1}{N_j}\sum_{k=1}^{N_j} a_j(t_k)\exp(-Qt_k) \tag{I-2}$$

Method 3 (TTCI at Given a_0)

$$a_j(0) = \text{EIFS} = a_0\exp(-Q\tau) \tag{I-3}$$

Stochastic-Based EIFS Method

An expression for determining stochastic-based EIFS is given in Eq. I-4 [1].

$$a_j(0) = \text{EIFS} = \exp\left\{\frac{\sum_{k=1}^{N_j} Y_k - Q_j\sum_{k=1}^{N_j} X_k}{N_j}\right\} \tag{I-4}$$

All terms in Eq. I-4 are the same as those defined in Eq. I-1 except Q_j = crack growth rate parameter for the jth fatigue crack (see Eq. 5).

EIFS and EIFS statistics (mean, standard deviation and coefficient of variation) were determined for both the deterministic and stochastic crack growth approaches using the WPF data set (uncensored). Results are summarized in Table I.1. The deterministic-based EIFSs were determined using Eqs. I-1 through I-3. A "pooled Q" value of 2.379×10^{-4} for the data set, based on Eq. F-5 and the modified secant method [27], was obtained using fractographic results in the AL-AU = 0.01" through 0.05" crack size region. The stochastic-based EIFSs were determined using Eq. I-4.

Fractographic results for 33 fatigue cracks were utilized for this investigation. EIFSs are ranked in descending order for the deterministic and stochastic approaches in Table I.1. Results are presented in a form for making direct comparisons. Similar EIFS studies have been reported for both straight-bore and countersunk fastener hole data sets [13-15].

The following conclusions are based on the results of Table I.1 and the experience gained during the course of this program.

1. Either Method 1, 2, or 3 can be used to determine deterministic-based EIFSs. However, Method 3 (i.e., TTCI for given time) is recommended for durability analysis because it is simpler, more convenient to implement and has comparable accuracy (except COV is slightly higher than for Methods 1 and 2) with the other two methods.

TABLE I.1. Comparison of Deterministic and Stochastic Based EIFSs and Statistics for WPF Data Set.

I	I/(N+1)	DETERMINISTIC-BASED EIFSs (IN.)			SCGA EIFSs (IN.)
		METHOD 1	METHOD 2	METHOD 3	
1	.029	.00596	.00598	.00655	.00398
2	.059	.00295	.00299	.00389	.00353
3	.088	.00234	.00235	.00206	.00244
4	.118	.00223	.00223	.00198	.00241
5	.147	.00199	.00199	.00185	.00189
6	.176	.00179	.00180	.00175	.00187
7	.206	.00164	.00165	.00163	.00182
8	.235	.00125	.00126	.00108	.00147
9	.265	.00123	.00124	.00107	.00139
10	.294	.00118	.00119	.00106	.00133
11	.324	.00113	.00113	.00104	.00109
12	.353	.00107	.00107	.00104	.00105
13	.382	.00103	.00103	.00101	.00105
14	.412	.00102	.00102	.000985	.00103
15	.441	.00100	.00100	.000958	.00102
16	.470	.000997	.000997	.000954	.00100
17	.500	.000994	.000997	.000908	.000962
18	.529	.000975	.000975	.000889	.000946
19	.559	.000974	.000975	.000866	.000713
20	.588	.000751	.000751	.000751	.000656
21	.618	.000743	.000743	.000744	.000628
22	.647	.000639	.000641	.000732	.000624
23	.676	.000633	.000633	.000653	.000582
24	.706	.000629	.000629	.000649	.000534
25	.735	.000558	.000559	.000455	.000523
26	.765	.000509	.000509	.000439	.000494
27	.794	.000501	.000501	.000418	.000486
28	.824	.000493	.000494	.000389	.000483
29	.853	.000448	.000448	.000387	.000459
30	.882	.000434	.000434	.000349	.000387
31	.912	.000374	.000374	.000335	.00038[illegible]
32	.941	.000356	.000356	.000330	.000[illegible]
33	.970	.000293	.000293	.000259	.000218
Mean EIFS		.00119	.00119	.00117	.00115
Std. Dev. EIFS		.00106	.00107	.00119	.000889
COV EIFS		.897	.899	1.029	.776

2. The stochastic-based EIFSs had a slightly smaller mean, standard deviation and COV than the comparable results for the deterministic-based EIFS.

3. As a result of extensive investigations conducted [12-15,17,42], the deterministic-based EIFS is recommended for durability analysis.

APPENDIX J

DEMONSTRATION OF PROBABILISTIC-BASED DURABILITY ANALYSIS METHOD FOR METALLIC AIRFRAMES

J. N. Yang[1], S. D Manning[2], A. Akbarpour[1], M. E. Artley[3]

Abstract

A probabilistic-based durability analysis method for metallic airframes is demonstrated for clearance-fit countersunk fastener holes in 7475-T7351 aluminum. This method can be used to analytically predict the probability of functional impairment due to excessive cracking, fuel leaks or ligament breakage. The method accounts for the initial fatigue quality variation, crack growth damage accumulation in a population of structural details (e.g., fastener holes, lugs, fillets, cutouts, ets.), load spectra and material properties. The extent of damage (i.e., the number of structural details exceeding specified crack sizes) can be quantitatively estimated at any service time. Also, the cumulative distribution of service time at any crack size can be predicted. The probability of functional impairment is obtained by growing the equivalent initial flaw size distribution (EIFSD) forward to any service time using two different crack growth approaches. Both approaches, referred to as: (1) the "deterministic-deterministic crack growth approach" (DCGA-DCGA) and (2) the "deterministic-stochastic crack growth approach" (DCGA-SCGA), respectively, are evaluated and compared. Analytical predictions are compared with experimental results for dog-bone specimens and for a fighter lower wing skin. Good correlations are obtained using both crack growth approaches. However, the DCGA-SCGA was found to be more accurate and slightly more conservative than the DCGA-DCGA.

Introduction

The fatigue crack growth accumulation in structural details (e.g., fastener holes, fillets, cutouts, etc.) affects structural integrity, reliability and maintainability requirements for metallic airframes. The U. S. Air Force has damage tolerance design specifications for ensuring structural safety [1-4], and durability design specifications [1,2,4] for minimizing functional impairment problems, such as excessive cracking (e.g., cracks < 2.54 mm), fuel leaks, and ligament breakage (e.g., cracks 12.7 mm - 19.0 mm). This paper is concerned with the structural durability problem which affects structural maintenance requirements, aircraft performance, and operational readiness.

Airframe manufacturers need effective analytical tools for ensuring structural safety and durability with a high degree of confidence. To effectively utilize existing aircraft fleets and limited resources (e.g., budget, manpower and facilities), the U. S. Air Force requires longer aircraft life, higher reliability, minimum maintenance requirements and an increased operational readiness. Hence, it is extremely important that effective analytical tools be used to accurately assess the expected extent of damage in a durability-critical aircraft component at any service time so that the liability and risks associated with a "structural warranty" can be quantified. The probabilistic-based durability analysis method described in this paper provides a powerful and comprehensive tool for quantitatively estimating the crack growth damage accumulation for a population of structural details.

A probabilistic-based durability analysis methodology has been developed and verified for full-scale aircraft structure for relatively small cracks (e.g., smaller than 2.54 mm) in fastener holes where excessive cracking is the issue [5-10]. This methodology has recently been extended to the large crack size region where functional impairment due to fuel leaks and ligament breakage are concerns [11-13]. Two different two-segment crack growth approaches have been developed for performing durability analysis in both the small and large crack size regions [11,12]. The two crack growth approaches are referred to as: (1) the "two-segment deterministic crack growth approach" or DCGA-DCGA and (2) the "two-segment deterministic-stochastic crack growth approach" or DCGA-SCGA.

Various deterministic and stochastic crack growth approaches have been developed for predicting the crack growth damage accumulation in a population of structural details [12]. These approaches have been evaluated for both small and large fatigue

1. School of Engineering and Applied Sciences, The George Washington University, Washington, D.C. 20052, Member AIAA.
2. General Dynamics, Fort Worth Division, P. O. Box 748, Fort Worth, TX 76101.
3. Air Force Wright Aeronautical Laboratories, Flight Dynamics Laboratory, AFWAL/FIBE, Wright-Patterson Air Force Base, OH 45433.

cracks in clearance-fit straight-bore and countersunk fastener holes in 7475-T7351 aluminum [13]. The one-segment deterministic crack growth approach (DCGA) and/or the one-segment stochastic crack growth approach (SCGA) have been previously evaluated using dog-bone specimens with clearance-fit fasteners [10].

The purpose of this paper is to compare, evaluate and demonstrate two different two-segment crack growth approaches for predicting statistically the extent of cracking in a durability-critical component associated with fuel leaks and ligament breakage (e.g., crack size 12.7 mm to 19.0 mm). Both approaches (i.e., DCGA-DCGA and DCGA-SCGA) are demonstrated using fractographic results for dog-bone specimens and for full-scale lower wing skins from a fighter aircraft. The demonstration is conducted using fractographic results for fatigue cracking in 7475-T7351 aluminum containing countersunk fastener holes and clearance fit fasteners. Good correlations are obtained between the analytical predictions and experimental results for both of the two-segment crack growth approaches in the large crack size region. However, based on the results presented the DCGA-SCGA is superior to the DCGA-DCGA.

Technical Approach

Initial Fatigue Quality

The initial fatigue quality (IFQ) defines the initially manufactured state of a structural detail or details with respect to initial flaws in a part, component, or airframe prior to service. The IFQ for a group of replicate details (e.g., fastener holes) is represented by an equivalent initial flaw size (EIFS) distribution. An equivalent initial flaw is an artificial initial crack size which results in an actual crack size at an actual point in time when the initial flaw is grown forward.

The Weibull compatible distribution function proposed by Yang and Manning [14, 15] has been found to be reasonable for representing the EIFS cumulative distribution [5-15]

$$F_{a(0)}(x) = \exp\left\{ - \left[\frac{\ln(x_u/x)}{\phi} \right]^{\alpha} \right\} ; \quad 0 \le x \le x_u \qquad (1)$$

$$= 1.0 \qquad ; \quad x > x_u$$

in which x_u = EIFS upper bound limit; α and ϕ are empirical parameters.

An EIFS value for a fastener hole is determined by back-extrapolating fractographic data in a selected crack size range (AL-AU) using a simple but versatile deterministic crack growth rate model recommended by Yang and Manning [14,15],

$$da(t)/dt = Q[a(t)]^b \qquad (2)$$

where da(t)/dt = crack growth rate, a(t) = crack size at any time t in flight hours, and Q and b are empirical crack growth rate parameters. In this paper, the special case b = 1 is used.

After EIFS values, a(0), are obtained from all available fractographic data, they are fitted by Eq. 1 to determine the EIFS distribution (EIFSD) parameters x_u, α, and ϕ. To predict the extent of cracking in service, the initial flaw size, a(0), is grown forward, and the statistical distribution of the crack size a(t) at any service time t can be derived from that of a(0) given by Eq. 1. The EIFSD is grown forward to predict: (1) the probability that a crack in the ith stress region at any service time, τ, will exceed any given crack size, x_1, denoted by $p(i,\tau)$, and (2) the cumulative distribution of service time, $F_{T(x_1)}(\tau)$, for a crack in the ith stress region to reach any given crack size x_1. $p(i,\tau)$ is referred to as the crack exceedance probability. Two different crack growth approaches are described below and in Fig. 1 for growing the EIFSD forward to predict $p(i,\tau)$ and/or $F_{T(x_1)}(\tau)$.

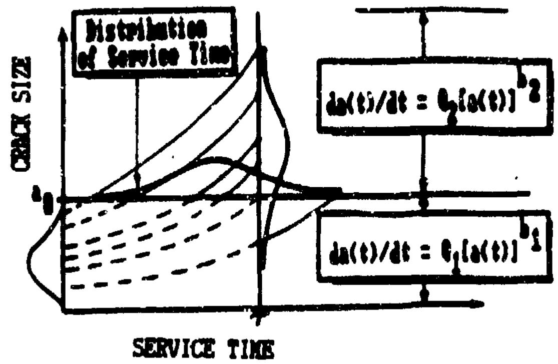

(a) Two-Segment Deterministic Crack Growth Approach (DCGA-DCGA)

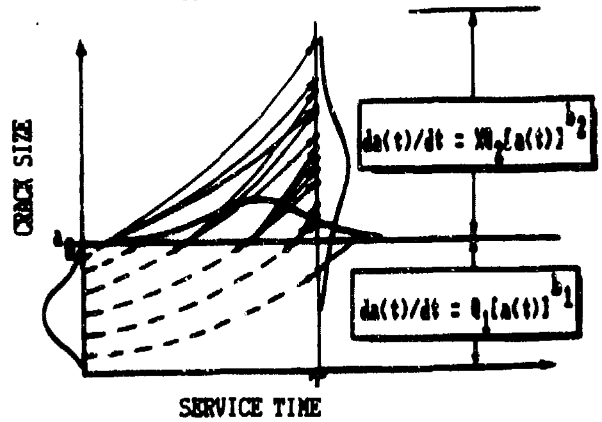

(b) Two-Segment Deterministic-Stochastic Crack Growth Approach (DCGA-SCGA)

Fig. 1 Two-Segment Crack Growth Approaches for Durability Analysis

Two-Segment Deterministic Crack Growth Approach (DCGA-DCGA)

The EIFSD given in Eq. 1 is grown forward using a service crack growth master curve (SCGMC) for a given stress region. To simplify the statistical analysis such a SCGMC can be fitted by an analytical crack growth rate equation. However, in some cases the SCGMC may not be fitted by a single equation, e.g., Eq. 2, with sufficient accuracy. Then, the SCGMC may be separated into two regions; one with the crack size smaller than the reference crack size, a_0, at crack initiation, and the other with crack size larger than a_0. The SCGMC can be represented in two regions using different crack growth rate equations or the same crack growth rate equation but with different crack growth rate parameters as follows:

$$da(t)/dt = Q_1[a(t)]^{b_1} \; ; \quad a(t)<a_0 \qquad (3)$$

$$da(t)/dt = Q_2[a(t)]^{b_2} \; ; \quad a(t)>a_0 \qquad (4)$$

The probability of crack exceedance, $p(i,\tau)$, can be derived by growing the initial flaw size distribution given in Eq. 1 using the crack growth rate equations given by Eqs. 3 and 4; with the results [see Refs. 11-12 for detailed derivations]

$$\begin{aligned} p(i,\tau) &= P[a(\tau) \geq x_1] = 1 - F_{a(\tau)}(x_1) \\ &= 1 - F_{a(0)}[y(x_1;\tau)] \end{aligned} \qquad (5)$$

in which $F_{a(0)}(x)$ is the distribution function of EIFS given by Eq. 1, $F_{a(\tau)}(x)$ is the cumulative distribution of the crack size, $a(\tau)$, at service time τ, and $y(x_1;\tau)$ is defined in Eqs. 6 and 7 for $b_1 = b_2 = 1$

$$y(x_1;\tau) = x_1 \exp(-Q_1\tau); \quad x_1<a_0 \qquad (6)$$

$$y(x_1;\tau) = (x_1)^{Q_1/Q_2} \exp(\Lambda - Q_1\tau); \quad x_1>a_0 \qquad (7)$$

where

$$\Lambda = [1 - (Q_1/Q_2)] \ln a_0 \qquad (8)$$

Let $T(x_1)$ be the time for a crack to reach any given crack size x_1 and $F_{T(x_1)}(\tau)$ be the corresponding cumulative distribution function, i.e., $F_{T(x_1)}(\tau) = P[T(x_1) \leq \tau]$. The distribution function of $T(x_1)$ is the probability that the crack will reach a crack size x_1 before service time τ. Such a probability is equal to the probability that the crack size $a(\tau)$ at service time τ will exceed x_1, which is simply the probability of crack exceedance. Hence,

$$\begin{aligned} F_{T(x_1)}(\tau) &= P[T(x_1) \leq \tau] \\ &= P[a(\tau) \geq x_1] = p(i,\tau) \end{aligned} \qquad (9)$$

Consequently, $F_{T(x_1)}(\tau)$ is obtained for any given crack size x_1 by computing the crack exceedance probability, $p(i,\tau)$, at different values of service time τ.

Deterministic-Stochastic Crack Growth Approach (DCGA-SCGA)

The crack growth damage accumulation is divided into two segments as shown in Fig. 1(b). For crack sizes $< a_0$, a deterministic crack growth rate model, Eq. 3, is used. The following stochastic crack growth rate model is used for crack sizes $> a_0$

$$da(t)/dt = XQ_2[a(t)]^{b_2}; \quad a(t)>a_0 \qquad (10)$$

in which X is a lognormal random variable with a median of one; Q_2 and b_2 are crack growth rate parameters. Equation 10 accounts for the crack growth rate variability and is referred to as the "lognormal random variable model" proposed by Yang et al [16-21].

The probability density function of the lognormal random variable X with a median 1.0 is given by

$$\begin{aligned} f_X(u) &= \frac{\log e}{\sqrt{2\pi}\; u\,\sigma_z} \exp\left\{-\frac{1}{2}\left[\frac{\log u}{\sigma_z}\right]^2\right\} \; ; \quad u \geq 0 \\ &= 0 \qquad ; \; u < 0 \end{aligned} \qquad (11)$$

in which σ_z is the standard deviation of the normal random variable $Z = \log X$. Equation 11 is used when σ_z is estimated using the log to base 10 form. If σ_z is based on the natural log form, $f_X(u)$ given in Eq. 12 should be used.

$$\begin{aligned} f_X(u) &= \frac{1}{\sqrt{2\pi}\; u\,\sigma_z} \exp\left\{-\frac{1}{2}\left[\frac{\ln u}{\sigma_z}\right]^2\right\} \; ; \quad u \geq 0 \\ &= 0 \qquad ; \; u < 0 \end{aligned} \qquad (12)$$

Note that σ_z based on the log to base 10 is equal to that based on the natural log divided by the natural log of 10. Details for estimating σ_z are given elsewhere [12, 13].

Let T be the time for an EIFS, $a(0)$, to reach the reference crack size a_0. Then, integrating Eq. 3 from $t = 0$ to $t = T$ for $b_1 = 1$, one obtains

$$T = Q_1^{-1} \ln[a_0/a(0)] \qquad (13)$$

in which it is understood that $a(T) = a_0$.

In the region where $a(\mathcal{T}) > a_0$ (or $\mathcal{T} > T$), Eq. 10 is integrated with $b_2 = 1$ from $t = T$ to $t = \mathcal{T}$ (or from $a(T) = a_0$ to $a(t) = a(\mathcal{T})$) with the result

$$T = \tau \cdot (XQ_2)^{-1} \ln[a(\tau)/a_0] \; ; \; a(\tau)>a_0 \qquad (14)$$

Equating Eqs. 13 and 14 leads to the following relation between $a(\mathcal{T})$ and $a(0)$

$$a(0) = a_0 \exp(-Q_1\tau)[a(\tau)/a_0]^{\gamma/X} \; ; \; a(\tau)>a_0 \qquad (15)$$

in which

$$\gamma = Q_1/Q_2 \qquad (16)$$

When the crack size, $a(\mathcal{T})$, at any service time $\mathcal{T}$ is smaller than a_0, the relation between $a(\mathcal{T})$ and $a(0)$ is obtained by integrating Eq. 3 for $b_1 = 1$ from $t = 0$ to $t = \mathcal{T}$ as follows:

$$a(0) = a(\tau)\exp(-Q_1\tau) \; ; \; a(\tau)<a_0 \qquad (17)$$

Depending on the crack size of interest x_1, the crack exceedance probability, $p(i, \mathcal{T})$, can be derived in the following manner.

(1) When the crack size of interest x_1 is smaller than the reference crack size a_0, the distribution function $F_{a(\mathcal{T})}(x_1) = P[a(\mathcal{T}) \le x_1]$ of the crack size, $a(\mathcal{T})$, for $x_1 < a_0$ can be derived from the distribution function of $a(0)$ through the transformation of Eq. (17),

$$F_{a(\tau)}(x_1) = F_{a(0)}[y(x_1;\tau)] \qquad (18)$$

in which

$$y(x_1;\tau) = x_1 \exp(-Q_1\tau) \qquad (19)$$

The crack exceedance probability, $p(i,\mathcal{T})$, is given by

$$p(i,\tau) = P[a(\tau)>x_1] = 1 - F_{a(\tau)}(x_1) = 1 - F_{a(0)}[y(x_1,\tau)] \; ; \; x_1 \le a_0 \qquad (20)$$

where $F_{a(0)}(x)$ is the distribution function of EIFS, $a(0)$, given by Eq. 1 or other suitable distribution functions.

(2) When the crack size of interest x_1 is larger than a_0, the conditional distribution function of $a(\mathcal{T})$ at any service time $\mathcal{T}$, given $X=u$, can be derived from that of $a(0)$ through the transformation of Eq. 15. Then, the unconditional distribution function, $F_{a(\mathcal{T})}(x_1)$, of $a(\mathcal{T})$ can be obtained using the theorem of total probability with the result

$$F_{a(\tau)}(x_1) = \int_0^{\infty} F_{a(0)}[G(x_1;\tau|X=u)] f_X(u) du \qquad (21)$$

in which the lognormal probability density function $f_X(u)$ is given by Eq. 11 or 12 and

$$G(x_1;\tau|X=u) = a_0 \exp(-Q_1\tau) [x_1/a_0]^{\gamma/u} \qquad (22)$$

The crack exceedance probability, $p(i, \mathcal{T})$, for $x_1>a_0$ is given by $p(i,\mathcal{T}) = 1 - F_{a(\mathcal{T})}(x_1)$, i.e.,

$$p(i,\tau) = 1 - \int_0^{\infty} F_{a(0)}[G(x_1;\tau|X=u)] f_X(u) du \qquad (23)$$

When the Weibull compatible distribution, Eq. 1, is used for the EIFS the condition that $F_{a(0)}[G(x_1;\tau|X=u)] = 1$ or $G(x_1; \mathcal{T}|X=u) \ge x_u$ should be reflected in the computer program for computing the crack exceedance probability $p(i,\mathcal{T})$ Eq. 23.

The cumulative distribution of service time, $F_{T(x_1)}(\mathcal{T})$ for a crack to reach any given crack size x_1 is determined using Eq. 9. $F_{T(x_1)}(\mathcal{T})$ is obtained for $x_1 < a_0$ and for $x_1 > a_0$ by computing $p(i, \mathcal{T})$ at different service times $\mathcal{T}$, using Eq. 20 and 23, respectively.

Durability Analysis Procedures

Durability analysis procedures for implementing the two approaches (Fig. 1) described above and demonstrated elsewhere [12,1 ,22] are summarized in the following four steps.

(1) Select a reasonable EIFS distribution function, $F_{a(0)}(x)$, to represent the initial fatigue quality (IFQ) (e.g., Eq. 1), and suitable base-line fractographic data sets (e.g., 23,24). For each base-line fractographic data set determine the EIFS master curve using (i) fractographic results in a selected crack size range AL-AU (e.g., 0.254 mm - 1.27 mm), (ii) the deterministic crack growth rate

model, Eqs. 2 or 3, and (iii) a least-squares fit procedure [12,13]. Select a reference crack size a_0 for AL $\le a_0 \le$ AU and determine the corresponding TTCI sample values for each data set. Then, for each data set the EIFS sample values are obtained by back-extrapolating the TTCI sample values at a_0 to time zero using the corresponding EIFS master curve [12, 13].

(2) Determine the IFQ or EIFSD for structural details in the durability critical components. Estimate/optimize the EIFSD parameters in Eq. 1 using: (i) the EIFS sample values from step (1), (ii) EIFS data pooling/global least squares fit procedures, and (iii) a statistical scaling technique [11-13]. Details of this step are given elsewhere [12,13]. The selected EIFSD is justified by checking the goodness-of-fit of crack exceedance predictions for $x_1 \le$ AU, Eq. 20 with $Q_1 = Q$, for the base-line fractographic data sets.

(3) The service crack growth master curve (SCGMC) in each stress region is determined by either available fractographic results or LEFM crack growth analysis. In the latter case, the LEFM crack growth computer program is "tuned" or "curve-fitted" to the EIFS master curve in the AL-AU crack size region where base-line fractographic data are available. Normal assumptions for the crack shape and geometry are reflected in the crack growth analysis. Then the SCGMC is fitted by Eqs. 3 and 4 for the DCGA-DCGA and by Eqs. 3 and 10 for the DCGA-SCGA using a least squares fit procedure [12, 13]. Equation 3 is used to obtain Q_1 for $a(t)<a_0$. For $a(t)>a_0$ Eq. 4 and 10 are used to estimate Q_2 for the DCGA-DCGA and the DCGA-SCGA, respectively. The standard deviation σ_z in Eqs. 11 or 12 can be estimated using available fractographic data or based on past experience [12,13].

(4) The probability of crack exceedance, $p(i,\tau)$, at any service time, τ, for each stress region, i, can be determined for the DCGA-DCGA and the DCGA-SCGA using Eqs. 5-8 and Eqs. 20-23, respectively. Then the statistics for the number of fastener holes that will have a crack size larger than x_1 in the entire durability critical component can be computed using the Binomial distribution [5,6,13].

The cumulative distribution of service time, $F_{T(x_1)}(\tau)$, to reach any given crack size, x_1, can be obtained using Eq. 9 and the applicable $p(i,\tau)$ expressions for the DCGA-DCGA and DCGA-SCGA, respectively.

Theoretical/Experimental Correlations

Theoretical and experimental correlations for the DCGA-DCGA and the DCGA-SCGA were conducted for clearance-fit countersunk fasteners for both coupon specimens and full-scale lower wing skins from a fighter aircraft. There are several facets to the investigation conducted. Because of space limitations a brief description of the investigation and the pertinent results obtained are described in the following. Details are given elsewhere [12,13].

The initial fatigue quality of clearance-fit countersunk fasteners (MS 90353-08) in 7475-T7351 aluminum was determined using fractographic results for 38.1 mm wide double-reversed dog-bone specimens with a 15% bolt load transfer design (Fig. 2) tested under spectrum loading. Three

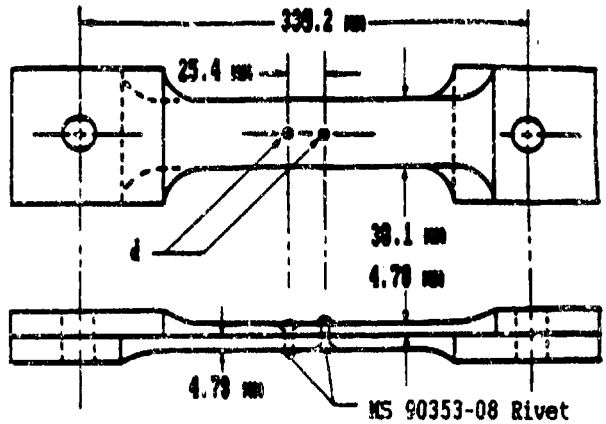

Fig. 2 Double Reversed Dog-Bone Specimen with 38.1 mm Width and 15% Load Transfer

different fractographic data sets (i.e., AFXLR4, AFXMR4 and AFXHR4) [23] were used to estimate the EIFSD parameters for the Weibull compatible distribution function given in Eq. 1. A statistical scaling technique and a data pooling procedure [12,13] were used to estimate the EIFSD parameters in a global sense. The resulting EIFSD parameters are summarized in Table 1, including the crack growth parameter Q for each of the three data sets, Eq. 2.

The EIFSD defined by Eq. 1 and the parameters in Table 1 were then used to make $p(i,\tau)$ predictions for 76.2 mm wide double-reversed dog-bone specimens (Fig. 3) and for the full-scale lower wing skins of a fighter using both crack growth approaches (Fig. 1). Predictions for $F_{T(x_1)}(\tau)$ were also made for the 76.2 mm wide dog-bone specimens (Fig. 3). Analytical predictions and experimental correlations for coupon specimens and lower wing skin are described and discussed in the following.

Table 1 EIFSD Parameters for Pooled Fractographic Data Sets Based on Double Reversed Dog-Bone Specimens with 38.1 mm Width and 15% Bolt Load Transfer

DATA SETS (1)	NO. SPEC.	σ (MPa)	% BOLT LT	ℓ (2)	x_u (mm)	α	ϕ	$Q \times 10^4$ (1/HR) (3)
AFXLR4	10	220.6	15	4	.762	1.716	6.308	2.101
AFXMR4	9	234.4	↓	↓	↓	↓	↓	2.514
AFXHR4	10	261.9	↓	↓	↓	↓	↓	6.062

Notes: (1) Specimen details shown in Fig. 2
(2) Statistical scaling factor [13]
(3) Fractographic crack size range used:
AL-AU = .254 mm - 1.27 mm

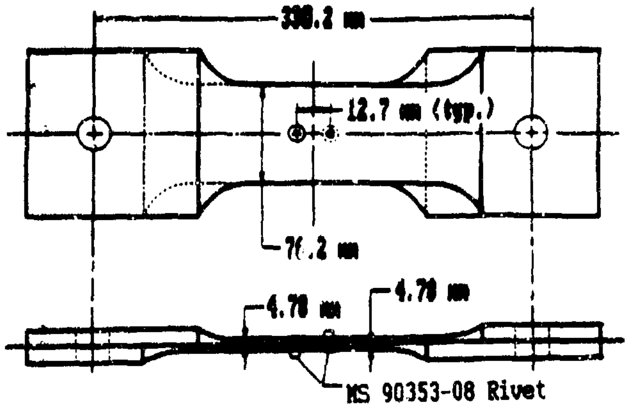

Fig. 3 Double Reversed Dog-Bone Specimen with 76.2 mm Width and 15% Bolt Load Transfer

Coupon Specimens

Fractographic results were available for 76.2 mm wide double reversed dog-bone specimen (Fig. 3) fatigue tested to failure under a fighter load spectrum [24]. Two fractographic data sets (i.e. WAFXMR4 and WAFXHR4) were used. Except for the width, these specimens are identical to the 38.1 mm wide specimens shown in Fig. 2. Crack growth parameters Q_1 and Q_2 for two segments of crack growth (i.e., AL-AU = .254 mm - 1.27 mm and 1.27 mm - 12.7 mm) were determined using fractographic results. The standard deviation, σ_z, was also determined for segment 2 (i.e., AL-AU = 1.27 mm - 12.7 mm) for implementing the DCGA-SCGA. Parameter results are summarized in Table 2. If applicable fractographic results are not available, Q_1 and Q_2 can be determined from the SCGMC based on a suitable analytical crack growth computer program.

Analytical predictions for the probability of crack exceedance, $p(i,\tau)$, for both crack growth approaches (Fig. 1) are correlated with experimental test results for the WAFXMR4 and WAFXHR4 data sets in Figs. 4 and 5, respectively. Predicted

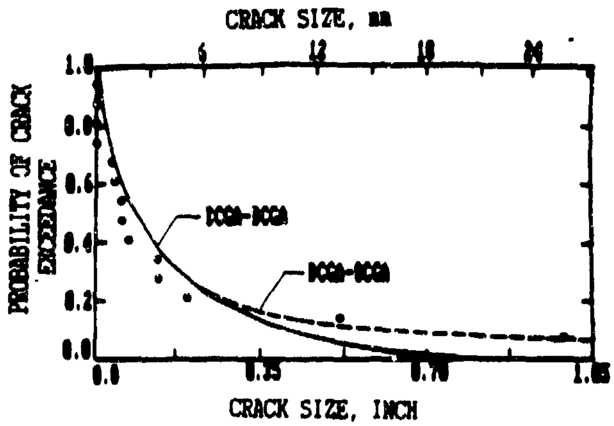

Fig. 4 Correlations Between Theoretical Predictions and Experimental Results (WAFXMR4 Data Set) for Crack Exceedance Probability $p(i,\tau)$ at τ = 11608 Flight Hours

Table 2 Summary of Crack Growth Parameters for Double Reversed Dog-Bone Specimen Data Sets with 76.2 mm Width and 15% Bolt Load Transfer

DATA SET (1)	NO. SPEC.	σ (MPa)	% BOLT LT	(2) $Q_1 \times 10^4$ (1/HR)	(3) $Q_2 \times 10^4$ (1/HR)	(4) σ_z
WAFXMR4	14	234.4	15	2.851	2.906	.449
WAFXHR4	12	261.3	15	9.126	3.854	.322

Notes: (1) Specimen details shown in Fig. 3
(2) AL-AU = .2564 mm - 1.27 mm
(3) AL-AU = 1.27 mm - 12.7 mm
(4) Natural log basis

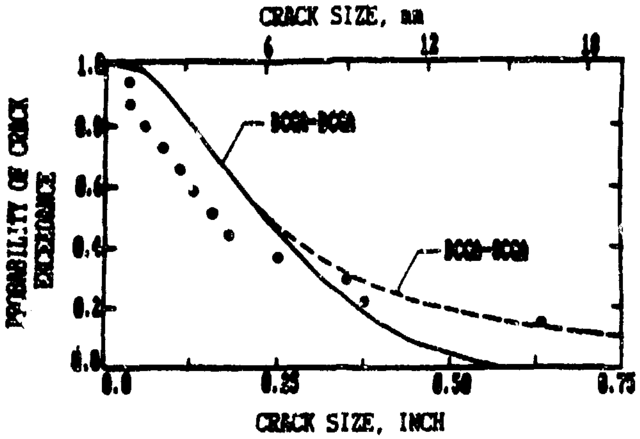

Fig. 5 Correlations Between Theoretical Predictions and Experimental Results (WAFXMR4 Data Set) for Crack Exceedance Probability $p(1,\tau)$ at τ = 7000 Flight Hours

crack exceedance probabilities at τ = 11608 flight hours are shown in Fig. 4; whereas those at τ = 7000 flight hours are presented in Fig 5. Results for the DCGA-DCGA are shown as a solid curve; whereas results for the DCGA-SCGA are shown as a dashed curve. Both crack growth approaches give the same results for crack sizes $\leq a_0$ (1.27 mm). Experimental results are shown as solid circles.

Theoretical predictions for the distribution of service time to reach any given crack size x_1, $F_{T(x_1)}(\tau)$, for both crack growth approaches (Fig. 1) are correlated with experimental test results for the WAFXMR4 and the WAFXHR4 data sets in Figs. 6 and 7, respectively. The results shown in Fig. 6 are for a crack size of x_1 = 18.54 mm and those in Fig. 7 are for x_1 = 14.99 mm. Predictions for the DCGA-DCGA and the DCGA-SCGA are displayed as solid

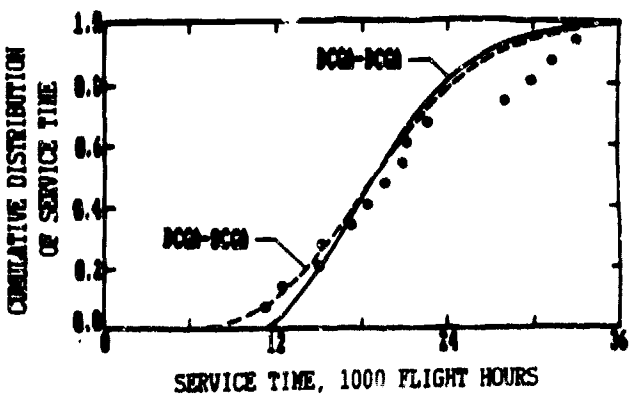

Fig. 6 Correlations Between Theoretical Predictions and Experimental Results (WAFXMR4 Data Set) for Cumulative Distribution of Service Time to Reach Crack Size x_1 = 18.54 mm

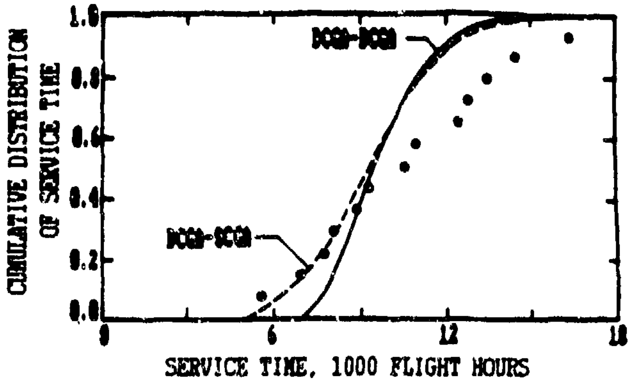

Fig. 7 Correlations Between Theoretical Predictions and Experimental Results (WAFXHR4 Data Set) for Cumulative Distribution of Service Time to Reach Crack Size x_1 = 14.99 mm

and dashed curves, respectively; whereas solid circles denote the experimental results.

From Figs. 4-7 it is observed that better overall correlations are obtained for the DCGA-SCGA than those for the DCGA-DCGA. Also, in the large crack size region (upper tail of Figs. 4 and 5) or the early service time (lower tail of Figs. 6 and 7), the DCGA-SCGA predictions are more accurate and conservative than those based on the DCGA-DCGA.

<u>Lower Wing Skins</u>

Fractographic results are available for the lower wing skins from a fighter durability test article [e.g., 25] that was fatigue tested under spectrum loading to 16000 flight hours. The wing skins are 7475-T7351 aluminum and include countersunk fasteners (i,e, MS 90353-08 blind pull-through rivets) of the same type used in the test specimens of Figs. 2 and 3. The durability analysis demonstration was conducted as follows:

1. The EIFSD parameters obtained previously for countersunk fastener holes were used for the fighter fastener holes, i.e., x_u = .762 mm, α = 1.716 and ϕ = 6.308. These EIFSD parameters, representing the IFQ, were determined from three narrow width specimen data sets, i.e., AFXLR4, AFXMR4 and AFXHR4.

2. The lower wing skin was divided into ten stress regions as shown in Fig. 8. The maximum stress level, σ_i, and the number of fastener holes, N_i, in each stress region are shown in Table 3. Service crack growth rate parameters Q_1 and Q_2 for each stress region in the small and large crack size regions were estimated using five fractographic data sets available and a crack growth model proposed by Yang and Manning [5,12-14].

$$Q_i = \xi \sigma_i^{\psi} \quad (24)$$

In Eq. 24, Q_i = service crack growth parameter for the ith stress region, σ_i = maximum stress level in the ith stress region; ξ and ψ are empirical constants determined from available base-line data or suitable analytical crack growth results. Fractographic results for three narrow width specimen data sets (i.e., AFXLR4, AFXMR4 and AFXHR4) and two 76.2 mm wide specimen data sets (i,e,, WAFXMR4 and WAFXHR4) were used in Eq. 24 to determine ξ and ψ; with the following results: ξ = 2.2274×10^{-19} and $\psi = 6.3744$ for $x_1 < a_0$; $\xi = 6.2883\times10^{-8}$ and $\psi = 1.5463$ for $x_1 > a_0$. Parameter values for ξ and ψ reflect σ_i in MPa units. Once ξ and ψ are determined from these base-line fractographic data, the crack growth rate parameter Q_i in each of the ten stress regions with a maximum stress level of σ_i is computed from Eq. 24. The resulting crack growth rate parameters Q_1 and Q_2 in the small and large crack size regions for each of the ten stress regions are presented in Table 3.

3. Typical predictions for crack exceedance probability, $p(i,\tau)$, in each of the ten stress regions at τ = 16000 flight hours for five different crack sizes (i.e., x_1 = .762 mm, 1.27 mm, 2.54 mm, 7.62 mm and 12.7 mm) are shown only for the DCGA-SCGA in Table 4, due to space limitations. Analysis details and results for both crack growth approaches, Fig. 1, are given elsewhere [13]. The analysis for the DCGA-SCGA was conducted using σ_z =.3 (natural log basis), which is reasonable for countersunk fastener holes in 7475-T7351 aluminum [13]. The average number of fastener holes, $\bar{N}(i,\tau)$, with a crack size > x_1 at τ = 16000 flight hours are predicted and shown in Table 4 for each of the ten stress regions. Further, predictions for the average number of fastener holes in the lower wing skin with a crack size > x_1 at 16000 flight hours, $\bar{L}(\tau)$, and its standard deviation, $\sigma_L(\tau)$, are shown in Table 5 for the DCGA-SCGA. $\bar{L}(\tau)$ and $\sigma_L(\tau)$ values are computed based on the Binomial distribution [12,13], as given by Eqs. 25 and 26.

$$\bar{L}(\tau) = \sum_{i=1}^{10} \bar{N}(i,\tau) \quad (25)$$

$$\sigma_L(\tau) = \left\{ \sum_{i=1}^{10} N_i \, p(i,\tau) \left[1 - p(i,\tau)\right] \right\}^{1/2} \quad (26)$$

Using $\bar{L}(\tau)$ and $\sigma_L(\tau)$, the extent of damage for the lower wing skin can be estimated for selected probabilities. Such results can be used to determine the mean and upper/lower bound limits for the extent of damage.

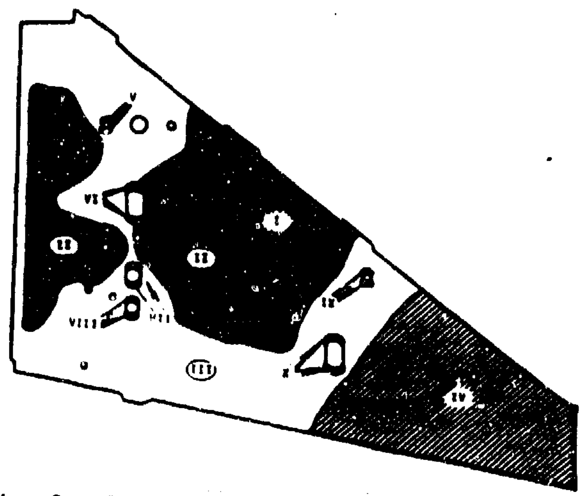

Fig. 8 Stress Regions for Fighter Lower Wing Skin

Table 3 Stress Levels, Number of Fastener Holes and Crack Growth Rate Parameters for Fighter Lower Wing Skin

STRESS REGION	MAX. STRESS σ_i(MPa)	NO. HOLES N_i	CRACK GROWTH PARAMETERS	
			$Q_1 \times 10^4$ (1/HR.)	$Q_2 \times 10^4$ (1/HR.)
1	195.1	59	.884	2.187
2	186.1	320	.655	2.033
3	167.5	680	.334	1.727
4	115.1	469	.031	.967
5	195.8	8	.904	2.199
6	201.3	30	1.080	2.296
7	223.4	8	2.097	2.697
8	180.6	8	.541	1.941
9	180.6	12	.541	1.941
10	177.2	20	.478	1.885

Theoretical predictions for the average number of fastener holes, $L(\tau)$, with a crack size > x_1 at τ = 16000 flight hours in the entire lower wing skin are plotted in Fig. 9 for both of the two-segment crack growth approaches. In this figure, the results for the DCGA-DCGA and the DCGA-SCGA are depicted by a solid curve and a dashed curve, respectively. Results for both approaches are identical for the crack size $x_1 \leq 1.27$ mm in the first crack growth segment. The tear-down inspection results are shown in Table 5 and Fig. 9 as solid circles for comparison. These results reflect the average extent of damage for a lower wing skin based on the total extent of damage for left and right lower wing skins combined.

It is observed that the durability analysis predictions based on specimen test results correlate well with the tear-down inspections results and that the predictions for the DCGA-SCGA are slightly more conservative than the results for the DCGA-DCGA.

Conclusions

Two different durability analysis approaches for the large crack size region have been demonstrated and evaluated using fractographic results for both coupon specimens and lower wing skins from a fighter aircraft. Both approaches (i.e., DCGA-DCGA and DCGA-SCGA) were evaluated for fatigue cracking in countersunk fastener holes with clearance-fit fasteners. Similar demonstrations and evaluations for straight-bore fastener hole fractographic data are given elsewhere [11,13]. Both two-segment crack growth approaches are considered reasonable for evaluating functional impairment due to fuel leakage/ligament breakage in metallic aircraft structures. However, the DCGA-SCGA is recommended for durability analysis because predictions are more accurate and slightly more conservative than those based on the DCGA-DCGA.

Acknowledgement

This research was sponsored by the Air Force Wright Aeronautical Laboratories, Wright-Patterson Air Force Base, under Contract No. F33615-84-C-3208.

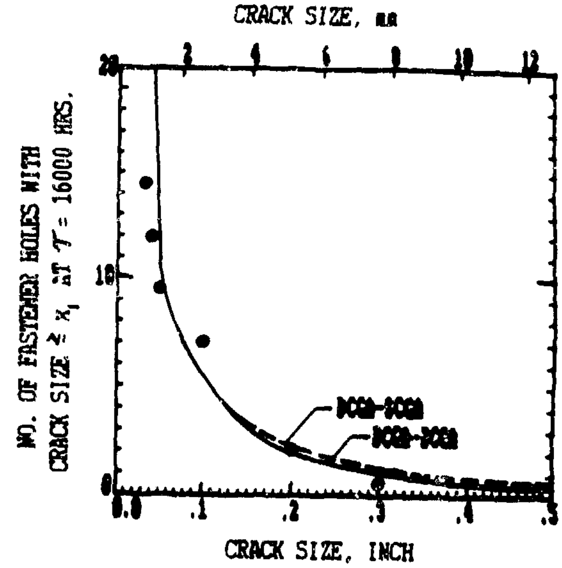

Fig. 9 Correlations Between Theoretical Predictions and Experimental Results for Fighter Lower Wing Skin for Extent of Damage at τ = 16000 Flight Hours

Table 5 Statistics for Number of Fastener Holes with Crack Size Exceeding x_1 in Fighter Lower Wing Skin

x_1 (mm)	$\bar{L}(\tau)$	$\sigma_L(\tau)$	EXPERIMENTAL RESULTS (Ave.)
.762	35.80	5.800	14.5
1.27	10.81	3.185	9.5
2.54	5.38	2.262	7.0
5.08	2.19	1.450	1.0
7.62	1.24	1.097	.5

Table 4 Crack Exceedance Probability and Average Number of Fastener Holes with Crack Exceeding x_1 at τ = 16000 Flight Hours in Each Stress Region

STRESS REGION	x_1 = .762 mm		x_1 = 1.27 mm		x_1 = 2.54 mm		x_1 = 5.08 mm		x_1 = 7.62 mm	
	$P(i,\tau)$	$\bar{N}(i,\tau)$	$P(i,\tau)$	$\bar{N}(i,\tau)$	$P(i,\tau)$	$\bar{N}(i,\tau)$	$P(i,\tau)$	$\bar{N}(i,\tau)$	$P(i,\tau)$	$\bar{N}(i,\tau)$
1	.0739	4.36	.0350	2.07	.0183	1.08	.0071	.42	.00348	.20
2	.0449	14.37	.0145	4.64	.00566	1.81	.00126	.40	.000419	.13
3	.0144	9.79	.0000643	.05	.0000066	.004	.0000066	.004	.0000066	.004
4	.000239	.11	.00	.00	.0000066	.003	.0000066	.003	.0000066	.003
5	.0768	.61	.0371	.29	.0196	.16	.00783	.06	.00392	.03
6	.103	3.09	.0577	1.73	.0335	1.00	.0158	.47	.00894	.27
7	.287	2.29	.225	1.80	.160	1.28	.104	.83	.0756	.60
8	.0326	.26	[illegible]	.06	.00187	.01	.000196	.002	.0000451	.00
9	.0326	.39	.00714	.09	.00187	.02	.000196	.002	.0000451	.00
10	.0264	.53	.00403	.08	.000621	.01	.000031	.001	.0000096	.00
		35.80		10.81		5.377		2.192		1.237

References

1. Military Specification, Aircraft Structures, Military Standard MIL-A-87221 (USAF), Air Force Aeronautical System Division, WPAFB, OH, February 28, 1985.

2. Aircraft Structural Integrity Program, Airplane Requirements, Military Standard MIL-STD-1530A, Air Force Aeronautical Systems Division, WPAFB, OH, December 1975.

3. Airplane Damage Tolerance Program Requirement, Military Standard MIL-A-83444, Air Force Aeronautical Systems Division, WPAFB, OH, July 1974.

4. Airplane Strength, Rigidity and Reliability Requirement; Repeated Loads and Fatigue, Military Standard MIL-A-8866B, Air Force Aeronautical Systems Division, WPAFB, OH, August 1975.

5. Manning, S. D. and Yang, J. N., USAF Durability Design Handbook; Guidelines for the Analysis and Design of Durable Aircraft Structures, AFWAL-TR-83-3027, Second Edition, Air Force Wright Aeronautical Laboratories, WPAFB, OH, August 1987.

6. Rudd, J. L., Yang, J. N., Manning, S. D., and Garver, W. R., "Durability Design Requirements and Analysis for Metallic Airframes," Design of Fatigue and Fracture Resistant Structures, ASTM STP 761, P. R. Abelkis and C. M. Hudson, Eds., American Society for Testing and Materials, 1982, pp. 133-151.

7. Rudd, J. L., Yang, J. N., Manning, S. D., and Yee, B. G. W., "Damage Assessment of Mechanical Fastened Joints in the Small Crack Size Range," Proc., Ninth U. S. National Congress of Applied Mechanics, Symposium on Structural Reliability and Damage Assessment, Cornell University, Ithaca, NY, June 21-25, 1982, pp. 329-338.

8. Rudd, J. L., Yang, J. N., Manning, S. D., and Yee, B. G. W., "Probabilistic Fracture Mechanics Analysis Methods for Structural Durability," Proc., Conference on the Behavior of Short Cracks in Airframe Components, AGARD-CP-328, Toronto, Canada, September 1982, pp. 10-1 through 10-23.

9. Yang, J. N., Manning, S. D., and Rudd, J. L., "Evaluation of a Stochastic Initial Fatigue Quality Model for Fastener Holes," Fatigue in Mechanically Fastened Composite and Metallic Joints, ASTM STP 927, John M. Potter, Ed., American Society for Testing and Materials, Philadelphia, 1986, pp. 118-149.

10. Yang, J. N., Manning, S. D., Rudd, J. L., and Artley, M. E., "Probabilistic Durability Analysis Methods for Metallic Airframes," Journal of Probabilistic Engineering Mechanics, Vol. 1, No. 4, December 1986.

11. Yang, J. N., Manning, S. D., Rudd, J. L., Artley, M. E., and Lincoln, J. W., "Stochastic Approach for Predicting Functional Impairment of Metallic Airframes," Proceedings of the 28th AIAA/ASME/ASCE/AHS Structures, Structural Dynamics and Materials Conference, Paper No. 8707520CP, Monterey, CA, April 6-8, 1987, pp. 215-223.

12. Manning, S. D., and Yang, J. N., "Advanced Durability Analysis, Volume I - Analytical Methods," AFWAL-TR-86-3017, Air Force Wright Aeronautical Laboratories, Wright-Patterson Air Force Base, OH, July 1987.

13. Manning, S. D., and Yang, J. N., "Advanced Durability Analysis, Volume II - Analytical Predictions, Test Results and Analytical Correlations," AFWAL-TR-86-3017, Air Force Wright Aeronautical Laboratories, Wright-Patterson Air Force Base, OH, August 1987.

14. Yang, J. N., Manning, S. D., and Garver, W. R., "Durability Methods Development, Volume V - Durability Analysis Methodology Development" AFFDL-TR-3118, Air Force Wright Aeronautical Laboratories, Wright-Patterson Air Force Base, OH, September 1979.

15. Yang, J. N., and Manning, S. D., "Distribution of Equivalent Initial Flaw Size," 1980 Proceedings of Annual Reliability and Maintainability Symposium, San Francisco, CA, 22-24 January 1980, pp. 112-120.

16. Yang, J. N., and Donath, R. C., "Statistical Fatigue Crack Propagation in Fastener Holes Under Spectrum Loading," Journal of Aircraft, AIAA, Vol. 20, No. 12, December 1983, pp. 1028-1032.

17. Yang, J. N., Manning, S. D., Rudd, J. L, and Hsi, W. H., "Stochastic Crack Propagation in Fastener Holes," Journal of Aircraft, AIAA, Vol. 22, No. 9, September 1985, 810-817.

18. Yang, J. N., Salivar, G. C., and Annis, C. G., "Statistical Modeling of Fatigue Crack Growth in a Nickel-Based Superalloy," Journal of Engineering Fracture Mechanics, Vol. 18, No. 2, June 1983, pp. 257-270.

19. Yang, J. N., and Chen, S., "Fatigue Reliability of Gas Turbine Engine Components Under Schedule Inspection Maintenance," Journal of Aircraft, AIAA, Vol. 22, No. 5, May 1985, pp. 415-422.

20. Yang, J. N., and Chen, S., "An Exploratory Study of Retirement-for-Cause for Gas Turbine Engine Components," Journal of Propulsion and Power, AIAA, Vol. 2, No. 1, January 1986, 38-49.

21. Yang, J. N., and Hsi, W. H., Manning, S. D., and Rudd, J. L., "Stochastic Crack Growth Models for Application to Aircraft Structures," Probabilistic Fracture Mechanics and Reliability, Edited by J. W. Provan, Chapter IV, Martinus Nijhoff Publishers, The Netherlands, 1987, pp. 171-211.

22. Manning, S. D., and Yang, J. N., "Advanced Durability Analysis, Volume IV - Executive Summary," AFWAL-TR-86-3017, Air Force Flight Dynamics Laboratory, Wright-Patterson Air Force Base, OH, September 1987.

23. Speaker, S. M., et al., "Durability Methods Development, Volume VIII - Test and Fractography Data," AFFDL-79-3118, Air Force Flight Dynamics Laboratory, Wright-Patterson Air Force Base, OH, November 1982.

24. Gordon, D. E., et al., "Advanced Durability Analysis, Volume III - Fractographic Data," AFWAL-TR-86-3017, Air Force Flight Dynamics Laboratory, Wright-Patterson Air Force Base, OH, August 1, 1986.

25. Manning, S. D., Yang, J. N., Shinozuka, M., Speaker, S. M., and Gordon, D. E., "Durability Methods Development, Volume VII - Phase II Documentation," AFFDL-TR-79-3118, Air Force Flight Dynamics Laboratory, Wright-Patterson Air Force Base, OH, January 1984.

Note: Appendix J is AIAA Paper No. 88-2421 presented at AIAA/ASME/ASCE/AHS 29th Structures, Structural Dynamics and Material Coonference, Williamsburg, VA, April 18-20, 1988.

U.S. GOVERNMENT PRINTING OFFICE: 1989-648-056